INVESTIGATING THE TARGETS AND MECHANISMS REGULATING SELF INCOMPATIBILITY IN *PAPAVER RHOEAS* POLLEN

by

TAMANNA HAQUE

A thesis submitted to
The University of Birmingham
for the degree of
DOCTOR OF PHILOSOPHY

School of Biosciences
The University of Birmingham
September 2015

ABSTRACT

Many higher plants use self-incompatibility (SI) mechanism to prevent inbreeding and thus encouraging out-crossing. Upon a self-challenge in *Papaver rhoeas,* a Ca^{2+}-dependent-signalling-cascade is initiated resulting in the destruction of the self-pollen by Programmed Cell Death (PCD). Upstream of PCD, several SI-specific events are triggered in incompatible pollen, including phosphorylation of soluble inorganic pyrophosphatases (sPPases); alterations to actin; increases in Reactive Oxygen Species (ROS) and Nitric Oxide (NO). In *Papaver* pollen, sPPases play an important role, as they provide the driving force for biosynthesis; data suggested that Ca^{2+} and phosphorylation inhibits the sPPases activities, contributing to pollen tube inhibition. Work presented in this thesis characterized Pr-p26.1 sPPases and the role of phosphomimic mutants in the SI signalling cascade. These studies provide good evidence that, together with Ca^{2+}, phosphorylation, H_2O_2 and pH dramatically affect sPPase activity.

As previous studies showed that increases in ROS and NO are triggered by SI in incompatible pollen, to provide insights into SI-mediated events, this project investigated protein-targets in pollen modified by oxidation and *S*-nitrosylations after SI, including actin and actin-associated proteins. Using a mass spectrometry approach we identified several proteins that were modified by oxidation and *S*-nitrosylation. This has provided us with several potential new mechanisms involved in SI.

Acknowledgement

Firstly, I would like to thank my supervisor, Professor Noni Franklin-Tong, for all her support and encouragement over the previous almost four years and for giving me the opportunity to work in a project that I have enjoyed a lot. I am also very thankful to Professor Chris Franklin for his critical advices and discussions, especially about actin cloning.

I would also like to express my gratefulness to the other members, staff and PIs on the second floor, past and present, who encouraged and helped me on many different levels, gave me the confidence, and provided an enjoyable working environment. In particular, I would like to thank Deborah J. Eaves for her valuable suggestions, support and comments during the experimental work and also on my thesis. Special thanks to Carlos Flores and Zongcheng Lin for being so helpful, for their valuable support and answering my questions all the time. I would like to thank Andrew Beacham, Javier Andrés Juárez Díaz, Katie Wilkins, Lijun Chai and Nianjun Teng for being wonderful lab mates. I also thank Kim Osman, Ruth Perry, Lisa Burke, Stefan Heckmann, Allan West for their valuable suggestions and help.

I would also like to acknowledge Nick Cotton and Dr. White for providing me some chemicals, giving me scientific and technical advices on the Pr-p26.1 project. My thanks go to the Proteomics Department, especially Laine Wallace and Cleidi Zampronio, who helped me with my samples for mass spectrometry and took the time to discuss the results with me.

I would like to thank the Commonwealth Scholarship Commission (CSC) for funding the PhD project.

Finally, but most importantly I would like to thank my friends and family members, specially my brother, sister and in-laws for all their moral support and encouragement. I would like to give a massive thank to my husband Zia and my daughter Zeba, who have been great support throughout the PhD, especially during the writing-up stage. I would like to thank my mum, without her moral support and unconditional love I would never have had the courage to pursue my PhD.

Table of contents

List of figures and tables

CHAPTER 1: Introduction

CHAPTER 2: Materials and methods

CHAPTER 3: Characterization of Pr-p26.1a and Pr-p26.1sPPase activity and investigations into how biologically relevant conditions might alter their activity

CHAPTER 4: Identification of proteins modified by ROS/NO during the SI response

CHAPTER 5: Actin as a target for SI signals

CHAPTER 6: General Discussion

ABBREVIATIONS

ABP: Actin binding protein

ADP: Adenosine diphoshate

ADF: Actin depolymerising factor

AEBSF: 4-(2-Aminoethyl) benzenesulfonyl fluoride hydrochloride

AmBic: Ammonium bicarbonate

ANSA: 1-amino-2-napthol-4-sulphonic acid

ASB: Actin stabilising buffer

ATP: Adenosine Triphosphate

BCECF AM: 2′,7′-bis-(2-carboxyethyl)-5-(and-6)-carboxyfluorescein ester

BSA: Bovine serum albumin

CAP: Cyclase associated protein

Caspase: Cysteinyl aspartate-specific protease

CCD: Cooled coupled device

c-DCFDA: 5-(and-6)-Carboxy-2',7'-dichlorofluorescein diacetate

c-PTIO: 2-(4-carboxyphenyl)-4,4,5,5- tetramethylimidazoline-1-oxyl-3-oxide

DEPC: Diethylpyrocarbonate

DMSO: Dimethyl Sulfoxide

ECL: Enhanced chemiluminescence

ECM: Extracellular Matrix

EDTA: Edetate disodium

EGTA: Ethylene glycol-bis(2-aminoethylether)-N,N,N′,N′-tetraacetic acid

ER: Endoplasmic reticulum

ETI: Effector-triggered immunity

ETS: Effector-triggered susceptibility

F-actin: Filamentous actin (actin MFs)

FITC: Fluorescein isothiocyanate

FT-ICR-MS: Fourrier transform ion cyclotron resonance mass spectrometry

GABA: Gamma-amino butyric acid

G-actin: Globular actin (actin monomers)

GC: Generative cell

GM: Germination Medium

GSH: Glutathione

GSI: Gametophytic SI

GSNO: *S*-nitrosoglutathione

HR: Hypersensitive Response

Jasp: Jasplakinolide

LatB: Latrunculin B

MAMP: Microbe- associated molecular pattern

MAPK: Mitogen-activated protein kinase

MBS: 3-Maleimidobenzoic acid N-hydroxysuccinimide ester

MF: Microfilament

MLPK: M-Locus Protein Kinase

MMTS: S-methyl methane thiosulfonate

MT: Microtubule

NO: Nitric oxide

PAGE: Polyacrylamide gel electrophoresis

PAMP: Pathogen-associated molecular pattern

PARP: Poly ADP Ribose Polymerase

PBS: Phosphate buffer saline

PCD: Programmed cell death

PCR: Polymerase Chain Reaction

Pi: Inorganic phosphate

PPi: inorganic Pyrophosphate

PrpS: *Papaver rhoeas* pollen S

PrsS: *Papaver rhoeas* stigma S

RNS: Reactive nitrogen species

ROS: Reactive oxygen species

Rh-Ph: Rhodamine Phalloidin

RT: Room temperature

RT-PCR: Reverse Transcription PCR

SA: Salicylic acid

SA-PMPs: Streptavidin MagneSphere Paramagnetic Particles

SAR: Systemic acquired resistance

SCR: S-locus Cysteine-Rich protein

SDS: Sodium dodecyl sulfate

SDW: Sterile distilled water

SI: Self-incompatibility

SLF: S-Locus F-box

SNO-RAC: Resin-assisted capture of *S*-nitrosothiols

sPPase: Soluble pyrophosphatase

SRK: S-locus Receptor Kinase

SSI: Sporophytic SI

TBS: Tris buffered saline

TBST: TBS + 0.1 % Tween 20

TEMED: N,N,N′,N′-Tetramethylethylenediamine

TLC: thin layer chromatography

TPS: Thiopropyl sepharose

TT: Transmitting-tissue

UT: Untreated

VCD: Vacuolar cell death

VN: Vegetative nucleus

Chapter 1

Introduction

1.1 Sexual Plant Reproduction

Sexual plant reproduction is an area of great scientific interest due to its enormous importance for crop science, biotechnology, medicine, conservation biology and evolution. Pollination is one of the very important steps during the life cycle of flowering plants, resulting in seeds which will give rise to new plants. Pollination starts when a pollen grain lands on the surface of a receptive stigma; the pollen hydrates and produces a pollen tube, which grows all the way down the style to the ovary following both internal and external stimuli. This pollen tube carries sperm cells through the transmitting tract of the pistil. When the pollen tube reaches the entry of the ovary, it will burst and delivers the sperm cells into the ovary. The sperm cell does double fertilization, fuging with the egg cell and the central cell. The fertilized ovule becomes a seed, which contains a food store and an embryo that will afterwards grow into a new plant (for recent reviews see Dresselhaus and Franklin-Tong, 2013, Linhart, 2014)

There are several plants (for examples, *Arabidopsis thaliana*) which produce their offspring through self-pollination as they are self-fertile plants. On the other hand, many sexually reproducing plants are self-incompatible (SI) (Self-incompatibility (SI)) and hence are not able to produce offspring by self-fertilization.

1.1.1 Self-Incompatibility (SI)

Higher plants produce seeds through pollination using specific interactions between pollen and pistil. The majority of plants develop both male and female organs on the same plants in close proximity. For most plants, inbreeding can

decreases fitness as the benefit of out-crossing are lost and inbreeding is encouraged with resulting loss of genetic variability (Lynch, 1991, reviewed by Charlesworth and Charlesworth, 1987). Self-incompatibility (SI) is an important mechanism used in many species to prevent inbreeding and thus encourage out crossing. SI is a genetically controlled cell-cell recognition system where self-pollen is recognised by pistil and inhibited in an S-specific manner. There are over 250,000 species of angiosperms and it is estimated more than half of these have evolved a form of SI (Igic and Kohn, 2006).

In homomorphic SI, the flowers are morphologically the same and use a recognition incident between the pollen and the pistil, which results in refusal of self-pollen and acceptance of non-self-pollen. In homomorphic self-incompatibility, if genetically unrelated pollen ('non-self') from the same species lands on the stigma, then germination, penetration of the stigmatic papilla cells and normal growth of the pollen tubes occurs, with the pollen finally reaching the ovule and fertilize the egg. If genetically identical pollen ('self') lands on the stigmas, its germination or growth is arrested, either on the stigma or during growth through the pistil (depending on the species) where the pollen is terminated (reviewed by Iwano and Takayama, 2012, Sawada *et al*., 2014).

1.1.1.1 Different mechanisms of self-incompatibility

There are two different mechanisms of SI (**Figure 1.1**). The first is sporophytic SI (SSI), where the SI phenotype of pollen is determined by the S-haplotypes

of diploid pollen donor. In contrast, pollen from plants with gametophytic SI (GSI) has an SI phenotype determined by its own haploid genotype.

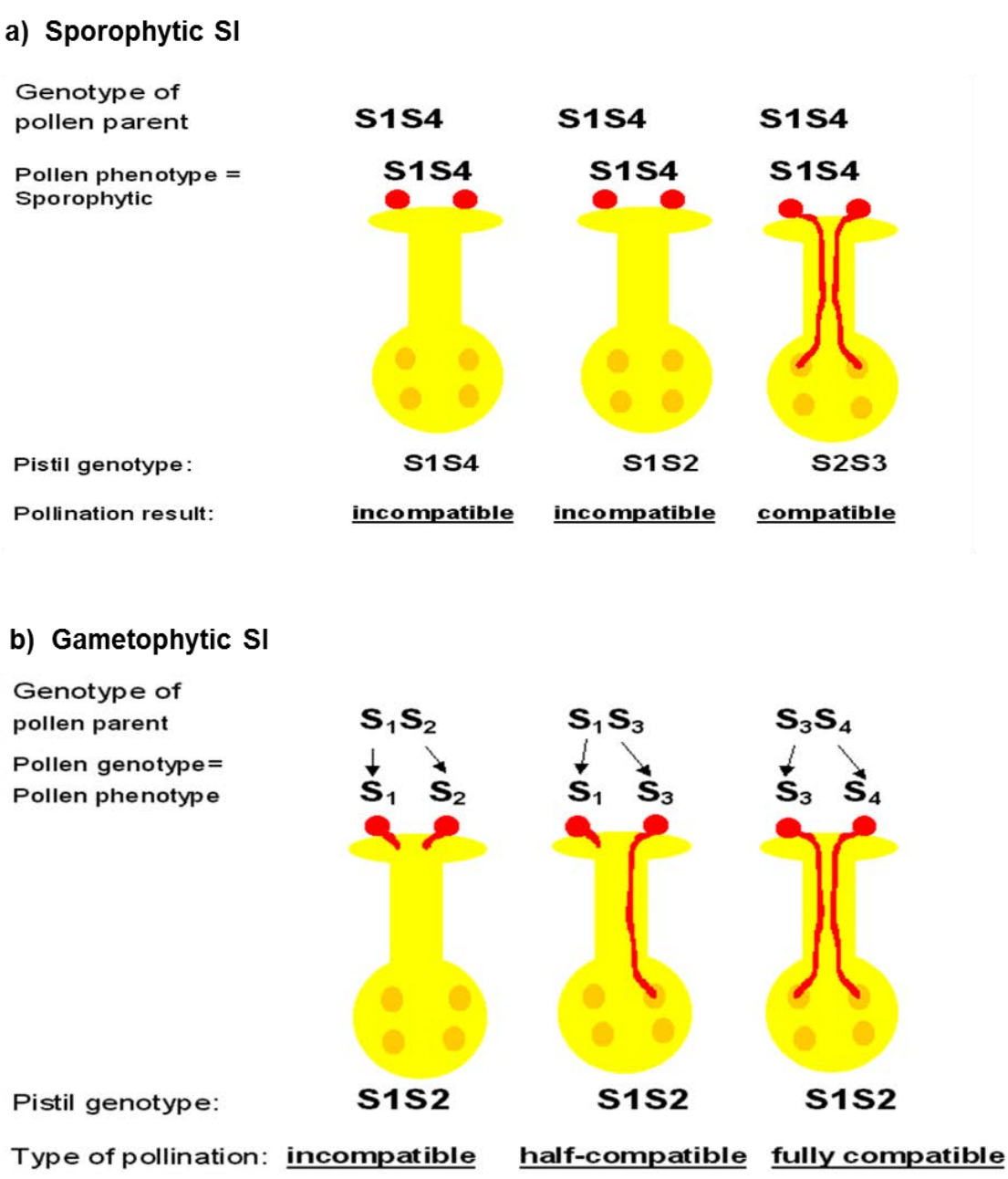

Fig. 1.1.Genetics of the two different types of SI

a) In sporophytic SI, pollen phenotype is identical as the parent plants diploid genotype. This produces either a compatible or incompatible outcome. b) In gametophytic SI, the phenotype of pollen is determined by the S-haplotype of haploid pollen, which results in three possible outcomes: fully compatible, half compatible or incompatible

GSI is more common type of SI, existing in the families: Solanaceae, Rosaceae, Plantaginaceae, Fabaceae, Onagraceae, Campanulaceae, Papavaraceae and Poaceae (reviewed by Hiscock and Allen, 2008).

SI is usually controlled by a single, polymorphic *S*-locus with multiple alleles. The *S*-locus comprises two tightly linked genes that code for the pistil (female) *S*-determinant and the pollen (male) *S*-determinant which are inherited as one segregating unit (Takayama and Isogai, 2005). Pollen that lands on stigma carrying the same *S*-allele is recognized as 'self' or 'incompatible' pollen and growth of the pollen tube, and therefore fertilization inhibited. Pollen that carries different alleles to those of the stigma is able to germinate and fertilisation is achieved. The rejection of incompatible pollen is governed by the interaction of pollen *S*-determinant with the pistil *S*-determinant. The SI-mechanisms involved in different SI systems will be discussed further in **section 1.6.**

Here we will consider pollen tubes and the mechanisms involved regulating their growth.

1.1.2 Pollen tubes

The pollen tube, the haploid male gametophyte is an important feature in plant sexual reproduction, which has been established as a model system for studying the molecular principles of polarised tip growth, organization of cytoskeleton, endo- and exocytosis, ion fluxes and cell-cell signalling (Cheung and Wu, 2008, Feijo *et al*., 2001, Hepler *et al*., 2001, Geitmann, 2010). This

has been possible because of high abundance of pollen and comparatively easy and rapid *in vitro* germination of pollen tubes.

During sexual reproduction of flowering plants, sperm cells are delivered to the egg through a long pollen tube. The pollen tube is a polarized structure that grows entirely at its tip. The tip growth rate of pollen is very fast, involving deposition of new cell and membrane material. A growing pollen tube consists of four distinct zones (**Figure1.2**).

1) The apical growth zone (the tip region)

2) The sub apical zone

3) The nuclear zone

4) The vacuolised and callose plug formation zone

The nuclear and vacuolisation zones are referred to as the shank.

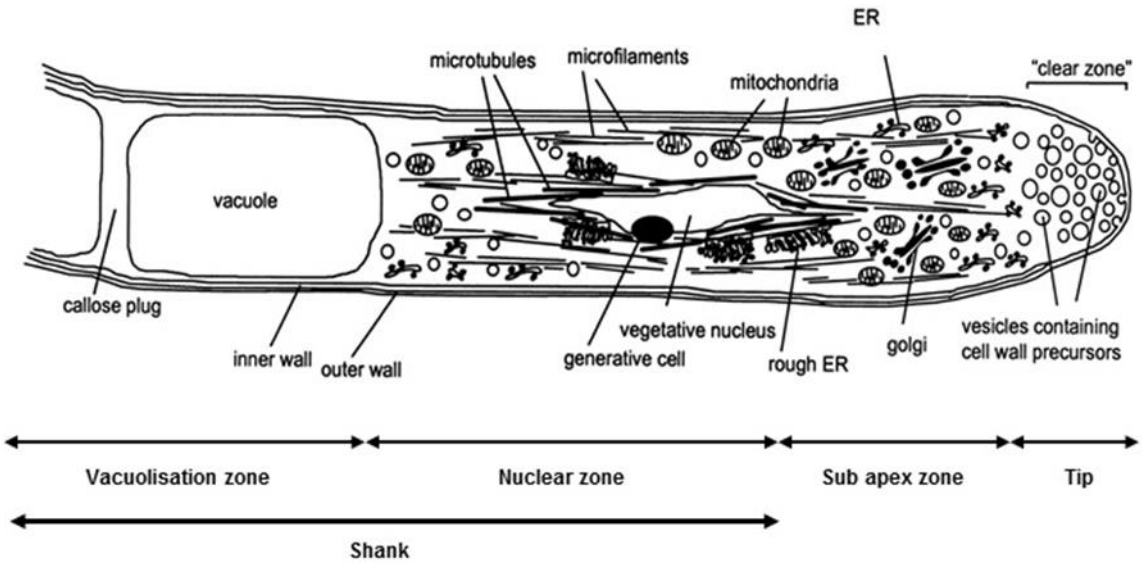

Figure 1.2. Structure of pollen tube

Diagram illustrating the relative positions of the 4 different zones of the pollen tube. (Figure adapted from Franklin-Tong, 1999).

The apical growth zone of actively growing pollen tube is a clear zone, which is free from large organelles but is full of small vesicles involved in the union of wall precursors of the tip (Franklin-Tong, 1999, Malhó, 2006). The sub-apical zone is just behind the tip region (**Figure 1.2**). The pollen tubes have 2 nuclei, the vegetative nucleus and generative cell. Callose plugs separate the cytoplasm from the rest of the pollen tube. The area behind the callose plug becomes vacuolated as the pollen tube grows.

The cell wall of the pollen tube is made up of two layers; the inner layer of callose and the outer wall made up with pectin, hemicelluloses and cellulose (reviewed by Franklin-Tong, 1999, Krichevsky *et al*., 2007). Callose is an important component of pollen mother cell and play role in different stages of its development (McCormick, 1993). Callose is a polysaccharide in the form of linear 1,3-β glucan polymer. It has some 1,6 branches and can be found in the cell walls of many higher plants (Aspinall and Kessler, 1957). Studies have shown that callose deposition is disrupted because of mutations of the *CalS5* gene in *Arabidopsis*. As a result, the pollen exine wall did not formed properly suggesting a vital function of callose synthase in building a proper exine wall, the integrity of which is essential for pollen viability (Dong *et al*., 2005). The tip region of the pollen is made up of a single layer of pectin, lacking callose and cellulose, which provides sufficient rigor to continue the cellular integrity, as well as plasticity to allow directional tube growth.

To fertilize the ovule, a pollen tube has to grow several cm and therefore, the growth rate of pollen tube is really vital. The growth of the highly polarized pollen tube generally occurs in the apical tip region of the pollen (Taylor and

Hepler, 1997). Endo and exo-cytosis play important role in regulating pollen tube growth. Secretory vesicles are carried by exocytosis to the pollen tip to deliver cell wall materials. These vesicles are fused to the membrane of the pollen tube at the tip region and thus facilitate the growth of pollen tubes (Steer and Steer, 1989). The excess amount of secretory vescicles are carried back and processed by endocytosis (Picton and Steer, 1983). Endo/exocytosis are supported by an intact actin cytoskeleton (Cárdenas *et al*., 2005), Ca^{2+} (Camacho and Malhó, 2003) and Rab-GTPase proteins (reviewed by Krichevsky *et al*., 2007). Pollen tubes are the fastest growing cell known and can grow as fast as 200-500 nm/s within the stigma (Cheung and Wu, 2008, Pierson *et al*., 1996).

Ca^{2+} has an important role in pollen tube growth which will be discussed in **Section 1.1.2.1**. An intact actin cytoskeletal network also plays a vital role to achieve the high rate of tube growth. Longitudinal actin filaments help to maintain the growth via cytoplasmic streaming and organelles movement. Various other factors are also involved in the growth of the pollen tube. For example, variation in Ca^{2+} concentrations, occurrence of gamma-amino butyric acid (GABA), transmitting-tissue specific (TTS) proteins, cysteine-rich attractant molecules LURES and secreted stylar tract proteins (Cheung and Wu, 2008, Malhó, 2006, Malho *et al*., 1994, Okuda *et al*., 2009).

1.1.2.1 The role of calcium in pollen tube growth

Calcium is crucial for pollen tube growth and plays an important role in its regulation. A strong tip-focused calcium gradient in growing pollen tube has

been found by calcium imaging studies while this gradient was not detected in non-growing pollen (Obermeyer and Weisenseel, 1991). This calcium gradient oscillates and this oscillatory activity is closely associated with pollen tube growth rate and they share the same periodicity (Holdaway-Clarke *et al*., 1997, Rathore *et al*., 1991). Calcium ion entry is restricted to the extreme apex of the pollen tube where growth takes places (Pierson *et al*., 1996), but later studies by Franklin-Tong *et al*. (2002) demonstrated that some calcium enters the tube via the shank, in poppy at least. Extracellular calcium goes into the pollen tube by means of ion channels at the tip region and, these channels are thought to be stretch-activated (Franklin-Tong, 1999, Hepler *et al*., 2001). When growth of pollen tubes stops, it is thought that the ion channels close, resulting in dissipation of the calcium gradient. When the calcium gradient is re-established, pollen tube growth starts again at the point of the highest calcium concentration (Hepler *et al*., 2001, Franklin-Tong and Franklin, 1993). Growth can be inhibited by increasing calcium levels within the tube. Upon returning to normal $[Ca^{2+}]_i$ levels, the tube restarts growth in a new direction. Using these methods it has been shown that calcium is involved in reorientation of the growing pollen tube, implicating calcium as a signal which allows pollen tubes to respond to directional signals in the style that guide it towards the ovary and a successful fertilisation (Malho *et al*., 1994).

1.1.2.2 Protons (H^+) in pollen tube growth

Protons (H^+) play an important role in the tip growth of pollen tubes. Extracellular H^+ interact with pectin, which is a major component of the cell wall, and can control pollen tube growth by regulating the mechanical

properties of pectin (Heslop Harrison, 1987). It has been demonstrated that an external pH ~ 4.5-6 is optimal for pollen growth, while a neutral pH ~ 7.0 can completely inhibit the growth (Holdaway-Clarke *et al*., 2003). In another studies in pear, an external acidic pH 6.5 was found to be ideal for germination and growth of the pollen tube (Zhang *et al*., 2004). Pollen tubes show sensitivity to pH change. Alteration of both external and internal pH might affect pollen tube growth (Feijó *et al*., 1999). Several groups have demonstrated that the pollen tube has no pH gradient (Fricker *et al.*, 1997). Other groups have evidence that there is a pH gradient in lily pollen tubes containing a slightly acidic pH around 6.8 at the tip. They also have shown that there is an alkaline band of pH ~7.5 at the base of the clear zone (Feijó *et al*., 1999). Using vibrating probes Malhó (2006) has shown that there is an influx of H^+ at the apex of pollen tube. During normal growth of pollen tubes, $[pH]_i$ also increases until it reaches to the maximum level and then the $[pH]_i$ decreases sharply. This oscillation of $[H^+]_i$ plays a role in pollen tube growth rates (Lovy-Wheeler *et al.*, 2006). A proton ATPase might play role to control this increase in $[pH]_i$ and consequently could be regulate pollen tube growth (Feijó *et al.*, 1999). Besides, artificial acidification in lily pollen showed destabilization of actin filaments, as a result pollen tube growth was halted (Lovy-Wheeler *et al*., 2006). This result demonstrated that pH has an important role in regulating in pollen tube growth.

1.1.2.3 Reactive oxygen species (ROS) and nitric oxide (NO)

In plant cells, various kinds of reactive oxygen species (ROS) can be produced during normal cellular metabolism and also in stress conditions. Molecular oxygen (O_2) is used as a terminal electron acceptor in plant cells and are reduced, thus ROS are produced as highly reactive intermediates (Halliwell, 2006). Superoxide ($O_2^{\bullet-}$), hydroperoxide ($HO^{\bullet}_2$), hydrogenperoxide (H_2O_2), singlet oxygen ($^1O_2$) are different forms of ROS generated in different organelles such as chloroplasts, mitochondria, peroxisomes, glyoxisomes. Plasma membrane-bound NADPH oxidases are also involved in the production of H_2O_2 in the apoplast (see **Figure 1.3**) (reviewed by Gechev *et al*., 2006, Jajic *et al*., 2015)

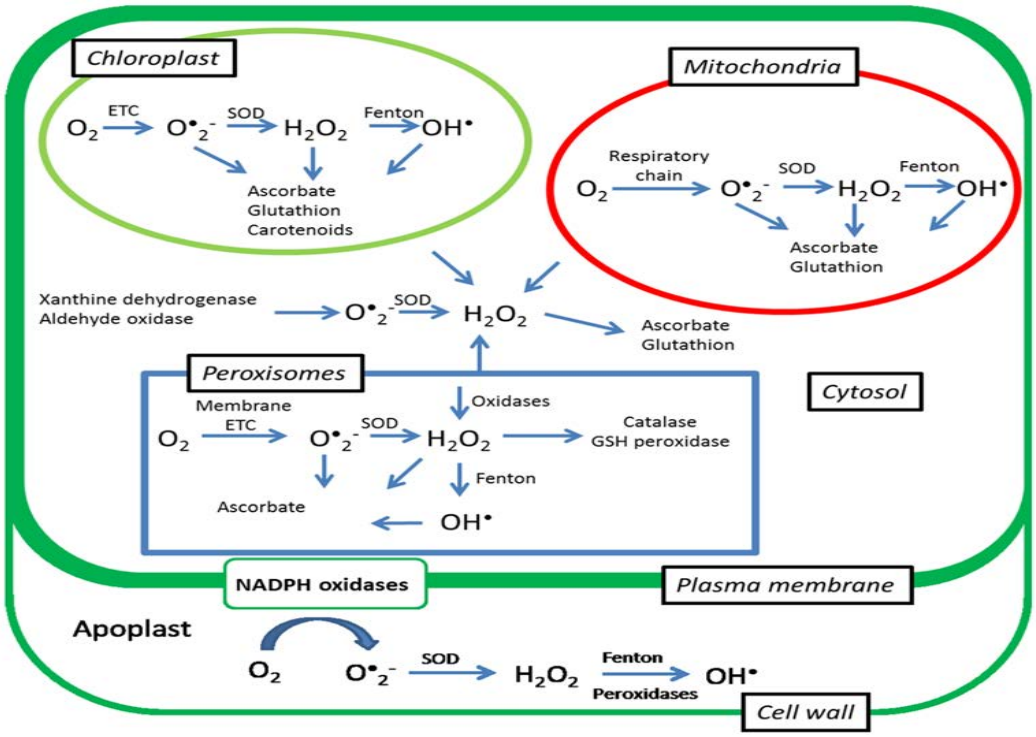

Figure 1.3. Schematic representation of production of different ROS in different organelles of plant cell. Figure adapted from Jajic *et al*. (2015).

Nitric oxide (NO) is also widely recognized as a key signalling molecule and regulator of plant. In plant NO can be produced by reductive or oxidative pathways. Reductive pathways involve nitrate reductase (NR), plasma membrane or mitochondria to produce NO. On the other hand, L-arginine, polyamine or hydroxylamine-mediated NO production follow the oxidative pathways (reviewed by Gupta *et al*., 2011).

Both ROS and NO are involved in different physiological functions of plant. Here we will discuss their role in pollen tube growth.

1.1.2.3.1 ROS and NO in pollen tube growth

ROS has been demonstrated to be an important regulator in pollen tubes growth (Potocký *et al*., 2007). Studies have shown that pollen tube growth was inhibited while ROS scavengers were used. Growth of the pollen tube was recovered by adding H_2O_2 which shows the importance of ROS for normal tube growth (Potocký *et al*., 2007). ROS was demonstrated as a fundamental signalling factor during the pollen tube growth, strongly associated with Ca^{2+} signalling. ROS is involved in the activation of Ca^{2+} channels which is essential for [Ca^{2+}] gradient and pollen tip growth (reviewed by Fu, 2010). Furthermore, Wang *et al*. (2010), suggested that during S-RNase-SI in *Pyrus*, ROS production was disrupted which causes actin depolymerization and DNA fragmentation. Another study shows that production of ROS by NADPH oxidases is crucial for proper pollen tube growth as mutation of NADPH oxidases inhibited pollen tube growth (Kaya et al., 2014b).

Involvement of NO in the pollen tube growth regulation has been demonstrated. In *Arabidopsis* and *Lilium,* NO has been shown to be involved in pollen tube growth regulation and reorientation (Prado *et al*., 2008, Prado *et al*., 2004). Extracellular nucleotides, mediated by NO participated in inhibition of pollen germination and elongation (Reichler *et al*., 2009). Another study demonstrated the negative role of NO in pollen tube growth. Pollen exposed to UV-B radiation increased NO levels in the pollen grain and tube, resulted in pollen tube growth inhibition (He *et al*., 2007). ROS and NO will be discussed further later in **section 1.4.2.4** and **1.6.2.1.6.**

1.2 The cytoskeleton

The cytoskeleton is an intracellular matrix of proteinaceous filaments found in the eukaryotic cell cytoplasm. The plant cytoskeleton comprises two interconnected arrays consisting of actin microfilaments (MFs or F-actin) and tubulin microtubules (MTs). The actin cytoskeleton continually experiences dynamic assembly and disassembly. Based on these rearrangements cells can modify signalling networks and form distinctive assemblies to perform various physiological cellular processes, including cell motility, cell division, cytokinesis, cell polarization, and cell growth, along with responses to various stimuli (Staiger, 2000, Pollard and Cooper, 2009). As the cytoskeleton is an important topic in this thesis, we will describe it in a little more detail here.

1.2.1 The actin cytoskeleton

Actin exists as actin monomers (globular (G)-actin), which form linear chains to make filamentous polymers (F-actin). Each G-actin binds to two other actin monomers in a head-to-tail manner to form actin filament which is a double-

stranded helix. The actin filaments have two ends; called the barbed end (+) and the pointed end (-), which are distinguishable from one another and have distinct polarity. The first step in actin polymerization is called nucleation, which involves three actin monomers to develop a small aggregate. After that, actin monomers start to accumulate at the end to grow actin filaments. The actin monomers bind ATP; only ATP-bound monomers assemble into MFs, which is hydrolyzed to ADP after filament assembly. Reversible polymerization of actin filaments can be depolymerized by the separation of actin subunits (reviewed by Korn *et al*., 1987, Dos Remedios *et al*., 2003).

1.2.1.1 The actin cytoskeleton in pollen tubes

The actin cytoskeleton is at the centre of many important processes in pollen tubes. In the pollen tube actin can be found at a high concentration, which supports driving the fast growth of pollen tube through cytoplasmic streaming and transport of secretory vesicles to the tip. F-actin is present in the form of long filamentous cable-like structures in the shank of the pollen tube, that are responsible for the organelle and vesicle movement and reverse cytoplasmic streaming (Cai and Cresti, 2009). Studies have shown that F-actin can regulate the calcium channels (Wang *et al*., 2004). Pollen tube growth inhibition and a rise of calcium conductance were observed when F-actin dynamics was disrupted using latrunculin A or cytochalasin. This indicates the requirement of intact actin cytoskeleton for the regulation of Ca^{2+} channels permeability (Wang *et al*., 2004).

Ca^{2+} is involved regulating actin cytoskeleton in pollen. F- actin fragmentation and inhibition of cytoplasmic streaming were observed when pollen tubes were microinjected with high concentrations of Ca^{2+}. As mentioned earlier, Ca^{2+} concentration is extremely high at the tip region of pollen. Interestingly, this region is free from F-actin. It is assumed that, polymerization of G-actin is inhibited because of that high $[Ca^{2+}]_i$ (Lovy-Wheeler *et al*., 2006). The integral dynamics of the actin cytoskeleton is crucial for pollen tube growth. The transportation of secretory vesicles to the pollen tube apex where they fuse to the cell membrane to assist pollen tube growth is dependent on actin cytoskeletal integrity (Cai *et al*., 2015).

1.2.1.2 Actin binding proteins (ABPs)

As mentioned in **section 1.2.1** the first step of actin filament formation is nucleation. Several ABPs are crucial to ensure the rapid nucleation and are involved in the regulation of the dynamics of the actin cytoskeleton (Pollard and Borisy, 2003). A large number of ABPs have been identified so far, Dos Remedios *et al*. (2003) reported 162 distinct and separate ABPs which can be classified in to seven groups.

Several actin-binding proteins, such as actin depolymerizing factor-cofilin, formin, profilin, and villin, and signalling proteins, like Rho-of-Plants (ROP) GTPases also have been implicated to play critical roles in pollen tube growth and actin dynamics (Fu *et al.*, 2001, Vidali *et al*., 2001, Allwood *et al*., 2002, Chen *et al*., 2002, Cheung and Wu, 2004, McKenna *et al.*, 2004, Gu *et al.*, 2005, Ye *et al.*, 2009, Cheung *et al.*, 2010, Staiger *et al.*, 2010, Zhang *et al*.,

2010, Qu *et al*., 2013, van Gisbergen and Bezanilla, 2013). More recently Su *et al*. (2012) showed that microinjection of an actin binding protein, fimbrin (Ll-FIM1) antibody into lily pollen tubes inhibited tip growth and interrupted the actin fringe, showing that fimbrin may stabilize the actin fringe by cross-linking actin filaments into bundles, which is important for proper tip growth of lily pollen tubes.

Also involved in the pollen tube growth, an important component of all eukaryotic living cells are soluble inorganic pyrophosphatase (sPPases). A major part of this thesis is about two *Papaver* sPPases (Pr-p26.1a/b) which will be discussed later in **section 1.6.2.1.7** and in **Chapter 3**. Here we will describe some important general aspects of sPPases.

1.3 Soluble inorganic pyrophosphatases (sPPases)

Soluble inorganic pyrophosphatase (sPPases) are very important for almost every cell and catalyse the hydrolysis of inorganic pyrophosphate (PPi) to two molecules of inorganic phosphate (Pi) (Kornberg, 1962).

Phosphoryl transfer enzymes are phosphate metabolising enzymes which form one of the largest classes of enzymes in the nature (Knowles, 1980), yet their mechanisms of action and structure are not fully understood (Heikinheimo *et al*., 1996b). These enzymes catalyse the removal of a phosphate group from phosphoric monoesters or anhydrides acting on the P-O bonds and transfer phosphate to water. sPPase is one of the phosphoryl transfer enzymes, which activity is essential for normal cell growth and function. They control the level of PPi in the cell which is generated as a by-

product during cellular processes such as polynucleotide synthesis (Kornberg, 1962). The very high levels of PPi that result from the absence of pyrophosphatases would undoubtedly be toxic to the cell. It has been demonstrated that without PPases activity, the PPi concentration in *Escherichia coli* cells (*E. coli*) would rise within one hour, from 1mM, the usual concentration of PPi to a very toxic concentration to the cell (3M) (Klemme, 1976).

Two families of soluble PPases are known: Family I and Family II. Family I, includes most of the currently known PPases, and Family II, comprises PPase of *Bacillus subtilis* as well as putative PPases of four other bacterial strains. These two families are non-homologous families and do not show any sequence or structural similarity. However, they show conservation of key amino acid residues at the active site (Gómez-García *et al.*, 2007). Their preference for divalent metal ion cofactors are also different (Sivula *et al.,* 1999). As Family II sPPases are not relevant to this PhD project, only Family I sPPases will be described in detail.

1.3.1 Family I PPases

Family I sPPases are the most studied class of sPPases (Sivula *et al*., 1999). Family I PPases are classified into three subfamilies: prokaryotic, plant and animal/fungal PPases. Plant PPases show a closer resemblance to prokaryotic than to animal and fungal PPases (Sivula *et al*., 1999). PPases are metal ion-dependent enzymes. They need three or four metal ions for their catalytic activity, amongst them Mg^{2+} is the most dominant. Zn^{2+}, Co^{2+}, Mn^{2+},

and Cd^{2+} also have favourable effect on Family I PPase activity (Cooperman *et al*., 1992).

The crystallographic structure of Family I sPPases including *Escherichia coli* (Kankare *et al*., 1996) and *Saccharomyces cerevisiae* (Heikinheimo *et al*., 1996a), and recently *Arabidopsis thaliana* (Grzechowiak *et al*., 2013) have been solved. In prokaryotes, their hexameric structure comprise of a dimer of trimers and in the eukaryotes the structure is dimeric (Gómez-García *et al.*, 2006). The subunit size of prokaryotic and eukaryotes PPases varies between 19-22 kDa and 30-44 kDa respectively (Cooperman *et al*., 1992, Gómez-García *et al*., 2006, Baykov *et al.*, 1999). 17 amino acids have been found conserved in all known sPPases; 13 are polar active site residues which are functionally important for catalysis.

The two best studied sPPases are the prokaryotic sPPases of *E. coli* (E-PPase) and the eukaryotic sPPase found in *S. cerevisiae* (Y-PPase). (Cooperman, 1982, Cooperman *et al*., 1992, Baykov *et al*., 1990, Gómez-García *et al*., 2007). For their catalytic activity, both E-PPase and Y-PPase require 3-4 divalent metal ions attached to their active site. In the presence of Mg^{2+}, PPi-hydrolysis activity is found to be maximum (Cooperman, 1982). During the hydrolysis process, at least 3 divalent metal ions are attached to the active site (Bond *et al*., 1980). The active site of both sPPases has an ability for binding 4 metal ions and it is thought that Ca^{2+}occupies the fourth binding site, inhibiting sPPase activity (Cooperman *et al*., 1992).

Site directed mutagenesis of E-PPase and Y-PPase has been studied. As mentioned earlier, the 17 conserved polar residues are found in Y-PPase,

which are at or near to pyrophosphate or metal ion binding site residues. As presented in **Figure 1.4**, the structural alignment of Y-PPase and E-PPase exhibits 13 polar active site residues which are significant for catalysis (Kankare *et al*., 1996, Sivula *et al.*, 1999).

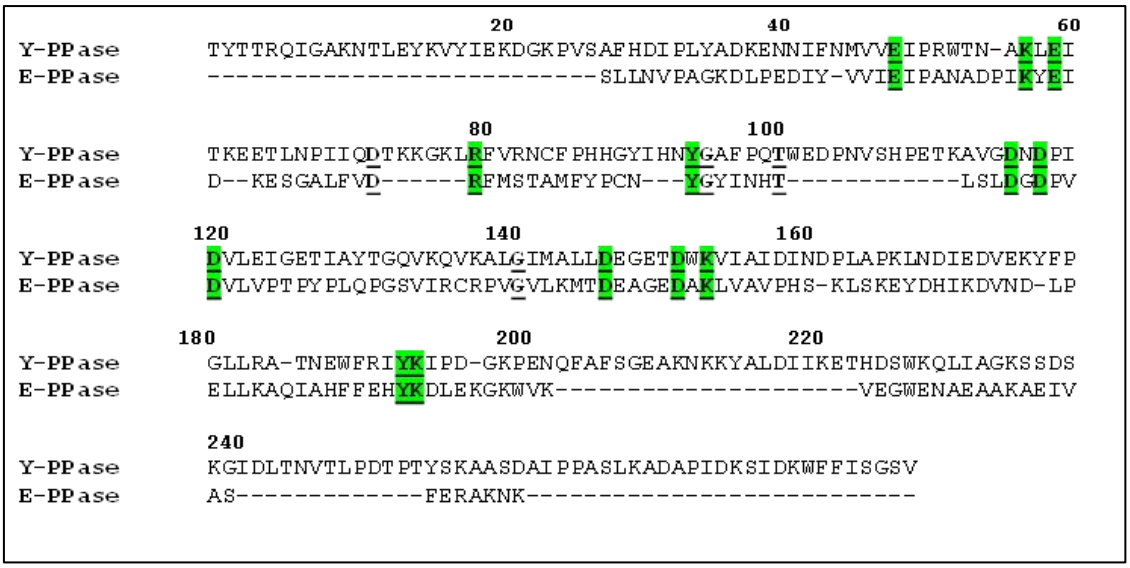

Figure 1.4 Figure showing the alignment between Y-PPases and E-PPase. Bold underlined letters show the conserved amino acids and the bold, green highlighted, underlined letters show the 13 amino acid functionally important for catalysis. Adapted from Sivula *et al*. (1999) with slight modifications.

For the catalysis in the active site of sPPase, an acidic and a basic group are required, where the basic group are absolutely indispensable to the reaction (Heikinheimo *et al*., 1996a). Because of the mutation of the polar active site residues sPPase activity was found to be inhibited. The apparent K_m of the enzyme is affected by the mutation and the pK_a of the basic group was increased by changing the 1-3 pH units. This suggested that hydroxide ion acts as the basic group but not an amino acid side chain (Heikinheimo *et al*., 2001).

1.3.2 Plant soluble inorganic pyrophosphatases

In plants, pyrophosphatase is not only involved in PPi hydrolysis but also functions as a regulator in primary metabolism, sulphur metabolism and growth (Farré *et al*., 2000, Farré *et al*., 2006). However, very little is known about these roles of sPPases (Farré *et al*., 2006, Pérez-Castiñeira *et al.*, 2001, Mi-Ichi *et al.*, 2009). Subcellular fractionation studies established that most, if not all, of the soluble PPase activity correspond to plastidic isoforms (Gross and Ap Rees, 1986, Weiner *et al*., 1987). The plant cytosol comprises a high concentration of PPi and low sPPase activity (Weiner *et al*., 1987). Nevertheless, the presence of soluble PPases in the cytosol cannot be ruled out. Certainly, a cytosolic soluble-PPase has been purified from the latex of *Hevea brasiliensis* which perhaps contributes in rubber synthesis (Jacob *et al*., 1989). Studies on overexpression of *Escherichia coli* sPPase showed that this eliminated cytoplasmic PPi pool impaired plant growth and development, showing the importance of the cytoplasmic PPi concentration (Jelitto *et al*., 1992, Sonnewald, 1992). Two cytosolic soluble inorganic pyrophosphatases were identified from *Papaver* pollen (Rudd *et al*., 1996, de Graaf *et al*., 2006). It was proposed they may be important for metabolic activity to produce new membrane and cell wall for pollen tube extension.

In contrast to the bacterial and fungal enzymes, sPPases from plants function as 25 kDa monomers (Navarro-De la Sancha *et al.*, 2007) rather than multimers. Recently the crystal structure for *Arabidopsis thaliana* inorganic sPPases (AtPPA1) has been solved; it is an alpha and beta protein fold

overlapping other structure of known bacterial and yeast sPPases (Grzechowiak *et al*., 2013).

Next, we are going to introduce programmed cell death (PCD) which is an important mechanism involved in SI and also related to ROS and NO which are two major parts of this thesis.

1.4 Programmed cell death (PCD)

PCD or apoptosis is a highly conserved process used by eukaryotes to remove unwanted cells. It involves the highly regulated death of redundant, misplaced or damaged cells (Mittler and Lam, 1996, Woltering *et al*., 2002) and is crucial for development and the correct maintenance of multicellular organisms. PCD is a genetically encoded cell suicide pathway that involves proteins for killing and dismantling the cell in an organism (Raff, 1998, Hoeberichts and Woltering, 2003). Cell death can be defined as an irreversible pathway in which the cell goes in a position from where it can not return to its previous state resulting in the death of the cell. This is an obligatory pathway for development and maintenance process. However, this pathway is not same in all cell and varies depending on the stimuli (Kroemer *et al*., 2009). An intracellular signalling programme is responsible to start this process in both mammalian and plant systems and is indispensable in many eukaryotic systems (Van Doorn *et al*., 2011). In mammals there are three main types of cell death distinguished: necrosis, autophagic cell death and apoptosis (Kroemer *et al*., 2009).

1.4.1 Apoptosis in mammalian cells

Apoptosis is a specialised form of PCD that occurs in animal cells. Key features of apoptosis includes chromatin condensation, cell shrinkage, nuclear segmentation, DNA fragmentation, caspase activation, membrane blebbing and production of 'apoptotic bodies' which consists of cytoplasm, organelles and sometimes nuclear fragments (Elmore, 2007). Some other cell death features are related with apoptosis. These features include fragmentation of DNA and the activation of caspases although they are not specific to apoptotic cell death.

Caspases are cysteine proteases which specifically cleave after an aspartic acid residue and act to accelerate the progression of cell death (Kumar, 2007). Caspases are involved in many cell death processes. Caspases can cleave proteins to dismantle the cell. Cell death occurs because of the degradation of DNA, by cleaving DNAse inhibiting proteins. Caspase activity is essential in apoptosis (Wolf *et al*., 2001). Caspases generally function in acidic conditions. During apoptosis the $[pH]_i$ of the cell cytosol decrease approximately 0.3–1.4 $[pH]_i$ units to achieve an acidic condition (for review see Matsuyama and Reed, 2000).

1.4.2 Plant PCD

Programmed cell death (PCD) is well recognized in plants. This cell death pathway has an important role during plant development, embryogenesis and senescence (reviewed by Lam, 2004). Plant PCD can be triggered by many external factors such as abiotic and biotic stresses (Zhang and Klessig, 2001), for example, high temperature (Qu *et al.*, 2009) and plant-pathogen

interactions (reviewed by Greenberg and Yao, 2004). Studies have been carried out that uncover PCD in both plant and mammalian systems, which reveals clear differences between plant and mammalian PCD. Recently a classification emerged that set the ground for morphological classification of plant PCD (Van Doorn *et al*., 2011). Two classes of PCD were distinguished: vacuolar cell death and necrosis.

1.4.2.1 Vacuolar cell death (VCD)

Vacuolar cell death is the most common type of plant PCD. It has been documented in a range of systems, caused by the cells as a part of normal developmental process or to prevent infection or diseases (reviewed by Hara-Nishimura and Hatsugai, 2011). VCD in plants is found during aerenchyma formation, xylem differentiation in vascular plants, leaf remodelling in *Monstera* or during the formation of embryo-suspensor (Gunawardena *et al*., 2004, Ohashi-Ito *et al*., 2010, Filonova *et al*., 2000). It is morphologically visible due to the increase of the volume of the vacuole, which contains hydrolytic enzymes that swallow up cell cytoplasm and degrade its contents. Other morphological features include actin cable formation, disassembly of nuclear envelop, and nuclear segmentation (Obara *et al*., 2001). At the end, the tonoplast (membrane of vacuole) ruptures to release of hydrolytic enzymes which destroys the protoplast (Van Doorn *et al*., 2011).

1.4.2.2 Necrotic PCD

During plant necrotic cell death, inflammation of the cell occurs which eventually bursts the cell to spill off their contents over neighbouring cells and damage the cells by an inflammatory response (Danon *et al*., 2000). The necrotic PCD usually occurs in pathogen recognition during the hypersensitive response (HR) or in cells challenged by necrotrophic pathogens (Van Doorn *et al*., 2011). Some of the key features for necrotic PCD include mitochondrial swelling and shrinkage of protoplasts caused by the early rupture of plasma membrane with spilled and unprocessed bodies of necrotic cells. Biochemically, necrosis can be detected by changes in mitochondria membrane potential, decreased respiration, accumulation of reactive oxygen species (ROS) and reactive nitrogen species (NS) as well as a drop in ATP level (Van Doorn *et al*., 2011, Christofferson and Yuan, 2010)

1.4.2.2.1 Plant caspase-like activities

As mentioned earlier, caspases play an important role in mammalian apoptosis. Although plant cells experiencing PCD display caspase-like activities, they do not have orthologues of mammalian caspases in their genomes (Bonneau *et al*., 2008). Many different caspase-like activities have been identified in plants to date, though caspases in plants posses different mechanisms than animal caspases (Bosch and Franklin-Tong, 2007). The most common form of caspase-like activities in plant is documented as caspase-1-like/YVADase and caspase-3-like/DEVDase activities (Bonneau *et al*., 2008). Studies have shown the involvement of casepase-3-like/DEVDase

activities in SI-PCD signalling in poppy SI (Thomas and Franklin-Tong, 2004, Bosch and Franklin-Tong, 2007).

1.4.2.3 The hypersensitive response (HR) and induction of PCD

The hypersensitive response (HR) is a mechanism of cell death and shows features of necrotic cell death like shrinkage and vacuolization of the cytoplasm, chromatin condensation, and membrane dysfunction and endonucleolytic cleavage of DNA. HR is also featured by rupture of vacuolar membrane to release the lytic vacuolar content. It is a genetically controlled mechanism which is involved in plant resistance by controlling the interaction of pathogen with the plant at the site of infection leading to rapid development of cell death at the site of infection. In this way plants protect themselves and prevent spread of pathogens into healthy tissues (Dangl and Jones, 2001, Greenberg and Yao, 2004, Coll *et al*., 2011). An interaction is termed as compatible when it leads to disease, and an incompatible interaction results in resistance (Dangl, 1995, Staskawicz *et al*., 1995). During the attack of a microbial pathogen in the plant tissue, a defence mechanism is triggered inside the plant tissue. Pathogens are inhibited by a combination of a layer of dead cells, locally produced antimicrobial compounds, and the induction of systemic acquired resistance (SAR) in the host (Dickman *et al*., 2001, Lincoln *et al*., 2002)

Plant immune systems are able to distinguish ‘self’ and ‘non-self’. In the recognition of ‘non-self’ two types of immune response have been documented: one against general microorganisms and the other is against

specific pathogens. The general defence mechanism recognizes pathogen- or microbe- associated molecular pattern (PAMP/MAMP) triggered immune signalling (Schwessinger and Zipfel, 2008, He *et al*., 2007). This is the first line of defence which is triggered by pattern-recognition receptors (PRRs) which are trans-membrane receptors (Postel and Kemmerling, 2009, Zipfel, 2009). Several approaches have been developed by plant pathogens to overcome PAMP triggered immunity (PTI), for example, effector-triggered susceptibility (ETS), which organizes PTI-suppressing pathogen effectors. The second and more precise defense mechanism against pathogen ETS is recognized as effector-triggered immunity (ETI), stimulated by plant resistance proteins (R proteins) identifying pathogens effector proteins, avirulence (Avr) proteins (Jones and Dangl, 2006, Boller and Felix, 2009).

During ETI in plant, several molecular events play roles that lead to HR. Some of these events are: the accumulation of salicylic acid (SA), generation of reactive oxygen species (ROS), for example, hydrogen peroxide (H_2O_2), hydroxyl radicals (•OH), superoxide anions (O_2•-) and nitric oxide (NO), activation of MAPK, alterations in calcium levels in the cell and development of localized PCD of infected cells, the final defense mechanism in plants (Nimchuk *et al*., 2003, Mur *et al.*, 2008). SA induces the induction of various pathogenesis-related (PR) genes and the activation of systemic acquired resistance (SAR) (Nimchuk *et al*., 2003). It is well known that plasma membrane NADPH oxidases are the main source of apoplastic ROS (superoxide). This ROS plays a very crucial role to develop HR and afterward activate the systemic immunity (Torres and Dangl, 2005). ROS generated in

other plant organelles like chloroplast, mitochondria and peroxisomes also play role to the HR (Torres, 2010).

The interplay between ROS and NO is of special interest in plant disease resistance initiation and execution. NO together with ROS have been recognized as indispensable molecules that mediate cell death in HR and defence gene activation (Lin *et al*., 2012, Zaninotto *et al*., 2006). It is thought that *S*-nitrosoglutathione, which might act both as NO reservoir and NO donor, performs as a long-distance signal in SAR (Lindermayr *et al*., 2005, Rustérucci *et al*., 2007); NO is indispensable to SA functioning as SAR inducer (Malik *et al*., 2011, Romero-Puertas and Delledonne, 2003). S-nitrosylation, addition of NO moiety to Cys thiol to form S-nitrosothiol (SNO), has arisen as a key redox-based posttranslational modification in plants and a major method for the transduction of the bioactivity of NO fundamental to plant immune function (Feechan *et al*., 2005, Lin *et al*., 2012, Malik *et al*., 2011). We will consider ROS and NO in more detail as they are a major topic of this thesis.

1.4.2.4 The role of ROS and NO in plant PCD

Fluctuations in levels of ROS observed during development or during environmental changes, are perceived as signals which act in association with other signalling molecules, like plant hormones and lipids messengers to modulate many plant processes, including PCD (Gechev *et al*., 2010). The first signs for involvement of ROS in PCD were documented by Levine *et al*. (1994). They demonstrated that increased level of ROS induced cell death by oxidative damage. It is well known that ROS act as an activator of oxidation

and are considered as harmful molecules. Studies have demonstrated their involvement in plant PCD signals. In cell suspensions, H_2O_2-induced cell death could be blocked by inhibitors of protein synthesis (Levine *et al*., 1994). Since then, a number of studies have been carried out to establish a role for ROS as a mediator of PCD. During various developmental or environmental process, ROS-mediated PCD happens; for example, leaf senescence, germination of seed, several abiotic stress, allelopathic plant–plant interactions, hypersensitive responses etc. (Bethke and Jones, 2001, Bais *et al*., 2003, Apel and Hirt, 2004). As mentioned earlier in **Section 1.4.2.3**, during HR burst of NADPH-dependent ROS production takes place for the initiation of PCD (Alvarez *et al*., 1998). ROS-mediated PCD has also been found in allelophathic plant-plant interaction. ROS accumulation in the root meristem of *Centaurea maculosa* can trigger a Ca^{2+}-dependent cell death to adjacent species to kill them (Bais *et al*., 2003). ROS-mediated cell death is featured by some distinct cellular lesions and a number of hallmarks of PCD, like DNA laddering, chromatin condensation and cytochrome c release (Lam, 2004).

ROS can strongly interact with many other signalling molecules, for examples NO, redox metabolites, lipid messengers or plant hormones. During PCD, this interplay can govern cell fate by altering the biological response to altered ROS levels (Foyer and Noctor, 2009). In recent years, the crosstalk between H_2O_2 and NO during plant cell death has been documented (Zago *et al*., 2006). To induce PCD, there should be a balance between ROS and NO (Gupta *et al*., 2011). The gathering indication suggests that both ROS and NO act as key regulators in PCD. ROS and NO can activate cell death either

independently or synergistically (reviewed by Wang *et al*., 2013). NO-dependent signalling pathways are involved in post-translational modifications (PTMs) of proteins (Leitner *et al*., 2009) and this PTMs which is mainly S-nitrosylation, is involved in PCD (Belenghi *et al*., 2007, Leitner *et al*., 2009).

Some reports also describe the cross-talk of ROS and NO in other kinds of cell death in plants. In pollen-pistil interactions, self-incompatibility (SI) induces comparatively rapid and transient upsurges in ROS and NO. Using ROS/NO scavengers, studies showed an alleviation of SI-induced actin punctate foci and activation of a DEVDase/caspase-3-like activity, which is a key hallmark for SI-mediated PCD (Wilkins *et al*., 2011). Other studies have shown in tobacco BY-2 cells, sphinganine or dihydrosphingosine (d18:0, DHS) encourage a calcium-dependent PCD, triggering the production of H_2O_2 via the activation of NADPH oxidase(s). They also promote NO production, vital for cell death induction (Da Silva *et al*., 2011). In *Arabidopsis*, NO promoted Cd-induced PCD by promoting MPK6-mediated caspase-3-like activation (Ye *et al*., 2013). Thus the different roles of reactive nitrogen species in PCD and their crosstalk with ROS depend on the plant species, growth conditions and redox status.

We will next consider how protein targets can be modified by ROS and NO

1.5 Oxidation and Nitrosylation of Proteins

Reactive oxygen species (ROS) and reactive nitrogen species (RNS) can be formed in various places within the living cells, and the rate of their production increased during biotic and abiotic stress. There are wide varieties of ROS

which can affect cell function. Many of these reactive species can interact with biomolecules and can result in oxidative post-translational modification of proteins (Wall *et al*., 2012). These modifications are mainly oxidation and S-nitrosylation of proteins which are described below

1.5.1 Oxidation of proteins

Elevated levels of ROS can modify proteins by oxidation. During aerobic metabolism, various ROS, such as, hydrogen peroxide (H_2O_2), superoxide ($O_2^{\bullet-}$), singlet oxygen ($^1O_2$) and hydroxyl radicals ($HO^{\bullet}$), can be produced and modify macromolecules (Halliwell and Gutteridge, 1999). ROS can attack the amino acid side chain of the protein directly by oxidation or can produce carbonyl-groups in the protein molecule by secondary reactions with aldehydic products of lipid peroxidation or glycosylation (Reinheckel *et al*., 1998). Most types of protein oxidation are essentially irreversible, while a few, which involves sulphur-containing amino acids, are reversible (Ghezzi and Bonetto, 2003). Cysteine and methionine residues are the most common amino acids, which can easily be oxidized by almost all forms of ROS. Because of their sensitivity to ROS, under even minor conditions cysteine can be changed to disulphides and methionine residues can be converted to methionine sulfoxide (MeSOX) residues. The oxidation of cysteine to disulfide (R_1-S-S-R_2, cystine; **Figure 1.5**) produced by a number of ROS, is a very significant metabolic redox regulation mechanism. Cysteine can be further oxidized to sulfenic acid and then sulfinic acid which are reversible modifications and thought to be involved in signalling pathways (Biteau *et al*., 2003). Oxidation of sulfinic acid

to Cysteic acid is the last stage of oxidation and at this point the modification is irreversible and damaging to the protein(Ghezzi and Bonetto, 2003)

As mentioned earlier, methionine is also very sensitive to oxidation. Methionine can be reversibly oxidized to methionine sulfoxide (**Figure 1.5**). When reversible modification occurs, the protein could be back to its previous state and play an important regulatory role (Sundby *et al*., 2005). Further oxidation of Met sulfoxide to the Met sulfone (**Figure 1.5**) is an irreversible modification which would permanently inhibit proteins function and eventually the proteins will be damaged (**Figure 1.5**). Another type of oxidation of protein is carbonylation which generally oxidized arginine, proline, lysine, histidintryptophane and threonine. Protein carbonylation is the most common type of oxidation which is generally irreversible (Shacter, 2000).

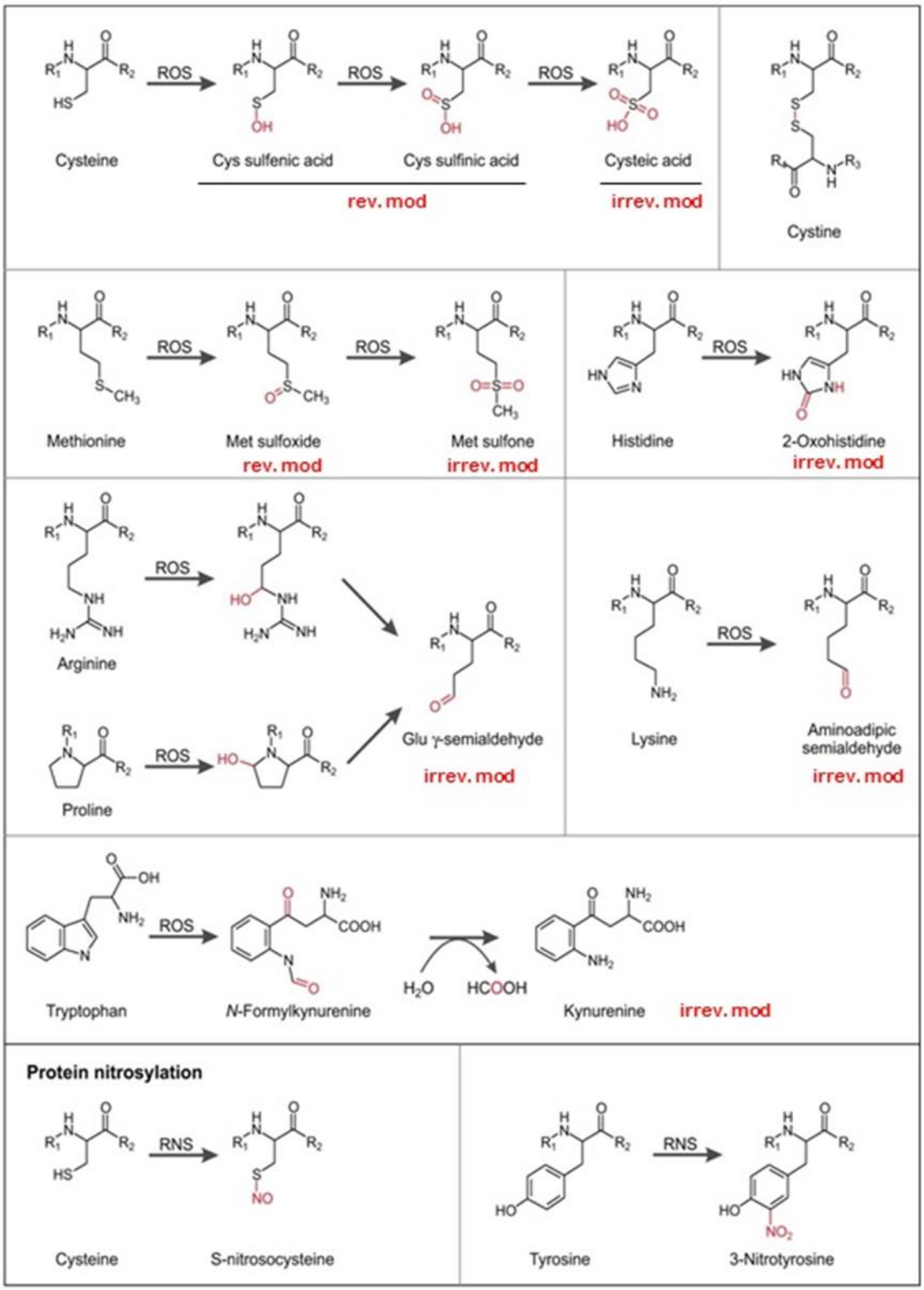

Figure 1.5. Commonly observed oxidative modifications of amino acids. Adapted and slightly modified from (Møller *et al*., 2007). Reversible modifications and irreversible modifications are indicated as rev. mod. and irrev. mod (in red) respectively

1.5.2 *S*-nitrosylation

S-Nitrosylation is a reversible posttranslational modification (PTM). This PTM is involved in the modification of the thiol group of cysteine to create S-nitrosothiol (SNO) by NO. Phosphorylation and S-nitrosylation are similar kinds of protein modifications. Within the cell, nitrosothiol can easily react with several reducing agents, such as glutathione (GSH), ascorbic acid or reduced metal ions (Cu^{+}). This reactivity makes them remarkably labile. Under almost all physiological conditions, presence of SNO-proteins is very low. The SNO-bond is easily breakable by homolytic and heterolytic decomposition.

Over the last decade, S-nitrosylation has been established to control an increasing number of signalling systems, structural proteins and metabolic processes in animals (Hess *et al*., 2005). In animal sytems, there are many examples of protein *S*-nitrosylation and functional consequences of alteration have been described. Many proteins involved in a variety of cellular processes undergo S-nitrosylation and thus their functions are regulated (Hess and Stamler, 2012). By regulating procaspase-3, *S*-nitrosylation can control basic cellular processes like apoptosis (Mannick and Schonhoff, 2004) by activating or disactivating many proteins functions (Stamler *et al*., 2001).

Comparing to the animal system, studies on protein modification by S-nitrosylation in the plant are in their infancy. Pioneer studies by Lindermayr *et al.* (2005) identified 63 *S*-nitrosylated proteins from cell cultures and 52 proteins from leaves of *Arabidopsis*. The identified proteins were mainly metabolic enzymes, stress related proteins, signalling/regulating proteins, redox-related proteins and cytoskeleton proteins, indicating the involvement of

NO in the regulation of all of these processes (Lindermayr *et al*., 2005). After that study, many groups have shown their interests in this area and, as a result, in recent years, important contributions towards the S-nitrosylated proteins in plants have been added. Numbers of S-nitrosylated proteins under hypersensitive response in *Arabidopsis* (Romero-Puertas *et al*., 2008), abiotic stress conditions in pea (Ortega-Galisteo *et al*., 2012) and salinity stress in citrus plant (Tanou *et al*., 2014) have been identified. However, what the S-nitrosylated proteins are involved in and when they are modified under biological relevant conditions is not known. Neither is how the modifications affect their functions. Part of this thesis investigated the effect of oxidation and *S*-nitrosylation of proteins by ROS and NO during SI in poppy.

In **section 1.1.1** we introduced self-incompatibility as an important genetical mechanism used by many plants to prevent inbreeding. Here we will describe three main SI systems including *Papaver* SI.

1.6 Molecular mechanisms involved in the three main SI systems

To date, three main SI systems are well characterised at the molecular level. These are: The Brassicacea*e,* the Papaveraceae and the S-RNase-type SI which includes the Solanaceae, Plantaginaceae and Rosaceae (Takayama and Isogai, 2005). Molecular mechanisms involved in these are covered in sections **1.6.1**, **1.6.2** and **1.6.3.**

1.6.1 Mechanisms involved in SI in Brassicaceae

Asteraceae, Brassicaceae and Convolvulaceae families utilise SSI system, but SSI in Brassicaceae has been studied and characterised extensively at the molecular level comparing to the other two families. The SI response of Brassicaceae family occurs very quickly on the surface of the stigma. The S-locus of Brassica is large and complex, spanning ~80-100 kb (Hiscock and McInnis, 2003). The female S-determinant is a serine/threonine receptor kinase (SRK) expressed in the stigma. The male S-determinant is a small (6 kDa), S-cysteine-rich pollen coat protein (SCR) which is also identified as S-protein 11(SP11) (Stein *et al*., 1991, Suzuki *et al*., 1999, Schopfer *et al*., 1999, Takayama *et al*., 2000, Takayama *et al*., 2001). The proposed mechanism of SI is presented in **Figure 1.6**. Incompatible pollen tube growth is rapidly inhibited at the surface of the stigma.

SRK is composed of an extracellular domain, a single pass transmembrane domain and a cytoplasmic Serine/Threonine domain, and is plasma membrane localized on the stigma epidermis, offering its highly polymorphic extracellular *S* domain to the ligand molecules on the pollen surface (Nasrallah *et al*., 2002). The extracellular domain is the site of interaction with pollen SCR ligands (Stein *et al*., 1991).

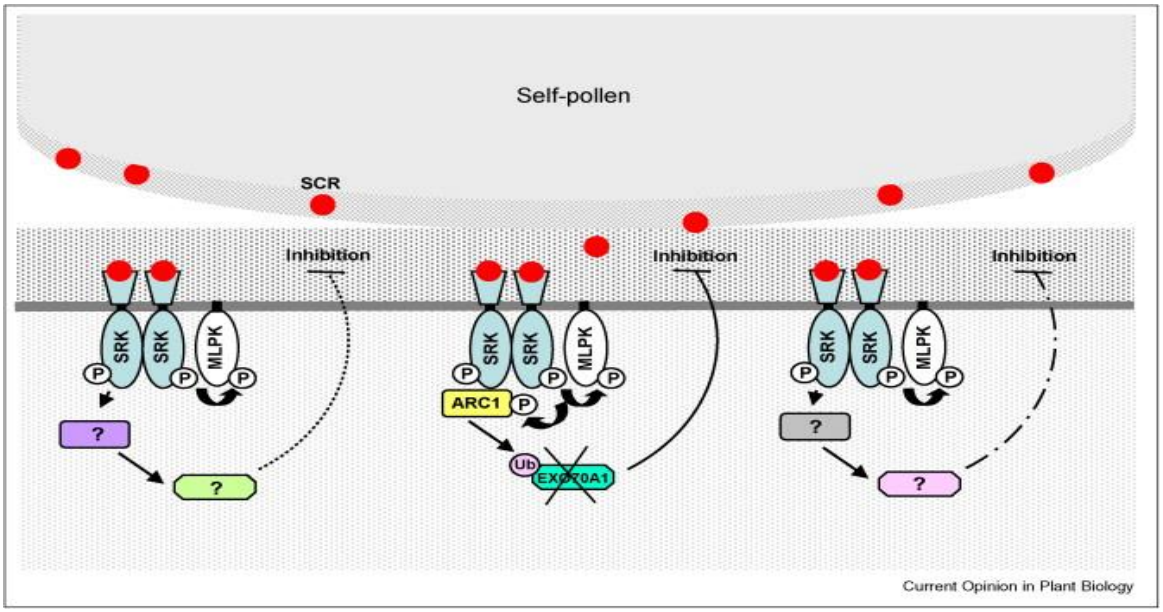

Figure 1.6. Schematic model for recognition of self-pollen and mechanism of sporophytic SI in *Brassica*. Male determinant of SI are SCR molecules expressed in pollen coat and female determinant are SRKs expressed in stigmatic epidermal cells. Upon landing of self-pollen on the stigma, SCR peptide is supplied to the stigma epidermal surface where it binds to the extracellular domain of associated SRK. This causes autophosphorylation of the receptor and triggers signalling cascade, the cartoon suggests three different SI cascades. MLPK acts as a signalling intermediate. The cartoon in the middle illustrates SI model involving ubiquitination of EXO70A1 by ARC1, whereas the cartoons on the side illustrate the presence of unknown compounds in the ARC1/ EXO70A1-independent signalling pathways. (Image adopted from Tantikanjana *et al*., 2010), Current Opinion in Plant Biology (http://www.sciencedirect.com/science/journal/13695266), 2010 Elsevier Ltd. All rights reserved.

The S-specific interaction of SRK with SP11/SCR is localised on the stigmatic papillae. Autophosphorylation of SRK is induced by the S-specific interaction, triggering a signalling cascade that results in the rapid rejection of self-pollen (Kachroo *et al*., 2001, Takayama *et al*., 2001, Ivanov *et al*., 2010). Current work is focusing on the downstream signalling components. To date, two positive mediators of *Brassica* SI have been identified: ARC1 (Armadillo-repeat-containing 1) and MLPK (*M*-locus protein kinase)(Gu *et al*., 1998,

Murase *et al*., 2004). ARC1 has been demonstrated to play a significant role in Brassicaceae SI (Goring *et al*., 2014). Studies demonstrated that over-expression of Exo70A1, which is a putative substrate of ARC1, partially overcome the SI in the transgenic *Brassica napus.* They also have shown by contrast that loss of expression leads compatible pollen tube rejection (Samuel *et al*., 2009). This suggests the contribution of Exo70A1 protein in the SI response of Brassicaceae by hindering the polarized secretion in the stigmatic papillae, since without this secretion pollen grains cannot be hydrated (Safavian and Goring, 2013).

M locus protein kinase (MLPK) is a second positive mediator of SI. It is a cytoplasmic serine/threonine protein kinase localised to the plasma membrane and creates a signalling complex with SRK to initiate an SI response (**Figure 1.6**) (Murase *et al*., 2004). Several negative regulators, like thioredoxin H-like proteins, THL1 and THL2 have been identified which interact with SRK through the kinase domain (Mazzurco *et al*., 2001). THL1 inhibits the autophosphorylation of SRK in the absence of pollen coat protein SP11/SCR (Cabrillac *et al*., 2001, Haffani *et al*., 2004), thus inhibits the activation of SRK results in the rejection of pollen (Takayama and Isogai, 2005). However, we don't know much about how incompatible pollen is inhibited/regulated, i.e. not much is known about the mechanisms involved in Brassica SI.

1.6.2 Mechanisms involved in S-RNase based gametophytic SI

In the Solanaceae (petunia, tobacco, potato, tomato, etc), Rosaceae (apple, cherry, pear, almond, etc) and Plantaginaceae (*Antirrhinum*) families share the same female S-determinant, an *S*-RNase. In these families rejection of

incompatible pollen occurs during pollen tube growth in the transmitting tract of the style and is therefore a much slower procedure than in Brassica, indicating a different mechanism of recognition and inhibition.

The female *S*-determinant in S-RNase based SI is a stigmatic protein which shows ribonuclease activity and thus called *S*-RNase (McClure *et al*., 2011, Murfett *et al*., 1994). The *S*-RNase was demonstrated as the *S*-determinant in *Petunia* using loss and gain of function experiments (Lee *et al*., 1994). *S*-RNase are produced in the transmitting cells and secreted into the transmitting tract where the pollen is growing. The ribonuclease activity of *S*-RNase has been shown to play a role in degrading RNA and play role for the rejection of self pollen (McClure *et al*., 2011, McClure *et al.*, 1989).

The male *S*-determinant in S-RNase SI is known by two names: the *S*-locus F-box protein (SLF,(Sijacic *et al.*, 2004)) and S-haplotype-specific-F-box protein (SFB,(Lai *et al*., 2002)). These genes are specifically expressed in the anther and pollen grain (Lai *et al*., 2002). SLF/SFB contains a motif called the F-box, which functions to bind specific substrate proteins to the E3-ubiquitin ligase complex and plays a role in the polyubiquitylating of non-self S-RNase. As a result, they permit the survival of compatible pollen. Studies in *Petunia* demonstrated that several types of SLF/SFB proteins encoded by numerous pollen S-determinants and each SLF/SFB-type identifies a range of S-RNase (Kubo *et al*., 2010).

There are two proposed models of S-RNase based SI, the degradation model and compartmentalization model, which can explain the self-compatibility and SI. These models are briefly described below and presented in the **Figure 1.7.**

1.6.2.1 Degradation Model

The degradation model of S-RNase-based SI is based on ubiquitylation and destruction of S-RNase after the interaction of SLF/SFB with S-RNase (Hua *et al*., 2008). According to this model when pollination occurs, S-RNase enter into the cytoplasm of pollen tube irrespective of their S-haploytpe (Luu *et al*., 2000) and they produce a SLF/SFB-S-RNase complex by interacting with SLF/SFB (**Figure1.7**). Through a compatible interaction, non-self S-RNase tags them with ubiquitin, so that the 26S proteasome can destroy them. As a result the pollen RNA remains intact and pollen tubes continue to grow (**Figure1.7)** (Kerscher *et al.*, 2006, Qiao *et al.*, 2004, Sijacic *et al*., 2004). On the other hand, in an incompatible response, the S-RNase interacts with SLF but is not degraded by the proteasome. Then the S-RNase degrades the RNA and inhibits further pollen tube growth (**Figure 1.7**) (Hua and Kao, 2006, Qiao *et al*., 2004).

1.6.2.2 The Compartmentalization Model

The S-RNase compartmentalization model involves S-RNase compartmentalization by the pollen tube endomembrane system (**Figure 1.7**) (McClure, 2009, Goldraij *et al*., 2006, McClure *et al*., 2011). The S-RNase forms complexes with 120K (a 120 kDa glycoprotein abundant in the stylar ECM) and HT-B (a small asparagine-rich protein)(McClure *et al*., 1999, Cruz-Garcia *et al.*, 2005). During endocytosis, these complexes are taken up and stored in the vacuole (Goldraij *et al*., 2006). In the vacuole they are separated from the cytoplasm. In a compatible reaction, HT-B levels are downregulated

by a hypothetical pollen protein (PP). S-RNase is compartmentalized and as result, pollen RNA remains intact, therefore pollen tube growth continue. In an incompatible interaction HT-B assists the transportation of S-RNase from endomembrane compartment to cytoplasm where S-RNase bound by 120K acts cytotoxicaly and degrade self-RNA, as a result pollen tube growth is halted (McClure, 2006, McClure *et al*., 2011, Goldraij *et al*., 2006).

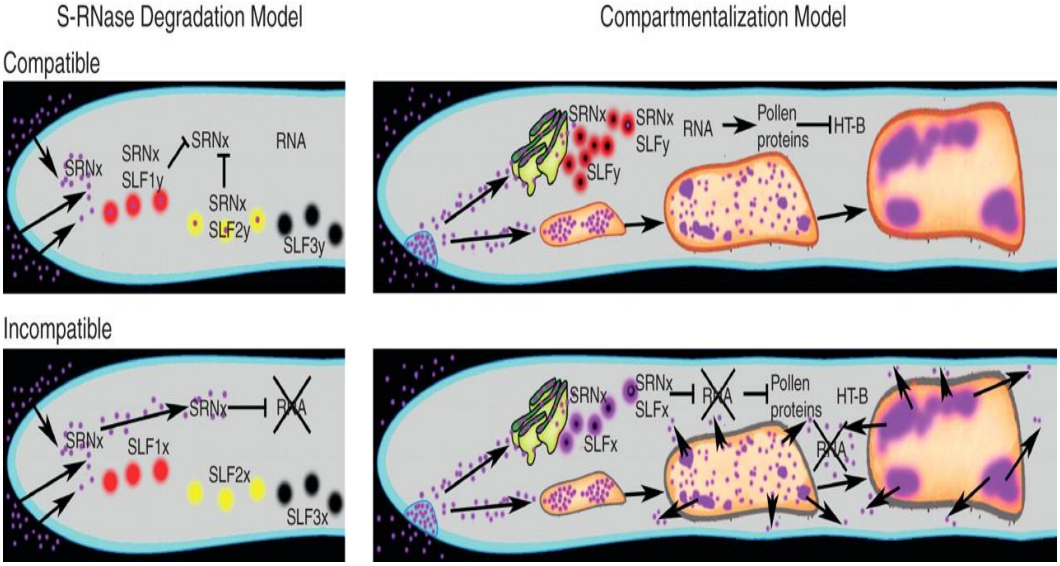

Figure 1.7. Two models for S-RNase-based SI. Degradation model: In compatible situation (left top) several SLF proteins (SLF1x, SLFy etc) bind to Sx-RNase and prevent the degradation of RNA in the pollen. During incompatible interaction (left bottom) SLF protein in the pollen (SLF1x, SLF2x, SLF3x etc) do not interact with self Sx-RNase. This Sx-RNase then degrades the RNA and thus pollen tube growth is inhibited.

The compartmentalization model: In compatible interaction (right top) the non-self S-RNase are taken up and compartmentalized by vacuoles and HT-B proteins are degraded. As a result RNA do not degraded. In incompatible pollination (right bottom) the S-RNase and HT-B enter into endomembrane system. S-RNase performs its cytotoxic function with the help of HT-B proteins. Interaction of S-RNase-SLF proteins inhibits several proteins which are involved in degredation of HT-B. So S-RNase works in association with HT-B protein to damage RNA and pollen tube growth is inhibited (McClure, 2006, Goldraij *et al*., 2006). Figure is adapted from McClure *et al*. (2011)

1.6.3 Gametophytic Self-incompatibility in Papavaraceae

The molecular and biochemical basis for the recognition, discrimination and selective rejection of incompatible pollen, observed during the SI response in *Papaver rhoeas* (Field Poppy), has been investigated since 1985. The ability to reproduce the SI response in *Papaver rhoeas* pollen *in vitro* (Franklin-Tong *et al*., 1988b) has allowed the dissection of signalling cascades triggered by SI (reviewed by Franklin-Tong and Franklin, 2003). Poppy regulating SI is regarded as one of the best characterised cell-cell signalling pathways involved in pollination/fertilization. This is a result of major advances in recent years that have revealed signalling components and targets involved in the SI response. It is quite distinct from the other two SI systems just described.

The *Papaver* SI system involves the two S-determinants at the *S* locus, which control a highly specific recognition between pistil and pollen. An *S*-allele-specific interaction occurs when pistil *S* gene products interact with pollen carrying a matching *S* allele so that 'self' ("incompatible") pollen is inhibited, while 'non-self' pollen is not. The pistil *S* determinant (PrsS, previously called "S protein", now renamed "PrsS": "*Papaver rhoeas* stigma S") is a novel small (~15kDa) secreted cysteine-rich protein (Foote *et al*., 1994). It interacts with incompatible pollen through the pollen "receptor" that interacts with the pistil "ligand". It is a gene encoding a novel transmembrane protein, PrpS ("*Papaver rhoeas* pollen S"). *PrpS* encodes a transmembrane ~20 kDa protein with no known homologues (Wheeler *et al*., 2009). *PrpS* is a single copy, novel, highly polymorphic pollen-expressed gene which is tightly linked to the pistil *S* gene.

1.6.3.1 Mechanisms involved in Self-Incompatibility in *Papaver*

When incompatible pollen lands on a receptive stigma, secreted *PrsS* proteins interact with pollen transmembrane *PrpS* and triggers almost instantaneous Ca^{2+}-dependent signalling cascade, which leads to the death of incompatible pollen tubes via programmed cell death (PCD). (Thomas and Franklin-Tong, 2004, Bosch and Franklin-Tong, 2007). Increases in Ca^{2+} mediate several SI-specific events in incompatible pollen. This is summarized in **Figure 1.8**. The SI response in poppy pollen can be divided into two phases. The first phase is relatively rapid, involves the inhibition of pollen tube growth. The second phase involves PCD to make the inhibition irreversible. As this thesis focuses on investigating mechanisms involved in mediating SI in incompatible pollen, it is appropriate to cover the events in detail here.

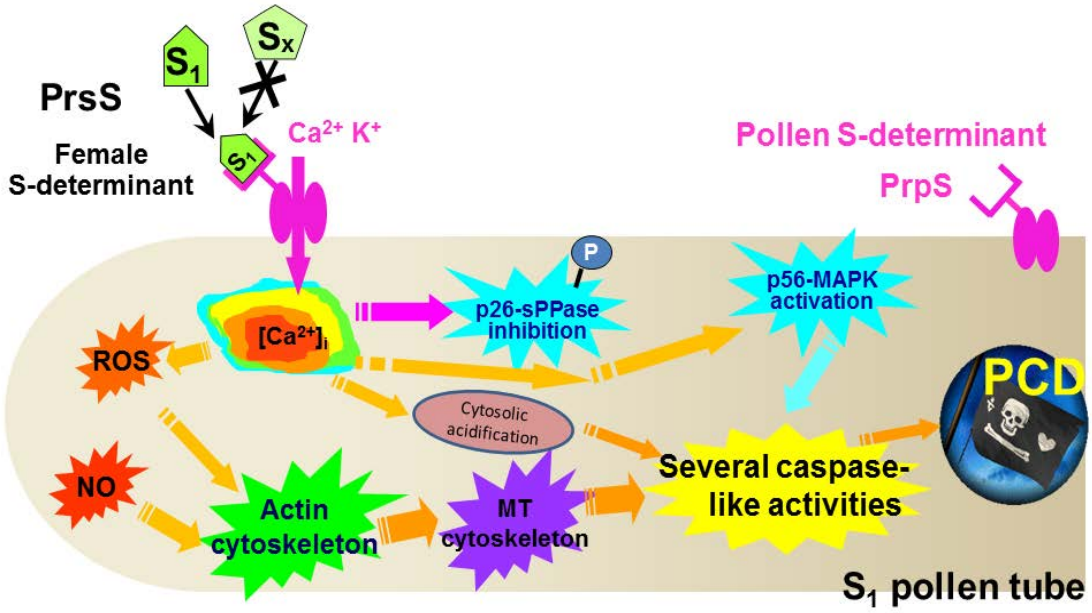

Figure 1.8. Model of *Papaver* SI mechanisms. A cartoon shows the self-incompatibility mechanism in *Papaver rhoeas* pollen tubes. For time line events of SI with more details, readers are referred to **Chapter 6 Figure 6.4.**

During an incompatible interaction between *Papaver rhoeas* stigmatic S (PrsS) and pollen S (PrpS), a rapid influx of Ca^{2+} and K^{+} is generated. Increases in Ca^{2+} mediate a signalling cascade, causing inhibition of pollen tip growth. Ca^{2+} dependent phosphorylation and inactivation of soluble inorganic pyrophosphatases (sPPases) Pr-p261a/b accur within 90s of SI. Ca^{2+} triggers alteration in the actin cytoskeleton and microtubule cytoskeleton. Rapid increases in both reactive oxygen species (ROS) and nitric oxide (NO) are related to actin foci formation. Rapid and dramatic acidification of cytosol occurs which is related to activation of several caspase-like activities. Mitogen activated protein kinase (MAPK) p56 is phosphorylated and activated which might be involved to PCD. Thus the incompatible pollen tube growth is inhibited and eventually destroed via PCD comfirming that self-fertilization cannot occur. Figure is adapted from Eaves *et al*. (2014).

1.6.3.1.1 Role of Ca^{2+} in the SI response

Calcium plays an important role in the SI-specific response in *Papaver rhoeas* pollen tube. Ca^{2+} imaging studies revealed a rapid, transient increase in pollen

$[Ca^{2+}]_i$, when pollen tubes were treated with incompatible but not compatible PrsS (Franklin-Tong *et al*., 1993, Franklin *et al.*, 1995, Franklin-Tong *et al*., 1997). Growing pollen tubes have a tip-focused Ca^{2+} gradiant, with a concentration of 1-2 μM, while the $[Ca^{2+}]_i$ in the shank region is comparatively low, ~ 200nM. SI-induction triggers rapid increases in Ca^{2+} in the shank region of the pollen tube and the characteristic tip-focused apical $[Ca^{2+}]_i$ gradient rapidly disappeared (Franklin-Tong *et al*., 1993, Franklin *et al*., 1995, Franklin-Tong *et al*., 2002). Influx of Ca^{2+} has been demonstrated to be essential for the increase in $[Ca^{2+}]_i$ during SI. Rapid increases in Ca^{2+} in the pollen tube during SI is necessary to trigger several downstream signalling components and events involved in mediating SI in incompatible pollen.

1.6.3.1.2 PCD and caspase-like activity in *Papaver*

PCD was first shown in incompatible *Papaver* pollen by Jordan *et al.* (2000) with the identification of nuclear DNA fragmentation and inhibition of pollen viability. The PCD was demonstrated in the PrsS challenged incompatible pollen by detecting the release of cytochrome *c,* cleavage of a classic substrate for caspase, bovine Poly-ADP-Ribose Polymerase (PARP) and activation of DEVDase activity (Bosch and Franklin-Tong, 2007, Thomas and Franklin-Tong, 2004, Franklin-Tong *et al*., 1996). Moreover, pre-treatment of pollen with DEVDase inhibitor, Ac-DEVD-CHO resulted in reduced DNA fragmaentation and significant alleviation in the SI-induced inhibition of pollen tube growth (Thomas and Franklin-Tong, 2004). These studies provide strong evidence that PCD is a novel mechanism for irreversible inhibition employed

during the SI response of poppy to ensure that self-fertilisation does not occur (**Figure 1.8**).

1.6.3.1.3 SI-induced pollen tube acidification

Recent study has shown that during SI in *Papaver,* there is a rapid and dramatic drop of cytosolic pH. The cytosolic pH of normally growing pollen tube is ~6.8. The studies shows that 10 min after SI-induction the pH drops to nearly 6.4 and 1-4 hours after SI induction, the pollen cytosolic pH drops to ~pH 5.5, which is its most acidic point (Wilkins *et al*., 2015). Previous studies have shown activation of caspase-like activities (DEVDase and VEIDase) to be involved in SI-induced PCD. These caspases have very narrow acidic pH optima of pH 5 (Bosch and Franklin-Tong, 2007). Thus, an acidic environment is required for caspase-like activities to be functional. So DEVDase activities are not active in normally growing pollen tube, but when the pH of SI-induced pollen tubes reaches pH ~ 5.5, the DEVDase would be active. Furthermore, the relationship between pH and caspase-like activities and actin alteration has been investigated by the use of propionic acid to manipulate $[pH]_i$. Activation of caspase-like-activities and also formation of actin foci was observed with artificial acidification treatment (Wilkins *et al.*, 2015). Moreover, caspase-3-like activity and formation of actin foci was prevented by blocking SI-induced acidification which suggests the requirement of cytosolic acidic pH for both caspase-3-like activities and actin foci formation and hence plays an important role in SI events (Wilkins *et al*., 2015).

1.6.3.1.4 Role of actin in poppy SI

One of the most rapid and dramatic physiological changes observed during *Papaver* SI response is a rearrangement of the actin cytoskeleton in the pollen tube, within 1-2 min after the challenge with incompatible PrsS protein. At first the F-actin filaments depolymerized and later stable actin puctate foci are formed and their size increases over time upto 3 h after SI-induction (Geitmann *et al*., 2000, Snowman *et al*., 2002, Poulter *et al*., 2010). An additional target of SI in incompatible pollen tube is the microtubule cytoskeleton. Microtubule and actin cytoskeleton show different temporal alteration upon SI. F-actin depolymerisation or stabilization can push the cell into PCD and the first indication of this in *Papaver* pollen tubes was provided when DNA fragmentation was observed by using latrunculin B, and by jasplakinolide that stabilizes actin filament, but was reduced when pollen was pre-treated with the inhibitor of DEVDase activity, AC-DEVD-CHO (Thomas *et al*., 2006). Despite the evidence for cross-talk between actin and microtubule cytoskeleton and the crucial role of actin cytoskeleton during the PCD, microtubule depolymerisation or stabilization alone does not trigger PCD (Poulter *et al*., 2008).

1.6.3.1.5 Recruitment of signalling for SI events in other species

Recent studies have started to explore the opportunity of efficient transfer of *Papaver* SI determinants into other species. It has recently been demonstrated that PrpS, the poppy pollen *S*-determinants, was expressed as a GFP-fusion protein and found to be functional in self-compatible *A. thaliana*

pollen (de Graaf *et al*., 2012). When *A. thaliana* pollen expressing PrpS-GFP was treated with recombinant PrsS (*Papaver* stigma S-determinant) the growth of the pollen tube was inhibited and the viability of pollen was decreased in an S-specific manner demonstrating PrpS functions as an S-determinant in *A. thaliana.* This S-specific reduction of pollen viability could be rescued by pre-treatment with the caspase 3 inhibitor, Ac-DEVD-CHO, demonstrated the association of PCD (de Graaf *et al*., 2012). S-specific actin foci formation was also observed in At-PrpS-GFP pollen after the treatment with recombinant PrsS, establishing that a signalling cascade comparable to that used in poppy SI response was triggered in the transgenic *A. thaliana* pollen.

The evolutionary distance between *P. rhoeas* and *A. thaliana* is ~144 million years (Bell *et al*., 2010) and from the all existing evidence it is clear that *Arabidopsis* does not have the *S*-determinants of *P. rhoeas*. Furthermore, *Papaver* and *Arabidopsis* don't have a common SI system. Even though, the poppy pollen S-determinants could be transferred successfully to *A. thaliana* which was evident by pollen rejection and exhibiting some hallmark features of the *Papaver* PCD (de Graaf *et al*., 2012). Thus detection of SI-induced PCD response similar to *Papaver* SI in *Arabidopsis* provides us good evidence that the interaction between PrpS and PrsS is adequate to achieve this PCD.

Recently, research has been performed to see whether SI response can be achieved in self-compatible *A. thaliana in vivo.* They transferred the *Papaver* female S-determinant, PrsS, into *A. thaliana*. Results demonstrated that when the stigma of transgenic *A. thaliana* expressing PrsS was pollinated with

pollen expressing PrpS:GFP, the pollen was rejected in an S-specific manner, and almost no seed was set. This suggests that the transformation of both PrpS:GFP and PrsS into *A. thaliana* to make self-incompatible plant was successfully achieved (Lin, 2015). Even though, *Papaver* and *Arabidopsis* are greatly diverged species, these studies showed that *Papaver* SI system could successfully and functionally be transferred to a self-compatible species.

1.6.3.1.6 Role of ROS and NO in *Papaver* SI

We previously discussed ROS and NO (**Section 1.1.2.3** and **1.4.2.4**). The role of ROS and NO signalling in the SI response has been demonstrated in the incompatible *Papaver* pollen (Wilkins *et al.*, 2011). Live-cell imaging was used to visualize reactive oxygen species (ROS) and nitric oxide (NO) in growing *Papaver* pollen tubes using CM-H_2DCF-DA (5-and-6)-chloromethyl-2',7'-dichlorodihydrofluorescein diacetate) and DAF-FM DA (4-amino-5-methylamino-2′,7′-difluorofluorescein diacetate). SI induced transient increases in ROS and NO (Wilkins *et al*., 2011). Crosstalk between the two signalling molecules was established, using H_2O_2 that stimulates ROS production and DPI that inhibit ROS. In incompatible pollen tubes, increases in cytosolic Ca^{2+} stimulated increase in ROS and NO.

A connection with the actin cytoskeleton and subsequent appearance of punctate actin foci and increase in DEVDase activity was also made, using ROS and NO scavenger demonstrating that alleviating ROS and NO production reduced the formation of punctate actin foci and DEVDase activity. This places ROS and NO production upstream of the actin cytoskeleton

alterations and DEVDase activity (Wilkins *et al*., 2011). However, the targets of ROS and NO signaling in pollen, especially in the context of SI response are not known.

1.6.3.1.7 Role of soluble in organic pyrophosphatases in poppy SI

We discussed sPPases earlier (**Section 1.3**). Rudd *et al*. (1996) showed that a rapid phosphorylation of a protein occur during *Papaver rhoeas* SI response. The phosphorylated protein was named as p26. Purification and cDNA sequencing of p26 deduced two full length structures of Pr-p26.1a and Pr-p26.1b (de Graaf *et al*., 2006). The Pr-p26.1a gene encodes a 24.4 kDa protein, Pr-p26.1b encodes a 26.5 kDa protein; they have slightly differing pI and Mr (de Graaf *et al*., 2006). Both proteins had high homology (~80%) to family 1 PPases. These inorganic pyrophosphatases (PPases Pr-p26.1a and b) are important ubiquitous enzymes that hydrolyse the inorganic pyrophosphate (PPi) which is generated as a by-product during cellular processes such as polynucleotide synthesis (Kornberg, 1962). This activity is essential to make a range of biosynthetic processes thermodynamically favourable. The activity of PPases enzymes is widely dependent on metal ions. Three or four divalent metal ions are necessary for their catalytic activity. Mg^{2+} is the most potent metal ion, while, Ca^{2+}, act as an inhibitor of magnesium pyrophosphate hydrolysis. Part of this project examined the effect of pH and metal ions on p26 sPPases activity (**Chapter 3**). In *Papaver* pollen the sPPases play an important role, as they provide the driving force for biosynthesis of pollen tube germination. SI stimulates Ca^{2+} increases and phosphorylation of soluble inorganic pyrophosphatases (sPPases). Both Ca^{2+}

and phosphorylation resulted in inhibition of sPPase activity. This inhibition of sPPase activity will contribute to inhibition of pollen tube growth, as they are essential enzymes for driving cellular biosynthesis.

1.7 Aims of this project

The work presented in this thesis studied the targets of *Papaver rhoeas* SI signalling network. The project comprises two main parts 1) Characterization of an important in organic pyrophosphatases, Pr-p26.1(**Chapter 3**), 2) Identification of proteins modified by ROS and NO during SI (**Chapter 4**) and also identify a link between actin and ROS/NO (**Chapter 5**).

- One objective was to characterize the soluble inorganic pyrophosphatases Pr-p26.1a and Pr-p26.1b (**Chapter 3**). It had previously been established that Pr-p26.1 sPPases were soluble inorganic pyrophosphatases, but a comprehensive characterization had not been performed. Hence, this part of project was to study the catalytic properties of these sPPase in the presence of different divalent and monovalent metal ions, Ca^{2+}, fluoride, substrates and pH to establish key factors involved in regulating their activity (**Chapter 3**). Previously it had been shown that phosphorylation affected the activity of these two sPPases, but the specific phosphorylation site is not known yet. So, we also carried out site-directed mutagenesis in an effort to mimic phosphorylation sites that might affect the sPPase activity of Pr-p26.1 and Pr-p26.1b (**Chapter 3**).
- ROS and NO were identified to be involved in the SI response, but the targets of these signalling molecules were not known. The major focus

of this thesis was to identify targets of ROS and NO during SI signalling (**Chapter 4**). Specific aims were to identify proteins that are modified by *S*-nitrosylation and oxidation as a result of SI signalling. As very little is known about the physiological functions of *S*-nitrosylation or oxidation in plants, especially in the context of a defined physiologically relevant stimulus, we hoped these studies would improve our understanding of this type of post-translational modification in plant cells in response to a specific stimuli and general stress conditions.

- In addition, we also investigated the possible role of actin and proteins associated with actin as targets of ROS and NO during SI response in order to attempt to establish further how actin may play a role in the SI response, as it seems to play such a central role (**Chapter 5**). We aimed to analyze post-translational modifications to actin and proteins associated with actin, to identify targets of ROS and NO after SI induction to obtain insights into additional potential, novel mechanisms or changes in modification status that might be involved in mediating SI-PCD through actin.

Chapter 2

Materials and Methods

2.1 Pollen tube growth *in vitro*

To investigate diffrent events and targets involved in SI signalling in *Papaver* pollen, an *in vitro* self-incompatibility assay has commonly been used in our lab. For *in vitro* experiment *Papaver* pollen was hydrated in a weighing boat for at least 45 minutes in a moist chamber at 26ºC. The shape of the pollen grains was used to assess the state of hydration. Desiccated pollen grains take an elliptical form and after hydration, pollen grains expand to a spherical form (Franklin-Tong *et al*., 1988a). Following hydration, pollen was suspended in 1ml liquid germination medium (GM) (See below for details) and then sown on to solid GM in 9 cm plates. Normally, for 10 mg of pollen,1.0-1.2ml of GM was required. Pollen was grown for at least 1hour, or until pollen tubes were visible. Following growth pollen was treated as required for the experiments.

Growth Medium Salt Stock (GM salt): 2 % (w/v) H_3BO_3, 2 % (w/v) KNO_3, 2 % (w/v) $Mg(NO_3)_2.6H_2O$, 7.2 % (w/v) $CaCl._2H_2O$, Sterile distilled water (SDW)

Liquid Growth Medium (GM): The solution was made as 13.5 % sucrose and then 0.5 % of GM salts was added to make up liquid GM.

Solid GM: Liquid GM supplimented with 1.2% agarose

2.2 Treatments to pollen tubes

With the intention of investigating the signalling events of *Papaver* SI, pollen was often treated with recombinant PrsS or different donors of ROS and NO.

2.2.1 *In vitro* induction of SI in pollen

In several previous PhD thesis, preparation of recombinant PrsS has been described in detail (Poulter, 2009 , Wilkins, 2013), therefore we will not cover this preparation steps here.

Recombinant PrsS was dialyzed overnight at 4ºC in to liquid GM using dialysis tubing with 12-14,000 kDa cut-off (Medicell International Ltd). For every 1ml of PrsS dialysed, 1 L of GM was needed. The next day, dialized PrsS was gently centrifuged and protein concentration was determined using the Bradford assay (Bradford, 1976). To induce an SI response, PrsS proteins of the same *S*-genotype as the pollen were added to pollen at the final concentration of 10 µg ml^{-1} (Snowman *et al.*, 2002). For each SI-induced sample, a non-induced control was prepared by adding only GM (Germination Medium) to the pollen.

2.2.2 H_2O_2 treatment

For mass spectrometry analysis (identification of protein targets of ROS) and imaging experiments of F-actin and foci, hydrated and germinated pollen was treated with H_2O_2 to final concentration of 2.5 mM. H_2O_2 treated pollen was collected at different time points from 5 min to 3 hr according to the experiment. .

2.2.3 NO donor GSNO

S-nitrosoglutathione (GSNO) (Sigma) was used as Nitric oxide donor. GSNO was added to the pollen tube to a final concentration of 500 µM from 5 mM stock for identification of S-nitrosylated proteins. For imaging experiments of

F-actin and foci in the pollen tubes the final concentration of GSNO was 250 µM. For both experiments pollen tubes were collected at different time points from 30 min to 3hr after treating with GSNO.

2.3 Visualisation of F-actin in *Papaver* pollen tube

Pollen was grown and treated using the treatments described above. For visualisation of F-actin in poppy pollen tube, we followed the procedure previously described in Poulter *et al*. (2010). Pollen was then fixed with 400 µM 3-maleimodobenzoic acid N-hydroxysuccinimide ester (MBS; (Pierce). 10 mM stock in DMSO) for ~6 min at room temperature, followed by 2% paraformaldehyde for 90 min at 4°C. Both fixatives were slowly added into the growing pollen tubes and the petri dish was gently tilted to distribute the chemicals evenly. Pollen tubes were collected using a pipette with a cut tip to enlarge the opening so that the pollen tubes could be transferred into a fresh microfuge tube with less damage. To remove the fixative the pollen was centrifuged at 4,000 rpm for 1.5 min. The pollen was washed with 3 changes of 1 x Tris buffered saline (TBS, pH 7.6) or actin stabilising buffer (ASB: 100 mM Pipes, pH 6.8, 1 mM MgCl2, 1 mM $CaCl_2$, and 75 mM KCl). Finally the pollen pellet was resuspended with 100 µl of TBS.

Actin in pollen tube was stained using 66 nM rhodamine-phalloidin (Rh-Ph) (Invitrogen). Phalloidin binds the F-actin form therefore G-actin is not visualised. This permits a clearer picture of the MF cytoskeleton since background signal created by monomeric actin is removed. The fixed pollen tubes were incubated with Rh-Ph for at least 30 min at 4ºC, but better results were achieved following overnight incubation at 4ºC.

2.4 Fluorescence microscopy

2.4.1 Epifluorescence imaging for F-actin analysis

Epifluorescence images were collected using a Nikon Eclipse Tε300 microscope attached to a cooled coupled device (CCD) camera supplied by Applied Imaging, UK. Fluorescence was detected using filters for FITC configured by Applied Imaging UK. Capture and analysis of images was achieved with a Nikon NIS elements 3.2 image analysis software. Images were saved as TIFF files and then analyzed in ImageJ or Microsoft PowerPoint. This system was used for F-actin analysis in the pollen tubes.

2.5 Extraction of Pollen Proteins

Pollen was hydrated and grown in a Petri dish as described in **Section 2.1**. The size of the Petri dish and the amount of pollen used depended on the experiment. After growth and/or treatment, pollen was collected from the Petri dish using a pipette with a cut tip and put into a 1.5 ml microfuge tube. The microfuge tubes were spun at full speed for 1 min and the liquid GM removed. For long pollen tubes additional spinning may be required to allow removal of as much liquid GM as possible.

Several different extraction buffers and methods of extracting the protein were used depending on the experiment:

2.5.1 Protein extraction for ROS/NO experiments

The pollen was collected from each dish and the GM removed. Approximately 200 µl of HEN buffer (250 mM HEPES, 1mM EDTA, 0.1mM neocuproine, pH 7.7) was added to the pollen were mixed by flicking and then transferred to a

glass homogenizer using a 1ml cut micro pipette tip. The pollen was ground on the ice for 10-15min, until the pollen appeared to be a homogenous liquid. Samples were checked under microscope to verify that the pollen grains and tubes had been ruptured to allow the proteins to be released. The ground pollen was transferred to a microfuge tube and centrifuged at 13,000 rpm for 10 min at 4ºC. The protein content of the supernatant was determined by Bradford assay (Bradford, 1976). These proteins were then stored in -20ºC until required.

2.5.2 Pollen protein extraction for F-actin isolation

The pollen was collected from each dish and the GM removed 200 µl of F-actin extraction buffer was added (10 mM HEPES (pH 6.8), 5 mM $MgCl_2$, 5 mM EGTA, 100 mM KCl , 0.6 µM Biotin-Phalloidin, 0.1 % NP-40, 1x protease inhibitor cocktail (Roche, Complete mini, EDTA-free)) to the microfuge tube. The pollen were mixed with extraction buffer by flicking the tubes and then transferred to a glass homogeniser using a cut 1 ml tip. The pollen was ground up keeping the homogeniser on ice as detailed in **Section 2.5.1**. The ground pollen was transferred to a microfuge tube and centrifuged at 6000 rpm for 30 min at 4^0C and the supernatant was collected. This centrifugation step was repeated to ensure that no debris such as pollen grains or tube walls remained in the supernatant. This protein extracts were then kept on ice ready for the next step (**Section 2.8**).

2.6 SDS-Polyacrylamide gel electrophoresis (SDS-PAGE)

Gels were prepared according to the BioRad self-assembly kits following standard SDS gel preparation protocol (Laemmli, 1970). 12.5% gel was

prepared for all experiment. 5-10 µg protein were mixed with 6x loading buffer and boiled for 5min before loaded to the gel. After electrophoresis, gels were soaked for 1h at room temperature in a Coomassie staining solution and then de-stained in several changes of de-staining solution until the bands were clearly visible.

2.7 Western blot

2.7.1 Protein transfer

After protein separation by SDS-PAGE protein was transferred to a nitrocellulose membrane (Hybond-C Extra, Amersham) using protein transfer buffer (0.2M Glycine, 25mM Tris, 20%(v/v) Methanol, pH 8.3) (Towbin *et al*., 1979) Protein transfer was performed by the electro blotting tank (BioRad), filled with protein transfer buffer. An ice block was also placed in the tank to prevent overheating due to the high voltage used for blotting. BioRad power packs were used to blot the gel at 400mA for 2h. Following transfer the nitrocellulose membrane was removed and washed briefly in 1XTBS (10x Tris Buffered Saline(TBS): 200 mM Tris-HCl pH 7.6, 730 mM NaCl, SDW) containing 0.1% Tween 20 (TBST) and then placed in blocking solution (5% skimmed milk powder in TBST) for at least 1 h at room temperature or overnight at 4˚C.

2.7.2 Antibody probing

After blocking the membrane, it was incubated with primary antibodies (see below for details) in blocking solution for 2h at room temperature or overnight at 4ºC. Then membrane was then washed 3 times 10 min each with blocking

solution and then incubated with secondary antibodies (see below for details) in blocking solution for 1h at room temperature. The blot was then washed 3x 10 min each in 1x TBS solution.

Primary antibodies:

Anti-TMT antibody (1:1000) in blocking solution (to detect *S*-nitrosylated proteins) from Pierce (Thermo scientific)

Anti-actin (Ab-1) Mouse mAb (JLA20) (1:5000) (Chembiochem) in blocking solution

Secondary antibodies

Anti-mouse IgG-HRP conjugate (1:5000) in blocking solution

2.7.3 Enhanced chemiluminescence detection (ECL)

ECL western blotting reagent (Amersham) was used to detect the secondary antibody. Solutions A and B were mixed 1:1 ratio (Yakunin and Hallenbeck, 1998) and immediately after mixing poured over the blot. After 1 min, excess reagents were removed. Blots were analysed using Curix 60 (AGFA) Photon imaging system.

2.8 F-actin enrichment using ultracentrifugation

Pollen proteins were extracted (**Section 2.5.2**) in a buffer containing 0.6 µM phalloidin that promotes F-actin stabilisation (Cano *et al.*, 1991). The extracted pollen protein was pipetted into 3 ml heat-sealable ultracentrifugation tubes keeping a volume of 50 µl for each sample to serve as the 'pre-spin' control. The volume was made up to the top of the tube using extraction buffer (10 mM

HEPES (pH 6.8), 5 mM MgCl2, 5 mM EGTA, 100mM KCl, 0.1% NP-40, 1x protease inhibitor cocktail). The tubes were sealed using a heat sealer. The protein extracts were then spun at 100,000 rpm at 4ºC in a Beckman TL-100 table top Ultracentrifuge (Beckman instruments, Inc) for 30 min to pellet the F-actin. The supernatant (the cytosolic fraction) was collected using a needle and syringe. The pellet (the F-actin enriched fraction) was resuspended into extraction buffer containing biotin-phalloidin. Depending on the size of the pellet 100-200 µl of the buffer was used. The pellet was then transferred to a glass homogeniser to re-suspend as well as possible. These samples were then stored at 4ºC as freezing causes F-actin depolymerisation

2.9 F-actin pull-down assay

F-actin was isolated from pollen protein extract using the property of phalloidin to bind specifically to F-actin. A biotin-phalloidin conjugate (Sigma-Aldrich) was used to bind to the F-actin. The biotin acted as a tag that could be used to pull-down the F-actin and its associated components by the high-affinity binding of biotin to avidin.

2.9.1 Streptavidin MagneSphere Paramagnetic Particles (SA- PMPs)

Pollen proteins were extracted as detailed in **Section 2.5.2** and the F-actin enriched by ultracentrifugation (**Section 2.8**). 400 µg of pollen extract was taken in a 1.5 ml microfuge tube and incubated with 4 µg of biotin-phalloidin, made up to a final volume of 500 µl with extraction buffer, for 2 h at 4ºC on a rotor. During this time, the SA-PMPs (Promega) were prepared for biotin binding by adding 100 µl of the fully re-suspended SA-PMPs into a 1.5 ml microfuge tube and washing in 3 x 100 µl of 2 x PBS and then once in 100 µl

of extraction buffer. During washing 100 µl solution was added to make sure everything was properly re-suspended and then the microfuge tube was placed into the Magnetic Separation Stand (Promega) which draws the magnetic particle to the side of the tube and allows the liquid to be pipetted off easily. After incubation, the 500 µl of extract with the biotin phalloidin was added to the SA-PMPs and left mixing on a rotor at room temperature for 1 h. The SA-PMPs were then captured using the magnetic stand and the liquid, which is the not bound fraction, was removed and kept. The beads were then washed three times with 500 µl of extraction buffer. Each wash was kept and labelled. The streptavidin-biotin binding of this method is irreversible. Therefore, to release the proteins from the SA-PMPs the SA-PMPs were re-suspended into 40 µl of 2 % SDS with 3 mM biotin made up in PBS. 10 µl of 5 x protein loading dye was then added to the protein and the mixture left to mix on the rotor for 15 min at room temperature. The protein was boiled for 15 min before loading onto SDS-PAGE. The input, not bound and wash fractions were combined with appropriate amounts of 5 x protein loading dye, boiled and loaded onto SDS-PAGE.

2.10 Analysis of F-actin containing fractions by FT-ICR MS

2.10.1 Sample preparation

60 µg of bound fraction from **Section 2.9.1** was loaded onto SDS-PAGE. All the proteins present in the extract were of interest, so the gel was only run for a very short time so that the proteins just entered the resolving part of the gel. The gel was then stained with coomassie blue and then destained so that the areas of the gel containing proetins could be clearly visible. These areas were

then cut out of the gel, and placed into a sterile microfuge tube. This was called a gel plug. The gel plugs were then sent to the Proteomics lab at the University of Birmingham for processing and analysis by FT-ICR MS. The samples were treated with trypsin and analysed by Mass Spectrometry.

2.11 Identification of proteins modified by ROS/NO using FT-ICR MS

2.11.1 Sample preparation for ROS experiment

Pollen protein was extracted as described in **Section 2.5.1**. Samples were prepared as described in **Section 2.10.1**

2.11.2 Resin-assisted capture of S-nitrosothiols(SNO-RAC)

We followed the protocol of Thompson *et al*. (2013) with slight modification to identify the S-nitrosylated protein using FT-ICR-MS.

2.11.2.1 Sample preparation

To generate S-nitrosylated proteins in *Papaver* pollen, we added either recombinant PrsS or treated the germinated pollen with 500 µM NO-donor S-nitrosoglutathione (GSNO). Pollen protein was extracted as detailed in **Section 2.5.1**. Protein concentration was determined with Bradford assay and adjusted to 3µg/µl in HEN buffer to get the final volume 75µl and kept in the dark at room temperature (RT) for 30 minutes.

2.11.2.2 Thiol Blocking

2.5% SDS (from 25% stock) and 0.2% S-methyl methane thiosulfonate (MMTS) (from freshly prepared 10% stock of MMTS in DMSO) were added to

the protein sample and incubated at 50°C for 20 minutes with frequent vortexing.

2.11.2.3 Removal of blocking reagent

Blocking reagent was removed by passing the sample through two Micro Bio Spin 6 columns (BioRad) equilibrated in HEN buffer according to the manufacturer's instructions.

2.11.2.4 SNO displacement and Cys capture with thiopropyl sepharose (TPS)

50 mM Ascorbate (Asc: freshly prepared in HEN buffer and kept away from dark on ice) and 60µl thiopropyl sepharose (TPS : swelled 1g in 4.5 ml HEN buffer, washed several times by centrifugations to remove preservatives. Re-suspended in HEN buffer) was added to the sample. The mixture was gently rotated overnight in dark at 4°C. The beads (TPS) were spun down in microfuge. Extreme care was taken to avoid sunlight exposure during SNO-RAC. At this stage the beads were divided into two parts; one part was used for western blot detection and the other part for mass spectrometry analysis.

2.11.2.5 Sample processing for western blot

S-nitrosylated proteins were detected using Pierce™ S-nitrosylation western blot kit (Thermo scientific) according to the manufacturer's instruction.

2.11.2.6 Sample preparation for mass spectrometry analysis

2.11.2.6.1 On resin digestion

Following protein capture, beads (TPS) were washed at least 5 times with wash buffer (25mM HEPES, pH 7.7, 1 mM EDTA, 600 mM NaCl and 0.5% Triton X-100) and then with 50mM ammonium bicarbonate (AmBic) to eliminate the detergent solution and to exchange TPS into an MS-compatible buffer. Two bed volume of 0.2% (w/v) Rapigest SF (Waters) in AmBic was added to the beads and this sample was sent to the proteomic lab for trypsin digestion (without adding DTT).

The digested supernatant ('SNO-sup') was separated from the SNO-site TPS-Resin (The supernatant contained all but the bound SNO-site peptide) and sent for MS-analysis as a negative control.

2.11.2.6.2 Preparation of SNO-site peptide from TPS Resin

The TPS- Resin (contained SNO-site) was washed at least three times with 200µl of each of the following buffers; HENS (HEN buffer with 1% SDS), AmBic (50 mM ammonium bicarbonate), 80/20/0.1 v/v/v Acetonitrile/H_2O/Trifluoro acetic acid and 50/50 MeOH/ H_2O.

The washed SNO-site peptides were eluted from the resin by treatment with DTT and iodoacetamide, purified and concentrated with Zip tip® clean up and then sent for mass spectrometry analysis.

2.11.3 Mass spectrometry analysis

Mass spectrometry analysis was performed by advanced mass spectrometry facilities provided by School of Biosciences, University of Birmingham. **Sections 2.11.3.1, 2.11.3.2 and 2.11.3.3** are written by Dr. Cleidiane Zampronio and she performed these parts of experiments using the following methods.

2.11.3.1 Liquid trypsin digestion

"Trypsin digestion was performed using 10 μL of samples (~1-100μg of protein) and added 40 μL of 100mM ammonium bicarbonate (pH 8). Samples were incubated at 56 ^{o}C for 30 mins after adding 50 μL 10 mM of dithiothreitol (DTT). Samples were cooled to room temperature and cysteines alkylated by addition of 50μl 50mM iodoacetamide, mixed and incubated at room temperature in the dark for 30 mins. 25 μl of trypsin gold (Promega, Southampton, Hampshire, UK, 6 ng/μl) was subsequently added to the samples, which were then incubated at 37 ^{o}C overnight."

2.11.3.2 Desalt samples

"The samples were desalted using millipore C18 ZipTips. Tips were prepared by pre-wetting in 100% acetonitrile and rinsed in 2x10 μL 0.1% trifluoroacetic acid. Samples were repeat pipetted throughout the volume of the samples five times. The tip was then washed with 3x10μl 0.1% trifluoroacetic acid to remove excess salts before elution of peptides with 10μL of 50% acetonitrile/water/0.1% trifluoroacetic acid. Samples were dried down to remove the acetonitrile, and then re-suspended in 0.1% formic acid solution in

water. All chemicals were purchased from Sigma (Gillingham, Dorset, UK), Fisher Scientific (Loughborough, Leicestershire, UK) and J.T. Baker (Philipsburg, NJ)."

2.11.3.3 LC-MS/MS Experiment

"NCS pump UltiMate® 3000 nano HPLC series (Dionex, Sunnyvale, CA USA) was used for peptide concentration and separation. Samples were trapped on uPrecolumn Cartridge, Acclaim PepMap 100 C18, 5 um, 100A 300um i.d. x 5mm (Dionex, Sunnyvale, CA USA) and separated in Nano Series™ Standard Columns 75 µm i.d. x 15 cm, packed with C18 PepMap100, 3 µm, 100Å (Dionex, Sunnyvale, CA USA). The gradient used was from 3.2% to 44% solvent B (0.1% formic acid in acetonitrile) for 30 min. Peptides were eluted directly (~ 300 nL min-1) via a Triversa Nanomate nanospray source (Advion Biosciences, NY) into a LTQ Orbitrap Velos ETD mass spectrometer (ThermoFisher Scientific, Germany). The data-dependent scanning acquisition was controlled by Xcalibur 2.7 software. The mass spectrometer alternated between a full FT-MS scan (m/z 380 – 1600) and subsequent collision-induced dissociation (CID) MS/MS scans of the 20 most abundant ions. Survey scans were acquired in the Orbitrap with a resolution of 30 000 at m/z 400 and automatic gain control (AGC) 1x106. Precursor ions were isolated and subjected to CID in the linear ion trap with AGC 1x105. Collision activation for the experiment was performed in the linear trap using helium gas at normalized collision energy to precursor m/z of 35% and activation Q 0.25. The width of the precursor isolation window was 2 m/z and only multiply-charged precursor ions were selected for MS/MS.

The MS and MS/MS scans were searched against NCBInr database using Mascot algorithm (Matrix Sciences). Variable modifications were deamidation (N and Q), oxidation (M) and phosphorylation (S, T and Y). The precursor mass tolerance was 5 ppm and the MS/MS mass tolerance was 0.8Da. Two missed cleavage was allowed and were accepted as a real hit proteins with at least two high confidence peptides."

Several additional modifications were searched in order to identify the modified targets for ROS and NO. These includes: S-nitrosylation (C), carbamidomethylation (C), carbonylation (K, P, R, H, W), Oxidation Met (M)

2.12 Growth and expression of recombinant Pr-p26.1a and Pr-p26.1b

Pr-p26.1 constructs transformed into *Escherichia coli* [BL21 (DE3)] kept frozen at -80^{0}C were used to start the growth. The construct contained an N-terminal His-Tag to aid protein purification. Samples of Pr-p26.1a and Pr-p26.1b from glycerol stock were streaked onto plates made of LB agar (LB medium with 15 g L^{-1} bacto-agar) containing 100µg.ml^{-1} ampicillin and incubated at 37°C overnight. The next day, 50ml LB medium supplemented with 100µg.ml^{-1} ampicillin was inoculated from a single colony and left shaking at 37°C and 200 rpm overnight. 4ml of the overnight culture was placed into 400ml LB broth/100µg.ml^{-1} ampicillin. 2 mM $MgCl_2$ was also added to the culture medium to promote the optimal Pr-p26.1 activity after purification, cultures were grown until an optical density, OD_{600nm} 0.7-0.8 was reached. To induce expression of the protein, 1mM IPTG was added to each culture and incubated overnight at 22°C with shaking at 200 rpm. The cells were harvested

at 8000 g at 4°C for 15 minutes and the resulting pellets were resuspended in Tris/NaCl buffer (50mM Tris HCl pH 8.0 ,0.1M NaCl, 2mM $MgCl_2$).Cells were collected by centrifugation at 14,000g at 4^0C for 15 min .

2.12.1 Purification of recombinant Pr-p26.1a and Pr-p26.1b

To purify the protein, the cell pellets were homogenised (800 ml culture equivalent) in cell re-suspension buffer(50 mM Tris HCl pH 8.0, 0.1 mM NaCl, 2mM $MgCl_2$, 0.5 mM AEBSF, 2 complete protease inhibitor tablets/25 ml, 0.5mg.ml^{-1} lysozyme) to a total volume of 25 ml. The re-suspended pellets were then sonicated on ice 6x15 seconds with 105 seconds intervals at power 3/4 microtip. Sonicated material was centrifuged at 45,000 rpm for 1 hour at 4°C. Supernatant was carefully separated and collected into a corning tube. Imidazole buffer (Imidazole dissolved in Tris/NaCl buffer) was added to the supernatant to final concentration of 10 mM for Pr-p26.1a and 15 mM for Pr-p26.1b.

This supernatant was mixed with 2 ml of pre-equilibrated Ni-NTA resin for 30 minutes at 4°C. The supernatant was poured into a 10ml disposable column and the flow through was collected in a beaker.

For Pr-p26.1a the column was first washed 4 times with 3 ml 10mM Imidazole (50mM Tris HCl, 0.1 mM NaCl, 2mM $MgCl_2$ pH 8.0). Second wash was done 4 times with 25mM Imidazole (25mM Imidazole, 50mM Tris HCl, 0.1M NaCl, 2mM $MgCl_2$ pH 8.0). Finally Pr-p26.1a protein was eluted using 300mM Imidazole (300 mM Imidazole, 50mM Tris HCl, 0.1M NaCl, 2mM $MgCl_2$ pH 8.0).

For Pr-p26.1b the column was washed 4 times with 3ml 15mM Imidazole (15mM Imidazole, 50mM Tris HCl, 0.1M NaCl, 2mM $MgCl_2$ pH 8.0). Second wash was done with 75 mM Imidazole (75 mM Imidazole, 50mM Tris HCl, 0.1M NaCl, 2mM $MgCl_2$ pH 8.0). Pr-p26.1b proteins were eluted using 300mM Imidazole (300 mM Imidazole, 50mM Tris HCl, 0.1M NaCl, 2mM $MgCl_2$ pH 8.0.). Glycerol was added to the protein to 30% (v/v) final concentration and snap frozen in liquid nitrogen in 500 ml aliquots and stored at -80^0C.

2.13 Site directed mutagenesis of Pr-p26.1 sPPases

2.13.1 Mutant Strand Synthesis Reaction

Site directed mutants of Pr-p26.1 were made using the Quick Change II Site-Directed Mutagenesis Kit (Agilent Technology) according to the manufacturer's instructions. The reaction mixtures included 40ng of pET21b+Pr-p26.1 templates, 125 ng of each of the oligonucleotide primers, 5µl of 10X reaction buffer, 1µl of dNTP mix, required amount of ddH_2O to a final volume of 50µl. Then 1µl of *PfuUltra* HF DNA polymerase (2.5 $U.\mu l^{-1}$) was added to the reaction mixture. The primers used for mutagenesis are listed in **Table 2.1**. The amplification reaction was carried out using the following programme:

95°C – 30s 1cycle

95°C – 30s
55°C – 1min
68°C – 6min 20s
} 18 cycles

68ºC – 7min

Following the temperature cycle the reaction was cooled down by placing them on the ice. The PCR product was treated with 1µl of *Dpn I* and incubated at 37°C for 1hr to digest the parental, non-mutated supercoiled DNA template. After 1hr, 1µl of digested DNA was transformed into 25µl of the XL-1 blue supercompetent cells (Agilent Technology). Transformant colonies were selected on LB-ampicillin agar plates containing 80µg/ml X-gal and 20mM IPTG. Single colony was picked and cultured in liquid LB containing ampicillin (100µg.ml^{-1}) followed by plasmid extraction using Wizard plus sv minipreps DNA purification system (Promega) following manufacturer's instruction. Mutant DNA isolated from XL1-Supercompetent Cells was sequenced in both directions to confirm the modification in the coding sequence.

Table 2.1 Sequences of primers used for site directed mutagenesis.

Oligo name And Substitutions	**Sequences (5'-3')**
p261b S35A S36A (t103g_t106ganti)	CTG GGC GTG CGT GAG CTG CAT AGC TTG CAG CCT TG
p261b S35A S36A (t103g_t106g)	CAA GGC TGC AAG CTA TGC AGC TCA CGC ACG CCC AG
p261b S48A S49A (t142g_t145ganti)	CTG CCC TCC GAG CCA TAG CTG CAA GGA TTC TTT CAT TAA G
p261b S48A S49A (t142g_t145g)	CTT AAT GAA AGA ATC CTT GCA GCT ATG GCT CGG AGG GCA G
p261b S35A S36A (t103g_t106gwtanti)	ATG GGC GTG CGT GAG CTG CAT AGC TTG CAG CCT TG
p261b S35A S36A (t103g_t106gwt)	CAA GGC TGC AAG CTA TGC AGC TCA CGC ACG CCC AT
p261a S28A S30A (t82g-t88ganti)	CAG CTA CAG ATC TCC TTG CTA GGG CTG CAA GAA TTC TCT CAT T
p261a S28A S30A (t82g-t88g)	AAT GAG AGA ATT CTT GCA GCC CTA GCA AGG AGA TCT GTA GCT G
p261a S11A S12A (t31g_t34ganti)	GTA CGC TTC ACA GCT GCT GCT CCA GTC TCG GTT GCA
p261a S11A S12A (t31g_t34g)	TGC AAC CGA GAC TGG AGC AGC AGC TGT GAA GCG TAC

2.13.1.1 DNA Sequencing

DNA sequencing of all the mutant proteins of Pr-p26.1 sPPases was carried out by the Genomic Lab at the School of Biosciences, University of Birmingham. 250ng of the plasmid DNA (miniprep) was mixed with 3.2 pmole of sequencing primer and sterile distilled water was added to make the volume 10µl. The sample was then loaded onto a 96 well plate and sent for sequencing. The output sequence data was examined using the Chromas 2.4 programme.

2.13.1.2 Overexpression of site-specific mutant

After confirming the desired mutation the construct expressing the mutant constructs were transformed into *E. coli* BL21 (DE3) for overexpression. 1µl of DNA construct (miniprep) was mixed gently with 50µl of the chemically competent cells and incubated on ice for 30 min. This was followed by a heat shock treatment for 90s at 42°C in a water bath and transferred back to ice. 500µl LB with 0.4% Glucose was added to the transformation tube and incubated at 37°C shaker for 1hr. The cells were spread onto LB/ampicillin (100µg.ml^{-1}). Next day, 1 single colony was picked and cultured in 50ml LB/ampicillin (100µg/ml) at 37°C shaker until an optical density, OD_{600nm} 0.7-0.8 was reached. To induce expression of the protein, 1mM IPTG was added to the sample and incubated overnight at 22° C shaker at 200 rpm.

2.13.1.3 Purification of the mutant

Protein was purified by Ni-NTA spin kit (QIAGEN) following Manufacturer's instructions (Ni-NTA spin kit handbook; page 23). Overexpressed cells from

50ml culture were re-suspended in 1.4ml lysis buffer(NPI-10: 50mM NaH_2PO_4, 300mM NaCl, 10mM imidazole,pH 8.0), 140 µl lysozyme, 10 µl DNAase and 150 µl protease inhibitor EDTA free cocktail. The lysate was centrifuged at 12,000 g (about 11,360 rpm) for 30min at 4°C to collect the supernatant. 600µl of cleared lysate was loaded onto the pre- equilibrated Ni-NTA spin column and centrifuged for 5min at 270 g (approximately 1600rpm) and the flow-through was collected. The Ni-NTA spin column was washed twice with 600µl Buffer NPI-20 (50 mM NaH_2PO_4, 300 mM NaCl, 20 mM imidazole, pH 8.0). Finally, the 6xHis-tagged protein was eluted with 300µl Buffer NPI-500 (50 mM NaH_2PO_4, 300 mM NaCl, 500 mM imidazole, pH 8.0) and kept the protein in 50µl aliquots in -20° C freezer. Samples from every step were analysed by SDS-PAGE (**Figure 2.1**). The purified proteins from lane 5 to 7 were then used for further studies.

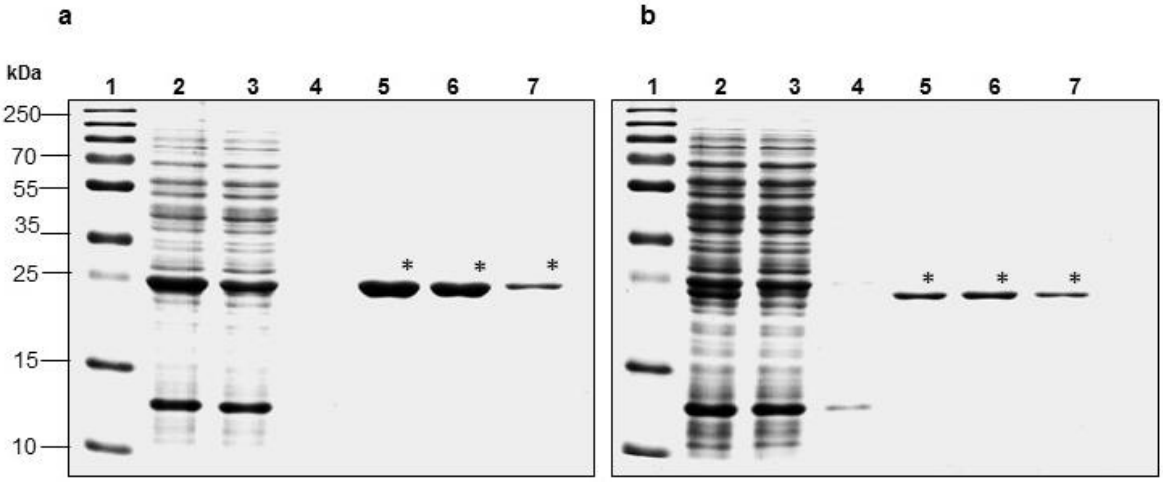

Figure 2.1. 12.5% SDS-PAGE showing purified site specific mutants of a)Pr-p26.1a and b)Pr-p26.1b. Lane 1-7 indicate Marker in kDa, Lysate, flow through, wash, elute 1, elute 2 and elute 3 respectively. * indicates the purified Pr-p26.1

2.14 Pyrophosphatase assay

The pyrophosphatase assay is a colorimetric method for the determination of inorganic phosphate, based on the production of a blue colour when the sample is treated with ammonium molybdate and 1-amino-2-napthol-4-sulfonic acid (ANSA).

2.14.1 Reagents required for pyrophophatase assay

Basic medium: 50 mM Hepes KOH pH 8.0, 50 µM EGTA, 2 mM $MgCl_2$

Substrate solution A: 100 mM Hepes, 2 mM Sodium Pyrophosphate (pH with NaOH to pH 7.0).

50mM propionic acid of different pH, 2 mM Sodium Pyrophosphate was used as substrate solution for most of the experiments.

Substrate solution B/ Metal ion stock solution: 0.1M $MgCl_2$

EGTA Solution: 50 mM EGTA stock

Stop Solution: 0.1 M EDTA (pH 7.0)

Ammonium Molybdate (2.5% w/v): 2.5 M H_2SO_4 (13.33 ml 98% sulphuric acid into 70 ml milli Q water), 2.5 g Ammonium Molybdate

ANSA Reagent (0.25% w/v): 0.25 g ANSA ((1-amino-2-napthol-4-sulphonic acid), 13.3 g Sodium Metabisulphite, 0.5 g Sodium Sulphite. Dissolved with mild heating making to 100ml (kept in the dark)

Fiske-Subbarow reagent: 9ml Milli Q, 2.5 ml (2.5%w/v) Ammonium Molybdate, 1.0 ml (0.25%w/v) ANSA.

Purified Pr-p26.1a-6His or Pr-p26.1b-6His or the substituted forms were diluted to 10 µM in 50 mM Hepes-KOH, pH 8.0, 50 µM EGTA, 2 mM $MgCl_2$. 250 ng aliquots were assayed for free phosphate using adaptations to the Fiske-Subbarow method (Fiske and Subbarow, 1925) using 2 mM sodium pyrophosphate (or other substrate as appropriate). The assay buffer was supplemented with 2 mM $MgCl_2$ (or other metal salts as appropriate) and 0.1 mM $CaCl_2$ (and/or 10 mM H_2O_2 as appropriate). For assays requiring a pH range observed during SI 100 mM sodium acetate pH 5.0 to 6.5, 50 mM propionic acid pH 5.0 to 7.0, or 100 mM Tris-HCl pH 7.0 to 9.0 were used as assay buffer at 30ºC. For measuring the effect of divalent cations other than Mg^{2+} on the enzyme activity, samples were incubated with the appropriate metal salts for 2 hours prior to assay.

For Substrate specificity study, 2 mM of the following substrates were used with 50mM propionic acid pH 7.0. Sodium pyrophosphate, Sodium tripolyphosphate, P',P-Di tetraphosphate, ATP, Beta-glycerophosphate, Adenosine 2' monophosphate, Adenosine 3' monophosphate, Adenosine 5' monophosphate, Adenosine 2'5' diphosphate, D-glucose-1-phosphate, D-glucose-6-phosphate.

For measuring the effect of Ca^{2+} and H_2O_2, enzymes were incubated with 0.1 mM $CaCl_2$ and/or 10mM H_2O_2 according to the treatments for at least 2hr.

To measure the activity of Pr-p26.1 sPPases an initial standard was constructed. 10 mM NaH_2PO_4 was diluted in Milli Q water with the concentration range between 0 to 0.4 µmol were obtained. The activity of enzyme was assayed at a regular interval of time (15s, 5min and 10min) .

Fiske-Subbarow reagent was added to each sample and left at room temperature for atleast 20 min. The absorbances of each sample were than read at OD_{691nm} and activity was calculated from the standard curve.

2.15 Cloning of *Papaver* actin from pollen

2.15.1 RNA extraction

Total RNA from *Papaver* pollen was extracted using RNeasy Mini Kit (Qiagen) following menufracturers insruction. All materials and water was pretreated with 0.05 % or 0.1 % diethylpyrocarbonate (DEPC) respectively. For each extraction, 100 mg pollen was used. Pollen was frozen in liquid nitrogen and grinded thoroughly in microfuge tube using a plastic rod. 450 µl of RLT buffer was added to the grounded pollen and mixed by vortexing. The sample was then added to a lilac QIA shredder spin column and centrifuged (2 min, 13,200 rpm). The flow-through was transferred to a new microfuge tube, 0.5 V of 100 % ethanol was added, the solution was mixed by pipetting, then immediately transferred to a pink RNeasy column and centrifuged (15s, 13,200 rpm). The flow-through was discarded and 700 µl RWI buffer was added to the new column before centrifugation (15s, 13,200 rpm). The flow-through was discarded and the column was transferred to a new collection tube. 500 µl RPE buffer was added to the column, centrifuged (15s, 13,200 rpm) and the flow-through discarded. Another 500 µL of RPE buffer was added to the column again and centrifuged (2 min, 10,000 rpm) to ensure the membrane was dry. The column was transferred into a new microfuge tube and centrifuged (1 min, 13,200 rpm). Finally, the column was transferred to a final microfuge tube, 30 µL of RNase free water added and centrifuged (1 min,

13,200 rpm). Then, another 10 µl of RNase free water was added to completely elute everything and centrifuged (1 min, 13,200 rpm). 5 µl of RNA was used to analyse by electrophoresis and the rest of the RNA was stored at -80 °C until required.

2.15.2 RNA analysis by agarose gel electrophoresis

Analysis of RNA samples was accomplished by electrophoresis on agarose gels using 5 µl of RNA loading dye. No ladder was used due to the possible contamination with RNases. 1 % agarose gel was made up in 0.5x TBE using RNase free SDW. Agarose was fused in 0.5X TBE by heating the solution until it was completely clear. Then, 0.5 µg ml^{-1} ethidium bromide was added to the molten agarose and poured in RNase free gel tank. Images of gels were captured using a Chemi Doc™ MP Imaging system (Bio-Rad) analysed using Quantity One software if necessary.

2.15.3 DNase treatment of RNA

In order to remove contaminating DNA, 10 µl of RNA was mixed with 10 µl of DNase solution and incubated at room temperature for 15 min. 2 µl of 25 mM EDTA was added and the mixture was incubated at 65ºC for 10 min. Then, 80 µl of RNase free water was added and extracted by addition of equal volume of phenol. The solution was mixed and centrifuged (5 min, 13,200 rpm). The upper aqueous layer was taken and transferred to a clean fresh tube and an equal volume of chloroform was added. After centrifugation the top layer with aqueous phase was taken, transferred to a fresh tube and 1 µl of glycogen (Roche) was added, which serves as a carrier to promote nucleic acids precipitation. RNA was precipitated by adding 2.5 V of 70% ethanol and

incubated at 70º C for 30 min and centrifuged (10 min, 13,200 rpm). Supernatant was carefully removed. RNA pellet was washed with 70% ethanol. The pellet was dried in a vacume chamber for 15 min and resuspended in 20 µl of RNase free water.

DNase solution: 2 µl 10x DNase I buffer 1 µl recombinant RNasin (Promega) 1 µl DNase (Invitrogen) 6 µl RNase free SDW.

2.15.4 cDNA synthesis by RT-PCR

Isolated total RNA was used in RT-PCR reaction using the Supersctipt™ II Reverse Transcriptase kit from Invitrogen following manufracturer's instruction:

RT-PCR mix: 1 µl Oligo(dT), 10 µl RNA, 1 µl dNTP mix, 4 µl 5X First-asatrand buffer, 2 µl 0.1 M DTT, 1 µl RNaseOUT™ , 1 µl SuperScript™ II RT.

RT-PCR condition: Incubation at 42ºC for 2 min, incubation at 42ºC for 50 min, inactivation the reaction by heating at 70ºC for 15 min.

After RT-PCR the obtained cDNA was used as a template for amplification in PCR

PCR mix: 12.5 µl My Taq Red mix(Bioline)
1 µl forward primer
1 µl reverse primer
2 µl cDNA
8.5 µl SDW(sterile distilled water)

PCR condition: 95ºC—1min 1cycle

95ºC—15s
48ºC—15s } 3 cycles
72ºC—1.3min

95ºC—15s
55ºC—15s } 32 cycles
72ºC—1.3min

72ºC—10min 1cycle

Primers:

Act forw: 5'-ATG GCC GAT GGT GAG GAT ATT CAG -3' Tm=62.7ºC

Act rev: 5'-TTA GAA GCA TTT CCT GTG AAC AAT CG -3' Tm=60.1ºC

To check the amplified DNA, PCR product was loaded on to agarose gel. 2.3.15 DNA analysis by agarose gel electrophoresis For the gel, agarose was fused in 0.5X TBE by heating the solution until it was completely clear. Then, 0.5 µg mL-1 ethidium bromide was added to the molten agarose. Gels were poured and electrophoresed using Biorad electrophoresis kits. Images of gels were captured using a Chemi Doc™ MP Imaging system (Bio-Rad) analysed using Quantity One software if necessary. An estimation of size was achieved by parallel electrophoresis of an aliquot of 1 kb ladder (Invitrogen).

10 x TBE:

0.9 M Tris

0.9 M Orthoboric acid

25 mM EDTA

DNA loading buffer:

40 % (v/v) glycerol

0.25 % (w/v) bromophenol blue

PCR product was purified using QIA quick PCR purification kit (QIAGEN) following the manufacturer's instructions.

2.15.5 Cloning of PCR product

Target DNA fragments were cloned into linearized pGEM®-T Easy Vectors through T4 DNA ligase mediated ligation using the pGEM®-T and pGEM®-T Easy vector system (Promega) following manufacturer's instruction. Ligation mixtures (see below) were incubated 1 h at room temperature before proceeding to transformation using JM109 High Efficiency Competent Cells (Promega) folloing manufacturer's instruction. Sequencing was performed using M13 forward and reverse primers.

Ligation mix

5 µl 2X Rapid Ligation Buffer, T4 DNA ligase

1 µl pGEM®-T easy vector

2 µl pure PCR product

1 µl T4 DNA ligase

1 µl nuclease free water

M13 Forward: 5' GTA AAA CGA CGG CCA G 3'

M13 Reverse: 5' CAG GAA ACA GCT ATG ACC 3'

Chapter 3

Characterization of Pr-p26.1a and Pr-p26.1b sPPase activity and investigations into how biologically relevant conditions might alter their activity

3.1 Introduction

As mentioned in **Chapter 1**, soluble inorganic pyrophosphatases (sPPases) are phosphate metabolising enzymes, recognized as phosphoryl transfer enzymes. These enzymes are ubiquitous enzymes and play a central role in cellular metabolism and are crucial for maintaining cellular level of Pi by catalysing the hydrolysis of PPi and provide the driving force for metabolism. (reviewed by Baykov *et al*., 1999). Thus, sPPase activity is essential for normal cell growth and function. It has been reported to be vital for the growth of *E. coli* (Chen *et al*., 1990) and *Bacillus subtilis* (Ogasawara, 2000) and for the mitochondrial function of yeast (Lundin *et a*l., 1991)

Like many other enzymes involved in metabolism of phosphate, sPPases are dependent on metal ions for their activity. Three to four divalent metal ions are essential per active site for catalytic activity with Mg^{2+} being preferred (Cooperman, 1982). In addition to Mg^{2+}, Zn^{2+}, Co^{2+} and Mn^{2+} can also stimulate pyrophosphate hydrolysis catalyses by pyrophosphatases (Heikinheimo *et al*., 1996a). Ca^{2+}, conversely, play a role as an inhibitor of the enzyme and therefore reduces sPPase activity (Cooperman *et al*., 1992) . In the presence of Mg^{2+}, sPPases show absolute substrate specificity. When other metal ions, for example Zn^{2+}, Co^{2+} and Mn^{2+} are used as cofactors, the specificity is lost. Inorganic pyrophosphate is the key substrate for soluble inorganic pyrophosphatase. Only linear polyphosphate such as inorganic tri- and tetra-phosphate are also hydrolysed in the presence of Mg^{2+} ion. However, the rate of hydrolysis is only 1/60 of that detected with pyrophosphate (Josse, 1966).

As mentioned earlier (**Chapter 1, Section 1.3**), to date, the soluble inorganic pyrophosphatases have been classified into two different families: Family I and Family II sPPases (Shintani *et al*., 1998, Young *et al*., 1998). The Family I sPPases are grouped into three subfamilies. Plant sPPases represent a separate group but have same type of deletions as prokaryotic sPPases and show a closer similarity to *E. coli* than to animal/fungal sPPases (Sivula *et al*., 1999). In the phylogenetic tree, the internal identities between plant and prokaryotic sPPases vary from 27% (*Chlamydia trachomatis* versus *Hordeum vulgare*) to 49% (*Methanobacterium thermoautotrophicum* versus *Oryza sativa*), whereas internal identities of plant versus animal/fungal sPPase vary from 20% (*Hordeum vulgare* versus *Saccharomyces cerevisiae*) to 29% (*Solanum tuberosum* versus *Bos Taurus*) (**Figure 3.1**). Several plant pyrophosphatases were characterized during 1970s and 1980s and reports show their existence in different cell compartments (Bucke, 1970, Maslowski *et al*., 1977, du Jardin *et al*., 1995, Visser *et al*., 1998). There are significant variations among their molecular mass, subunit conformation, metal ion requirements and substrate specificity (Bucke, 1970, Simmons and Butler, 1969, Klemme and Jacobi, 1974, Pwee, 1995). From the sequence alignments of Family I sPPases, it has been found that plant sPPases have an extended N-terminal region (not present in bacterial E-PPases or Y-PPases) of unknown function (Sivula *et al*., 1999).

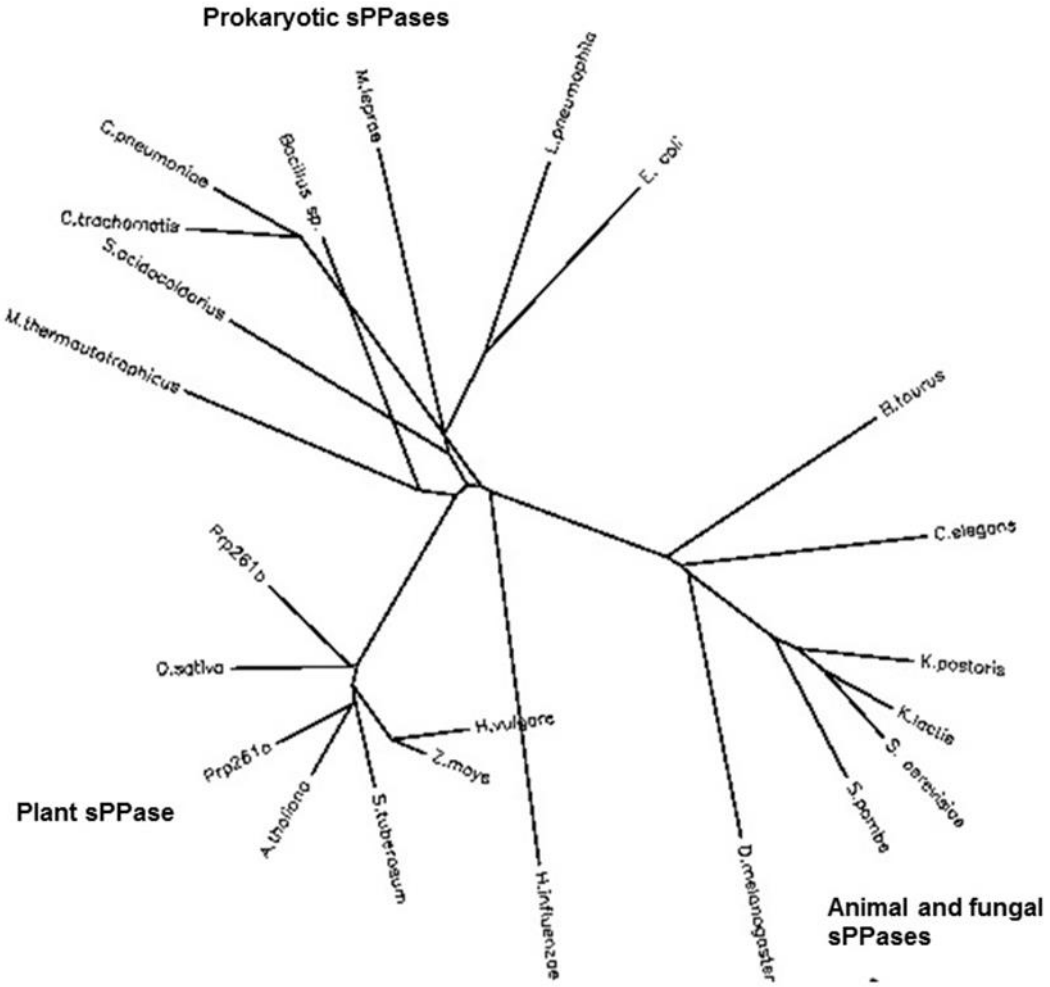

Figure 3.1. Phylogenetic tree of Family I sPPases.

Prokaryotic sPPases: *Methanothermobacter thermautotrophicus*, *Sulfolobus acidocaldarius, Chlamydia trachomatis, Chlamydophila pneumonia, Bacillus sp., Mycobacterium leprae, Legionella pneumophila, Escherichia coli, Haemophilus influenzae*

Plant sPPases: Papaver rhoeas (Pr-p26.1b)*, Oryza sativa, Papave rhoeas* (Pr-p26.1a), *Arabidopsis thaliana, Solanum tuberosum, Zea mays, Hordeum vulgare;*

Animal and fungal sPPases: *Drosophila melanogaster Schizosaccharomyces pombe, Saccharomyces cerevisiae, Kluyveromyces lactis, Komagataella pastoris, Caenorhabditis elegans, Bos Taurus.* Figure adapted and modified from Sivula *et al.* (1999)

Recently the crystal structure for *Arabidopsis thaliana* inorganic sPPases (AtPPA1) has been solved; it overlaps the other structures of known bacterial and yeast sPPases (Grzechowiak *et al*., 2013). In contrast to the bacterial and fungal enzymes, the eukaryotic sPPases from *Arabidopsis thaliana* (Gómez-García *et al*., 2006, Navarro-De la Sancha *et al*., 2007) *Chlamydomonas reinhardtii* (Gómez-García *et al*., 2006) and *Leshmania major* (Gómez-García et al., 2004, Gómez-García *et al*., 2007) are active monomers.

As described in **Chapter 1**, **Section 1.6.2.1.7**, two sPPases; Pr-p26.1a and Pr-p26.1b were identified as early targets for SI-Ca^{2+} and phosphorylation signals in incompatible pollen of *Papaver* (Rudd *et al.*, 1996, de Graaf *et al*., 2006). Pr-p26.1a and Pr-p26.1b from *Papaver rhoeas* shows strong homology to other plant sPPases. Pr-p26.1 are Mg^{2+}-dependent, Family I sPPases (de Graaf *et al*., 2006). In *Papaver* pollen they are thought to play an important role, by providing the driving force for the biosynthesis of pollen tube growth as this involves extensive biosynthesis of new membrane and cell wall. During SI in *Papaver* increases in $[Ca^{2+}]_i$ inhibit sPPase activity and also activates a calcium dependent protein kinase. This protein kinase is thought to be responsible for the phosphorylation of Pr-p26.1 sPPases causing a further decrease of their activity contributing to the pollen tube growth inhibition (de Graaf *et al*., 2006).

Phosphorylation of eukaryotic sPPases and their involvement in the signalling cascade have not been well reported to date. We know that the Pr-p26.1 sPPases are phosphorylated in a Ca^{2+} dependent manner, but it is unknown

where or on what specific sites the phosphorylation occurs. Our lab recently identified several phosphorylation sites on these two sPPases (Eaves, *et. al*.; unpublished data). We have examined the effect of mutating several of these phosphorylation sites and examined their effect on sPPases activity. We performed site directed mutagenesis in an attempt to identify phosphorylation site that might affect the sPPase activity of Pr-p26.1 and Pr-p26.1b.

As mentioned previously (**Chapter 1, Section 1.6.2.1.3**) it has been shown that during SI in *Papaver*, there is a dramatic drop of cytosolic pH. Within 10 min of SI pH drops from ~7.0 to pH ~ 6.4 and reaches to pH 5.5 after 60 min of SI (Wilkins *et al*., 2015). Cytosolic acidification is essential and sufficient to trigger numerous important hallmark features of the SI-PCD signalling pathway, particularly the activation of a DEVDase/caspase-3-like activity and SI-induced punctate foci formation. Alterations in cytosolic pH in the physiological conditions and its effect in the SI-induced events has been demonstrated (Wilkins *et al*., 2015). In this chapter we also investigated whether pH might affect the activity of the Pr-p26.1 sPPase. The effect of pH and divalent cations on the p26.1 sPPase activity *in vitro* was investigated.

As mentioned earlier (**Chapter 1, Section 1.6.2.1.6**) previous studies have shown that during SI signalling in *Papaver,* there is an increase in Reactive oxygen species (ROS) and Nitric oxide (NO) in a Ca^{2+} dependent manner and this event is involved in SI mediated PCD (Wilkins *et al*., 2011). In this chapter we also investigated the effect of H_2O_2, which is a form of ROS, in the presence and absence of Ca^{2+} to gain insights into how SI might affect Pr-p26.1 sPPases activity.

So far we have been unable to find any differences between Pr-p26.1a and Pr-p26.1b or explain why there are two sPPases. Hence we decided to study the further characteristics of Pr-p26.1 sPPases and to examine whether we could find any key differences between them. Although it had been established that Pr-p26.1a and Pr-p26.1b were sPPases, a detailed characterization of these enzymes had not been carried out. We therefore examined their catalytic properties in the presence of different divalent and monovalent metal ions, Ca^{2+}, fluoride, substrate specificity and pH.

3.2 Results

3.2.1 Effect of divalent metal ions on Pr-p26.1 sPPases activity

3.2.1.1 Effect of Mg^{2+} on recombinant Pr-p26.1 pyrophosphatase activity

It has been established that the Pr-p26.1 proteins are a family I soluble inorganic pyrophosphatases (sPPases). We have previously shown that Pr-p26.1a and 1b have a classic Mg^{2+} dependent sPPase activity (de Graaf et al., 2006).To determine the concentration of Mg^{2+} required for optimal activity Pr-p26.1 proteins were assayed using a range of $MgCl_2$ concentrations up to 10 mM (**Figure 3.2**). As expected, in the absence of $MgCl_2$ pyrophosphatase activity could not be detected. Maximal activity was observed at 2 mM $MgCl_2$ which was significantly higher than any other concentrations used (p=0.000***, **Figure 3.2**).

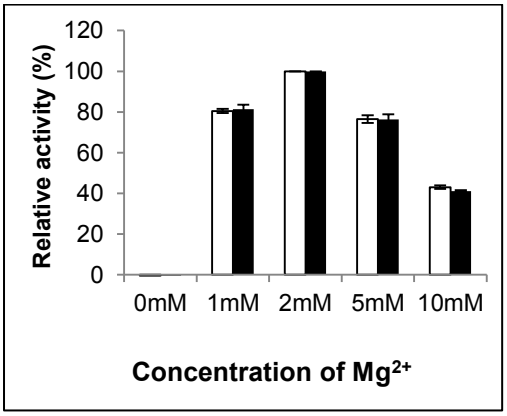

Figure 3.2. Effect of Mg^{2+} on the activity of Pr-p26.1a and Pr-p26.1b sPPases.

Pr-p26.1a and 1b enzymes (0.25µg) were assayed for pyrophosphatase activity in 50 mM propionic acid pH7.0 containing 2mM sodium pyrophosphate, 50µM EGTA and supplemented with different concentrations of $MgCl_2$. sPPase activity in the presence of 2mM $MgCl_2$ was considered as 100% activity. White bars and black bars represent the activity of Pr-p26.1a and Pr-p26.1b respectively. Data are mean ± SEM. (n=4).

In **Figure 3.2**, Pr-p26.1a and Pr-p26.1b showed 80.48% and 81.38% of maximal activity respectively at 1mM concentration and at 5mM concentration the activity was 76.47% and 76.35% for Pr-p26.1a and Pr-p26.1b respectively. There was no significant difference in activity of Pr-p26.1 sPPases between these two Mg^{2+} concentrations (1 mM and 5 mM) [Pr-p26.1a (NS, p=0.120, **Figure 3.2**), Pr-p26.1b (NS, p=0.088, **Figure 3.2**)]. Concentrations of $MgCl_2$ above 5mM were inhibitory to pyrophosphatase activity and significantly lower than the activity observed at 1mM, 2mM and 5mM concentration of $MgCl_2$ (p=0.000***, **Figure 3.2**). There was no significant difference between the activity of two sPPases, Pr-p26.1a and Pr-p26.1b at any concentration of $MgCl_2$ used for this experiment (NS, p=0.994, **Figure 3.2**).

Zn^{2+}, Co^{2+} and Mn^{2+} have favourable effects on the activity of prokaryotic sPPases. We investigated the effect of these cations on the activity of Pr-p26.1 sPPases and if there was any difference between Pr-p26.1a and Pr-p26.1b sPPases.

3.2.1.2 Effect of $ZnCl_2$ on Pr-p26.1 activity

Figure 3.3a shows that the Pr-p26.1 enzymes were able to effectively use 2mM $ZnCl_2$ for pyrophosphatase activity, although this activity was reduced to 62.98% for Pr-p26.1a and 59.45% for Pr-p26.1b compared to activity in 2mM $MgCl_2$ shown in **Figure 3.2**. The activity at 2mM $ZnCl_2$ was significantly higher than all other concentrations used (p=0.000***, **Figure 3.3a**). Activity with 5mM $ZnCl_2$ was 47.77% and 44.43% for p26.1a and p26.1b respectively. The lowest activity was obtained at 1mM $ZnCl_2$ which was 16.26% and 13.54% for

Pr-p26.1a and Pr-p26.1b respectively compared to the activity found at 2mM $MgCl_2$ (**Figure 3.2**). There was no significant difference between Pr-p26.1a and Pr-p26.1b in their activities at any concentration of $ZnCl_2$ used (NS., p=0.890; **Figure 3.3a**).

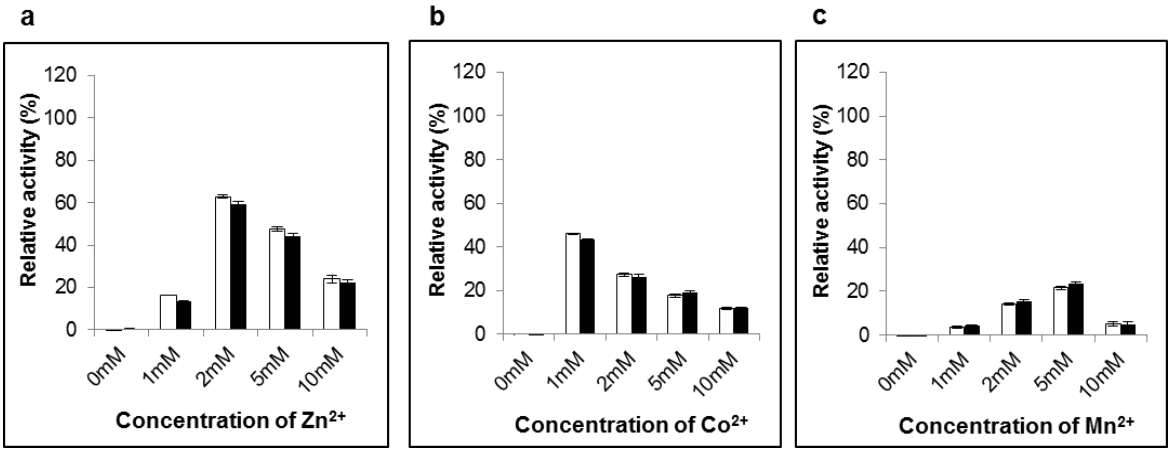

Figure 3.3. Effect of divalent metal ions on the activity of Pr-p26.1 pyrophosphatases.

Pr-p26.1 enzymes (0.25µg) were assayed for pyrophosphatase activity in 50mM propionic acid pH7.0 containing 2mM sodium pyrophosphate, 50µM EGTA and supplemented with a) $ZnCl_2$, b) $CoCl_2$ or c) $MnCl_2$ sPPase activity in the presence of 2mM $MgCl_2$ was considered as 100% activity. White bars and black bars represent the activity of Pr-p26.1a and Pr-p26.1b respectively. Data are mean ± SEM. (n=4).

3.2.1.3 Effect of $CoCl_2$ on Pr-p26.1a/1b sPPase activity

Cobalt also proved favourable for pyrophosphatase activity at 1mM concentrations of $CoCl_2$, significantly higher than any other concentration of $CoCl_2$ used (p=0.000***, **Figure 3.3b**). However this activity was 46.08% for Pr-p26.1a and 43.38% for Pr-p26.1b of the maximum obtainable activity with $MgCl_2$. Concentrations of $CoCl_2$ above 1mM became increasingly inhibitory

(**Figure 3.3b**). Again there was no difference between Pr-p26.1a and Pr-p26.1b observed.

3.2.1.4 Effect of $MnCl_2$ on the activity of Pr-p26.1 sPPase

A concentration of 5mM $MnCl_2$ was required to give a maximum activity of 21.46% for Pr-p26.1a and 23.58% for Pr-p26.1b with this ion (**Figure 3.3c**). Activity of Pr-p26.1 with 1mM, 2mM, 7mM and 10mM were significantly lower than the activity found at 5mM concentration (p=0.000***, **Figure.3.3c**).

Figure 3.2 and 3.3 illustrates that, Pr-p26.1 sPPases did not show any activity in the absence of the metal ions (**Figure 3.2 and 3.3a, b, c**). This demonstrates that, presence of divalent metal ions is essential for the hydrolysis of PPi by Pr-p26.1a and Pr-p26.1b and the order of metal ion preference is Mg^{2+}> Zn^{2+}> Co^{2+} > Mn^{2+}.

3.2.1.5 Ca^{2+} acts as an inhibitor of Pr-p26.1 pyrophosphatases

It is well known that Ca^{2+} is an inhibitor to family I sPPases (Cooperman *et al*., 1992). Previously we have shown Ca^{2+} to be a competitive inhibitor of Pr-p26.1a and 1b (de Graaf *et al*., 2006). We wanted to assess whether the $[Ca^{2+}]_i$ involved in *Papaver rhoeas* SI response can reduce Pr-p26.1 pyrophosphatase activity. We therefore examined in detail the Ca^{2+} concentrations required to inhibit Pr-p26.1 sPPase activity, in the presence of Mg^{2+}, as this was required for their activities.

Figure 3.4 shows that increasing concentrations of $CaCl_2$ up to 1mM in the presence of 2mM $MgCl_2$ results in total loss of Mg^{2+}-dependent

pyrophosphatase activity. Taking the activity at 0mM $CaCl_2$ (2mM $MgCl_2$, control) as 100%, 0.05 mM $CaCl_2$ reduced activity to 61.95% and 62.68% of the control for Pr-p26.1a and Pr-p26.1b respectively (**Figure 3.4**). 0.1 mM $CaCl_2$ reduced activity to 35.03% and 37.09% for Pr-p26.1a and Pr-p26.1b respectively. The activity of Pr-p26.1 pyrophosphatase at and above 0.2 mM $CaCl_2$ concentrations was significantly lower than the activity found using 0.1 mM $CaCl_2$ (p=0.000***, **Figure 3.4**). These results demonstrate that Ca^{2+} inhibits the activity of Pr-p26.1 sPPases at and above 0.2 mM concentrations, and that there is no significant difference between Pr-p26.1a and Pr-p26.1b in response to Ca^{2+}.

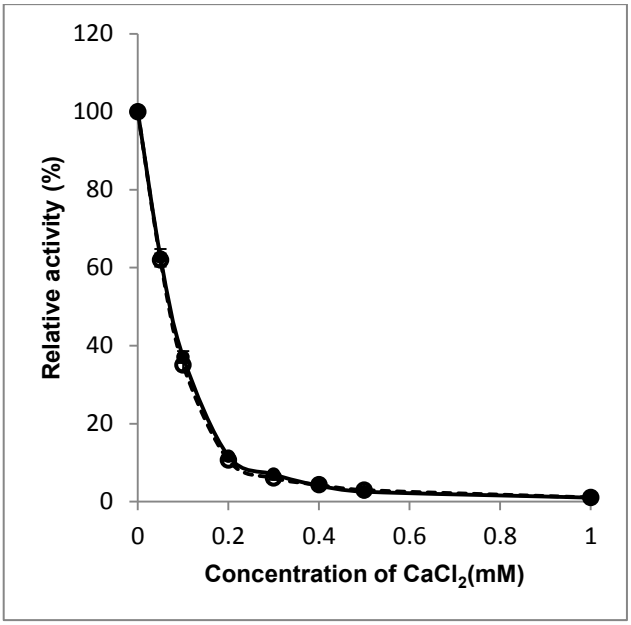

Figure 3.4. Effect of $CaCl_2$ on the activity of Pr-p26.1 pyrophosphatase.

50 mM propionic acid pH 7.0 containing 2mM sodium pyrophosphate was used as the assay buffer. 2mM $MgCl_2$ was added to the assay buffer along with $CaCl_2$. The discontinuous, Fiske-Subbarow method was used to determine inorganic phosphate release from 0.25µg inorganic pyrophosphatase Pr-p26.1 activity. The activity of Pr-p26.1a and Pr-p26.1b are shown by white bars and black bars respectively. Data are mean ± SEM. (n=4). Dashed line open circle Pr-p26.1a, Solid line solid circle Pr-p26.1b

3.2.1.6 Effect of fluoride on the activity of Pr-p26.1 sPPases

It is known that fluoride ions can strongly inhibit eukaryotic PPases by inhibiting hydrolysis at the attacking nucleophile site by freezing the reaction in the enzyme-substrate form (Baykov *et al*., 2000). This is a distinguishing feature between Family I and Family II pyrophosphatases. Varying concentrations of NaF ranging from 0 mM to 1.0 mM were used to investigate the influence of fluoride on Pr-p26.1 pyrophosphatases (**Figure 3.5**).

The Pr-p26.1a and Pr-p261b enzymes were inhibited to 45.87% and 47.13% respectively by 0.2 mM NaF and were completely inhibited by NaF at concentrations at and above 0.8mM (**Figure 3.5**). The sensitivity of these enzymes to F^- provides good evidence that they are Family I sPPases. However, again no difference between Pr-p26.1a and 1b was observed.

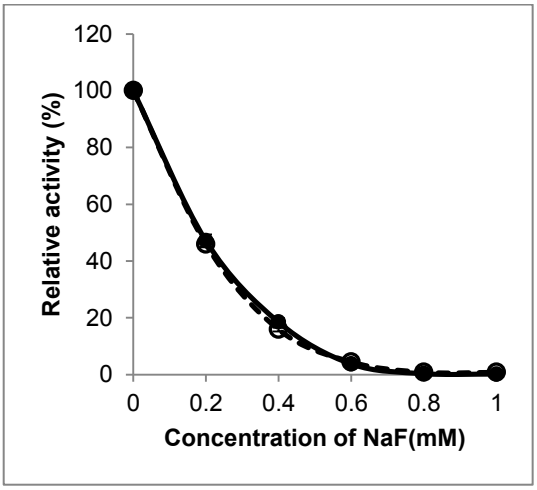

Figure 3.5. Effect of NaF on the activity of Pr-p26.1 pyrophosphatases.

Pr-p26.1 enzymes (0.25µg) were assayed for pyrophosphatase activity in 50mM propionic acid pH 7.0 containing 2mM sodium pyrophosphate, 5mM $MgCl_2$, 50µM EGTA and supplemented with varying concentrations of NaF ranging from 0mM to 1.0mM. Activity of the enzymes without NaF was considered as 100% activity. Data are mean ± SEM (n=4). Dashed line open circle represents Pr-p26.1a, solid line solid circle represents Pr-p26.1b

3.2.2 Effect of monovalent metal ions on Pr-p26.1 activity

3.2.2.1 Effect of KCl and NaCl on the Pr-p26.1 sPPases activity

Recent studies using electrophysiological method has demonstrated evidence for a large influx of K^+ in addition to Ca^{2+} influx in incompatible pollen (Wu *et al*., 2011). To assess whether monovalent metal ions have any effect on Pr-p26.1 sPPases activity, we investigated the effect of different concentrations of KCl and NaCl. **Figure 3.6** shows that there was no significant difference between the Pr-p26.1 pyrophosphatases activity for the concentrations used for both KCl (**Figure 3.6a**) and NaCl (**Figure 3.6b**) [KCl (Pr-p26.1a: p=0.353; Pr-p26.1b: p=0.101) NaCl (Pr-p26.1a: p=0.409; Pr-p26.1b: p=0.721)]. The enzymes showed full activity only in the presence of 2mM $MgCl_2$ with KCl or NaCl, however without $MgCl_2$ the activity of the enzymes were negligible for both of the metal ions at all concentrations (data not presented). This result demonstrates that monovalent metal ions like K^+ and Na^+ do not have any effect on the activity of the Pr-p26.1a and Pr-p26.1b sPPases.

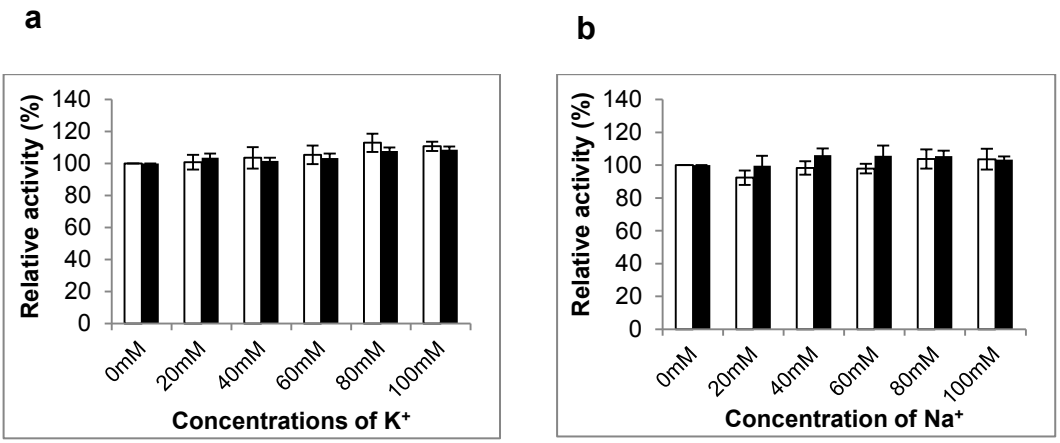

Figure 3.6. Effect of different concentrations of KCl (a) and NaCl (b) on Pr-p26.1a (white bars) and Pr-p26.1b (black bars) sPPases activity. 0.25µg enzymes were assayed in 50mM propionic acid pH 7.0 supplemented with 2mM sodium pyrophosphate using Fiske-Subbarow method. Different concentrations of a) KCl + 2mM $MgCl_2$ and b) NaCl + 2mM $MgCl_2$ were assayed. Data are mean ± SEM (n=4).

3.2.3 Effect of different ratios of Pr-p26.1a and Pr-p26.1b on their activity

To date, the crystal structure of the Pr-p26.1 sPPases is not available. However, the crystallographic structures of Family I sPPases from *E. coli* (Kankare *et al*., 1996) and *S. cerevisiae* (Heikinheimo *et al*., 1996b) have been solved and demonstrated that the active form of bacterial and yeast sPPases is oligomeric. So far we have been unable to find any differences between Pr-p26.1a and Pr-p26.1b. But the fact that we have 2 enzymes with different sequences suggests functional difference. We wondered whether the two forms might form an oligomer and wondered if this might change their characteristics.

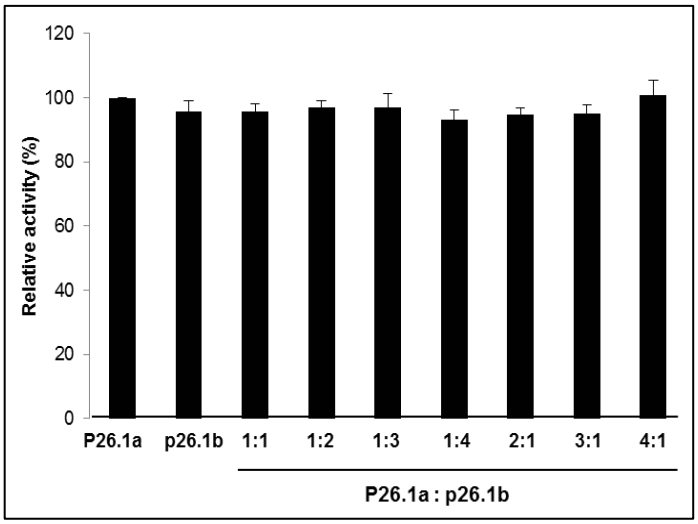

Figure 3.7. Effect of different ratio of Pr-p26.1a and Pr-p26.1b on their activity

Pr-p26.1a and Pr-p26.1b were mixed in different ratio keeping the total amount of protein 0.25µg and assayed in 50mM propionic acid pH 7.0 supplemented with 2mM sodium pyrophosphate using Fiske-Subbarow method. Data are mean ± SEM (n=4).

To investigate this, we mixed Pr-p26.1a and Pr-p26.1b at different ratios keeping an equal amount of total protein and tested the sPPase activity of the mixture. **Figure 3.7** shows that mixing of two enzymes at various ratios does not have any effect on their activity, though it was predicted that the association of subunits might interfere with their activity.

3.2.4 Substrate specificity

Generally inorganic pyrophosphate is the primary substrate for sPPases in the presence of divalent metal ions. Several other naturally occurring substrates are available including tri-phosphate and tetra-phosphate (Josse, 1966). In order to determine the substrate specificity of Pr-p26.1a and Pr-p26.1b enzymes the free phosphate released from various polyphosphates, nucleotide phosphates and sugar phosphates was determined using the

pyrophosphatase assay (See **Chapter 2**, **Section 2.14**). Pr-p26.1 sPPases exhibited very high pyrophosphatase activity for sodium pyrophosphate (100%) which is significantly higher than other substrates used (p=0.000***; **Table 3.1**). Both Pr-p26.1a and Pr-p26.1b enzymes could utilize sodium tripolyphosphate as a substrate releasing free phosphate to 23.32% and 26.84% of the true substrate sodium pyrophosphate (100%) by p26.1a and p26.1b respectively. The enzymes could also release phosphate from adenosine triphosphate and P', P-di tetraphosphate but at a rate of less than 6%. Phosphate released from all other derivatives was less than 2% (**Table 3.1**). This shows that Pr-p26.1 sPPase have similar characteristics to other Family I sPPase regarding substrate specificity.

Table 3.1. Substrate specificity of Pr-p26.1 sPPases. Phosphatase activity of Pr-p26.1a and Pr-p26.1b assayed in 50mM propionic acid pH 7.0 containing 2mM of different polyphosphate, nucleotide phosphate or sugar phosphate substrates, 2mM $MgCl_2$ and 50µM EGTA.

Substrates	**Specific activity (%)**	
	Pr-p26.1a	**Pr-p26.1b**
Sodium pyrophosphate	100	100
Sodium tripolyphosphate	23.32	26.84
P',P- Di tetraphosphate	4.53	5.67
ATP	4.49	3.65
Beta-glycerophosphate	<2	<2
Adenosine 2' monophosphate	<1	<1
Adenosine 3' monophosphate	<1	<1
Adenosine 5' monophosphate	<1	<1
Adenosine 2' 5' diphosphate	<1	<1
Adenosine 5' diphosphate	<1	<1
D-glucose-1-phosphate	<1	<1
D-glucose-6-phosphate	<1	<1

3.2.5 Effect of pH on Pr-p261a and Pr-p261b activity

Previous research showed that during SI the pollen cytosolic pH drops rapidly and dramatically from 7.0 to pH 5.5 (Wilkins *et al*., 2015).This is an early event of SI. We therefore investigated the effect of pH on Pr-p26.1 sPPases activity *in vitro*. We examined the activity of Pr-p26.1 sPPases in two different ways. Firstly, we investigated the effect of pH with a range from pH 5.0 to 9.0 which is normally used to characterise prokaryotic sPPases, secondly we used a pH range 5.0 to 7.0 which is biologically relevant to *Papaver* SI system.

3.2.5.1 Activity in acetate (pH 5.0-6.5) and Tris-HCl (pH 7.0-9.0) buffers

Firstly, we examined the effect of pH on the activity of Pr-p26.1 sPPases using a wider range of pH (pH 5.0-9.0), traditionally used for characterising the activity of *E. coli* sPPases. Here we used sodium acetate and Tris-HCl, which are the standard buffer for pyrophosphatase activity assays. The Pr-p26.1 sPPases showed highest activity at pH 8.0, reducing to 80.0% for Pr-p26.1a and 78.58% for Pr-p26.1b at pH7.5 (**Figure 3.8**). At pH 7.0 the activity of Pr-p26.1a and Pr-p26.1b was 74.8% and 72.1% respectively. The activity was trending towards 0% at pH 5.0. At alkaline conditions, at pH 9.0, 47.8% and 41.9% activity was observed for Pr-p26.1a and Pr-p26.1b respectively (**Figure 3.8**). Both Pr-p26.1a and Pr-p26.1b had similar pH profiles which demonstrate that a decrease in the pH causes reduction in pyrophosphatase activity, and also (yet again) reveals no difference between the propreties of Pr-p26.1a and 1b forms of the protein.

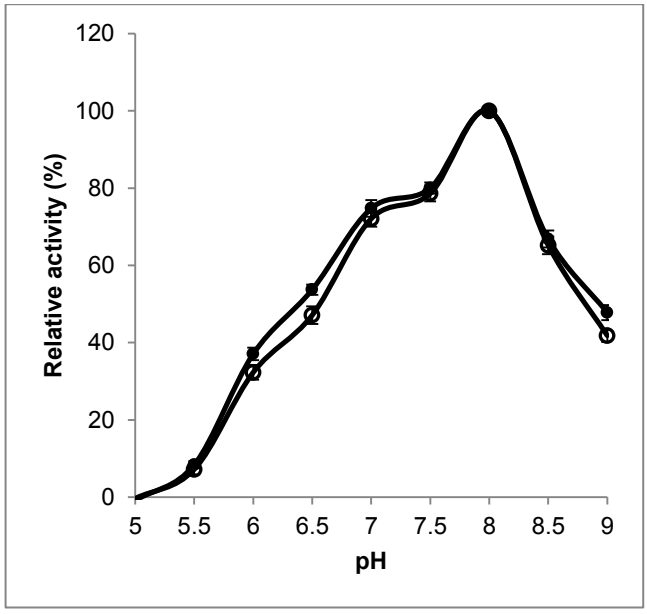

Figure 3.8. Effect of pH on the activity of Pr-p26.1 soluble pyrophosphatases.

Fiske-Subbarow method was used to determine the release of inorganic phosphate from 0.25µg inorganic pyrophosphatase Pr-p26.1 activity using 100mM sodium acetate (pH5-7) or 100mM Tris-HCl (pH7-9). Buffers contained 2mM sodium pyrophosphate, 2mM $MgCl_2$ and 50µM EGTA. Solid circle represents Pr-p26.1a, open circle is Pr-p26.1b. Data are mean ± SEM (n=4).

Though the highest activity of Pr-p26.1 sPPaes was observed at pH 8.0 we decided to look at the activity of these enzymes at a biologically relevant pH (pH 5.0- 7.0) in more detail.

3.2.5.2 Activity in propionic acid (pH 5.0-7.0) buffer

We used propionic acid to test the activity of Pr-p26.1a and Pr-p26.1b pyrophosphatases within the biological range of pH altered during SI-response, using pH 5.0 to pH 7.0. Propionic acid was chosen as buffer as

previously this weak acid was used to mimic the induction of cytosolic acidification in the pollen tube by SI response (Wilkins et al., 2015). At pH 7.0, which is normal physiological cytosolic pH of pollen, the Pr-p26.1 sPPases activity was high (shown as 100%, **Figure 3.9**).

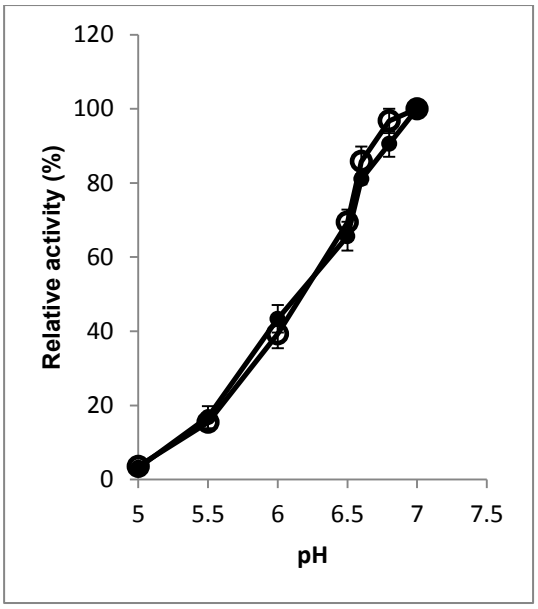

Figure 3.9. Effect of pH on the activity of Pr-p26.1a and Pr-p26.1b sPPases.

0.25µg enzymes were assayed in 50mM propionic acid (pH5.0-7.0) supplemented with 2mM sodium pyrophosphate using Fiske-Subbarow method. Solid circle represents Pr-p26.1a, open circle is Pr-p26.1b. Data are mean ± SEM (n=4).

At pH ~6.5, which reached within 10 minutes of SI induction, the sPPases activity of Pr-p26.1a and Pr-p26.1b was significantly reduced to 65.64% and 69.40% of their highest activity (p=0.000***; **Figure 3.9**). At pH 5.5 (cytosolic pH, 1hr after SI), sPPase activity was only 16.83% and 15.42% for Pr-p26.1a and Pr-p26.1b respectively. Thus, pH has a major effect on Pr-p26.1 sPPases activity. This work has been published in Plant Physiology:

WILKINS, K. A., BOSCH, M., HAQUE, T., TENG, N., POULTER, N. S. & FRANKLIN-TONG, V. E. 2015. Self-Incompatibility-induced Programmed Cell Death in poppy pollen involves dramatic acidification of the incompatible pollen tube cytosol. Plant Physiology, 167, 766-779.

See inserted paper in appendix I

My contribution: I investigated the effect of pH on Pr-p26.1a and Pr-p26.1b sPPases activity (Figure 5)

3.2.6 Site directed mutagenesis of Pr-p26.1 sPPases

3.2.6.1 Identification of *in vitro* phosphorylation sites of Pr-p26.1

Previous work has shown that SI-induced Ca^{2+}-dependent hyper-phosphorylation of Pr-p26.1 proteins occurs *in vitro* (Rudd *et al*., 1996, de Graaf *et al*., 2006). We determined the location of these phosphorylation sites, using two different approaches to phosphorylate the recombinant Pr-p26.1 sPPases *in vitro* (Eaves *et al*., unpublished). Firstly, recombinant Pr-p26.1 sPPases were phosphorylated using crude pollen extracts. Secondly, we used recombinant calcium dependent protein kinases identified as likely candidates responsible for phosphorylation of Pr-p26.1a (Tudor *et al*., unpublished data). Several different phosphorylation sites were identified from mass spectrometry analysis shown in **Figure 3.10**. These data were kindly provided by Dr. Deborah J. Eaves.

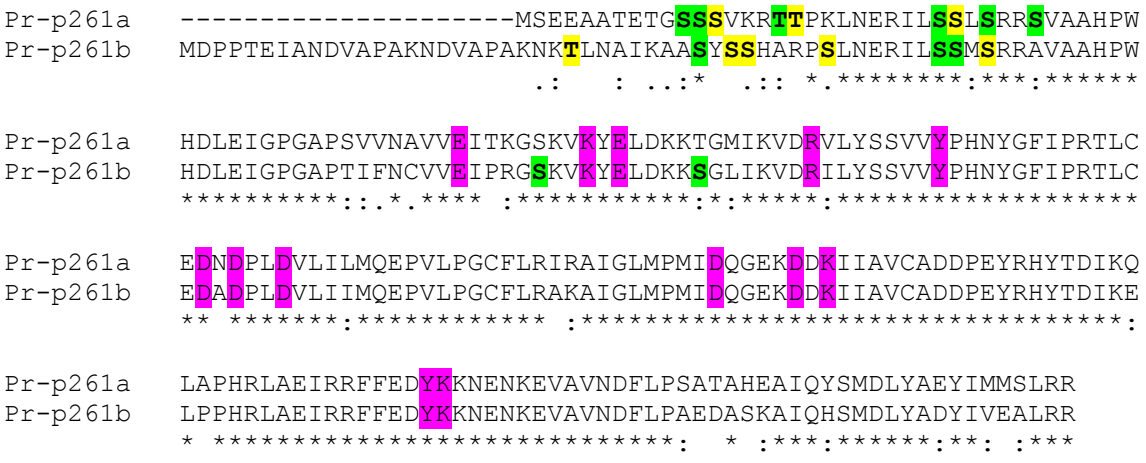

Figure 3.10. Phosphorylation sites on Pr-p26.1a and Pr-p26.1b.

Yellow highlighted amino acids are phosphorylated by endogenous pollen extracts and green amino acids are phosphorylated by recombinant protein kinases. Purple highlighted letters show functionally important active site residues.

Figure 3.10 shows that the identified phosphorylation sites are mainly in the N-terminal region, but not at/near the active site which might explain changes in activity. However, Pr-p26.1a and Pr-p26.1b phosphorylated differentially by both pollen extract and recombinant protein kinases. This is the first difference we have found between these two sPPases. Therefore it is of great interest to see if this might affect Pr-p26.1 activity as sPPases.

As mentioned earlier, SI-induced phosphorylation of Pr-p26.1 sPPases inhibits their activity (de Graaf *et al*., 2006). So first we wanted to investigate whether the phosphorylated residues identified in Pr-p26.1a and Pr-p26.1b were responsible for inactivation of the enzyme. Our approach was to use site directed mutagenesis.

3.2.6.2 Generation of site specific mutants

Phospho-mimic mutants can be constructed by replacing serine, tyrosine or threonine with aspartate (D) or glutamate (E) residues. The D or E provides a negative charge that can mimic phosphorylated proteins, thereby creating a "phospho-mimic" form of the protein. Mutating phosphorylation sites to an Alanine (A) provides a nonphosphorylatable control(phospho-null) form of the protein (Harper *et al*., 2004).

To make phospho-mimic mutants we substituted the phosphorylated sites with glutamic acid (E). We constructed several site specific mutants based on the phosphorylation sites identified (**Figure 3.10**). We constructed 3-site, 5-site or 7-site mutants by substituting with 3, 5 or 7 glutamate residues respectively (**Figure 3.11; Table 3.2a & b**). We also made phospho-null mutants by making Alanine substitutes. The procedure followed for mutagenesis is described in **Chapter 2** (**Section 2.13**).

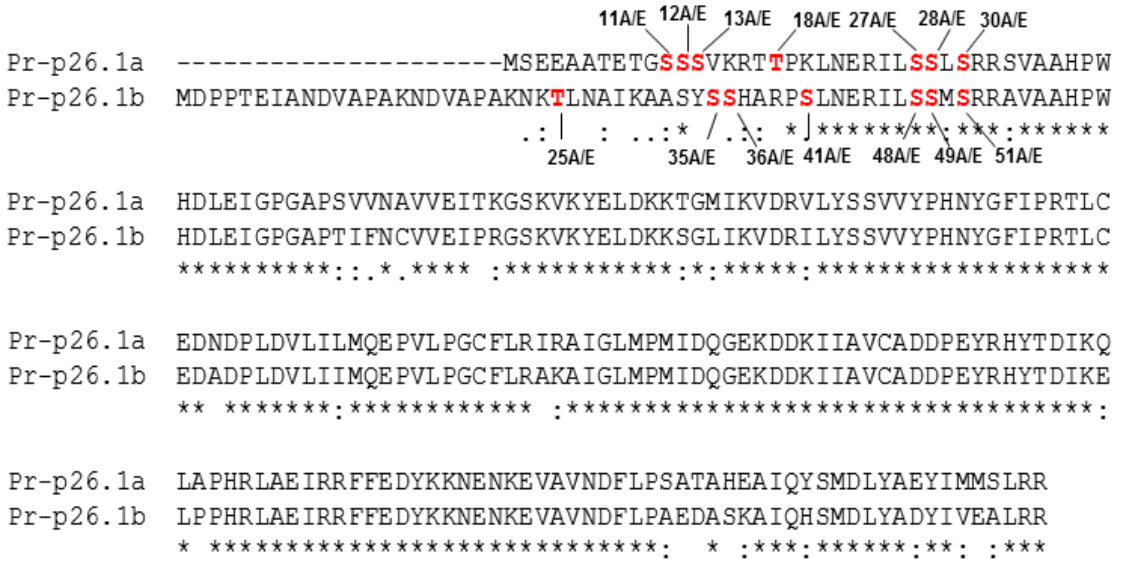

Figure 3.11. Phosphorylation sites on Pr-p26.1a and Pr-p26.1b (red letters; highlighted). Substitutions of alanine or glutamic acid on Pr-p261a are located at Ser11, Ser12, Ser13, Thr18, Ser27, Ser28 and Ser30. On Pr-p26.1b the location of substituted alanine and glutamic acid are on Thr25, Ser35, Ser36, Ser41, Ser48, Ser49 and Ser51. Phopho-mimic and phopho-null mutant shown in Table 3.1a and 3.1b are constructed based on these phosphorylation sites.

Table 3.2 a. Phospho-mimic (E) and Phospho-null (A) mutants Construct in pET21.b for overexpression of phosphorylation site substitution in Pr-p26.1a.

Protein/plasmid name		Substitutions	Constructed by
(3A; phospho-null)	3X	S13A, T18A, S27A	Richard Tudor
(3E; phospho-mimic)		S13E, T18E, S27E	Richard Tudor
(3A; phospho-null; Different sites)		S27A, S28A, S30A	Tamanna Haque
(3E; phospho-mimic)		S27E, S28E, S30E	Deborah J. Eaves
(5A; phospho-null)	5X	S13A, T18A, S27A, S28A, S30A	Tamanna Haque
(5E; phospho-mimic)		S13E, T18E, S27E, S28E, S30E	Deborah J. Eaves
(7A;phospho-null)	7X	S11A, S12A, S13A, T18A, S27A, S28A, S30A	Tamanna Haque
(7E; phospho-mimic)		S11E, S12E, S13E, T18E, S27E, S28E, S30E	Deborah J. Eaves

Figure 3.11 and **Table 3.2a & b** show the mutants constructed based on the phosphaorylated sites found previously (**Section 3.2.6.1**; **Figure 3.10**). 3XA/E, 5XA/E and 7XA/E indicate the 3-site, 5-site and 7-site mutations. The substitution column on **Table 3.2a & b** describes mutation on that particular site which was substituted by Alanine (A) for a phospho-null mutation or Glutamate (E) for a phospho-mimic mutation. For example, S13A indicates a mutation on Ser13 (See **Figure 3.11**) where Serine (Ser) was substituted by Alanine to create a phospho-null mutation on this amino acid.

Table 3.2b. Phospho-mimic (E) and Phospho-null (A) mutants construct in pET21.b for overexpression of phosphorylation site substitution in Pr-p26.1b

Protein/plasmid name		Substitutions	Constructed by
(3A;phospho-null)	3X	T25A, S41A, S51A	Richard Tudor
(3E;phospho-mimic)		T25E, S41E, S51E	Richard Tudor
(5A;phospho-null)	5X	T25A, S35A, S36A, S41A, S51A	Tamanna Haque
(5E;phospho-mimic)		T25E, S35E, S36E, S41E, S51E	Deborah J. Eaves
(7A;phospho-null)	7X	T25A, S35A, S36A, S41A, S48A, S49A, S51A	Tamanna Haque
(7E;phospho-mimic)		T25E, S35E, S36E, S41E, S48E, S49E, S51E	Deborah J. Eaves

The recombinant protrein mutants shown in the **Table 3.2a & b** were studied to investigate their sPPase activities in the presence of different metal ions (3-site mutants), pH, Ca^{2+} and H_2O_2 to establish if the mutation had any effect on sPPase activity.

3.2.7 Effect of different metal ions on phospho-mimic mutant Pr-p26.1 (3E, triple)

Previous studies demonstrated that SI induced phosphorylation of Pr-p26.1 sPPase reduced their activity and inhibited pollen tube growth (de Graaf *et al*., 2006). We wished to investigate whether the phospho-mimic mutants constructed on the basis of the identified phosphorylation sites in Pr-p26.1a

and Pr-p26.1b could inhibit their activities. We therefore measured the catalytic properties of these sPPases phospho-mimic mutants (0.25 μM) with the different metal ions used before (see **Section 3.2.1**). We chose the optimal concentrations of metal ions (2mM $MgCl_2$, 2mM $ZnCl_2$, 1mM $CoCl_2$ and 5mM $MnCl_2$) to determine their effect on phospho-mimic mutants at which Pr-p26.1a and Pr-p26.1b showed their highest activity (**Section 3.2.1**). The phospho-null (Alanine substituted) Pr-p26.1 enzymes (S13A, T18A and S27A) and the triple phospho-mimic (Glutamate substituted) enzymes (S13E, T18E and S27E) were assayed for sPPase activity in the presence of the different metal ions. To compare the activity between mutant and wild type enzymes, Pr-p26.1a and Pr-p26.1b were also assayed for sPPase activity along with their correspondent mutants (**Figure 3.12a and b**).

Figure 3.12a shows that there were no significant differences in sPPases activities between the wild type Pr-p26.1a, phospho-null and phospho-mimic enzymes using any of the specific metal ions (NS, p=0.205; **Figure 3.12a**). All three enzymes exhibited highest activities with 2mM $MgCl_2$ which was significantly different from the activity with other metal ions (p=0.000; **Figure 3.12a**). The effectiveness of cations as cofactors for Pr-p26.1a, phospho-null (3A) and phospho-mimic (3E) was in order of Mg^{2+}> Zn^{2+}> Co^{2+}> Mn^{2+}. The phospho-null triple (Alanine substituted) Pr-p26.1b enzyme (T25A, S41A and S51A) and the triple phospho-mimic mutants (Glutamate substituted) (T25E, S41E and S51E) also showed similar sPPase activity as we found with the Pr-p26.1a mutants (**Figure 3.12b**). These data show that phosphorylation at these three sites have no effect on sPPase activity.

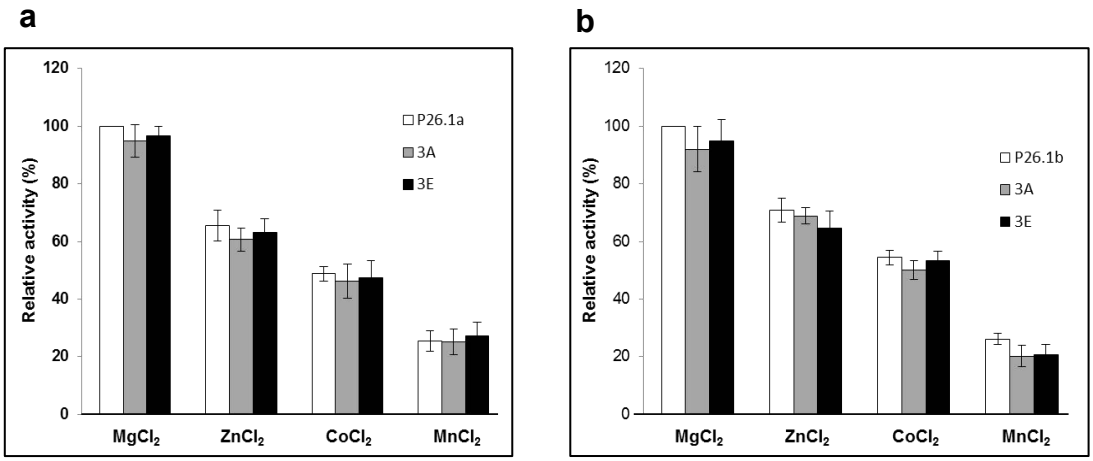

Figure 3.12. Effect of Mg^{2+}, Zn^{2+}, Co^{2+} and Mn^{2+} on a) Pr-p26.1a, Alanine substituted Pr-p26.1a (3A) and Glutamic acid substituted Pr-p26.1a (3E) and b) Pr-p26.1b, Alanine substituted Pr-p26.1b(3A) and Glutamic acid substituted Pr-p26.1b(3E). 0.25µg enzymes were assayed in 50mM propionic acid pH 7.0 supplemented with 2mM sodium pyrophosphate. 2mM $MgCl_2$, 2mM $ZnCl_2$, 1mM $CoCl_2$ or 5mM $MnCl_2$ were used to determine the activity of the enzymes. White, grey and black bars represent the activity of a) Pr-p26.1a, Alanine substituted Pr-p26.1a (3A) and Glutamic acid substituted Pr-p26.1a (3E) and b) Pr-p26.1b, Alanine substituted Pr-p26.1b (3A) and Glutamic acid substituted Pr-p26.1b (3E) respectively. Data are mean ± SEM (n=4).

3.2.8 Effect of different ratios of mutants on their activity

We also investigated the effect of different ratios of Pr-p26.1a and Pr-p26.1b in **section 3.2.3** hoping that mixing of two enzymes might change their properties and hence might affect sPPase activity. However, we didn't get any effect on the sPPase activity. However, we wondered if the mixing of different ratio of phospho-mimic mutants might change their sPPase activity. We mixed 3E, 5E and 7E phospho-mimic mutants of Pr-p26.1a with 3E, 5E and 7E phospho-mimic mutants of Pr-p26.1b at different ratio keeping equal amount of total protein. **Figure 3.13** shows that mixing of two phospho-mimic mutants at various ratios did not have any effect on their activity either (**Figure 3.13 a,**

b, c) though it was predicted that the association of subunits might interfere their activity. There was no significant difference between any comparison [(NS, p= 0.308; **Figure 3.13 a**); (NS, p=0.861; **Figure 3.13 b**); (NS, p=0.690; **Figure 3.13 c**)]

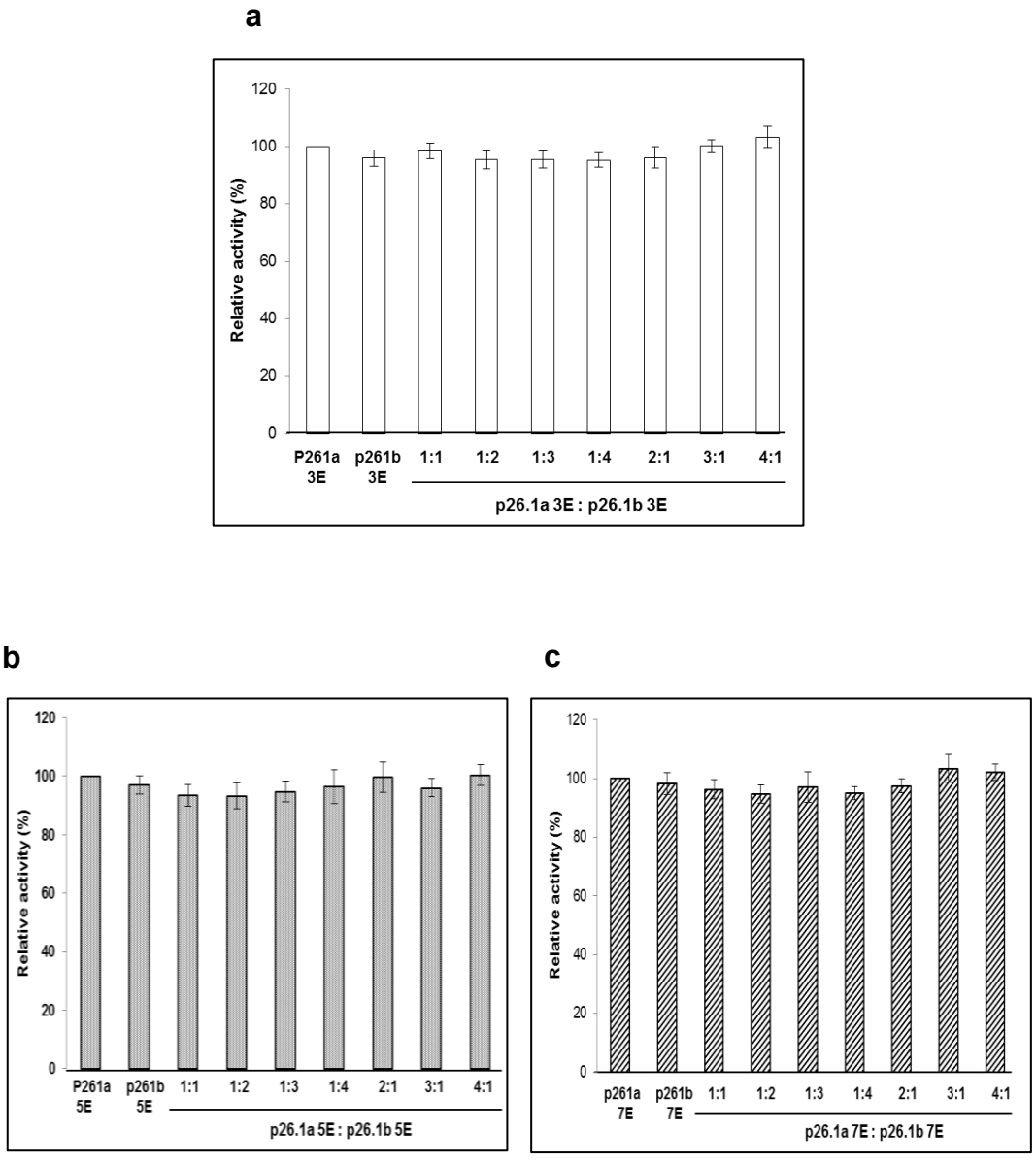

Figure 3.13. Effect of different ratios between a) Pr-p26.1a and Pr-p26.1b b) Pr-p26.1a 3E and Pr-p26.1b 3E; c) Pr-p26.1a 5E and Pr-p26.1b 5E d) Prp26.1a 7E and Prp26.1b 7E on their activity. Pr-p26.1a and Pr-p26.1b and their multiple site glutamic acid substituted mutants (3E, 5E, 7E = 3, 5, 7 glutamic acid substitutions respectively) were assayed in propionic acid pH 7.0 buffer. Data are mean ± SEM (n=4).

3.2.9 Effect of pH on the phospho-mimic mutant

Previously we showed that pH has a dramatic effect on the activity of Pr-p26.1 sPPases (**Section 3.2.5**). We wished to investigate whether pH affected the sPPase activity of phospho-mimic mutant in the same manner comparing with the wild type Pr-p26.1 at different pH. **Figure 3.14** and **3.15** show that sPPase activity of the phospho-mimic mutants were affected dramatically and differentially by pH. There was no significant difference of activity between the Pr-p26.1 wild type and phospho-null and phopho-mimic mutants at pH 7.0 [Pr-p26.1a (NS, P= 0.772) **Figure 3.14;** Pr-p26.1b (NS, p= 0.109) **Figure 3.15**].

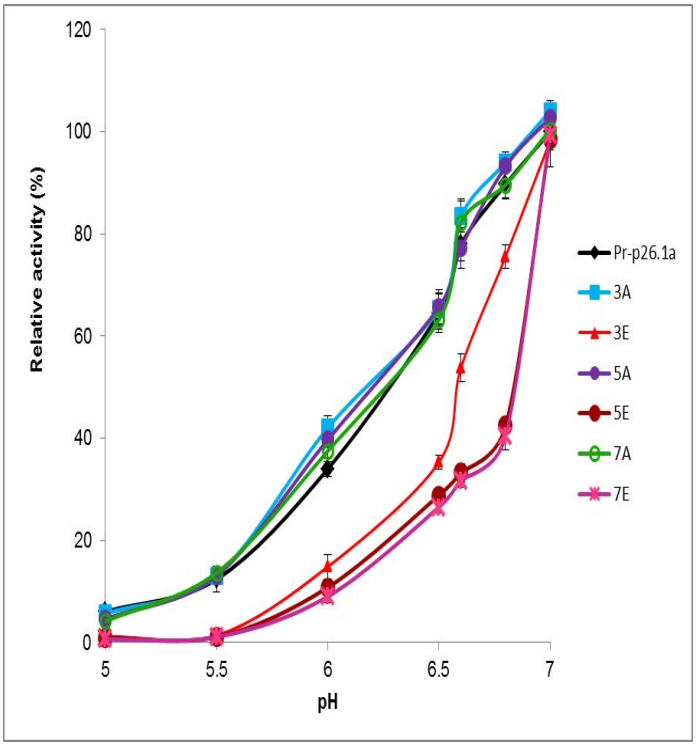

Figure 3.14. Effect of pH on the activity of phospho-mimic mutant of Pr-p26.1a soluble pyrophosphatases.

Pr-p26.1a , different site phospho-null (3A, 5A, 7A), phospho-mimic mutant (3E, 5E, 7E) were assayed with 50mM propionic acid with varying pH containing 2mM sodium pyrophosphate and 50μM EGTA . Data are mean ± SEM (n=4).

However, at pH 6.8 there was a large drop in sPPase activity of all the phospho-mimic mutants, reducing to 75.61% for Pr-p26.1a 3E (**Figure 3.14**) and 69.52% for Pr-p26.1b 3E (**Figure 3.15**) which was significantly lower than wild type and phopho-null mutants (p=0.000***; **Figure 3.14 & 3.15**). The drop in sPPase activity at pH 6.8 for 5E and 7E mutants was even more dramatic, reducing to 42.53% and 40.72% for Pr-p26.1a 5E and 7E (**Figure 3.14**) and 39.38% and 37.46% for Pr-p26.1b 5E and 7E (**Figure 3.15**) respectively. Up to pH 6.5 the 5E and 7E mutant showed significant differences in sPPase activity compared to the 3E mutant (p=0.000***; **Figure 3.14 & 3.15**). The sPPase activity of Pr-p26.1a 3E, 5E and 7E at pH 6.5 was 39.01%, 28.84% and 26.53% (**Figure 3.14**) and for Pr-p26.1b 3E, 5E, and 7E was 34.67%, 19.43% and 22.81% respectively (**Figure 3.15**). Once the sPPase activity had dropped to this level, there was no further significant difference of activity between the 3E, 5E and 7E mutants at pH 6.0, 5.5 and 5.0 for both Pr-p26.1a and Pr-p26.1b. The activity of phosphomimic mutants was significantly lower compared to the wild type and phospho-null mutant at pH 5.0, 5.5 and 6.0. [(p=0.002**; **Figure 3.14**); (p=0.000***; **Figure 3.15**)]. This provides evidence that phosphorylation has an effect on Pr-p26.1 sPPases activity in the presence of varying pH. Moreover, it also revealed differences between Pr-p26.1a and Pr-p26.1b activities

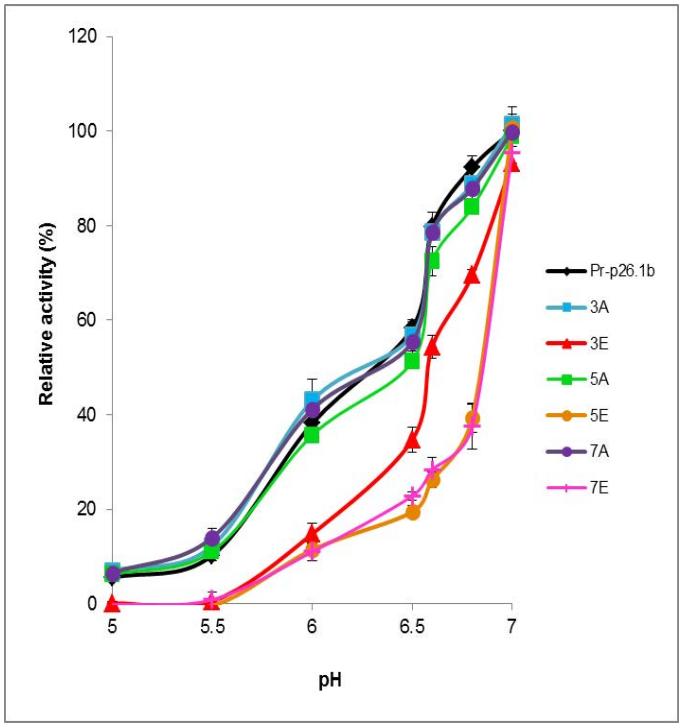

Figure 3.15. Effect of pH on the activity of phospho-mimic mutant of Pr-p26.1b soluble pyrophosphatases.

Pr-p26.1b, phospho null (3A, 5A,7A), phospho mimic mutant (3E, 5E,7E) were assayed with 50mM propionic acid with varying pH containing 2mM sodium pyrophosphate and 50µM EGTA . Data are mean ± SEM (n=4).

The phospho-mimic mutants from Pr-p26.1a and Pr-p26.1b did not show significant differences in sPPase activity compared to each other except for the 5E mutant. The activity of 5E mutant from Pr-p26.1a and Pr-p26.1b was significantly different at pH 6.5, 6.6 and 6.8 (p=0.001***; p=0.009**; p=0.024* respectively) although no significant difference was observed at other pH points. This provides the first data showing a difference between Pr-p26.1a and Pr-p26.1b sPPases activity.

These data demonstrate that phospho-mimic mutants behave differently with different pH. At lower pH the sPPase activity of phospho-mimic mutants is

nearly zero. The difference in sPPase activity between the 3E, 5E and 7E mutants suggests that the phosphorylation site has an effect on sPPase activity.

3.2.10 Effect of Ca^{2+} and H_2O_2 on the activity of phospho-null and phospho-mimic mutants of Pr-p26.1

It has been shown in previous studies that during SI there is a rise of ROS and NO in incompatible pollen of *Papaver* and they are dependent on Ca^{2+} influx (Wilkins *et al*., 2011). Increases in both ROS and NO have been shown to be involved in the SI mediated PCD in *Papaver.* As increases in ROS are a key pivotal early event of SI and related to increases in Ca^{2+}which we know affects on sPPase activity, we wished to investigate whether ROS had any effect on Pr-p26.1 sPPases and their phospho-mimic mutants because Ca^{2+} dependent phosphorylation of Pr-p26.1 is also an early event of SI.

We assayed the effect of Ca^{2+} and H_2O_2 on the activity of Pr-p26.1 sPPases and their multiple site mutants. Either 0.1mM $CaCl_2$ or 10mM H_2O_2 or combination of $CaCl_2$ and H_2O_2 were added to the assay buffer to determine their effect on the wild type enzymes (either Pr-p26.1a or Pr-p26.1b) and the various phopho mutants (Phospho-null = alanine substitution, 3A, 5A, 7A; Phospho-mimic = Glutamate substitution, 3E, 5E, 7E; See **table 3.2a & b**)

There were no significant differences between the sPPase activities of Pr-p26.1a wild type, phospho-null mutants 3A, 5A and 7A and phopho-mimic mutants 3E, 5E and 7E in the absence of Ca^{2+} or H_2O_2 (using Pr-p26.1a wild type as 100%; p=0.674; NS, **Figure 3.16**).

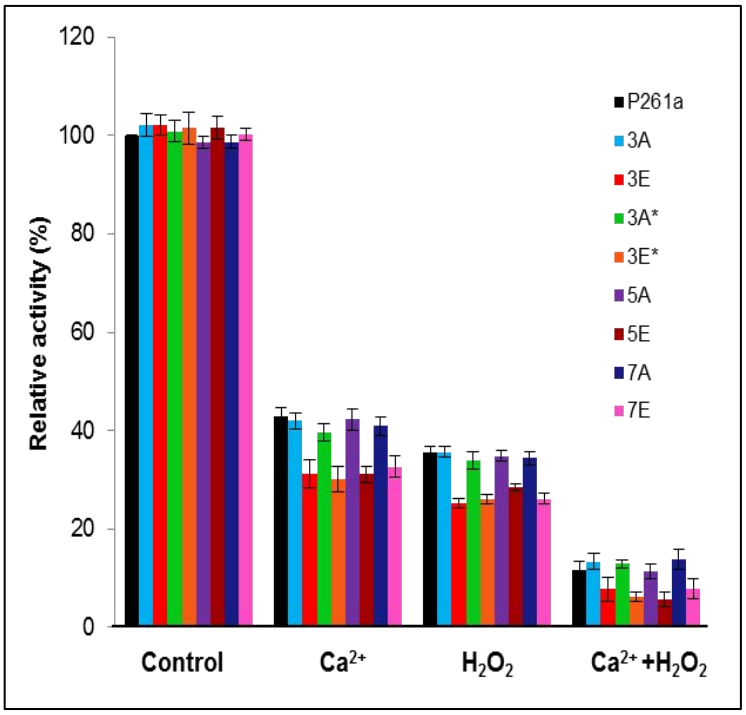

Figure 3.16. Effect of Ca^{2+} and H_2O_2 on Pr-p26.1a (wild type), phospho-null mutants [3A, 3A*(different site), 5A, 7A] and phospho-mimic mutant [3E, 3E*(different site), 5E, 7E].

Control data represent the activities of wild type and multiple site mutants without any treatment; (i.e. without Ca^{2+} or H_2O_2) Multiple site mutants (3A, 5A and 7A=3, 5, 7 alanine substitutions respectively; 3E, 5E, 7E = 3, 5, 7 glutamic acid substitutions respectively) were assayed along with their wild type non-mutated enzymes in propionic acid pH 7.0 buffer. Data are mean ± SEM (n=4).

As expected, Ca^{2+} showed a significant inhibitory effect, reducing the activities of non-mutated wild type, phospho-null and phospho-mimic mutants to less than 50% compared to the control (p=0.000***; **Figure 3.16**). There was no significant difference between the sPPase activity of the wild type and phopho-null mutant in the presence of Ca^{2+} (NS, p=0.899). However the sPPase activities of all the phopho-mimic mutants (3E, 3E*, 5E, 7E) were significantly less than their corresponding phospho-null mutants (3A, 3A*, 5A, 7A)

[(p=0.022*; 3A versus 3E); (p=0.018*; 5A versus 5E);(p=0.038*; 7A versus 7E); **Figure 3.16**]. This result suggests phosphorylation of Ser11, Ser12, Ser13, Thr18, Ser27, Ser28 and Ser30 amino acids has an effect on Pr-p26.1 sPPase activity in the presence of Ca^{2+}.

H_2O_2 also demonstrated an inhibitory effect on the activity of all the enzymes used in this experiment. Similar to the effect of Ca^{2+}, the sPPase activity of all the phopho-mimic mutants was significantly lower compared to their corresponding phopho-null mutants [(p=0.038*; 3A versus 3E);(p=0.030*; 5A versus 5E);(p=0.022*; 7A versus 7E); **Figure 3.16**]. These data demonstrate that phopho-mimic mutant has lower sPPase activity than the wild type and phospho-null mutants in the presence of H_2O_2.

Strikingly, the additive effects of Ca^{2+} and H_2O_2 was much larger than their individual effect. All the mutants showed less than 20% activity than the control when Ca^{2+} and H_2O_2 were added together, which was significantly lower than the activity found using the Ca^{2+} and H_2O_2 separately (p=0.000***; **Figure 3.16**). The phospho-mimic mutants also showed significantly lower sPPases activity than their comparable same site phospho-null mutants [(p=0.027*; 3A versus 3E); (p=0.002**; 5A versus 5E); (p=0.007**; 7A versus 7E); **Figure 3.16**].

Pr-p26.1b wild type and its phopho-null and phospho-mimic mutants also showed similar response as we observed in **Figure 3.16** using $CaCl_2$, H_2O_2 and addition of $CaCl_2$ and H_2O_2 together (**Figure 3.17**).

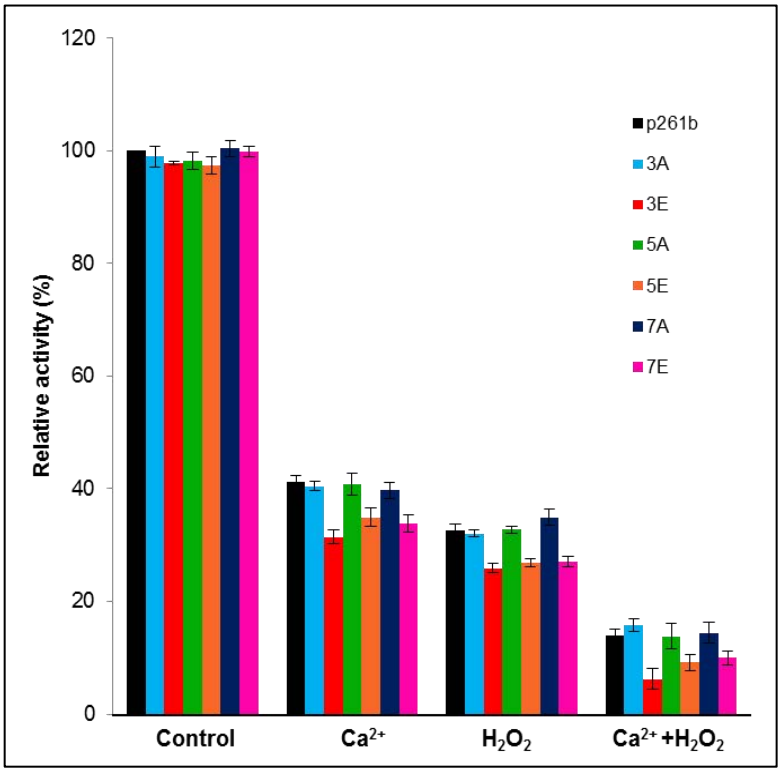

Figure 3.17. Effect of $CaCl_2$ and H_2O_2 Pr-p26.1b (wild type), phospho-null (3A, 5A, 7A) and phospho-mimic mutants (3E, 5E, 7E).

Multiple site mutants (3A, 5A and 7A=3, 5, 7 alanine substitutions respectively; 3E, 5E, 7E = 3, 5, 7 glutamic acid substitutions respectively) were assayed along with their wild type enzymes in propionic acid pH 7.0 buffer. Data are mean ± SEM (n=4).

The activity of wild type and all the mutants was reduced significantly comparing to the control treatment when Ca^{2+} or H_2O_2 was added to the assay buffer (p=0.000***; **Figure 3.17**). The activity of the wild type and mutants was reduced to less than 50% and 40% when Ca^{2+} and H_2O_2 were added to the assay buffer respectively. Thus Ca^{2+} and H_2O_2 strongly inhibit sPPase activity. Phopho-mimic mutants (3E, 5E, 7E) showed significantly lower activity than

the wild type and phopho-null mutants (3A, 5A, 7A) when Ca^{2+} was added (p=0.000***; **Figure 3.17**).

Similarly, there were significant differences between the sPPase activity of wild type and phospho-null with the phospho-mimic mutants with H_2O_2 treatment (P=0.012*; **Figure 3.17**). The sPPase activity of Pr-p26.1b wild type, and its phospho-null and phospho-mimic mutant showed less than 20% activity when Ca^{2+} and H_2O_2 were added together. Here as well, the sPPase activity of phospho-mimic mutants was significantly lower than the wild type or phospho-null mutant (p=0.000***; **Figure 3.17**). This provides evidence that phosphorylation can affect sPPase activity in the presence of Ca^{2+} and H_2O_2.

3.3 Discussion

Soluble inorganic pyrophosphatases are crucial for life. They affect essential biosynthetic reactions such as protein, DNA/RNA and polysaccharides synthesis (Cooperman *et al*., 1992). The sPPases identified in *Papaver rhoeas*, the Pr-p26.1 proteins have a vital function in pollen tube growth and were found to play a key role in SI (de Graaf *et al*., 2006). When Pr-p26.1 proteins are phosphorylated during SI, the activities of these sPPases are reduced; as a result, the pollen tube growth in inhibited (de Graaf *et al*., 2006).

As Pr-p26.1a/b had both previously been poorly characterized, the aim of this part of the project was to characterize Pr-p26.1a and Pr-p26.1b using different metal ions standard for sPPases. We also examined the effect of several biologically relevant events that are involved in *Papaver* SI: the effect of Ca^{2+}, pH and ROS on their own and combined effect. We also examined the effect of mutating several phosphorylation sites on Pr-p26.1a and Pr-p26.1b recently identified by our lab to examine if the identified phosphorylation sites are involved in regulation of sPPases activity and so potential role in SI.

3.3.1 Metal ion requirements

It has been established that plant sPPases are more closely related to prokaryotic sPPases than animal/fungal sPPases (Sivula *et al*., 1999). Thus plant pyrophosphatases might be expected to have similar properties to prokaryotic sPPases. The ideal concentration of divalent metal ions for prokaryotic sPPases activity is 5mM at pH 7.2 (Heikinheimo *et al.*, 1996a). The optimum Mg^{2+} concentration for Pr-p26.1 pyrophosphatases was 2mM at pH 7.0, although high activity was obtained using 1mM and 5mM Mg^{2+}. The

activity of Pr-p26.1 using Mg^{2+} concentration above 5mM showed a reduction in activity. This result suggests that the optimum Mg^{2+} concentration for Pr-p26.1 activity is between 1-5 mM. The optimum charge at the active site of the enzyme is suitable for the Mg^{2+} ions. The hydroxide ion binds to two metal ions to become stabilized (**Figure 3.18**). A third metal ion is used to bring together a water molecule and protonate the leaving group (Heikinheimo *et al*., 1996a). The activity of the enzyme reduced when more than 5mM Mg^{2+} was added. Presence of too many Mg^{2+} ions might be responsible to lower the pH. Accordingly the pK_a of the catalytic environment is altered. This altered environment is not suitable for the metal ions to coordinate as it could do between 1-5 mM Mg^{2+}.

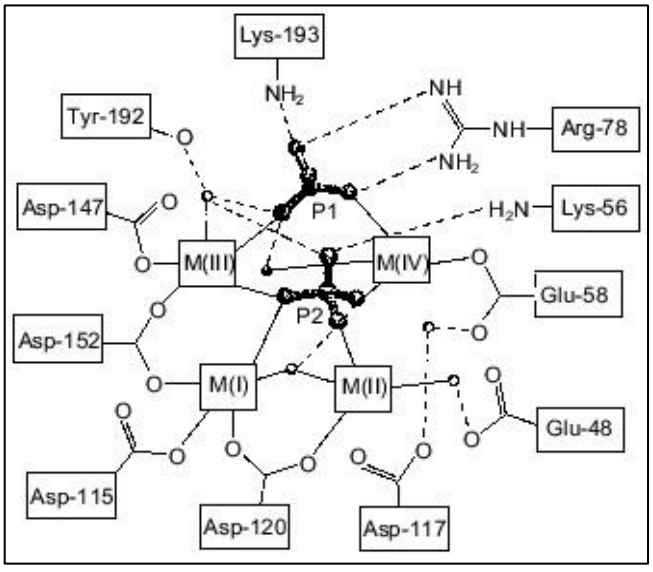

Figure 3.18. Structure of Y-PPase showing phosphates (P1 & P2) and metal ions disposition. Four metal ion binding sites are shown as M (I-IV). PPi hydrolysis rate is maximal by the enzyme when the sites are accupied by 3/4 Mg^{2+}. Binding of Ca^{2+} in M (IV) is inhibitory. Small circles represented the water molecules. Solid lines represented contacts of metal ions and dotted lines show the hydrogen bond. Figure is adapted from Avaeva (2000).

Research has revealed that sPPases have highest activity when Mg^{2+} is used as the cofactor for the enzymes active site. After Mg^{2+}, significant activity is also observed in the presence of Zn^{2+}, Co^{2+} or Mn^{2+} (Cooperman *et al*., 1992). *Pyrococcus horikoshii,* a family I sPPases also utilise these metal ions effectively for its activity (Jeon and Ishikawa, 2005). This is in agreement with the results obtained in this chapter. Pr-p26.1 pyrophosphatases showed appreciable activity using 2mM Zn^{2+}, 1mM Co^{2+} and 5mM Mn^{2+}. The effectiveness of the cations as cofactors can be arranged in order of Mg^{2+}> Zn^{2+}> Co^{2+} > Mn^{2+}.

3.3.2 Inhibitors of Pr-p26.1 sPPases

Ca^{2+} is an effective inhibitor of magnesium pyrophosphate hydrolysis. At concentrations above the physiological level (normal intercellular Ca^{2+} concentration is 10^{-7} to 10^{-6} M (Uribe *et al*., 1993, Williams, 1998), Ca^{2+} ions are strongly inhibitory to Family I sPPases because of the development of Ca.PPi complex (Kurilova *et al*., 1984), which acts as a competitive inhibitor of Mg.PPi . In *E. coli*, Ca^{2+} ions are able to replace Mg^{2+} ions from the substrate and also from the enzyme to inhibit enzymes activity (Kurilova *et al*., 1983). All other sPPases also showed similar results (Fraichard *et al*., 1996, Uribe *et al*., 1993, Davidson and Halestrap, 1989). This suggests that inhibition by Ca^{2+} is common to all sPPases.

Ca^{2+} is the sPPase's natural inhibitor, and here we have shown that it reduces Pr-p26.1 sPPases activity at concentrations above 0.05mM and completely inhibited at 0.2mM concentration. During *Papaver* SI, $[Ca^{2+}]_i$ concentration increases in the sub apical region of the pollen tube up to 1-2μM (Franklin-

Tong *et al*., 1997) and after that Pr-p26.1 sPPases are phosphorylated and their activity decreased. Here the Ca^{2+} concentration finding is far higher than that during SI. This is probably because of the difference between *in vivo* and *in vitro* experiments.

In addition to Ca^{2+}, fluoride also inhibited the sPPase activity of Pr-p26.1a, which was expected as sensitivity to fluoride is an important characteristics of Family I sPPases. Hydrolysis of PPi in Family I pyrophophatases is carried out by an associative mechanism in which the electrophilic phosphate moiety of PPi is attacked by an activated water molecule nucleophile. The metal-coordination of the nucleophile makes Family I sPPases very vulnerable to fluoride inhibition as this ion can easily substitute the emerging hydroxide ion, through stabilizing the enzyme-substrate complex, apparently due to replacement of the nucleophilic water molecule in the active site (Baykov *et al*., 1992).

3.3.3 Substrate specificity of Pr-p26.1a/b

sPPases display absolute substrate specificity in the presence of its physiological activator Mg^{2+}. Inorganic pyrophosphate is generally the main substrate for soluble sPPase. Two other naturally occurring substrates are tri-phosphate and tetra-phosphate, which are also hydrolysed in the presence of Mg^{2+} ions (Josse, 1966). Here we have shown that Pr-p26.1 sPPases from *Papaver* also showed the highest activity in the presence of inorganic pyrophosphate. This was expected. However we also found that Pr-p26.1 sPPases were able to hydrolyse tri- and tetra-polyphosphates at a rate of about 25% and 5% of that observed with PPi. This result is in agreement with

the previous findings; Y-PPase from *Saccharomyces cerevisiae* can hydrolyse tri-polyphosphate at a rate of less than 0.1% comparing with the PPi at pH 7.0 (Shafranskii *et al*., 1977). This suggests a similarity between Y-PPase and Pr-p26.1 sPPase. The substrate specificity of sPPases is generally lost when transitional metal ions such as Co^{2+} , Mn^{2+} and Zn^{2+} are used as cofactors (Höhne and Heitmann, 1973). The effectiveness of metal ions as cofactors of Y-PPase falls in the order of Mg^{2+}> Zn^{2+}> Mn^{2+} >Co^{2+} (Baykov *et al*., 1999) which is also in an agreement with Pr-p26.1 sPPases which suggests that the Pr-p26.1 sPPases bear similar characteristics to other sPPases.

3.3.4 pH dramatically affects the activity of Pr-p26.1a sPPases

pH plays an important role in the activity of soluble inorganic pyrophosphatases. The optimal pH for most Family I sPPases ranged from 5.0 to 8.0 (Hoe *et al*., 2001). However some unusual bacterial sPPases like *Vibrio cholera* prefer highly alkaline pH 9.0 (Rodina *et al*., 2009). Here we investigated the effect of pH on Pr-p26.1 sPPases using varying range. We have shown that optimal sPPase activity of Pr-p26.1 was at pH 8.0, which suggests its similarity with other Family I sPPase. Previous studies have shown that during SI-induction in *Papaver* rapid acidification of pollen tube occurs which is very rapid (Wilkins *et al*., 2015). Within 10 min of SI the cytosolic pH dropped from ~7.0 to pH 6.4 (Wilkins *et al*., 2015). Our studies showed a remarkable effect on the activity of Pr-p26.1 sPPases. At pH 6.4 the activity of Pr-p26.1 almost halved. This would occur within 10 min of SI. So, the SI-induced acidification dramatically affect the activity of sPPase. This

suggests that, within a few minutes of the SI response in poppy pollen, many important enzymes essential for pollen tube growth might be inhibited.

We also examined the effect of pH on the phopho-mimic mutant to test if phosphorylation might affect the activity of the sPPases. There was a very sharp drop of activity of phospho-mimic mutants (3E, 5E and 7E) after only 0.2 unit of pH change from pH 7.0 to pH 6.8. At pH 5.5, which is the most acidic state of the pollen tube after SI-induction, the activity of the phopho-mimic mutants was nearly zero. The 5-site and 7-site phopho-mimic mutants were more affected by pH than 3-site mutation, although at pH 5.0-6.0 the activity of these three mutants was so low that they did not show any significant difference.

Here we have shown that under natural conditions (normal pH) phospho-mimic mutants have no different activity to wild type non-mutated Pr-p26.1 or phospho-null mutants. However, we were surprised to see that there was not only an effect but a differential effect of pH on phospho-mimic mutants having more greatly reduced sPPase activity comparing to the wild type and phopho-null mutants (~ 45%). So although phosphorylation has no effect on sPPase activity on its own, in combination with pH, phosphorylation increases the effect. This suggests that phosphorylation has a biological relevant effect on the activity of Pr-p26.1a/b in the presence of pH effect.

We have also presented data which shows that 5-site and 7-site phospho-mimic mutant showed less activity compared to the 3-site mutant. However 5-site and 7-site phospho-mimic mutant did not show any significant difference between them. This result suggests that those two sites which are present in

the 7-site mutant probably have no additional effect on phosphorylation and hence on the sPPase activity of Pr-p26.1 sPPases.

The data presented here suggests that during early SI, cytosolic acidification dramatically affects Pr-p26.1 activity and effect of phosphorylation further reduces the activity. This provides a further mechanism whereby the activity of Pr-p26.1 sPPases can be inhibited during early SI. As mentioned earlier that within a few seconds of SI Ca^{2+} increases and within 90 s of SI Pr-p26.1 sPPase are phosphorylated (Rudd *et al*., 1996). In this chapter we have established that pH has a dramatic effect on phosphorylated Pr-p26.1 sPPases. It is widely accepted that protein phosphorylation is a reversible mechanism. During early SI phosphorylation of Pr-p26.1 sPPases reduces its activity and pollen tube growth is inhibited. Cytosolic acidification of the pollen tubes would completely inactivate of this enzyme so that the dephosphorylation could not recover the activity of Pr-p26.1 sPPases.

3.3.5 Both Ca^{2+} and H_2O_2 inhibit the activity of Pr-p26.1 and the phosphomimic mutants

Ca^{2+} is well established as an inhibitor of soluble inorganic pyrophosphatases as well as Pr-p26.1 sPPases (de Graaf *et al*., 2006). Here we have investigated and established that H_2O_2 also has inhibitory effect on the activity of Pr-p26.1 sPPases and their multiple site mutants. Data presented here showed that H_2O_2 alone can effectively reduce the sPPase activity of these enzymes. This is comparable to the effect of Ca^{2+}. However the activity was reduced to less than 20% when H_2O_2 and Ca^{2+} were added together. As both Ca^{2+} and H_2O_2 increase during SI in *Papaver*, this finding is therefore

biologically and physiologically relevant. As mentioned earlier, increases in $[Ca^{2+}]_{cyt}$ are triggered by SI in *Papaver.* Previous studies showed that increase in $[Ca^{2+}]_{cyt}$ stimulated increases in ROS and NO in *Papaver* pollen tube (Wilkins et al., 2011). An increase in ROS was observed as early as 4-5 min after SI induction. This suggests that ROS might play an important role in the inhibition of the activity of the Pr-p26.1 sPPases. The effect of H_2O_2 on the survival and activity of some enzymes from *Saccharomyces cerevisiae* has demonstrated that the H_2O_2 can lead to either an increase or decrease in activities of enzymes depending on the H_2O_2 concentration used or the yeast strain specificity (Bayliak *et al.*, 2006).

We have demonstrated here that H_2O_2 alone and in the combination of Ca^{2+} have significant effect on the sPPase activity of the phospho-mimic mutants. The sPPase activity of phospho-mimic mutants showed greater loss of activity compared to the wild type non-mutated Pr-p26.1 and phospho-null mutants. This suggests that phosphorylation has a further effect on sPPase activity under these SI-induced conditions.

In conclusion, data presented in this chapter has characterized the sPPases Pr-p26.1 and their multiple site phospho-mimic mutants for the first time. Pr-p26.1 prefers Mg^{2+} as a cofactor for their activity though appreciable activity was found in the presence of Zn^{2+} Co^{2+} and Mn^{2+} which is comparable to other sPPases. Ca^{2+} as well as pH and H_2O_2 showed inhibitory effect on the activity of Pr-p26.1 sPPase. The activity of the phospho-mimic mutants reduced more sharply and dramatically than the wild type and their phospho-null mutants by Ca^{2+}, acidic pH and H_2O_2. These data suggest that phosphorylation of these

sites plays an important role in regulation of sPPase activity. This suggests that during SI in *Papaver* phosphorylation of Pr-p26.1 makes this enzyme more vulnerable to the effect of Ca^{2+}, acidic pH and H_2O_2. During SI in *Papaver* an incompatible interaction triggers an increase of $[Ca^{2+}]_{cyt}$ almost instantaneously and within 90s of SI-induction the Pr-p26.1 is phosphorylated. Within 5-10 min of SI increases in ROS and cytosolic acidification occur in the cytosol of pollen tube which play important role to inhibit the activity of the phosphorylated enzyme as low as 0%. Together these events confirm the total inhibition of this sPPases under SI-induced conditions, so that it cannot be dephosphorylated. These studies provide good evidence that together with Ca^{2+}, ROS and pH dramatically affect sPPase activity. This would provide a neat way to effectively and rapidly inhibit pollen tube growth. Thus, these sPPases clearly play a key role in mediating the SI response in *Papaver.*

Chapter 4

Identification of proteins modified by ROS/NO during the SI response

4.1 Introduction

Reactive oxygen species (ROS) and nitric oxide (NO) play a role as signalling molecules. In plant cells, ROS has been demonstrated to be involved in numerous biological responses, like gravitropism (Joo *et al*., 2001), root growth (Foreman *et al*., 2003), signalling of extracellular ATP (Song *et al*., 2006), pollen-tube growth (Potocký et al., 2007, Kaya et al., 2014a) and rupture of pollen tubes (Duan *et al.*, 2014). ROS can activate Ca^{2+} channels and thus increase Ca^{2+} levels in the cytosol, activate MAPKs, depolymerise microtubules, activate defence gene and cell death (Lecourieux *et al*., 2002, Levine *et al*., 1996, Rentel *et al*., 2004). NO signalling also plays role in stomatal closing, abiotic stress and disease resistance (Delledonne, 2005, Neill *et al.*, 2003). Moreover, NO is involved in regulating many developmental processes in plants. Involvement of NO has been documented in leaf expansion, encouraging seed germination, root development and fruit maturation delaying (Kopyra and Gwóźdź, 2003, Lombardo *et al*., 2006).

During biotic and abiotic stress condition, ROS is produced at an increased rate. Extreme temperature, ultra-violet (UV) radiation, excess excitation energy, exposure of ozone, water deficiency, attack of pathogen and wounding are examples of stimuli that are responsible for ROS induction in plants (Tsikas *et al*., 1999, Berlett and Stadtman, 1997, Pena *et al*., 2012, Costa *et al*., 2008, Guan *et al*., 2015, Gechev *et al.*, 2006, Chi *et al*., 2013, Halliwell, 2006). Chloroplasts, Mitochondria, and microbodies are considered as main sources of production of ROS and the level of ROS in the cells are regulated by their production and scavenging systems (Mittler *et al*., 2004,

Apel and Hirt, 2004). During the plant hypersensitive response against avirulent pathogens, host cells vigorously produce high levels of ROS (Berlett and Stadtman, 1997). This “oxidative burst” is contributed mostly by plasma membrane-bound NADPH oxidases (Berlett and Stadtman, 1997, Jajic *et al*., 2015). Pathogen infection also activates production of nitric oxide (NO) which coordinates with ROS to control hypersensitive cell death and induction of defence genes (Gupta *et al*., 2011).

ROS and reactive nitrogen species (RNS) play significant physiological functions but also can cause widespread cellular damage too. The negative role of ROS is related to oxidative stress which can impair function of major cellular components including lipids, proteins, carbohydrates, and DNA. At an optimal concentrations, ROS plays a positive role in cellular functions since it is also a signalling molecule that governs programmed cell death (PCD) during unfavourable environmental conditions (Wituszyńska and Karpiński, 2013, Van Breusegem and Dat, 2006, Woo *et al*., 2013, Coll *et al*., 2014). Under unfavourable biotic and abiotic stress conditions, when production of ROS exceeds the ROS-scavenging capability in plant tissues, surplus ROS induces necrotic lesions as cytotoxins and modifies the expression of genes involved in signal transduction and ultimately causes cell death (Mittler, 2002).

A highly regulated biological process called “autophagy” initiates PCD during plant aging (Pennell and Lamb, 1997). Senescence and autophagy are genetically controlled terminal stages of the plant life which play significant roles on degradation and recycling of organelles, macromolecules, and cytoplasm throughout PCD (Lim *et al*., 2007, Karuppanapandian *et al*., 2011).

It has been described that the spatial-temporal correlation between upsurges in ROS and cell death serve as the early sign of ROS-mediated PCD (Vranová *et al*., 2002, Apel and Hirt, 2004). ROS such as O^{2-} and H_2O_2 are also known as key coordinators of senescence (Kim *et al*., 2009).

As mentioned earlier (**Chapter 1, Section 1.6.2.1.6**) in recent years, involvement of ROS and NO in the Self-incompatibility (SI) response, eventually triggering PCD has been documented (Bosch *et al*., 2010, Wilkins *et al*., 2011, Serrano *et al*., 2011, Serrano *et al*., 2012, Jiang *et al*., 2014). Using both *in vivo* and *in vitro* experiments in the olive (*Olea europaea* L.), the role of ROS and RNS has been investigated in the pollen-pistil interaction. These studies demonstrated a bidirectional signals between the stigma and the pollen that seems to control the production of ROS and RNS in both tissues (Serrano *et al*., 2011). The first data involving ROS throughout the SI-mediated signalling events were described in *Pyrus pyrifolia* (Wang *et al*., 2010) and *Papaver rhoeas* (Wilkins *et al*., 2011).

ROS and NO have been shown to be involved in *Papaver rhoeas* SI-mediated PCD (Wilkins *et al*., 2011). Studies showed that SI induces comparatively rapid increases in ROS and NO in *Papaver* pollen tubes. Investigations using the ROS and NO scavengers provided evidence that ROS and NO were involved in the formation of the SI-induced punctate actin foci and the activation of a DEVDase/caspase-3-like activity (Wilkins *et al*., 2011) which are key features of SI response. However, exactly how ROS and NO signal to mediate SI-induction is not known.

To apply their effects, ROS and NO must alter target proteins. So far, these types of research in plant have been very limited and rather little is known about exactly how ROS and NO regulate plant responses. However, NO is well known to modify proteins by *S*-nitrosylation (Lindermayr *et al*., 2005). It is thought that NO signalling in plants uses *S*-nitrosylation of cysteine residues of redox-sensitive proteins (Moreau *et al*., 2010, Wang *et al*., 2006). Proteomic studies of *Arabidopsis* have identified some nitrosylated proteins (Lindermayr et al., 2005), and this combined with mass spectrometry, offers a powerful approach for the identification and analysis of the targets of ROS and NO.

In this chapter, we used the approach of using H_2O_2 as a ROS donor and GSNO (*S*-nitrosoglutathione) as a NO donor to analyse their specific modifications to protein targets of *Papaver* pollen tubes. We also identified protein targets that were modified by ROS and NO during SI-signailing using recombinant PrsS for SI-induction. We used a mass spectrometry approach generally used for post-translational modification (PTM) proteomic studies to identify and analysed the modifications to the proteins by ROS and NO. These data represent the first studies to analyse the protein targets of ROS and NO in the context of SI induction and identification of specific modifications. This provides insights into novel additional mechanisms potential to be involved in mediating SI-PCD.

For this chapter, we will describe the results and discussion together as this is the easier way of presenting these data without repetition.

4.2 Results and Discussion

In order to identify protein targets of ROS and NO in poppy pollen tubes, we treated germinated pollen tubes growing *in vitro* (see **Chapter 2**, **Section 2.1 and 2.2** for details). We added ROS donor H_2O_2 to increase [ROS] or the NO donor GSNO (*S*-nitrosoglutathione) to increase [NO] in the pollen tubes. To identify protein targets that were modified by ROS and NO during SI-signalling, we induced SI using recombinant PrsS. We analysed untreated samples side by side to verify and compare the modifications to target proteins from each treatment. Results under these three treatments will be discussed in separate sections below.

4.2.1 Oxidative modification of pollen proteins by adding H_2O_2 to poppy pollen tube

Pollen tubes normally exhibit steady levels of ROS. As an approach to identify the modified proteins that could be targets of ROS, we added 2.5 mM H_2O_2 to increase the ROS levels in germinated pollen tubes. After 5-12 min of the treatment, which is the time point for the maximum increase of SI-induced ROS in the poppy pollen was identified (Wilkins *et al*., 2011), we extracted pollen proteins from H_2O_2 treated samples, loaded these onto SDS-PAGE gel and gel plugs digested using trypsin before analysis using mass spectrometry (see **Chapter 2**, **Section 2.5.1 & 2.10.1**). Fourier transform ion cyclotron resonance mass spectrometry (FT-ICR-MS) can be used to determine masses with high accuracy. FT-ICR-MS is convenient for analysis of complex mixtures because it has a high resolution which allows the signals of two ions of similar mass to charge (m/z) to be detected as separate ions (Sleno *et al*., 2005,

Bossio and Marshall, 2002, He *et al.*, 2001). Metabolomic fingerprinting using FTICR-MS demonstrated the effectiveness of this method by profiling more than 400 metabolites within 24 h (Han *et al*., 2008). Studies on compositional based fingerprints using FT-ICR MS resolved and identified a huge number of distinct chemical components of commercial canola, olive, and soybean oils (Wu *et al*., 2004). As we had to identify proteins that were modified by H_2O_2 from hundreds of pollen proteins, FT-ICR-MS technique seemed to be the most appropriate.

University of Birmingham Proteomics Unit provided a service that analyses samples digested by trypsin by FT-ICR-MS (see **Chapter 2**, **Section 2.11.3** for details). The identified peptides were searched against NCBI Green Plant database using the SEQUEST algorithm (Thermo Scientific). As the complete and annotated genome sequence for *Papaver rhoeas* is not currently available, the identifications were limited to peptides identical to those found in other green plants or the few sequences of *Papaver rhoeas* submitted to EMBL (European molecular biology laboratory) by our laboratory namely; Pr-p26.1a, Pr-p26.1b and MAPK. The initial data from mass spectrometer contained hundreds of proteins as 'hits'. However, not all the proteins in the list were confirmed as modified. First we looked at the proteins listed as modified. Criteria for 'real hit proteins' were accepted as those containing at least two high confidence peptides. For example, **Figure 4.1** shows that three different peptides of 14-3-3 like proteins were modified, all of which were with high confidence and hence considered as 'real hits'.

18411901	14-3-3-like protein GF14 omega [Arabid	27.11	28.57	101	1	6	10
	A2	Sequence	# PSMs	Protein	tein G	Protein Group Accessions	Modifications
	High	LAEQAERYEEMVEFMEK	2	100	5	18411901;2492487;3517	
	High	SKIETELSGIcDGILK	1	5	1	18411901	C11(Carbamidomethyl)
	High	QAFDEAIAELDTLGEESYK	2	66	3	18411901;351725929;32	
	High	IISSIEQKEESR	1	102	5	18411901;351725929;32	
	High	YEEMVEFMEK	1	100	5	18411901;2492487;3517	
	High	LAEQAERYEEMVEFMEk	1	100	5	18411901;2492487;3517	K17(AASA)
	High	QAFDEAIAELDTLGEESYkDSTLIMQL	1	63	3	18411901;351725929;32	K19(AASA)
	High	QAFDEAIAELDTLGEESYKDSTLIMQI	1	63	3	18411901;351725929;32	

Figure 4.1. An example of the Excel data sheet shows the protein targets identified by mass spectrometry. Proteins containing two or more different high confident modified peptides were considered as real hits.

The full list of the protein hits identified for both untreated and H_2O_2 treated samples can be found in the **Appendix II.**

4.2.1.1 Distribution of H_2O_2-modified proteins into different functional groups

To obtain an insight into the functions of modified proteins identified by mass spectrometry, the protein candidates from untreated and H_2O_2-treated samples were categorised based on their general functions (**Figure 4.2**). Compared to the untreated sample, the H_2O_2-treated samples showed an increased proportion of modified cytoskeletal proteins (16% versus 9%; 16 different peptides in H_2O_2 and 8 different peptides in untreated samples), stress related proteins (14% versus 8%; 23 peptides versus 11 peptides), signalling proteins (14% versus 7%; 21 peptides versus 7 peptides) and redox proteins (4% versus 0%; 9 peptides versus 0 peptide). Clearly, the H_2O_2-treated sample showed almost double proportion of modified peptides in these

groups of proteins than untreated sample, showing real differences caused by the treatment.

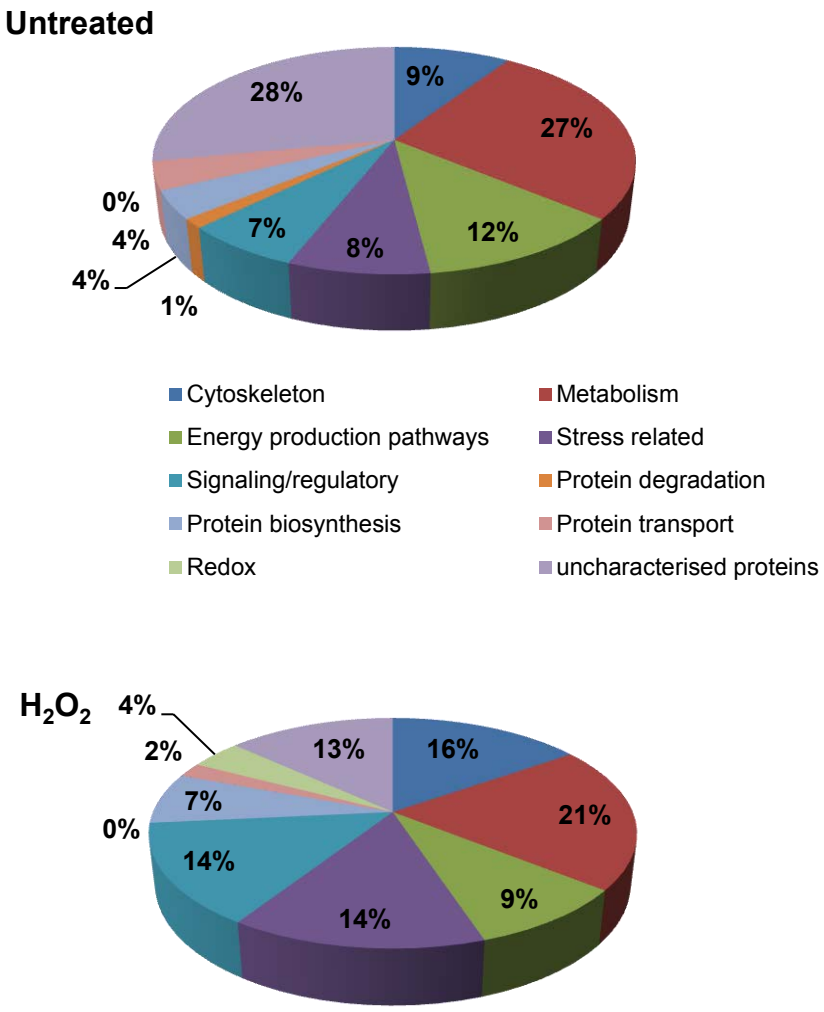

Figure 4.2. Distribution of modified proteins with H_2O_2 treatment identified by mass spectrometry into functional groups

A pie chart representation of the percentage of the modified proteins identified by FT-ICR-MS that fall into each of the functional groups for untreated (UT), and H_2O_2 treated samples.

Among the identified proteins in the H_2O_2 samples, 56% (79% of the identified peptides) were specifically identified in the H_2O_2 sample, i.e. the protein

identification number was not found in the untreated sample. However 41% of these proteins (20% of the identified peptides) had proteins of similar function in the untreated sample, for example, different sub-units of the same complex or different isoforms.

The extent and types of oxidative modification of protein was an important aspect for analysing the target proteins for oxidation. Among the identified peptides in the untreated samples, 14% of them were modified irreversibly. The rest of the peptides showed reversible modification. In contrast, 87% of the identified peptides in the H_2O_2 treated samples were modified irreversibly. We identified some proteins common to both untreated and H_2O_2 treated samples. However, the types of oxidative modification of those proteins were different in untreated sample compared to H_2O_2 treated sample. For example, peptide EITALAPSS**mk** identical to *Arabidopsis* actin 12 was identified in both untreated and H_2O_2 treated samples. In the untreated sample, methionine was oxidised to methionine sulfoxide, which is a reversible modification. In contrast, the same peptides identified in the H_2O_2 treated samples showed irreversible modifications of methionine (m) and lysine (k). Methionine was modified to met sulfone and lysine was modified to Aminoadepic semialdehyde which are two step-modifications and irreversible (see **Chapter 1, Figure 1.5**). It has been suggested that the reversible modification of methionine may be an important regulatory mechanism (Sundby *et al*., 2005) and therefore it is expected as intermediates in untreated samples. Further oxidation of methionine to met sulfone is irreversible and permanently damaging to the protein (Møller *et al.*, 2007). Modification of lysine to

aminoadepic semialdehyde is a carbonylation modification which is the most common type of oxidative modification to a protein. There is no indication that carbonylation is reversible (Shacter, 2000). So this is likely to be damaging to the proteins. These data suggest that oxidative stress might cause damage to several proteins which might have important role in the cell.

As mentioned earlier, H_2O_2 treated samples contained increased levels of cytoskeletal proteins, signalling or regulatory proteins, stress related proteins and redox related proteins that were oxidatively modified, compared to the untreated samples. This suggests that these groups of proteins are the target of an oxidative stress response in the poppy pollen. We will therefore now consider each of these classes of ROS-modified protein and discuss their identity, the modification and possible implications for biological function.

4.2.1.1.1 Cytoskeletal proteins modified after H_2O_2 treatment

Several cytoskeletal proteins, primarily actin and tubulin were identified as targets of oxidative modification from untreated and H_2O_2 treated samples. The modifications are shown in **Table 4.1**. Eight different modified peptides identical to actin and tubulin were identified in the untreated sample. The modified amino acid in most of the peptides (7 out of 8) was methionine; it was modified to met fulfoxide, which is a reversible modification. Only one peptide was identified where proline was modified irreversibly to Glu-γ-semialdehyde. In contrast, 16 different peptides identical to actin and tubulin were identified from H_2O_2-treated samples. The modified amino acids were mainly methionine, tryptophan, lysine, proline, arginine and cysteine. Methionine was

modified to met sulfone, tryptophan to kynurenine, lysine to aminoadipic semialdehyde, proline and arginine to glu-γ-semialdehyde; all these modifications are irreversible modifications and likely to be damaging to the proteins. Cysteine was modified to carbamidomethyl which is a reversible modification. One fimbrin-like protein was identified from H_2O_2-treated samples but not in the untreated sample. The peptides identical to fimbrin identified in the H_2O_2-treated samples where proline, tryptophan, methionine and arginine were modifies to glu-γ-semialdehyde, kynurenine, met sulfone and glu-γ-semialdehyde respectively. All these modifications are irreversible modifications, therefore, likely to be damaging to the protein.

Actin and tubulin have been reported as target of oxidative modifications in animal cells (Dalle-Donne *et al*., 2001a, Lassing *et al*., 2007). It has been reported that oxidation of actin in mammalian cells induces the disruption and inhibition of actin filament formation (Dalle-Donne *et al*., 2001a). In yeast, actin is considered as oxidative stress sensor and its oxidation regulates stress-triggered cell death (Farah and Amberg, 2007). In plants, it has been reported that 2,4-D, a commonly used herbicide, affects the actin cytoskeleton by encouraging oxidative and *S*-nitrosylated modifications on the actin, thus interrupting actin polymerization and compromising the dynamics of peroxisomes and mitochondria (Rodríguez-Serrano *et al.*, 2014). Thus, the oxidative modifications to actin identified in this current study are likely to affect actin polymerization and its function and might affect pollen tube growth, as actin plays a key role in pollen tube growth.

Table 4.1. Modified cytoskeletal proteins found in the untreated and H_2O_2 treated samples by mass spectrometry analysis

Proteins	UT		H_2O_2	
	Identified peptides	Type of modification	Identified peptides	Type of modification
Actin-1, 2,	DLYGNIVLSGGTT**m**FPGIADR EITALAPSS**m**K	Met sulfoxide (rev.) Met sulfoxide (rev.)	DLYGNIVLSGGTT**m**FPGIADR EITALAPSS**m**K YPIEHGIVTN**w**DD**m**EK	Met sulfone (irrev.) Met sulfone (irrev.) Kynurenine (irrev); Met sulfone (irrev.)
Actin 3	n.d	n.d	DLYGNIVLSGGTT**m**FPGIADR YPIEHGIVTN**w**DD**m**EK	Met sulfone (irrev.) Kynurenine (irrev); Met sulfone (irrev.)
Actin 4	EITALAPSS**m**K AVF**p**SIVGRPR	Met sulfoxide (rev.) Glu y-semialdehyde(irrev)	n.d	n.d
Actin 12	EITALAPSSmK LDLAGRDLTDHLmK	Met sulfoxide (rev.) Met sulfoxide (rev.)	EITALAPSS**m**K CDVDI**r**KDLYGNIVLSGGTTMFGGIGD**r**	Met sulfone (irrev.) Glu y-semialdehyde(irrev)
Alpha-tubulin	n.d	n.d	**k**LADN**c**TGLQGFLVFNAVGGGTGSGLGSLLL ER AV**cm**ISNSTSVAEVFSR TIQFVDW**c**PTGF**k** EIVDL**c**LD**r**	AASA (irrev); Carbamidomethylation (rev.) Carbamidomethylation (rev.); Met sulfone (irrev.) Carbamidomethylation (rev.); AASA (irrev) Carbamidomethylation (rev.); Glu-y-semialdehyde (irrev.)
Beta-tubulin	**m**ASTFIGNSTSIQE**m**FR M**m**LTFSVFPSPK LHFF**m**VGFAPLTSR VSEQFTA**m**FR	Met sulfoxide (rev.) Met sulfoxide (rev.) Met sulfoxide (rev.) Met sulfoxide (rev.)	SG**p**YGQIFRPDNFVFGQSGAGNNWAK LHFF**m**VGFA**p**LTSR **m**MLTFSVFPSPK LTTPSFGDLNHLISATMSGVT**cc**LR NSSYFVE**w**l**p**NNVk	Glu y-semialdehyde (irrev.) Met sulfone (irrev.); Glu y-semialdehyde (irrev.) Met sulfone (irrev.) Carbamidomethylation (rev.) Kynurenine (irrev); Glu y-semialdehyde(irrev)
fimbrin-like protein	n.d	n.d	VS**p**GSVN**w**KHANKP**p**IK**m**PFK LLLAFLWQL**mr**YT**m**LQILNNL**r**	Glu y-semialdehyde (irrev.) Kynurenine (irrev); Met sulfone (irrev.); Met sulfone (irrev.); Glu y-semialdehyde (irrev.)

Lowercase bold letters in the identified peptide column indicate the modified amino acids. UT=Untreated samples, H_2O_2= H_2O_2 treated samples. In the types of modification column AASA indicates Aminoadepic semialdehyde. Rev=Reversible modification; irrev= irreversible modification; n.d=not detected

4.2.1.1.2 Signalling or regulatory proteins modified after H_2O_2 treatment

We identified several signalling proteins that were oxidatively modified in the untreated and H_2O_2 treated pollen samples. The identified signalling proteins were mainly, 14-3-3 protein, elongation factors, initiation factor and Rab-GDP dissociation proteins (**Table 4.2**). From the untreated control samples 4 signalling proteins with 7 different modified peptides were identified. In the untreated sample all the modifications on these peptides were reversible modification of methionine and glutamine; where methionine was modified to met sulfoxide and modification for glutamine was deamidation. Therefore, these modifications are likely to be involved in the regulatory functions of these proteins.

Different isoforms of 14-3-3 protein and Rab family proteins had previously been identified as actin-associated proteins with a potential role in SI signal in *Papaver* (Poulter *et al*., 2011). In the current study we identified 14-3-3 protein and Rab family protein as a target of oxidative modification from H_2O_2-treated poppy pollen extract. These proteins may be involved in the SI signalling probably via actin, as 14-3-3 proteins have been shown to be involved in many cellular processes including reorganization of actin cytoskeleton, biotic and abiotic stress response and apoptosis (van Hemert *et al*., 2001, Ferl *et al*., 2002, Denison *et al*., 2011). The SI response in poppy can be considered as a stress response which involves reorganization of the cytoskeleton and consequences in PCD (Bosch *et al*., 2008).

Table 4.2. Identified signalling proteins by mass spectrometry analysis modified after H_2O_2 treatments

Proteins	UT		H_2O_2	
	Identified peptides	Type of modification	Identified peptides	Type of modification
Elongation factor 1-alpha	**n.d**	**n.d**	VETGVIKPGMVVTFGPTGLTTEV**k** MI**p**TK**p**MVVETFAQYPPLGR	AASA (irrev.) Glu y-semialdehyde (irrev.); Glu y-semialdehyde (irrev.);
elongation factor 1-alpha 1	**n.d**	**n.d**	VGYN**p**E**k**IPFVPISGFEGDNMIER YY**c**TVIDAPGHR	Glu y-semialdehyde (irrev.); AASA (irrev.) Carbamidomethyl (rev.)
elongation factor 2-like	EVAGDVR**m**TDTRADEAERGIT QRVIENANVI**m**ATYED	Met sulfoxide (rev.) Met sulfoxide (rev.)	GVQYLNEIKDSVVAGFQ**w**AS**k** VIENANVIMATYEDPLLGDVQVYPE**k** N**c**DPDGPL**m**LYVSK LYMEAR**p**LEDGLAEAIDDGR	Kynurenine (irrev.); AASA (irrev.) AASA (irrev.) Carbamidomethyl (rev.); Met sulfone (irrev.) Glu y-semialdehyde (irrev.);
elongation factor 2-like isoform 1	**n.d**	**n.d**	GVQYLNEIKDSVVAGFQ**w**AS**k** VIENANVIMATYEDPLLGDVQVYPE**k**	Kynurenine (irrev.); AASA (irrev.) AASA (irrev.)
EIF4A-2; ATP-dependent helicase/ translation initiation factor	**n.d**	**n.d**	**r**QSLRPD**c**IKMFVLDEADEMLS**r** DIIMREF**r**SGSS**r**	Glu y-semialdehyde (irrev.); S-nitrosocysteine (rev.); Glu y-semialdehyde (irrev.) Glu y-semialdehyde (irrev.); Glu y-semialdehyde (irrev.);
Eukaryotic initiation factor 4A-8;	n.d	n.d	GLDVIQQA**q**SGTG**k** LETL**c**DLYETLAITQSVIFVNTR	Deamidation (rev.); AASA (irrev.) Carbamidomethyl (rev.)
initiation factor eIF4A-15	n.d	n.d	LETL**c**DLYETLAITQSVIFVNTR VQVGVFSATM**p**PEALEITR	Carbamidomethyl (rev.) Glu y-semialdehyde (irrev.);
putative 14-3-3 regulatory	LAEQAERYEE**m**VEFMEK IISSIE**q**KEESR	Met sulfoxide (rev.) Deamidation (rev.)	SAQDIALAELA**p**THPIR QAFDEAISELDSLGEESY**k**DSTLI**m**QLLR LAEQAERYEEMVEFME**k**	Glu y-semialdehyde (irrev.); AASA (irrev.); Met sulfone (irrev.) AASA (irrev.)
14-3-3 protein 3	n.d	n.d	LAEQAERYEEMVEFME**k** QAFDEAIAELDTLGEESY**k**DSTLI**m**QLLR	AASA (irrev.) AASA (irrev.); Met sulfone (irrev.)
14-3-3-like protein GF14 omega	n.d	n.d	SKIETELSGI**c**DGILK LAEQAERYEEMVEFME**k**	Carbamidomethyl (rev.) AASA (irrev.)

14-3-3 protein SGF14h	QAFDEAIAELDTLGEESYKDST LI**m**QLLR IISSIE**q**KEESR	Met sulfoxide (rev.) Deamidation (rev.)	LAEQAERYEEMVEFME**k** QAFDEAIAELDTLGEESY**k**DSTLI**m**QLLR	AASA (irrev.) AASA (irrev.); Met sulfone (irrev.)
PREDICTED: rab GDP dissociation inhibitor alpha	n.d	n.d	IHKVPATDVEAL**k**SPLMGLFEK VPATDVEALKS**p**LMGLFEk	AASA (irrev.) Glu y-semialdehyde (irrev.);
rab GDP dissociation inhibitor alpha	n.d	n.d	IHKVPATDVEAL**k**SPLMGLFEK VPATDVEALKSPLMGLFE**k**	AASA (irrev.) AASA (irrev.)
Rab1/RabD-family small GTPase	n.d	n.d	FADDSYLESYISTIGVDF**k** LLLIGDSGVG**k**	AASA (irrev.) AASA (irrev.)
AtRABH1c GTP binding / protein binding	LVFLGD**q**SVGK EYGV**m**FIETSAK	Deamidation (rev.) Met sulfoxide (rev.)	n.d	n.d

In the identified peptides column lowercase bold letters indicate the modified amino acids. UT=Untreated samples, H_2O_2= H_2O_2 treated samples. In the types of modification column AASA indicates Aminoadepic semialdehyde. Rev=Reversible modification; irrev= irreversible modification; n.d=not detected

Therefore, the oxidative modification of 14-3-3 proteins identified in this study could play a role in the SI response of poppy incompatible pollen tubes.

Irreversible modifications of several amino acids were identified on elongation factors (EF1α) in the H_2O_2-treated samples which are likely to be damaging to the protein (**Table 4.2**). EF1α protein plays a role in protein synthesis. Studies show that oxidative stress is involved in the modifications of EF-2 and this modification could account for the decline in protein synthesis in old animals (Parrado *et al*., 1999). Besides peptide elongation, EF1α play role in translation and also functions in the regulation of the cytoskeletal dynamics (Liu *et al*., 1996a). There is evidence that EF1α-F-actin complex create a scaffold which is important to bind β-actin mRNA. If the complex disrupted for any reason, mRNA would be delocalized and probably would not bind to actin (Liu *et al*., 2002). Oxidative modification of EF1α could hamper the binding of actin to this protein and eventually would disrupt the protein synthesis. 14-3-3 proteins and EF1α proteins and their association with actin will be discussed in more detail in **Chapter 5**.

4.2.1.1.3 Stress related proteins modified by H_2O_2 treatment

Another class of modified proteins that presented at a higher frequency in the H_2O_2-treated sample compared to the untreated sample were stress-related proteins; especially heat shock proteins (HSPs) and chaperonins. Other stress proteins like luminal-binding proteins and ERD2 (Early-responsive to dehydration 2) proteins were also identified. Eleven different peptides were identified in the untreated sample, while 23 different peptides were identified in

the H_2O_2-treated sample. Thus the H_2O_2-treated sample had over twice the number of modified peptides compared to the untreated sample, leading confidence this is an authentic response. Methionine was reversibly modified to met sulfoxide in almost all peptides (10 out of 11) identified from the untreated sample. One proline was modified to Glu-γ-semialdehyde which is an irreversible modification. Conversely, in the H_2O_2-treated sample the modified amino acids were methionine, proline, lysine, arginine, tryptophan and cysteine on the identified peptides (**Table 4.3**) Methionine was modified to met sulfon, proline and arginine were modified to Glu-γ-semialdehyde, lysine to aminoadepic semialdehyde, tryptophan to kynurenin, and cysteine was modified to either S-nitrosocysteine or carbamidomethyl. Except for the cysteine modification, the other modifications were all irreversible modifications. So, nearly all H_2O_2 -treated samples were irreversibly modified, while virtually none of the untreated samples were.

Almost all stresses (eg. drought, salinity, cold oxidative stress, chemicals) induce the production of heat shock proteins (reviewed by Al-Whaibi, 2011). So it is not surprising that HSPs are more abundant in the H_2O_2-treated sample, as it caused stress to the pollen tube. HSPs generally protect cells against many stresses. They have some roles in regulating a variety of components, all of which contribute to existence under abiotic stress by checking misfolding and aggregation of proteins, along with its role as chaperones (reviewed by Al-Whaibi, 2011).

Table 4.3. Stress related proteins modified after H_2O_2 treatment identified by mass spectrometry analysis

Proteins	UT		H_2O_2	
	Identified peptides	**Type of modification**	**Identified peptides**	**Type of modification**
Heat shock protein	**n.d**	**n.d**	SIN**p**DEAVAYGAAVQAAILSGEGNE**k** NQVAMN**p**VNTVFDAK	Glu γ-semialdehyde (irrev.); AASA (irrev.) Glu-γ-semialdehyde (irrev.)
HSP60 ; ATP binding	**n.d**	**n.d**	MS**w**SRNYAAKEIK GIS**m**AVDAVVTNLK	Kynurenine (irrev.); Met sulfone (irrev.)
heat shock protein 70	**n.d**	**n.d**	SIN**p**DEAVAYGAAVQAAILSGEGNE**k** IINEPTAAAIAYGLDK**k**	Glu γ-semialdehyde (irrev.); AASA (irrev.) AASA (irrev.)
HSP70	**n.d**	**n.d**	LGTVIGIDLGTTYS**c**VGVY**k** DILLLDVAPLTLGIETVGGVMT**k**	Carbamidomethyl (rev.); AASA (irrev.) AASA (irrev.)
Putative heat shock 70 KD protein, mitochondrial precursor	GVNPDEAVA**m**GAAIQGGILR ATNGDTFLGGEDFD**n**TLLEFL VSEFKR	Met sulfoxide (rev.) Deamidation (rev.)	**n.d**	**n.d**
HSC70-1 (ATP binding)	**n.d**	**n.d**	NALENYAYN**m**R ITITNDKG**r**	Met sulfone (irrev.) Glu-γ-semialdehyde (irrev.)
MTHSC70-2	GVNPDEAVA**m**GAALQGGILR IINEPTAAALSYG**m**TNK	Met sulfoxide (rev.) Met sulfoxide (rev.)	GVNPDEAVA**m**GAALQGGILR **m**V**p**YKIV**r**	Met sulfone (irrev.) Met sulfone (irrev.); Glu-γ-semialdehyde (irrev.); Glu-γ-semialdehyde (irrev.)
Heat shock cognate 70 kDa protein 3	NQVA**m**NPINTVFDAK **m**VNHFVQEFK	Met sulfoxide (rev.) Met sulfoxide (rev.)	NQVA**m**NPINTVFDAK NALENYAYN**m**R	Met sulfone (irrev.) Met sulfone (irrev.)
heat shock protein 70-3	LIGDAAKNQVA**m**NPINT QFAAEEISS**m**VLIK	Met sulfoxide (rev.) Met sulfoxide (rev.)	SINpDEAVAYGAAVQAAILSGEGNE**k** NQVAMN**p**INTVFDAK	Glu γ-semialdehyde (irrev.); AASA (irrev.) Glu-γ-semialdehyde (irrev.)

Hsp70b ATP binding	**n.d**	**n.d**	IINEPTAAAIAYGLDK**k** **cm**DPVEKVLK	AASA (irrev.) *S*-nitrosocystein (rev.); Met sulfone (irrev.)
HSP81-2 ATP binding	GYEVLY**m**VDAIDEYAVGQLK AVENS**p**FLER	Met sulfoxide (rev.) Glu-γ-semialdehyde (irrev.)	DSS**m**AGYMSS**k** NLKLGIHEDSQN**r**TK	Met sulfone (irrev.); AASA (irrev.) Glu-γ-semialdehyde (irrev.)
chaperonin, putative	EERNYILG**m**IKK ILKITGIKD**m**GR	Met sulfoxide (rev.) Met sulfoxide (rev.)	**n.d**	**n.d**
Chaperonin CPN60-2	**n.d**	**n.d**	QRPLLIVAEDIESDALATLILN**k** GYIS**p**YFITNQ**k**	AASA (irrev.) Glu-γ-semialdehyde (irrev.); AASA (irrev.)
luminal binding protein	**n.d**	**n.d**	VFSPEEISA**m**ILTK **m**KETTEAYLGKK DAVVTV**p**AYFNDAQ**r**QATK	Met sulfone (irrev.) Met sulfone (irrev.) Glu-γ-semialdehyde (irrev.); Glu-γ-semialdehyde (irrev.)
PREDICTED: luminal-binding protein 5	**n.d**	**n.d**	LGTVIGIDLGTTYS**c**VGVY**k** LKEVEAV**c**NPIITAVYQR	Carbamidomethyl (rev.); AASA (irrev.) Carbamidomethyl (rev.)
ERD2 (EARLY-RESPONSIVE TO DEHYDRATION 2); ATP binding	**n.d**	**n.d**	QFAAEEISS**m**VLIK **m**VNHFVQEFK ELESV**w**STIITK**m**YQG	Met sulfone (irrev.) Met sulfone (irrev.) Kynurenine (irrev.); Met sulfone (irrev.)

Lowercase bold letters indicate the modified amino acids in the identified peptides column. UT=Untreated samples for control, H_2O_2= H_2O_2 treated pollen protein samples. In the types of modification column AASA indicates Aminoadepic semialdehyde. Rev=Reversible modification; irrev= irreversible modification; n.d=not detected; i.e.; that particular protein was not detected under that treatment.

Irreversible modifications identified on amino acids would likely hamper the activity of these HSPs and might interfere with their function of protection during stress conditions. Stress related proteins and their involvement in the stress response will be further discussed in **Chapter 5**.

4.2.1.1.4 Redox proteins modified by H_2O_2 treatment

Ten different peptides from four modified redox-related proteins were identified in the H_2O_2 treated samples (**Table 4.4**), and none of them were identified in the untreated sample. Methionine was modified to met sulfone, proline and arginine were modified to glu-γ-semialdehyde and lysine was modified to aminoadepic semialdehyde; all these modifications are irreversible modifications. In one peptide, cysteine was modified to carbamidomethyl which is a reversible modification.

Table 4.4. Modified redox related proteins in H_2O_2 treated samples from mass spectrometry analysis.

Treatments	Proteins	Sequences	Site and type of modifications
H_2O_2	SKS11 (SKU5 Similar 11)	DYY**m**VASSR SGKGDGSDA**p**LFTLK**p**GK YALNGVSHTD**p**ETPLK	Met sulfone (irrev.) Glu y-semialdehyde (irrev.); Glu y-semialdehyde (irrev.) Glu y-semialdehyde (irrev.)
	2-oxoglutarate dehydrogenas, E1 subunit-like protein	EAMN**m**GAFSYIS**p**R EKIETPT**p**W**r**YNR RTPVSGPKG**k**PQALQV**k**	Met sulfone (irrev.); Glu y-semialdehyde (irrev.) Glu y-semialdehyde (irrev.) Glu y-semialdehyde (irrev.) AASA (irrev.); AASA (irrev.);
	ferric leghemoglobin reductase-2 precursor	LTLE**p**AAGGDQTTLEADVVLVS AGR AEEDGVA**c**VEYIAGK	Glu y-semialdehyde (irrev.) Carbamidomethyl (rev.)
	putative ascorbate peroxidase	EILSGEKEGLLQLPTD**k** TKTGG**p**FGTIR	AASA (irrev.); AASA (irrev.); Glu y-semialdehyde (irrev.)

Amongst the redox related proteins, 3 peptides identical to *Arabidopsis* SKS11 copper binding protein were identified in the H_2O_2 sample. SKS11 (SKU5 similar 11) belongs to a gene family entitled SKS (SKU5 Similar). Investigations of plants revealed that SKU5 was expressed strongly in growing tissues (Sedbrook *et al*., 2002). The authors suggested that two directional growth processes were affected by SKU5, possibly by participating in cell wall expansion. A loss-of-function mutant has twisted roots and exhibits directional growth defects compared to wild type. In another study, *BcSKS11, which* has several features of SKS proteins, was expressed in microspores, mature pollen grains and growing pollen tubes. This suggests that mature pollen grain might store BcSKS11 protein, which would be using to prepare the pollen to germinate and afterward provide energy for pollen-tube growth (Zhang *et al*., 2013). In this current study we identified SKS11 as a target of oxidative modification from poppy pollen. These data suggest that this protein might potentially have a role in the growth of poppy pollen tubes and that modification of this protein is likely to affect the activity of SKS11 protein.

Here we identified several oxidatively modified peptides using ROS donor H_2O_2. We also wanted to study a potential role for NO, as both ROS and NO increased in incompatible pollen during the SI response. We therefore investigated the role of NO by using the NO donor, *S*-nitrosoglutathione (GSNO) on protein modifications in poppy pollen tubes.

4.2.1.2 Pollen proteins modified by a NO donor

In order to identify proteins modified by NO we treated poppy pollen growing *in vitro* with the NO donor GSNO to increase the NO levels in the pollen tubes. Pollen tubes were treated with GSNO for ~30 min as at this time point SI-induced increases in NO reaches its peak (Wilkins *et al*., 2011). An untreated control pollen sample prepared side by side was also analysed for comparison. Detection of NO modifications is quite challenging and more difficult than oxidative modifications. To detect *S*-nitrosylated proteins in the pollen extract we used a method developed by Thompson *et al*. (2013) with some modifications. The levels of endogenous *S*-nitrosylation are usually very low. The *S*-NO bond has the tendency to undergo homolytic and heterolytic decomposition, so using a suitable method is one of the most important aspects for the analysis of the SNO-proteome. The biotin switch technique (BST) (Jaffrey and Snyder, 2001) is the most regularly used method to detect cellular *S*-nitrosylation. This method requires blocking of free thiols, ascorbate-based denitrosylation of SNO-Cys, biotinylation of emerging thiol and avidin-based affinity isolation. However, in this current study we used resin-assisted capture of S-nitrosothiols (SNO-RAC) method to identify S-nitrosylated proteins from *Papaver* pollen during SI response as it contains fewer steps than BST reducing potential loss. Resin assisted-capture of SNO-proteins substitutes Thiopropyl Sepharose (TPS) for biotin-avidin. This method combines thiol labelling and protein enrichment into a single step, thus excludes the need of removal of excess biotinylating agent and avidin pull-down. Furthermore, SNO-RAC has better sensitivity for high MW SNO

proteins (Forrester *et al.*, 2009). Additionally, SNO-RAC is able to identify SNO-site more easily than BST approach. By using several available quantitative mass spectrometry approaches, this technique allows both SNO-site and protein level quantitation.

To generate S-nitrosylated proteins in *Papaver* pollen, germinated pollen was treated with 500 µM NO donor *S*-nitrosoglutathione (GSNO). After performing all the steps (see **Chapter 2, Section 2.11.2**) for protein capture, the beads were sent to the proteomic lab for trypsin digestion without adding the DTT. It was important not to expose samples to disulfide reductants (e.g. DTT) or UV light (e.g.sunlight) prior to or during sample handling as SNOs are a labile PTM and sensitive to homolytic or heterolytic degradation (Stamler and Toone, 2002). Washed and processed samples were sent for analyzed by mass spectrometry (see **Chapter 2, Section 2.11.3**).

4.2.1.3 Analysis of *S*-nitrosylated proteins after NO donor treatment

Fourteen proteins were identified from the NO donor treated pollen sample as candidates of *S*-nitrosylation. In contrast, mass spectrometry did not identify any proteins as candidates of S-nitrosylation from the untreated pollen sample. This gives us confidence that the identified modifications are likely to be authentic. The identified modified proteins were categorized according to their general function into different functional groups (see **Table 4.5**).

Two metabolic enzymes; fructose-bisphosphate adolase (FBA) and glyceraldehyde-3-phosphate dehydrogenase (GAPDH) were identified as *S*-

nitrosylated from the NO donor-treated pollen sample. Fructose-bisphosphate aldolase (FBA) has previously been described to undergo S-nitrosylation in various plants (Lindermayr *et al*., 2005, Abat *et al*., 2008, Tanou *et al*., 2009). In yeast cell FBA was modified by H_2O_2 stress without dramatic effect on the enzyme activity.

Table 4.5. Identified candidates of S-nitrosylated proteins from *Papaver* pollen extract treated with NO donor GSNO

Functional groups	Protein	Acc.No.	NO-peptides
Metabolism	Glyceraldehyde-3-phosphate dehydrogenase C subunit	AAM65189	VSNAScTTNc
	Fructose-bisphosphate aldolase,putative	NP_181187	AqEAFLVRcK
Cytokinesis and cell patterning	Callose synthase 10	ACV04899	EmDLLSIPSNTGS LRLVQWPLFLLcS K
Protein synthesis/signallin g	Putative elongation factor 1-a	AAL32631	YYcTVIDAPGHR
Protein synthesis	40S ribosomal protein S2 (RPS2D)	NP_191308	ATFDcLQK
	40S ribosomal protein S8 (RPS8A)	NP_197529	LLAcISSRPGQcG R
	40S ribosomal protein S3 (RPS3C)	NP_198403	GLcAIAQAESLR
	60S ribosomal protein L10 (RPL10B)	NP_174013	ALGtcARVAIGQVL LSVRcK
	putative ribosomal protein	BAA11393	GcIVSQDLSVLNL VIVK
Amino acid synthesis	5-methyltetrahydropteroyltriglutamate-homocysteine S-methyltransferase -like protein	BAF01079	cVTGFGFDLVR
	Cobalamin-independent methionine synthase	CAE55865	cVTGFGFDLVR
Transporter and channels	AHA4; ATPase/ hydrogen-exporting ATPase	NP_190378	VKRLQARKHIcGM TGD
Uncharacterized	predicted protein [Populus trichocarpa]	XP_0023374 43.1	GLcAIAQAESLR
	Hypothetical protein ZEAMMB73_875183	AFW74913	IIAVcADDPEYR

GAPDH was another metabolic protein identified in the NO donor-treated sample as being S-nitrosylated. The identified peptide was identical to an *Arabidopsis* peptide sequence and Cys-155 and Cys-159 were modified as a target of NO. It has been reported in *Arabidopsis* that S-nitrosylation on cys-155 and cys-159 is the primary target of post translational modification which decreases its enzymatic activity (Lindermayr *et al*., 2005, Holtgrefe *et al*., 2008). Therefore, modification identified on GAPDH in *Papaver* pollen sample is also expected to reduce the activity of this enzyme. This modification of cysteine in GAPDH seems to be quite an important and general one, affecting catalytic activity.

In yeast cells, oxidative stress conditions induced S-thiolation onto the GAPDH enzyme and this inhibited its activity (Shenton and Grant, 2003). It has also been demonstrated that very small concentration of NO donor sodium nitroprusside (SNP) not only inactivated GAPDH by S-nitrosylation of the enzyme thiol but also reduced the binding affinity of GAPDH for the red blood cells in mammalian cells (Galli *et al*., 1998). Recently, it has been shown that GAPDH is *S*-nitrosylated by NO resulting in the loss of its catalytic activity (Sen *et al*., 2008, Tristan *et al.*, 2011) and this S-nitrosylation confers the capability of GAPDH to bind to Siah-1. The GAPDH-Shih-1 complex is translocated into the nucleus and afterward causes apoptosis (Lee *et al.*, 2012, Hara *et al.*, 2005). Thus, this modification may be involved in a PCD process in poppy pollen.

Another protein that has been identified as being *S*-nitrosylated in poppy pollen is callose synthase. Callose can be found in almost all higher plants. At

particular stages of cell wall growth and differentiation, callose functions as important component. Callose is involved at numerous developmental stages of pollen (Stone and Clarke, 1992). It has been reported in numerous plant species that callose is synthesized by callose synthases (Verma and Hong, 2001, Brownfield *et al*., 2007, Brownfield *et al*., 2008). In *Arabidopsis thaliana*, twelve callose synthase genes have been identified by two research groups (Verma and Hong, 2001, Richmond and Somerville, 2000). It has been demonstrated that one of these genes, *CalS5*, encodes a callose synthase which is responsible for the synthesis of callose deposited at the cell wall of meiocytes, tetrads and microspores, and the expression of this gene is crucial for the formation of exine in pollen wall (Dong *et al.*, 2005). Although the effect of *S*-nitrosylation of callose synthase has not previously been reported, the implication is that it would probably affect its function towards the formation of callose in poppy pollen and eventually affect pollen tube germination and growth and thus play role in the SI.

Four ribosomal proteins (three 40S and one was 60S) were identified as being *S*-nitrosylated in the NO donor-treated pollen samples. Ribosomal proteins have been identified previously as candidates of S-nitrosylation in *Arabidopsis (*Fares *et al*., 2011). Although the consequences were not investigated, the authors suggested that nitrosylation of those ribosomal proteins could affect the protein synthesis machinery. The 60S ribosomal protein identified in this current study is L10 (RPL10B), which is a ubiquitous protein that takes part to joinup the 40S and 60S subunits into 80S functional unit (Eisinger *et al*., 1997, Loftus *et al*., 1997). However, collective evidence shows that RPL10 has

extra-ribosomal functions (Wool, 1996, Nika *et al*., 1997, Chávez-Rios *et al*., 2003). Previous studies showed in maize and *A. thaliana,* after treatment with UV-B radiation, protein biosynthesis was reduced. The auther hypothesized that protein biosynthesis was reduced probably because of ribosomal damage (Casati and Walbot, 2004, Ferreyra *et al*., 2010). Thus S-nitrosylation of the ribosomal proteins could affect their function, and hence protein synthesis.

Elongation factor 1-a (EF1-a), also involved in protein synthesis, was also detected as a target of NO. Identification of EF1a is quite interesting as different isoforms of this protein were also identified from the H_2O_2-treated samples suggesting a role of EF1a in the stress response. This will be discussed further later in this chapter and in **Chapter 5**.

In summary, we identified several important proteins which were modified by the artificial treatments of ROS and NO donors and found to be involved in various mechanisms related to pollen tube growth, stress, reorganization of actin cytoskeleton etc.

In order to provide further information and links between ROS and NO protein modifications in poppy pollen, we also performed mass spectrometry analysis on pollen that was SI-induced. We hoped this might provide data linking some general ROS and NO modifications to the biological phenomenon of SI.

4.2.2 Identification of proteins modified by oxidation during SI response to PrsS challange

As with previous experiments, we prepared untreated samples side by side to SI-induced pollen. The SI samples were taken at 5-12 min after the treatment. As mentioned earlier in **Section 4.2.1**, SI-induced increases in ROS reached its peak at ~10min. This is why we considered this time point for treatment. The extracted pollen proteins were analysed for oxidative modifications using FT-ICR-MS (for detail see **Chapter 2, Section 2.11.3**). The full list of the protein hits for both untreated and SI-induced samples can be found in the Appendix II.

4.2.2.1 Distribution of SI-induced modified proteins into different functional groups

To get an overall idea of the proteins modified by ROS during SI in poppy pollen, the protein 'hits' for both untreated and SI-induced samples were categorised according to the general functions (see **Figure 4.3**). The identified modified proteins were divided into: cytoskeletal proteins, metabolic enzymes, proteins involved in energy production, stress related proteins, signalling or regulatory proteins, protein degradation pathways, proteins related to biosynthesis, ion transport, protein transport, redox related proteins and others. The proportion of proteins involved in energy production was comparable between SI and untreated samples (10% versus 12%). Compared to the untreated controls, SI-induced pollen samples showed increased levels of modified cytoskeletal proteins (15% versus 10% in untreated; 26 different

peptides for SI and 8 different peptides for untreated from different proteins), stress related proteins (14% versus 10%; 19 peptides versus 11 peptides), signalling or regulatory proteins (12% versus 7%; 21 peptides versus 7 peptides) and redox related proteins (3% versus 0%; 6 peptides versus no peptide). The SI-induced samples showed clearly increased levels of modified proteins than untreated samples which gave us confidence that the modifications were authentic.

Of the proteins identified in the SI-induced samples as being modified 49% were specific to SI, i.e. the protein identification number was not found in the untreated samples. However, the untreated samples contained 57% modified proteins in common which were found in SI-induced samples. These were generally different sub-units of same complex or different isoforms.

As mentioned earlier (**Section 4.2.1.1**) that, types of modification play important role in the protein function. Among the identified peptides in the untreated samples, only 17% of them were modified irreversibly; the rest of the peptides showed reversible modification. In contrast, 85% of the identified peptides in the SI-induced samples were modified irreversibly. There is clearly a major difference between what is happening to the proteins in the SI samples.

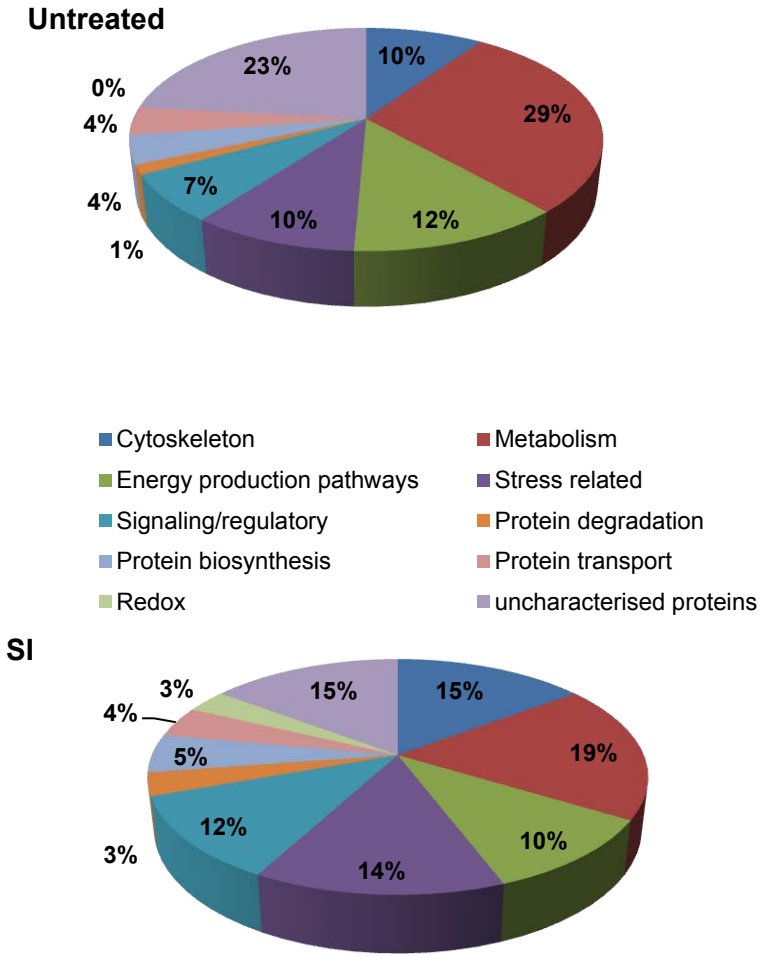

Figure 4.3. Distribution of SI-induced oxidatively modified proteins into functional groups

A graphical representation for Untreated and SI treated samples of the percentage of the modified proteins identified by FT-ICR-MS that fall into each of the different functional groups.

Although we identified some proteins common in both untreated and SI treated samples, types of oxidative modification of those proteins were different. For example, Actin7 was identified in both untreated and SI-induced samples. 2 peptides identical to actin 7 were identified in untreated samples and 3 peptides from SI-induced samples where 2 peptides were common in

both of these samples. In the untreated sample, methionine was oxidised to methionine sulfoxide which is a reversible modification. In contrast, the same peptides identified in the SI treated samples showed irreversible modifications of methionine and proline. Methionine was modified to met sulfone and proline was modified to Glu-γ-semialdehyde which are two steps modifications and irreversible, hence likely to be damaging to the proteins. These data suggest that during the SI response ROS might cause damage to several proteins which might affect their function in incompatible pollen.

4.2.2.2 Soluble inorganic pyrophosphatases are targets of ROS during SI

Mass spectrometry analysis identified peptides of soluble inorganic pyrophosphatase (sPPases) from *Papaver;* Pr-p26.1 as a target of ROS during SI response (**Table 4.6**). This was of considerable interest, as Pr-p26.1 sPPases are known to be important during SI and modified by Ca^{2+}, phosphorylation and by artificially added H_2O_2 (see **Chapter 3**). Peptides identical to Pr-p26.1a were identified in both untreated and SI samples and Pr-p26.1b were identified only in SI sample. Two different peptides from the untreated sample and three different peptides from SI samples were identified; the peptide AIGL**mp**MIDQGEKDDK was identified in both samples. In the untreated sample methionine was modified to met sulfoxide, which is a reversible modification. In the SI sample, methionine was irreversibly modified to met sulfone. In the same peptide proline was also irreversibly modified to glu-γ-semialdehyde in the SI sample, but not in the untreated sample. In the SI sample some other amino acid modifications were identified. Tryptophan

was modified to kynurenine, histidine was modified to 2-Oxohistidine and lysine was modified to aminoadepic semialdehyde where all these modifications were irreversible. Thus, most of the modifications observed were irreversible and likely to be damaging. Reversible modifications were observed on cysteine and asparagine where the modifications were carbamidomethyl and deamidation respectively.

Table 4.6. Identified peptides of Pr-p26.1a and Pr-p26.1b modified by ROS during SI signalling in poppy

Treatments	Proteins	Identified peptides	Site and type of modification
UT	**Pr-p26.1a**	AIGL**m**PMIDQGEKDDK EVAVNDFLPSATAHEAIQYS**m**DLYA EYI**m**MSLR	Met sulfoxide (rev) Met sulfoxide (rev)
SI	**Pr-p26.1a**	AIGL**mp**MIDQGEKDDK SVAAH**pwh**DLEIGPGAPSVVNAVVE IT**k** TL**c**EDNDPLDVLILMQE**p**VLPG**c**FLR	Met sulfone (irrev); Glu-γ-semialdehyde (irrev.) Glu-γ-semialdehyde (irrev.); Kynurenine (irrev.); 2- Oxohistidine (irrev.); AASA (irrev.) Carbamidomethyl (rev.); Glu- γ-semialdehyde (irrev.); Carbamidomethyl (rev.)
	Pr-p26.1b	AIGL**mp**MIDQGEKDDK KNEN**k**EVAVNDFLPAEDAS**k** TLNAIKAAS**y**SS**h**ARPSL**n**ER	Met sulfone (irrev); Glu-γ-semialdehyde (irrev.); AASA (irrev.) Phosphorylation; 2- Oxohistidine (irrev.); Deamidation (rev.)

Bold lowercase letters indicate the modified amino acids. UT= Untreated sample, SI=Recombinant PrsS treated sample. AASA=Aminoadipic semialdehyde, rev=reversible modifications, irrev= irreversible modifications

Identification of Pr-p26.1 pyrophosphatases as a target of ROS during SI response is an important finding. We showed in **Chapter 3** that the activity of Pr-p26.1 was reduced dramatically with H_2O_2 treatment. It is worth mentioning here that the same peptides of Pr-p26.1a were also identified in the H_2O_2-

treated pollen samples with same modifications on the amino acids. However, Pr-p26.1b was not identified as modified by H_2O_2-treated samples. In this current study we identified the Pr-p26.1 pyrophosphatases as a target of ROS, which clearly suggests that during SI-signalling ROS also affects the activity of Pr-p26.1 sPPases by modifying several amino acid residues. These data provide us with a further potential mechanism whereby Pr-p26.1 sPPases activity can be inhibited during SI signalling. Moreover it places this enzyme firmly as a key target for SI signals.

4.2.2.3 Other proteins modified by oxidation during SI

Besides Pr-p26.1 pyrophosphatases modified by oxidation, mass spectrometry analysis identified several groups of proteins which were of interest in the context of SI. As mentioned in S**ection 4.2.2.1** the SI-induced sample contained a greater number of modified cytoskeletal proteins, signalling proteins, stress-related proteins and redox proteins compared to control samples. Therefore these groups of proteins might be involved in the SI signalling in incompatible poppy pollen. These will be discussed below.

4.2.2.3.1 Cytoskeletal proteins modified after SI-induction

In total, 14 actin, tubulin and actin binding proteins were identified by mass spectrometry from SI-induced pollen samples as target of ROS. Six actin and tubulin (8 different peptides) were also identified from the untreated sample (**Table 4.7**). All these modifications to these proteins in the untreated sample

were on methionine which was reversibly modified to met sulfoxide. In the SI sample 26 different peptide hits were identified and most of them were irreversible modifications. Methionine was modified to met sulfone, proline to glu-γ-semialdehyde, lysine to aminoadipic semialdehyde and tryptophan was modified to kynurenine; all these modifications are irreversible. Cysteine was modified to cysteic acid (irreversible), carbamedomethyl or S-nitrosocysteine (reversible) modifications.

It is of interest that 48% of the modified peptides of actin in the SI-induced samples were also identified with same modifications in the H_2O_2-treated samples described in **Section 4.2.1.1.1**. These data suggest that SI-induced ROS might have similar effect as artificial H_2O_2-treated oxidative stress response. H_2O_2 is authentic ROS and SI involves ROS signalling. Here we have identified authentic identical modifications verifying similar biochemical processes involved in SI, so authentic SI-ROS mediated events. Three actin binding proteins (one profilin and two fimbrin) with 6 different peptides identical to *Arabidopsis* sequences were identified as modified by oxidation in the SI induced sample. Two peptides of profilin were identified where methionine was modified to either reversibly to met sulfoxide or irreversibly to met sulfone. Cysteine was modified to S-nitrosocystein which is a reversible modification.

Table 4.7. Modified cytoskeletal proteins found in the untreated and SI-induced samples by mass spectrometry analysis

Proteins	UT		SI	
	Identified peptides	Type of modification	Identified peptides	Type of modification
Actin 2	DLYGNIVLSGGTT**m**FPGIADR EITALAPSS**m**K	Met sulfoxide (rev.) Met sulfoxide (rev.)	DLYGNIVLSGGSTMF**p**GIADR YPIEHGIVTN**w**DDMEK	Glu y-semialdehyde (irrev.) Kynurenine (irrev)
Actin 3	n.d	n.d	DLYGNIVLSGGSTMF**p**GIADR LAYIALDYEQELETA**k** EITALA**p**SSMK	Glu y-semialdehyde (irrev.) AASA (irrev) Glu y-semialdehyde (irrev.)
Actin 4	EITALAPSS**m**K AVF**p**SIVGRPR	Met sulfoxide (rev.) Glu y-semialdehyde(irrev)	VAPEEH**p**VLLTEAPLNPK EITALAPSS**m**K	Glu y-semialdehyde (irrev.) Met sulfone (irrev.)
Actin 7	DLYGNIVLSGGST**m**FPGIADR EITALAPSS**m**K	Met sulfoxide (rev.) Met sulfoxide (rev.)	DLYGNIVLSGGST**m**F**p**GIADR YPIEHGIVSNWDD**m**EK EITALAPSS**m**K	Glu y-semialdehyde (irrev.); Met sulfone (irrev.) Met sulfone (irrev.) Met sulfone (irrev.)
Actin 11	n.d	n.d	DLYGNIVLSGGTT**m**FPGIADR EITALAPSS**m**K	Met sulfone (irrev.) Met sulfone (irrev.)
Actin 12	EITALAPSS**m**K LDLAGRDLTDHL**m**K	Met sulfoxide (rev.) Met sulfoxide (rev.)	SFEL**p**DGQVITIGAER AGFAGDDA**p**R EITALAPSS**m**K	Glu y-semialdehyde(irrev) Glu y-semialdehyde(irrev) Met sulfone (irrev.)
Alpha-tubulin	n.d	n.d	FDGALNVDVTEFQTNLV**p**YPR TVGGGDDAFNTFFSETGAG**k** QLFH**p**EQLISGKEDAANNFAR RTIQFVDW**c**PTGFKCGINYQPPSVVPGGDLAK **k**LADN**c**TGLQGFLVFNAVGGGTGSGLGSLLLER TIQFVDW**c**PTGFK	Glu y-semialdehyde(irrev) AASA (irrev); Glu y-semialdehyde(irrev) Carbamidomethylation (rev.) AASA (irrev); Carbamidomethylation (rev.) Carbamidomethylation (rev.)

Beta-tubulin	**m**ASTFIGNSTSIQE**m**FR LHFF**m**VGFAPLTSR	Met sulfoxide (rev.) Met sulfoxide (rev.)	NSSYFVE**w**l**p**NNV**k** GHYTEGAELIDSVLDVVR**k** AVL**m**DLEPGTMDSLR **m**MLTFSVFPSPK LAVNLI**p**FPR	Kynurenine (irrev); Glu y-semialdehyde(irrev); AASA (irrev) AASA (irrev); Met sulfone (irrev.) Met sulfone (irrev.) Glu y-semialdehyde(irrev)
fimbrin-like protein 2	n.d	n.d	KVEN**c**NEVIKIGK KVLEQAEKLD**c**k	Carbamidomethylation (rev.) Carbamidomethylation (rev.)
ATFIM1; actin binding	n.d	n.d	VVN**w**NLVTK A**c**TTTLLHTIYQSEKGPFVQHINR	Kynurenine (irrev) Carbamidomethylation (rev.)
Profilin	n.d	n.d	Y**m**VIQGEPGAVIR GAGGITIKKTGQSCVFGIYEEPVTPGQ**c**N**m**VVER	Met sulfoxide (rev.) S-nitrosocystein ;Met sulfone (irrev.)

In the identified peptide column lowercase bold letters show the modified amino acids. UT=Untreated samples as control treatments, SI=Recombinant PrsS treated samples. In the types of modification column Aminoadepic semialdehyde is shown as AASA;. Rev = reversible modification; irrev= irreversible modification; n.d=not detected.

Profilin generally binds to monomeric actin with high affinity (Perelroizen *et al*., 1996) and stimulates nucleotide exchange (ADP to ATP) in monomers released from the microfilaments (Goldschmidt-Clermont *et al*., 1991). Profilin is involved in maintaining a pool of ATP-G-actin in the cell by preventing hydrolysis of ATP (Ampe *et al*., 1988). This prepares actin for polymerisation, as it has a high affinity for the growing barbed end of the MF and profilin can then increase polymerisation by transporting G-actin to these barbed ends (Dos Remedios *et al*., 2003). Profilin can act to prevent spontaneous nucleation of filaments and also sequesters actin monomers when the barbed ends of filaments are capped (Pantaloni and Carlier, 1993). Modification of profilin identified in this study might alter its affinity for binding to actin filaments or could affect its actin sequestering property. This would likely impact on the organization of the actin cytoskeleton in incompatible pollen.

Four different peptides of fimbrin were identified as modified by oxidation in the SI-induced sample (**Table 4.7**). Fimbrin acts as an actin filament bundling protein (Glenney *et al*., 1981, Bretscher, 1981). The plant fimbrin AtFim1 has been shown to stabilise F-actin against profilin-induced depolymerisation *in vitro* and *in vivo* (Kovar *et al*., 2000). In this current study we identified the irreversible modification of tryptophan, cysteine and lysine on 4 peptides identical to *Arabidopsis* fimbrin which would affect the binding of fimbrin with actin and thus affect the bundling of actin filament.

Mass spectrometry analysis identified several peptides of actin and tubulin from the SI induced sample, which will be discussed further in detail in **Chapter 5,** which focuses on actin.

4.2.2.3.2 Signalling proteins modified by SI-induction

Several signalling proteins were identified as modified by ROS in incompatible pollen from SI induced samples. Peptides identical to several proteins like 14-3-3 proteins, elongation factors, initiation factors and Rab family proteins were identified. 21 different peptides were identified in the SI induced sample (**Table 4.8**). Lysine was modified to aminoadipic semialdehyde, proline to glu-γ-semialdehyde and methionine was modified to met sulfone which were all irreversible modifications of these amino acids. Methionine was also reversibly modified to met sulfoxide. Cysteine was also reversibly modified to carbamedomethyl and S-nitrosocysteine. Mass spectrometry identified 5 signalling proteins with 9 different peptides in the untreated sample. In the untreated sample methionine was modified to met sulfoxide and glutamine was deamidated. Both of the modifications were reversible. Proline was found to be modified to glu-γ-semialdehyde in one peptide where the modification was irreversible. 14-3-3 proteins and elongation factors were thought to be interesting as those proteins were also identified in the H_2O_2-treated sample described in **Section 4.2.1.1.2** and also found in association with actin which will be described further in detail in **Chapter 5**.

Table 4.8. Modified signalling/regulatory proteins found in the untreated and SI-induced samples by mass spectrometry analysis

Proteins	UT		SI	
	Identified peptides	Type of modification	Identified peptides	Type of modification
RAB GTPase homolog 1C	n.d	n.d	NVNKLLVGNK**c**DLTSQKVVS TRMASQ**p**AGGSKPPTVQIRGQPVN	Carbamidomethyl (rev.) Glu y-semialdehyde (irrev.)
Rab GDP dissociation inhibitor	n.d	n.d	NDYYGGESTSLNLIQLW**k** LSAVYGGTYMLNK**p**E**c**K	AASA (irrev.) Glu y-semialdehyde (irrev.); Carbamidomethyl (rev.)
RAB6A; GTP binding / protein binding	LVFLGDqSVGK ELNVmFIETSAK	Deamidation (rev.) Met sulfoxide (rev.)	n.d	n.d
Rab1/RabD-family small GTPase	n.d	n.d	FADDSYLESYISTIGVDF**k** LLLIGDSGVG**k**	AASA (irrev.) AASA (irrev.)
14-3-3-like protein GF14 omega	LAEQAERYEE**m**VEFMEK IISSIE**q**KEESR	Met sulfoxide (rev.) Deamidation (rev.)	QAFDEAIAELDTLGEESY**k** SKIETELSGI**c**DGILK	AASA (irrev.) Carbamidomethyl (rev.)
14-3-3-like protein GF14 iota	n.d	n.d	QAFDEAIAELDTLSEESY**k**DSTLI**m**QLLR DSTLI**m**QLLR	AASA (irrev.); Met sulfone (irrev.) Met sulfone (irrev.)
14-3-3-like protein AFT1	n.d	n.d	QAFEEAIAELDTLGEESY**k**DSTLI**m**QLLR DSTLI**m**QLLR **m**AATLGRDQYVYMAK VESELSSV**c**SGILK	AASA (irrev.); Met sulfone (irrev.) Met sulfone (irrev.) Met sulfone (irrev.) Carbamidomethyl (rev.)
elongation factor 2-like	EVAGDVR**m**TDTRADEAERG IT QRVIENANVI**m**ATYED	Met sulfoxide (rev.) Met sulfoxide (rev.)	GVQYLNEIKDSVVAGFQ**w**AS**k** ITDGALVVVD**c**IEGV**c**VQTETVLR N**c**DPDGPL**m**LYVSK LYMEAR**p**LEDGLAEAIDDGR GFVQF**c**YEPI**k**	Kynurenine (irrev.); AASA (irrev.) Carbamidomethyl (rev.) Carbamidomethyl (rev.) Carbamidomethyl (rev.); Met sulfone (irrev.) Glu y-semialdehyde (irrev) Carbamidomethyl (rev.); AASA (irrev.)
putative elongation factor	n.d	n.d	GVQYLNEIKDSVVAGFQ**w**AS**k** GHVFEE**m**QRPGTPLYNIK	Kynurenine (irrev.); AASA (irrev.) Met sulfone (irrev.)

elongation factor 1-alpha	n.d	n.d	YY**c**TVIDAPGHR GPTLLEALDLINE**p**KRPSDKPLR	Carbamidomethyl (rev.) Glu y-semialdehyde (irrev.)
initiation factor eIF4A-15	VQVGVFSAT**m**PPEALEITR **m**FVLDEADEMLSR	Met sulfoxide (rev.) Met sulfoxide (rev.)	LETL**c**DLYETLAITQSVIFVNTR VQVGVFSATM**p**PEALEITR	Carbamidomethyl (rev.) Glu y-semialdehyde (irrev.)
GRF7 (general regulatory factor 7)	n.d	n.d	LAEQAERYEE**m**VEFMEK DSTLI**m**QLLR QAFDEAISELDTLGEESY**k**DSTLI**m**QLLR	Met sulfone (irrev.) Met sulfone (irrev.) AASA (irrev.); Met sulfone (irrev.)

Two Rab GTPases and one Rab GDP dissociation inhibitor with 6 different modified peptide hits were identified in the SI induced sample. The identified Rab proteins all belong to the Rab family of small GTPase found in the plants. Small GTPases work as molecular switches in cells, cycling between an active, GTP-bound state and an inactive, GDP-bound state. The Rab GTPases act as key regulatory factors that impact on all the steps involved in endocytosis and intracellular membrane trafficking (reviewed by Bou Daher and Geitmann, 2011). The Rab-GTPases had been identified to be significant for pollen tube growth with overexpression experiments in tobacco (de Graaf *et al*., 2005, Cheung *et al*., 2002). Alteration/mutation of Rab resulted in inhibition of pollen tube growth and loss of directionality. In *Arabidopsis*, disruption of polar growth and alteration of cell wall patterning were observed because of loss of the pollen expressed RABA4D. (Szumlanski and Nielsen, 2009). Rab-GTPases also play a part in intracellular signalling with membrane trafficking as many receptor-ligand pairs continue to release signals in the course of the endocytic pathway (Miaczynska *et al*., 2004). So, the modifications identified on the Rab-GTPases in the SI-induced pollen sample likely to interrupt pollen tube growth or its proper directionality and thus would play a role in the SI in poppy incompatible pollen. Considering the involvement of Rab GTPase in the pollen tube growth and vesicle trafficking, we assumed that the modification identified during SI signalling might inhibit Rab GTPase activity and thus inhibit pollen tube growth. Further investigation should be carried out to confirm this hypothesis.

4.2.2.3.3 Redox related protein modified after SI-induction

Three redox related proteins modified by oxidation were identified in SI induced pollen samples as targets of ROS and not in the untreated samples. Six different peptides identical to those from *A. thaliana* and *Theobroma cacao* were identified (see **Table 4.9**). Modified amino acids were proline, lysine, arginine, methionine and cysteine where all the amino acids were modified irreversibly except for the cysteine which was modified reversibly to S-nitrosocysteine (**Table 4.9**).

Table 4.9. Identified redox related proteins modified by ROS after SI-induction in *Papaver* pollen

Treatments	Proteins	sequences	Types of modification
SI	sks11(copper ion binding)	YALNGVSHTD**p**ETPLK **k**NYNLLDAVS**r**	Glu y-semialdehyde (irrev) AASA(irrev.);Glu-y-semialdehyde (irrev)
	superoxide dismutase (Mn) (SOD)	LVVETTANQD**p**LVT**k** **m**TTTVIIIIFVAIFATTLHDARG AT**m**EP**c**LES**m**K	Glu y-semialdehyde (irrev.); AASA (irrev.) Met sulfone (irrev); Met sulfone (irrev); Met sulfone (irrev); S-nitrosocysteine (rev.); Met sulfone (irrev.)
	2-oxoacid dehydrogenases acyltransferase family protein	RTPVSGPKG**k**PQALQV**k** EEVA**p**AVPAAAPVAPAVWS**p** **k**	AASA (irrev.); AASA (irrev.); Glu y-semialdehyde (irrev); Glu y-semialdehyde AASA (irrev.);

In the sequence column bold lowercase letters indicate the modified amino acids. In the types of modification column AASA indicates aminoadipic semialdehyde. Rev=reversible modification; irrev.= irreversible modification

Among these 3 proteins, SKS11 and 2-oxoacid dehydrogenase proteins were also identified in the H_2O_2 treated sample; SKS11 was described earlier in **Section 4.2.1.1.4**. Superoxide dismutase (SOD) was unique to SI-induced

sample. SOD is a metalloenzyme that catalyzes the disproportionation of superoxide to produce H_2O_2 and molecular oxygen and protect cells from the toxic effect of ROS (Fridovich, 1995). Various efforts have been made to increase stress tolerance in plants by modifying the production of SOD enzymes. Ectopic production of cytosolic Cu/Zn SOD enhanced tolerance to stress in potato (Perl *et al*., 1993), sugar beet (Tertivanidis *et al*., 2004), tobacco (Faize *et al*., 2011), and plum (Diaz-Vivancos *et al*., 2013). A characteristic expression of manganese SOD 1 (MSD1) in a heat-stress-tolerant cultivar of rice (Oryza sativa) has been identified (Shiraya *et al*., 2014). The studies showed that MSD1-knock-down rice was strikingly susceptible to heat stress, while the quality of rice grain with constitutive high expression of MSD1 grown at 33/28 °C, was significantly better than that of the wild type. The authors proposed that MSD1 plays an important role in the adaptation of heat tolerance. SI can also be considered as a stress response. The irreversible modification found in this current study is likely to damage this protein and hence would affect protective characteristics of the protein. Thus the SI ROS-induced modifications of SOD are likely to be damaging.

The third redox related protein identified was 2-oxoacid dehydrogenases, which is a multi-enzymes play an important role in the redox regulation in the cell and also probably involve in the protection of the cell during oxidative damage (reviewed by Bunik, 2003). Although the effect of oxidative modification of this multienzyme is not known, we presumed that irreversible modification of this enzyme would affect its activity of protecting the cells during oxidative stress.

4.2.2.3.4 Oxidative modification of stress-related protein by SI-induction

In total, 13 stress related proteins with 19 different peptides were identified from the SI induced sample by mass spectrometry. In contrast, 6 stress-related proteins (9 different peptides) were identified from untreated sample where the modification occured on methionine for all the peptides (reversibly modified to met sulfoxide). The modified amino acids on the identified peptides from the SI induced samples were lysine, proline, methionine and cysteine. Lysine was modified to aminoadipic semialdehyde, proline to glu-γ-semialdehyde and methionine was modified to met sulfone, which were all irreversible modifications. Cysteine was either irreversibly modified to cysteic acid or reversibly modified to carbamedomethyl or S-nitrosocysteine (**Table 4.10**).

Among the identified peptides of HSPs in the SI induced sample, 57% of the peptides were also identified in the H_2O_2 treated sample described in **Section 4.2.1.1.3.** The identified proteins from the SI induced samples were mainly different isoforms of HSPs, chaperonin, luminal binding protein (BiP) and early responsive to dehydration 2 (ERD 2) proteins.

The molecular chaperone BiP belongs to the HSP 70 superfamily and has ATPase activity which binds to nascent polypeptides to induce their correct folding (Rothman, 1989). BiP supports in the folding of proteins and also acts in the quality control mechanism of endoplasmic reticulum (ER) that recognizes unfolded or abnormally folded proteins and drives them out of the

organelle for degradation (Ma and Hendershot, 2004). BiP has been shown to confer drought tolerance through an as yet unknown mechanism when constitutively overexpressed in *N. tabacum* (Alvim *et al*., 2001). It has been demonstrated in mice that BiP is oxidatively modified in liver of the aged mice with definitive decreases in BiP ATPase activity measured. This suggests that protein folding and other activities mediated by BiP are reduced during aging. Moreover, the loss of these chaperone-like activities could directly contribute to the age-dependent accumulation of misfolded proteins, a characteristic of the aging phenotype (Nuss *et al*., 2008). Identification of modifications on several peptides of BiP in this current study therefore might reduce the activity of this protein in the incompatible pollen tube. This might affect protein folding and protective characteristics against stress response.

Having identified oxidatively modified peptides during SI, we also wished to examine a potential role for NO, as we had previously shown that both ROS and NO increased in incompatible pollen during the SI response. We therefore investigated NO modification of protein after SI.

Table 4.10 Modified stress related proteins identified in untreated and SI treated pollen samples by mass spectrometry analysis

Proteins	UT		SI	
	Identified peptides	Type of modification	Identified peptides	Type of modification
Heat shock cognate 70 kDa protein isoform 1	**n.d**	**n.d**	SIN**p**DEAVAYGAAVQAAILSGEGNE**k** NQVAMN**p**INTVFDAK	Glu-γ-semialdehyde (irrev.); AASA (irrev.) Glu-γ-semialdehyde (irrev.)
heat shock protein 70	GVNPDEAVA**m**GAAIQGGIL R ATNGDTFLGGEDFD**n**TLLE FLVSEFKR	Met sulfoxide (rev.) Deamidation (rev.)	EVDEVLLVGG**m**TR SP**c**QN**c**LKDAGVTIKEVDEVLLVGGM TR	Met sulfone (irrev.) S-nitrosocysteine (rev.); Cysteic acid (irrev.)
Heat shock cognate 70 kDa protein, putative, expressed	**n.d**	**n.d**	EQVFSTYSDNQ**p**GVLIQVYEGER NQVAMN**p**INTVFDAK	Glu-γ-semialdehyde (irrev.) Glu-γ-semialdehyde (irrev.)
Hsp70b ATP binding	**n.d**	**n.d**	NEEKQFSPEEISS**m**VLVK**m**K IQQLLQDFFNGKEL**c**K	Met sulfone (irrev.); Met sulfone (irrev.) Cysteic acid (irrev.)
HSC70-1 ATP binding	**n.d**	**n.d**	IINE**p**TAAAIAYGLDK DAGVIAGLNV**m**R NQVA**m**NPVNTVFDAKRLIGR	Glu-γ-semialdehyde (irrev.) Met sulfone (irrev.) Met sulfone (irrev.)
heat shock cognate 70 kDa protein 2-like isoform 1	GVNPDEAVA**m**GAALQGGIL R IINEPTAAALSYG**m**TNK	Met sulfoxide (rev.) Met sulfoxide (rev.)	SIN**p**DEAVAYGAAVQAAILSGEGNE**k** NQVAMN**p**VNTVFDAK	Glu-γ-semialdehyde (irrev.); AASA (irrev.) Glu-γ-semialdehyde (irrev.)
heat shock protein 70-3	LIGDAAKNQVA**m**NPINT QFAAEEISS**m**VLIK	Met sulfoxide (rev.) Met sulfoxide (rev.)	SIN**p**DEAVAYGAAVQAAILSGEGNE**k** NQVAMN**p**INTVFDAK	Glu-γ-semialdehyde (irrev.); AASA (irrev.) Glu-γ-semialdehyde (irrev.)
heat shock protein 81-4	GYEVLY**m**VDAIDEYAVGQL K AVENS**p**FLER	Met sulfoxide (rev.) Glu-γ-semialdehyde (irrev.)	l**m**KAQALK EKFEGL**c**KVIK	Met sulfone (irrev.) S-nitrosocysteine (rev.);

PREDICTED: luminal-binding protein 5	**n.d**	**n.d**	VFS**p**EEISAMILTK LKEVEAV**c**NPIITAVYQR DILLLDVAPLTLGIETVGGVMT**k**	Glu-γ-semialdehyde (irrev.) Carbamidomethyl (rev.) AASA (irrev.)
luminal binding protein	**n.d**	**n.d**	VFSPEEISAMILT**k** DILLLDVAPLTLGIETVGGV**m**TK	AASA (irrev.) Met sulfone (irrev.)
chaperonin, putative	EERNYILG**m**IKK ILKITGIKD**m**GR	Met sulfoxide (rev.) Met sulfoxide (rev.)	TQDEEVGDGTTSVIVLAGE**m**LHVAEA FLEK LEEEYIENI**c**VQILK	Met sulfone (irrev.) S-nitrosocysteine (rev.);
Chaperonin CPN60-2	**n.d**	**n.d**	TQDEEVGDGTTSVIVLAGE**m**LHVAEA FLEK GYIS**p**YFITNQ**k**	Met sulfone (irrev.) Glu-γ-semialdehyde (irrev.); AASA (irrev.)
ERD2 (early-responsive to dehydration 2); ATP binding	**m**VNHFVQEFK QFAAEEISS**m**VLIK	Met sulfoxide (rev.) Met sulfoxide (rev.)	NQVA**m**NPVNTVFDAKRLIGR SIN**p**DEAVAYGAAVQAAILSGEGNE**k**	Met sulfone (irrev.) Glu-γ-semialdehyde (irrev.);

4.2.3 Identification of proteins modified by NO during SI response

In order to identify *S*-nitrosylated proteins modified by NO during SI in poppy pollen, we treated the germinated pollen with recombinant PrsS to induce SI and followed the method described in **Section 4.2.1.2** (see **Chapter 2**, **section 2.11.2** for further detail). Before being analysed by mass spectrometry, S-nitrosylated proteins were analysed by western blotting. (see **Chapter 2**, **section 2.7**). **Figure 4.4.a** shows that both SI and NO donor GSNO treated samples (samples from **section 4.2.1.2**) had heavy staining of many proteins indicating *S*-nitrosylation, whereas there was little or no staining of proteins detectable in the GSH treated samples used as a negative control. When DDT was used with the *S*-nitrosylated proteins treated with SI and GSNO no bands could be identified which suggests that DDT totally reduced the S-nitrosylated proteins. This verifies that we are authentically obtaining much more S-nitrosylated proteins in the SI and GSNO samples, leading confidence to further analysis.

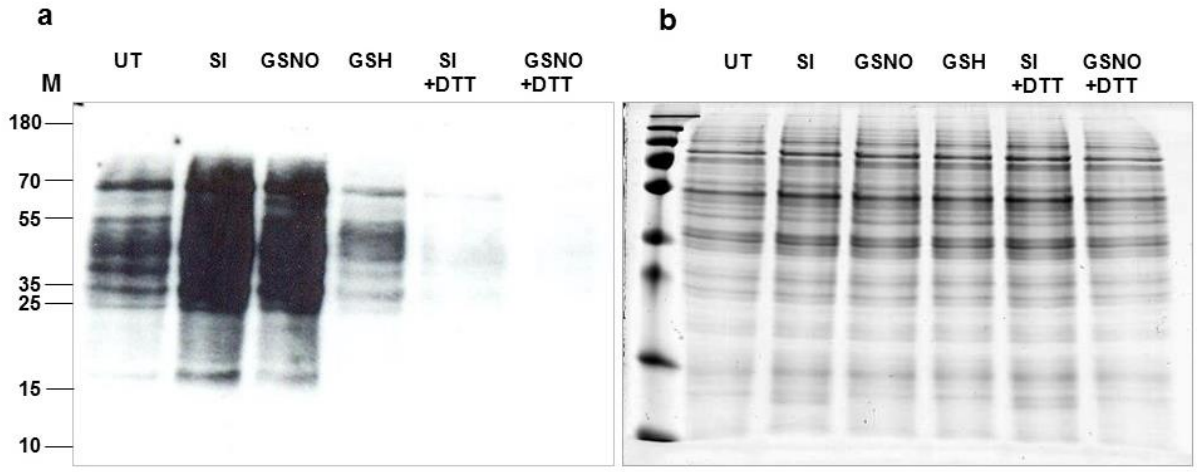

Figure 4.4 Detection of S-nitrosylated proteins from pollen tubes by Western blot analysis.

Western blot for S-nitrosylated proteins. UT=Untreated sample, SI=Recombinant PrsS induced sample, GSNO=NO donor S-nitrosoglutathion, GSH= Reducing agent glutathione, SI+DTT=SI induced S-nitrosylated proteins were reduced by DDT, GSNO+DTT= NO donor treated S-nitrosylated proteins were reduced with DTT. Western blot detection was performed with Pierce^{TM} S-nitrosylation western blot kit (Thermo scientific). M= Molecular marker (kDa)

Coomassie blue staining of S-nitrosylated proteins on 12.5% SDS-PAGE shows equal loading of proteins

4.2.3.1 Analysis of *S*-nitrosylated proteins during SI-induction identified by mass spectrometry

Strong positive staining for *S*-nitrosylated proteins in the SI samples and mass spectrometry analysis identified 12 *S*-nitrosylated proteins from the SI induced sample (**Table 4.11**). No peptides were identified by mass spectrometry analysis from the untreated samples; the visible bands detected on the western blot for the untreated sample might be because of background cross-reactivity. Among the 12 S-nitrosylated SI proteins identified, 4 proteins were

also identified in the NO donor treated samples described in **section 4.2.1.2**. These are: glyceraldehyde-3-phosphate dehydrogenase (GAPDH), elongation factor 1-a, callose synthase and 60S ribosomal protein L10 (RPL10B). We hypothesize these 4 proteins are important in the context of SI response as they were identified in both of the samples and also because of their functions described in **Section 4.2.1.2**.

Table 4.11. Identified candidates of S-nitrosylated proteins from *Papaver* pollen extract treated with recombinant PrsS (SI induced)

Functional groups	Proteins	Acc.No.	NO-peptide sequence
Metabolism	glyceraldehyde-3-phosphate dehydrogenase	AAM65189	VSNAS**c**TTN**c**
Protein synthesis/signalling	Putative elongation factor 1-a	AAL32631	YY**c**TVIDAPGHR
Protein synthesis	60S ribosomal protein L10 (RPL10B)	NP_174013	IRIYDVGMKRKGVDEF PY**c**VHLV
Cytokinesis and cell patterning	Callose synthase	ACV04899	E**m**DLLSIPSNTGSLRL VQWPLFLL**c**SK
Small secreted protein	PREDICTED: tyrosine-sulfated glycopeptide receptor 1-like	XP_004235 515	LSRLEQLLLHINNLNGT VPPSLMT**c**TR
Uncharacterized proteins	Stem-specific protein TSJT1, partial	XP_003637 634	VDSSGQV**c**GATFK
	Hypothetical protein OsI_06487	EAY85133	IA**c**YVTVR
	Ferric leghemoglobin reductase-2 precursor	NP_001237 764	AEEDGVA**c**VEYIAGK
	unknown	ACF86001	TVVSIP**c**GPSALAVK
	unnamed protein product	BAG94605	NPGDEVFSGST**c**K
	unknown	AFK48639	AG**c**YAANVIIQR

Proteins written in **red** are also identified as being modified in the GSNO pollen samples

A tyrosine-sulfated glycopeptide receptor protein was identified in the SI induced sample as a candidate of *S*-nitrosylation. A number of genes encoding small secreted peptides have been identified in *Arabidopsis* (Lease and Walker, 2006, Silverstein *et al*., 2007, Ohyama *et al*., 2008) and a certain part of their products are likely to comprise candidates for ligands (i.e. hormones). In *Arabidopsis* cell suspension culture medium, a tyrosine-sulfated glycopeptide has been identified and named as PSY1. This peptide, even at nanomolar concentration, significantly promotes cellular proliferation and expansion (Amano *et al*., 2007). So far, three tyrosine-sulfated peptide hormones, PSK, PSY1 and RGF1, have been identified in plants and all are related to cell elongation activity. Recent evidence has shown that secreted peptide hormones often undergo post-translational modification which are critical for their function (reviewed by Matsubayashi, 2011). Besides, a loss-of-function mutant of AtTPST (tpst-1) exhibited a noticeable dwarf phenotype accompanied by stunted roots, disorganized root meristem, pale green leaves, reduction in higher order veins and early senescence, suggesting various roles for tyrosine-sulfated peptides in plant growth and development (Komori *et al*., 2009). In this current study we identified a tyrosine-sulfated glycopeptide receptor 1-like protein which was S-nitrosylated. This modification might affect its function of cell elongation of the pollen tube.

In summary, in this chapter, we identified for the first time several potentially important protein targets of ROS and NO during SI induction in incompatible *Papaver* pollen. We identified hundreds of oxidatively modified proteins from the mass spectrometry analysis in both SI induced and H_2O_2 treated samples.

However, the number of S-nitrosylated proteins in both SI-induced and NO donor GSNO treated samples was very low. Mass spectrometry analysis identified several similarities between SI-induced and ROS and NO donor treated samples and clear differences between SI/ROS/NO and untreated samples. Detailed analysis of the overall function will be discussed in **Chapter 6**, where we will further discuss a few aspects that relate to their potential biological function in SI dealing with both oxidative modifications and nitrosylation.

Chapter 5

Actin as a target for SI signals

5.1 Introduction

As mentioned in **Chapter 1** (**Section 1.2**) the cytoskeleton comprises a dynamic network of actin microfilaments (MFs or F-actin), microtubules (MTs), and accessory proteins. Actin is a crucial element of the cytoskeleton and plays an important role in maintaining cell morphology and polarity, functions to regulate endocytosis and intracellular trafficking (Winder and Ayscough, 2005). There are many other proteins which interact with the cytoskeleton. For instance, motor proteins used for intracellular transportation along the cytoskeletal 'tracks', such as myosin and dynein and also proteins involved in controlling MF and MT dynamics. In cells, the actin filaments can be assembled or disassembled. Many actin-binding proteins (ABPs) are involved in controlling organisation of actin filaments into functional networks (Dos Remedios *et al*., 2003).

The dynamics of the actin cytoskeleton are controlled by signalling pathways which permit the cell to respond to exterior stimuli and acclimatize successfully to new environments. In mammalian cells, actin plays a vital role in organelle and vesicle transport, and in the motility of the cell itself. In plant cells, the actin cytoskeleton plays a role in various processes such as, cytoplasmic streaming, co-ordinating endo- and exocytosis, guiding the plane of cell division, cell wall synthesis and response to pathogen attack (Meagher and Williamson, 1994, Kobayashi *et al*., 1994, Fowler and Quatrano, 1997, Kobayashi *et al*., 1997a, Kobayashi *et al*., 1997b, Kropf *et al.*, 1998, Nick, 1999, McCurdy *et al*., 2001). Actin has also been found to be involved in

programmed cell death pathways in plant, yeast and mammalian cells (Franklin-Tong and Gourlay, 2008).

The actin cytoskeleton is a major target for signalling cascades in both plants and animals. In plants, a wide range of biotic and abiotic stimuli, for example light, pathogen attack and SI can trigger actin alteration (Nick, 1999, Staiger, 2000). The continuous and rapid actin filament reorganization system during cell motility and migration, mitogenesis, and phagocytosis depends on nucleation, elongation and depolymerisation of actin filaments as the basic process (Small *et al*., 2002, Pollard and Borisy, 2003). The actin binding proteins (ABPs) are generally thought to be responsible for transducing the extracellular signals into changes in cytoarchitecture and the function of actin.

Many of the ABPs identified in plants so far have their activity controlled by phospholipids, calcium and post-translational modifications (PTMs) suggesting that they are responding to external signals (Dos Remedios *et al*., 2003, Winder and Ayscough, 2005). It has recently been reported that actin is a major substrate for at least 17 post-translational modifications. These PTMs of actin are extensively employed, occur through enzymatic and non-enzymatic mechanisms, control the equilibrium of monomer-polymer and organisation of actin and regulate both physiological and pathological processes (Terman and Kashina, 2013). The dynamic reorganization of cellular actin is greatly controlled and ROS seem to be one of the vital regulatory elements (Moldovan *et al*., 2006). The activity of signalling pathways can be affected by ROS through direct modification of regulatory proteins via disulphide bond formation, nitrosylation, carbonylation or glutathionylation (England and Cotter,

2005). Glutathionylated actin is documented to be present in human cells in many conditions of oxidative stress (Fratelli *et al*., 2002, Pastore *et al*., 2003). Notably, glutathionylation of actin can prevent actin polymerization. This is a reversible alteration which suggests that actin glutathionylation might prevent irreversible organization of F-actin inside the cells by extreme actin polymerization under oxidative stress conditions (Dalle-Donne *et al*., 2001b).

The actin cytoskeleton is crucial for the tip growth of pollen tubes (Gibbon *et al*., 1999, Vidali *et al*., 2001). It is widely believed that three different structures of actin cytoskeleton are observed into the pollen tubes (Staiger *et al*., 2010). Longitudinal actin cables are distributed in the shank region throughout the cytoplasm. Following this actin cable arrangement, movement of organelle and vesicle trafficking are controlled within the cell. In the subapex, dense mesh of short actin filaments are found which are involved in the cytoplasmic streaming and elongation of pollen tubes (Hepler *et al*., 2001). Very fine and short actin filaments of the apical region probably regulate the fusion of vesicles through exocytosis (Bou Daher and Geitmann, 2011)

It has been shown in previous studies that the actin cytoskeleton is an early target of the SI signalling cascade in *Papaver* (Geitmann *et al*., 2000, Snowman *et al*., 2002). The alterations of cytoskeleton during SI follow a distinctive and reproducible pattern that begins with a depolymerisation of the F-actin in the pollen tube (Snowman *et al*., 2002), subsequently the formation of small actin foci and later, larger, stable punctate F-actin foci (Geitmann *et al*., 2000, Snowman *et al*., 2002, Poulter *et al*., 2010). The early depolymerisation of F-actin during SI contributes to the inhibition of pollen tube

growth and recent work has shown that F-actin depolymerisation and stabilization is necessary and sufficient for beginning of PCD (Thomas *et al*., 2006).

More recently, studies have shown that, actin cytoskeleton is a target of ROS and NO signals during SI in *Papaver* incompatible pollen (Wilkins *et al*., 2011). Increases in both ROS and NO contribute to the signalling events that mediate the formation of the actin punctate foci which are characteristic of the SI response in incompatible pollen of *Papaver.* Studies showed that untreated pollen tubes contained negligible number of actin foci, while SI induced pollen tubes had high levels, and when pollen was pre-treated with the ROS scavenger TEMPOL (4-Hydroxy-2,2,6,6-tetramethylpiperidine 1-oxyl) and/or c-PTIO (2-(4-carboxyphenyl)-4,4,5,5-tetramethylimidazoline-1-oxyl-3-oxide) prior to SI-induction, the number of actin foci was significantly reduced (Wilkins et al., 2011), demonstrating that ROS and NO are important signal for formation of foci.

Chapter 4 identified and characterized some of the protein targets that are modified by ROS and NO signalling during SI in *Papaver*. We identified hundreds of proteins and amongst them actin was identified as a target of ROS and NO. Considering the importance of the involvement of actin changes/depolymerisation and actin binding proteins in the SI signal, we decided to investigate the possible role of actin and actin binding proteins as target of ROS and NO signalling more intensively.

In this chapter we used H_2O_2 and the NO donor GSNO (*S*-nitrosoglutathione) to increase the levels of ROS and NO respectively in the pollen tube to

artificially observe their effect more clearly *in vitro*. Unfortunately we could not detect any proteins that were modified by NO donor GSNO using the actin pull down assay. However, we could see the formation of actin foci after NO donor treatment in the pollen tube. We also used SI treated pollen samples to investigate the role of ROS and NO during SI. We took the approach of isolating the modified F-actin from SI-induced, H_2O_2 and NO donor GSNO treated pollen extracts and used mass spectrometry to identify modified proteins associated with actin. F-actin from untreated pollen was also examined as control to make comparisons with components that were related with the F-actin under normal conditions and those that were induced by artificial and *in vivo* SI conditions. We also cloned and sequenced *Papaver* pollen actin in order to identify the exact modifications identified by mass spectrometry. Thus this chapter comprises the first studies to analyse the actin cytoskeleton and its associated proteins as targets of ROS after SI induction and identify their modifications providing insights into novel additional mechanisms expected to be involved in mediating SI-PCD through actin.

5.2 Results

5.2.1 F-actin enrichment using ultracentrifugation

To explore the possible role of actin and ABPs as a target of ROS and NO signalling we performed a two-step purification protocol developed by Poulter *et al*. (2011). The first step involved F-actin enrichment using ultracentrifugation. Pollen tube proteins from untreated, SI-induced pollen at 12 min and H_2O_2-treated pollen at 12 min were extracted in the presence of phalloidin to stabilise the F-actin during the extraction procedure. The pollen extracts were centrifuged to sediment the majority of F-actin (see **Chapter 2**, **Section 2.8** for details). The total protein (pre-spin), supernatant and pellet fractions were analysed using SDS-PAGE and Western blotting to observe the presence of actin and ABPs. **Figure 5.1a** shows that the ultracentrifugation procedure enriched F-actin in all the samples. The amount of F-actin in the pellet fractions for untreated, SI induced and H_2O_2 treated samples were greatly increased than in the total protein. The supernatant fractions did not contain any F-actin detectable by western blot. The coomassie blue staining of the gel in **Figure 5.1b** shows equal loading of proteins.

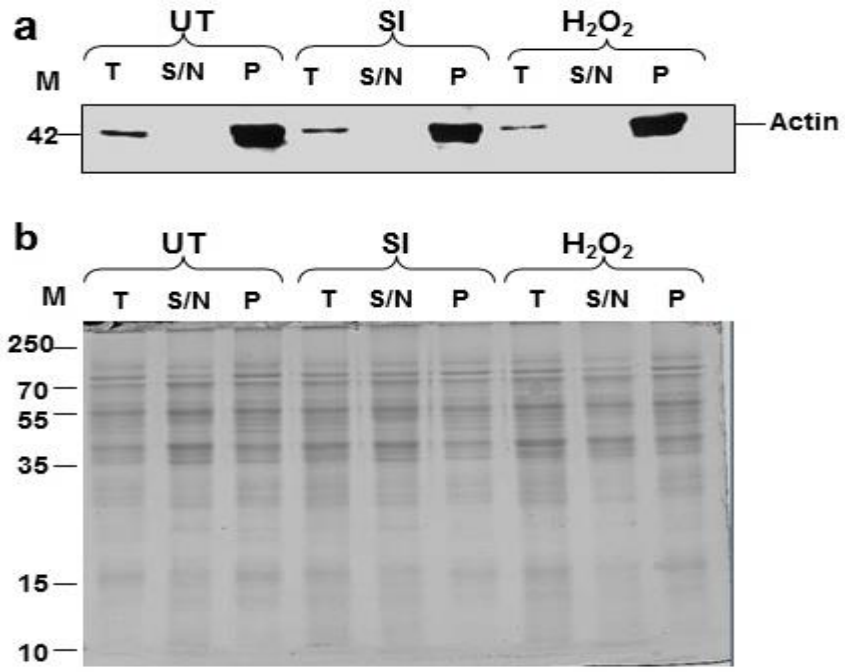

Figure 5.1. Western blot analysis of Enrichment of F-actin from poppy pollen tubes by ultracentrifugation

UT = untreated extracts, SI = Self-incompatible extracts, H_2O_2 = H_2O_2 treated extracted

T= total protein, S/N = supernatant, P = pellet

a. Western blot analysis of actin in pollen. Proteins from each of the three fractions were separated by SDS-PAGE and blotted onto nitrocellulose membrane. The membranes were then probed with the antibodies Anti-Actin mouse mAb (Ab-1,JLA 20, 1:5000). Detection was carried out with ECL.

b. Coomassie blue staining of total protein on 12.5% SDS-PAGE shows equal loading of proteins

5.2.2 F-actin isolation using actin pull down assay

The second step in the isolation and purification of F-actin from pollen protein extracts was an F-actin pull-down assay from the pellet fraction prepared in the ultracentrifugation step. Biotin phalloidin was added to the re-suspended pellet fraction during incubation of the F-actin pellet, which allowed the phalloidin to bind the F-actin. The biotin-phalloidin F-actin complex was pulled out of the extract using Streptavidin Magne Sphere Paramagnetic Particle

(SA-PMPs; magnetite beads coated in streptavidin; see **Chapter 2**, **Section 2.9** for detail). Unbound proteins were washed from the SA-PMPs. The resultant SA-PMPs, which were binding F-actin and associated proteins linked with F-actin, were analysed using SDS-PAGE and western blotting. **Figure 5.2a** shows that non-bound and wash fractions were completely actin free, a considerable amount of bound actin was successfully enriched from the pollen extract from all untreated, SI induced and H_2O_2 treated extracts.

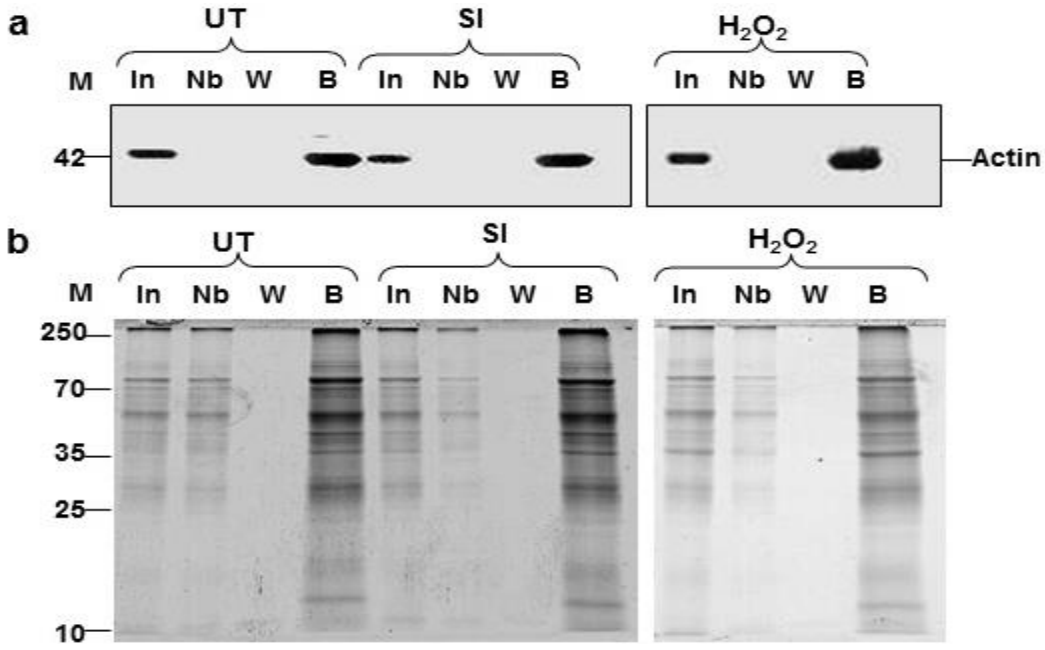

Figure 5.2. Western Blot analysis of poppy pollen tube F-actin pull-down using SA-PMPs.

Proteins were extracted from untreated pollen or SI-induced or H_2O_2 treated pollen and subjected to F-actin enrichment using ultracentrifugation. The pellet containing the F-actin was re-suspended, incubated with biotin-phalloidin and subjected to an F-actin pull-down assay using SA-PMPs.

(a) Western blot for actin. The untreated, SI and H_2O_2 samples had actin in the input (In). The non-bound (Nb) and washes (W) fractions were actin-free. The SA-PMPs containing the bound F-actin (B) were boiled to release the F-actin and its associated proteins. M = marker (kDa), the blot was probed with Anti-Actin mouse mAb (Ab-1,JLA 20, 1:5000). Detection was carried out with ECL.

(b) Coomassie blue stain of 12.5% SDS PAGE showing loading of the different fractions of the pull-down assay.

This demonstrates that the SA-PMPs could purify actin effectively. The Coomassie blue stain of the gel (**Figure 5.2b**) shows that in the bound fraction there were many proteins; as these proteins were potentially came down in the actin fraction they are interacting with the F-actin.

5.2.3 Analysis of F-actin and actin binding proteins using mass spectrometry

After isolation of the F-actin and its associated proteins from the pollen protein extracts by the actin pull down assay, they were analysed by mass spectrometry discussed in **Chapter 4** (**Section 4.2.1**). Unfortunately we could not identify any peptide from NO donor treated sample. This is not very surprising, because the *S*-nitrosylated proteins are very labile post translational modifications and sensitive to homolytic or heterolytic degredation (Stamler and Toone, 2002). As samples had to go through a multistep procedure before analysing them by mass spectrometry, the *S*-nitrosylated protein might be degraded and as a result could not be identified. The full list of the actin and its associated proteins identified in untreated, SI-induced and H_2O_2 treated samples can be found in the Appendix II.

To get a general idea of the type of proteins being identified as modified proteins by the mass spectrometer, we categorised the 'protein hits' identified from the untreated (UT), SI and H_2O_2 treated samples into different functional groups shown in **Figure 5.3**.

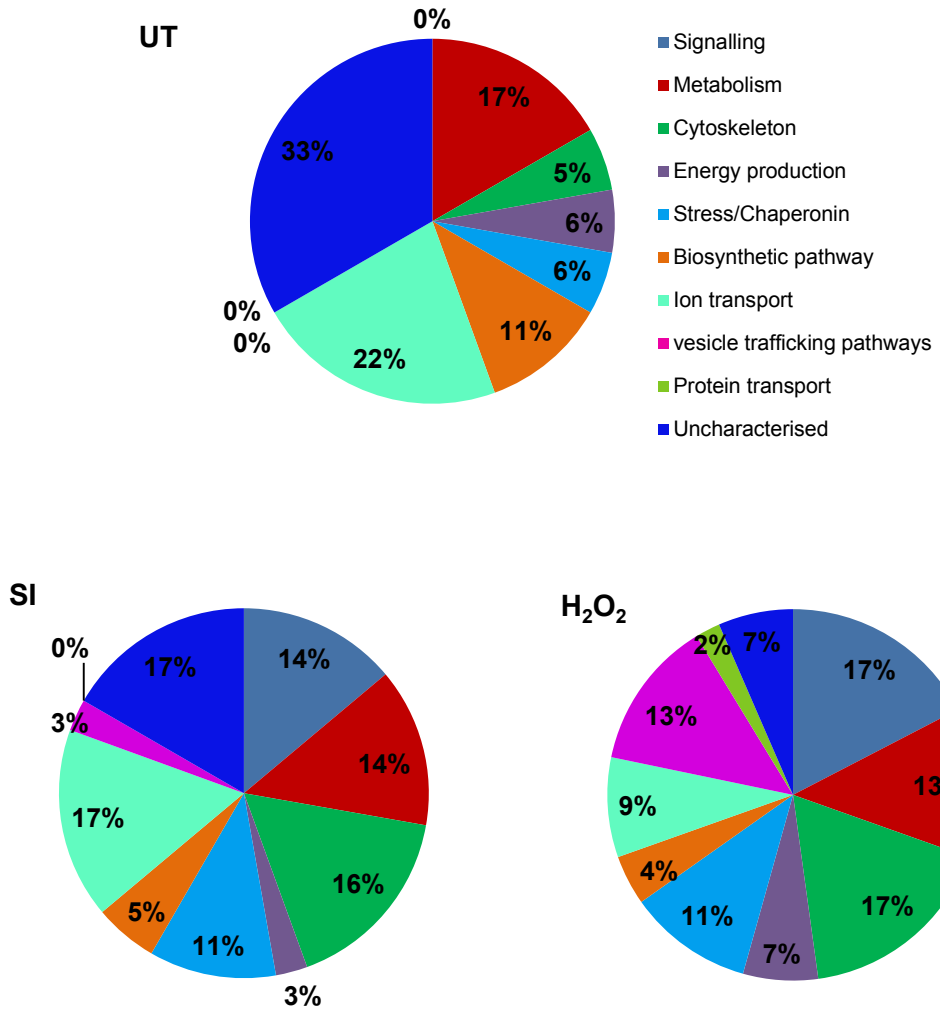

Figure 5.3. % Distribution of identified modified actin and actin binding proteins into different functional group

A pie chart representation of the percentage of the proteins identified by FT-ICR-MS that fall into each of the functional groups. for untreated (UT), SI and H_2O_2 treated samples.

The identified modified proteins are divided into signalling proteins, metabolic enzymes, cytoskeletal proteins, proteins involved in energy production, stress related proteins, proteins related to biosynthetic path ways, ion transport, proteins involved in vesicle trafficking pathways, protein transport and others. In the untreated samples 124 proteins were identified, among them 17

proteins were found to be modified with 30 different peptides. In total 36 proteins (62 different peptides) and 46 proteins (92 different peptides) were identified as modified proteins from SI treated and H_2O_2 treated samples respectively.

SI and H_2O_2 treated samples were more similar to each other than untreated samples. Compared to the untreated control, SI and H_2O_2 treated samples showed increased levels of signalling proteins (14% in SI; 17% in H_2O_2; 0% in UT), increased Cytoskeletal proteins (16% in SI; 17% in H_2O_2; 5% in UT), increased stress related proteins (11% in SI; 11% in H_2O_2; 6% in UT) and increased proportions of proteins involved in vesicle trafficking pathways (3% in SI; 13% in H_2O_2; 0% in UT). Among the identified proteins in the SI and H_2O_2 treated samples, more than 50% of proteins (and 44% of peptides) were common in both the samples. Some of the proteins were specifically found in these two samples but not in the untreated samples. For instance, there were no signalling proteins or vesicle trafficking proteins found in the untreated samples which suggest that these groups of proteins might be involved in the SI signalling as well as stress response. However, untreated samples contained 47% proteins in common which were found in either SI or H_2O_2 treated samples. These were mainly different sub units of same complex or different isoforms. This analysis had been carried out against green plant data base; as a result there were several peptides which could be identified as identical to those found in one or more plant species. If the modification was in same in all peptides we choose one protein among those common proteins.

Mass spectrometry allows sensitive detection of modified proteins. The extent and types of oxidative modification of protein was another important aspect for analysing the proteins. There were 5 proteins which were identified in all the three samples (UT, SI & H_2O_2). However, the type of modifications identified on these proteins varied. In most of the cases (in 4 proteins), the modification in the untreated samples were reversible, while the same proteins in SI treated or H_2O_2 treated samples showed irreversible modification. For example, Actin 3 of *Populus trichocarpa* was identified in untreated, SI and H_2O_2 treated samples. In the untreated sample, two peptides were identified where methionine was oxidised to methionine sulfoxide which is a reversible modification (**Chapter 1, Figure 1.4**). On the other hand, the same peptides identified in the SI and H_2O_2 treated samples showed irreversible modifications of methionine and proline. Methionine modified to Met sulfone and proline was modified to Glu-γ-semialdehyde (**Chapter 1, Figure 1.4**). Reversible oxidative modification might involve in important regulatory mechanism while irreversible oxidative modifications are damaging to the proteins (Møller *et al*., 2007). These data suggest that during SI response ROS might cause damage to several proteins which might play important role in the cell.

The alteration of the F-actin during SI is thought to be an active process. Previous studies have shown that alteration of F-actin as a result of the increase of ROS and NO are involved in SI mediated PCD (Wilkins *et al*., 2011) pointed towards a role for the alteration in SI signalling cascade.

Therefore, the identified modified proteins that were involved in signalling were investigated more thoroughly in the current study. The SI and H_2O_2 treated samples exhibited an increase in the modification status of cytoskeletal proteins; proteins involved in signal transduction, stress related proteins and vesicle trafficking proteins compared to the untreated samples and therefore were of more interest as candidates for detailed investigation.

5.2.3.1 Actin as a target of ROS

Several cytoskeletal proteins; primarily actin and one tubulin were identified as targets of oxidative modification from SI and H_2O_2 treated samples. The modifications are shown in **Table 5.1**. Several proteins were found to be modified in both SI and H_2O_2 treated samples. Peptides of Actin 3 protein identical to *Populus trichocarpa* was the only peptides found in all three types of samples (UT, SI, H_2O_2) though the type of modification was different. The EITALAPSS**m**K peptide was identified in both untreated and SI treated samples. In the untreated sample the methionine was modified to Met sulfoxide which is a reversible modification, while in SI sample methionine was irreversibly modified to Met sulfone.

Table 5.1. Actins found in the untreated (UT), SI and H_2O_2 treated samples.

Proteins	UT		SI		H_2O_2	
	Identified peptides	Type of modifications	Identified peptides	Type of modifications	Identified peptides	Type of modifications
alpha-tubulin [*P. vulgaris*]	n.d	n.d	AIFVDLE**p**TVIDEVR TVGGGDDAFNTFFSETGAG**k**	Glu-y-semialdehyde (irrev.) AASA (irrev.)	AIFVDLE**p**TVIDEVR TVGGGDDAFNTFFSETGAG**k**	Glu-y-semialdehyde (irrev.) AASA (irrev.)
actin 3 [*P. trichocarpa*]	NGTG**m**VKAGFAG DDAPRAV EITALAPSS**m**K	Met sulfoxide (rev.) Met sulfoxide (rev.)	VAPEEH**p**VLLTEAPLNPK EITALAPSS**m**K	Glu-y-semialdehyde (irrev.) Met sulfone (irrev.)	NGTG**m**V**k**AGFAGDDAPRAV VAPEEH**p**VLLTEAPLNPK	Met sulfone (irrev.); AASA (irrev) Glu-y-semialdehyde (irrev.)
Actin [*C. sinensis*]	n.d	n.d	SYEL**p**DGQVITIGAER EITALAPSS**m**K	Glu-y-semialdehyde (irrev.) Met sulfone (irrev.)	SYEL**p**DGQVITIGAER EITALAPSS**m**K	Glu-y-semialdehyde (irrev.) Met sulfone (irrev.)
Actin 7 [*A. thaliana*]	n.d	n.d	VAPEEH**p**VLLTEAPLNPK DLYGNIVLSGGSTmF**p**GIADR NYELPDG**q**VITIGAER	Glu-y-semialdehyde (irrev.) Met sulfone (irrev.) Glu-y-semialdehyde (irrev.) Deamidation	VAPEEH**p**VLLTEAPLNPK DLYGNIVLSGGST**m**F**p**GIADR NYELPDG**q**VITIGAER	Glu-y-semialdehyde (irrev.) Met sulfone (irrev.); Glu-y-semialdehyde (irrev.) Deamidation
actin 4 [*G. max*]	n.d	n.d	LAYIALDYEQELETS**k** SYEL**p**DG**q**VITIGAER	AASA (irrev.) Glu-y-semialdehyde (irrev.) Deamidation	n.d	n.d
Actin, partial *[G. max]*	n.d	n.d	LAYIALDYEQELETS**k** SYEL**p**DGQVITIGSER	AASA (irrev.) Glu-y-semialdehyde (irrev.)	LAYIALDYEQELETS**k** LDLAGRDLTDAL**m**KILTER DLTDAL**m**KILTER SYEL**p**DGQVITIGSER	AASA (irrev.) Met sulfone (irrev.) Met sulfone (irrev.) Glu-y-semialdehyde (irrev.)

actin [*M. acuminata*]	n.d	n.d	n.d	n.d	DLYGNIVLSGGSTMF**p**GIADR MSKEITALAPSS**m**K YPIEHGIVSNWDD**m**E**k** **c**DVDIRRDLYGNIVLSGGST**m** FPGIADR HTGV**m**VG**m**GQKDAYVGDE AQSKR	Glu-y-semialdehyde (irrev.) Met sulfone (irrev.) Met sulfone (irrev.); AASA (irrev.) S-nitrosocysteine (rev.); Met sulfone (irrev.) Met sulfone (irrev.)
Actin 2 [*P. abies*]	n.d	n.d	n.d	n.d	DLYGNIVLSGGSTMF**p**GIADR LDLAGRDLTDAL**m**KILTER YPIEHGIVSNWDD**m**EKIWHH TFYNELR	Glu-y-semialdehyde (irrev.) Met sulfone (irrev.) Met sulfone (irrev.)
Actin-like [*G. max*]	n.d	n.d	n.d	n.d	DLYGNIVLSGGSTMF**p**GIADR FR**c**PEVLFQPSMIG**m**EAVGIH ETTYNSI**m**K	Glu-y-semialdehyde (irrev.) S-nitrosocysteine (rev.); Met sulfone (irrev.)

In the identified peptide column lowercase bold letters indicate the modified amino acids. UT=Untreated samples, SI=Recombinant PrsS treated samples, H_2O_2= H_2O_2 treated samples. In the types of modification column AASA indicates Aminoadepic semialdehyde. Rev=Reversible modification; irrev= irreversible modification; n.d=not detected

Some of the peptides were identified in several proteins with the same modifications in both SI and H_2O_2 treated samples. For example, the DLYGNIVLSGGSTmFpGIADR peptide was identified in 4 different proteins identical to different green plants, where either methionine (m) or proline (p) or both of them were modified in an irreversible way. Methionine was modified to Met sulfone and proline was modified to Glu-γ-semialdehyde. This indicates that these amino acids might be real target of ROS during SI signal. This will be further discussed in **Section 5.2.3.1.1**.

Two peptides of alpha-tubulin identical to *Phaseolus vulgaris* were identified from both SI and H_2O_2 treated samples associated with actin, where the modifications were exactly the same on the same amino acid residues (**Table 5.1; Figure 5.4**).

MRECISIHIGQAGIQVGNACWELYCLEHGIQPDGQMPSDKTVGGGDDAFNTFFSETGAGkHVPRAIFVD
LEpTVIDEVRSGPYRQLFHPEQLISGKEDAANNFARGHYTIGKEVVDLCLDRIRKLADNCTSA

Figure 5.4. Sequence of alpha-tubulin of *Phaseolus vulgaris* showing the identified peptides (yellow highlighting) with modified amino acid residues (red highlight) found in both SI and H_2O_2 treated samples.

Proline (p) was modified to Glu-γ-semialdehyde and Lysine (k) was modified to Aminoadepic semialdehyde, where both of these modifications were irreversible. Previous studies have shown that microtubules are a target of SI signalling where signal integration between F-actin filaments and microtubules is required for triggering PCD (Poulter *et al*., 2008). Here we also identified microtubules not only associated with actin but also modified by SI induced ROS signalling suggesting its involvement in the ROS mediated SI-PCD pathways.

5.2.3.1.1 Cloning of *Papaver* actin

As mentioned earlier (**Section 5.2.2**), we used an actin pull down assay and mass spectrometry analysis to identify the modified proteins as target of ROS during SI signalling. To identify the modified peptides, a green plant data base was used as a best option since *Papaver rhoeas* genomic data is not currently available. Though we used a "green plant" data base including some *Papaver rhoeas* sequence informations, the identification of modified proteins had to rely on sequence identity to other plant homologues. Therefore we decided to clone *Papaver* actin, obtain the DNA sequence and subsequently predict the primary protein sequence. This would allow us to assess how closely related it was to other plant actins found in the database and to analyse the modified peptides directly in relation to the poppy actin sequence. We used the *Arabidopsis* actin sequence to initiate cloning of *Papaver* pollen cDNA (see **Chapter 2**, **Section 2.15**). We obtained full length nucleotide sequence for poppy actin which was translated into the full length amino acid sequence. **Figure 5.5** shows the predicted sequence alignment of poppy actin with other plant actin sequences. Actin is a highly conserved protein. Poppy actin shows 82.93% identity to *Saccharomyces cerevisiae* actin, 95.48% identity to *Glycine max* actin, 96.29% identity with *Arabidopsis thaliana* and *Oryza sativa* and 98.67% with *Populus trichocarpa's* actin sequences.

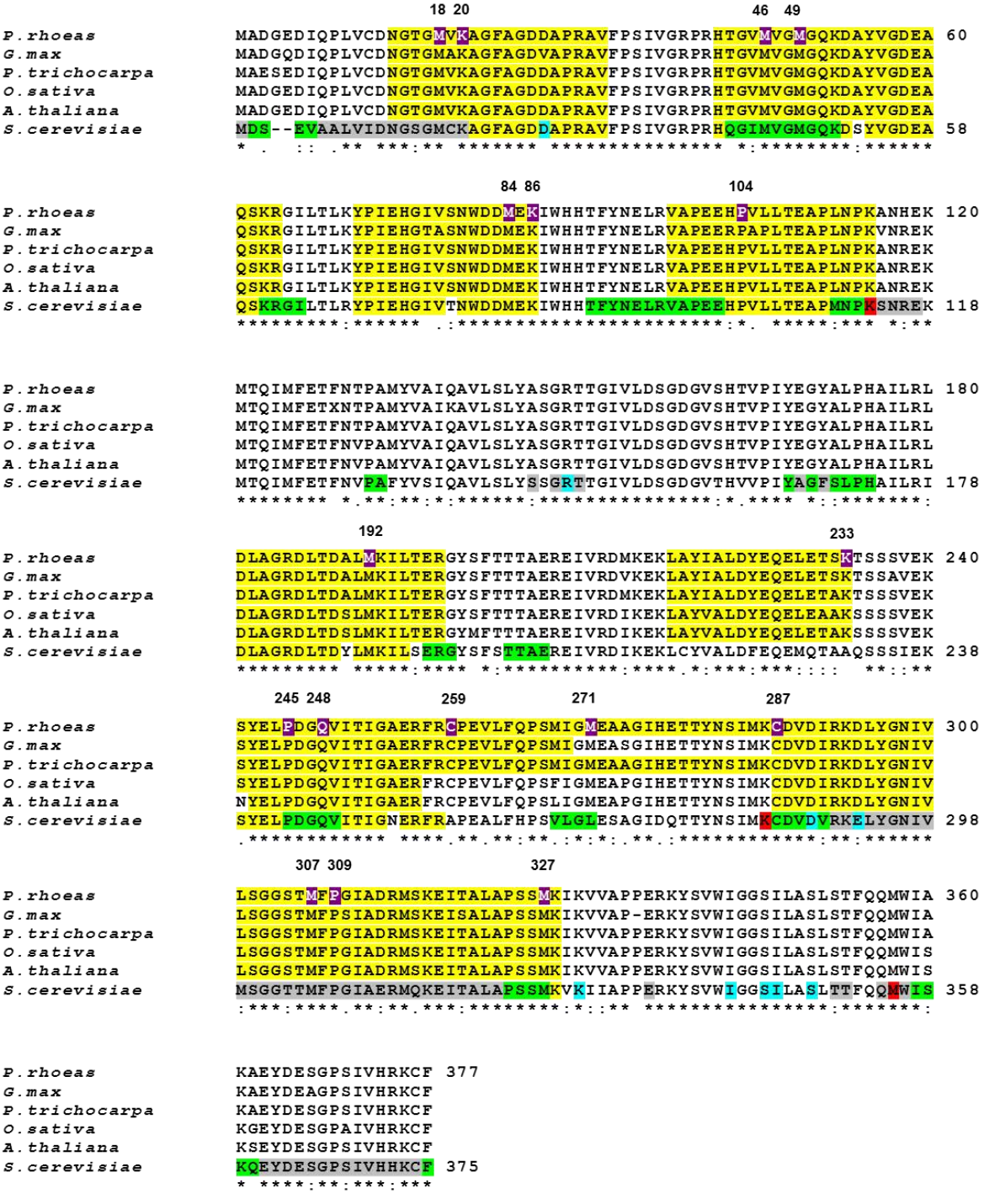

Figure 5.5. Sequence alignment of several plant and yeast actins.

An alignment of amino acid sequences of *Papaver* actin with actins from *Glycine max, Populus trichocarpa, Oryza sativa, Arabidopsis thaliana* actin 7 and *Saccharomyces cerevisiae.* The modified peptides are plotted on the sequences (yellow highlight) and are highlighted in purple in poppy actin sequence. Actin and actint binding proteins binding sites on yeast actin sequence are shown by highlighting with green for actin, light blue for ADF/cofilin, red for profilin and grey for gelsolin.

The FT-ICR-MS identified a number of actin peptide sequences identical to different green plants from SI and H_2O_2 treated samples that were modified by ROS. We plotted the identified peptides onto the *Papaver* actin sequence. **Figure 5.5** shows the peptides and modified amino acids identified on the poppy actin sequence. Modified amino acids were distributed throughout the sequence. Several residues on actin have been identified on yeast and other animals actin as binding domains where actin and other actin binding protins (ABPs) bind to actin (Dos Remedios *et al*., 2003). These binding sites are shown in the **Table 5.2**.

Table 5.2. Different binding sites on actin. Poppy actin modifications have been fond in the underlined domains

Actin binding proteins	Actin	ADF/Cofilin	Profilin	Gelsolin
Amino acid residues on actin that bind ABPs	2–5, 40–50, 61–64, 89–100, 110–112, 130–131, 166–173, 195–197, 202–205, 243–247, 266–269, 285–289, 322–325, 357–360, and 375	1–12, 25, 147, 167, 288, 292, 328, 334, 341, 344, 345, 348, 357–375 (304)	113, 166, 167, 169, 171–173, 284, 286–288, 290, 354, 355, 361, 364, 369, 371–373 and 375	1–18, 112–117, 144, 146, 148, 167, 169, 285–375, 334, 350, 351, 354, 356–375, 374 and 375

ABP=actin binding protein, ADF= actin depolymerizing factor. Table is adabted from Dos Remedios *et al*. (2003)

Figure 5.5 shows several amino acids that were modified by ROS are located on some of these binding domains. Met-48, Met-49 (within 40-50 residue domain, **Table 5.2**), Pro-245 (243-247 residue domain, **Table 5.2**) and Cys-287 (285-289 domain, **Table 5.2**) were all oxidatively modified and they are all located in the small actin binding domains on actin (Holmes *et al*., 1990). Oxidatively modified Met-18 (1-18 residue domain, **Table 5.2**) and Cys-287(285-375 residue domain, **Table 5.2**) lie in the gelsolin binding domain on

actin (McLaughlin *et al.*, 1993). These modified amino acids on these actin and gelsolin binding domain might interfere the binding of G-actin and gelsolin which is required for actin cytoskeleton dynamics.

Several studies have shown that fimbrin, α-actinin, and other actin cross-linking proteins share a conserved actin-binding domain and all might bind to the same region of actin (McGough *et al*., 1994, Mimura and Asano, 1987). Honts *et al*. (1994) identified a likely site of interaction of fimbrin on actin while working on yeast fimbrin Sac6p. They suggested that the small domain of interaction comprised residues 1-32, 70-144 and 338-375. In other studies it has been shown that conserved actin binding domain comprises residues 1-12, 83-125 and residues 350-375 (Mimura and Asano, 1987, Lebart *et al*., 1990, Fabbrizio *et al.*, 1993).

The poppy actin sequence in **Figure 5.5** and **Figure 5.6** shows that there are several peptides are found to be modified by oxidation in the above mentioned domains. Lys-20 (within the 1-32 residue domain), Met-84, Lys-86 and Pro-104 (within 83-125/70-144 residue domain) are all identified as being oxidatively modified by ROS in the current study and all lie within the small conserved binding domain for fimbrin. The modification of these amino acids on these sites might affect the ability of actin to bind several ABPs which are important for the controlling actin dynamics.

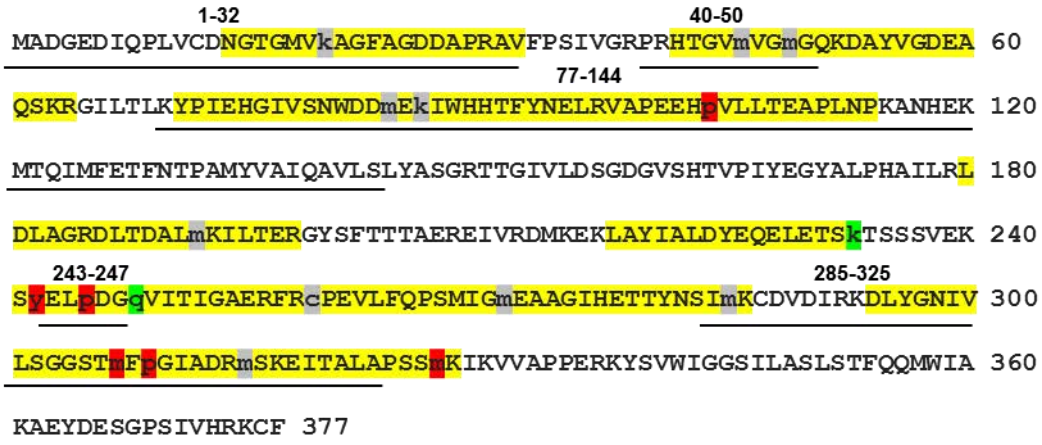

Figure 5.6. Amino acid sequence of *Papaver* actin showing the modified amino acids

Peptides identified from mass spectrometry were plotted onto the poppy actin sequence (yellow highlight). Green, grey and red highlighted amino acids are the modified amino acids where green represents the modified peptides identified only in the SI samples, purple for the modified peptides identified only in the H_2O_2 samples and red represents the peptide identified in both SI and H_2O_2 treated samples. The underlined regions indicate the conserved binding domain for actin, gelsolin and fimbrin.

Several amino acids were identified as targets of ROS during SI-induction (**Figure 5.6**). Some of the identified amino acids in this study have been identified as being modified by different post translational modifications (PTMs) of mammalian actin. Met-84/82 (Poppy/mammalian), Met-192/190, Tyr-242/240, Cys-259/257 and Met-271/269 are amino acid residues which have been reported to be modified by different PTMs (reviewed by Terman and Kashina, 2013). It has been reported that addition of an oxidizing agent prevents polymerization of globular actin and even destroys polymerised actin (Feuer and Molnar, 1948). There are several cysteines and methionine within the actin which are susceptible to oxidation. Redox-modification of some cysteine has been linked to reduced polymerization and altered interactions

with ABPs (Terman and Kashina, 2013). Oxidation of methionine has long been assumed to functionally impair actin (Milzani *et al*., 2000, Dalle-Donne *et al*., 2002). Therefore, the identified methionine, cysteine and other amino acids in this study might also affect polymerization of actin and might play a role in the impairment of actin function.

5.2.3.2 Modification of signalling proteins

We identified oxidative modification of several signalling proteins associated with actin in the pull down from SI and H_2O_2 treated samples. Importantly, none of them were detected in untreated sample. Amongst them, two particular proteins; elongation factors and 14-3-3 proteins were thought to be of most interest. 14-3-3 protein had previously been identified as a actin binding protein with a potential role in SI signal in *Papaver* (Poulter *et al*., 2011). In the current study we identified 14-3-3 protein as a target of oxidative modification from both SI and H_2O_2 treated samples. This suggests that this protein is modified during SI. **Figure 5.7** shows the sequence of a 14-3-3 protein annotated with the identified peptides and modified amino acids.

MLLTESSREENVYMAKLAEQAERYEEmVEFmEKVAKTVEVEELTVEERNLLSVAYKNVIGARRA
SWRIISSIEQkEESRGNEDHVAIIKDYRATIEAELSKICDGILSLLESHLIPSAVIAESKVFYL
KMKGDYHRYLAEFKTGPGRKEAAESTLLAYKSAQDIALAELApThpIRLGLALNFSVFYYEILN
SPDRACNLAKQAFDEAISELDTLGEESYkDSTLImQLLRDNLTLWTSDITDDAGDDIKEASKRE
SGEGQP

Figure 5.7. Sequence of 14-3-3-like protein from *Vitis vinifera* shows the identified peptides (yellow highlight) and the modified amino acids (red, grey and green highlight). Red highlighted amino acids are identified in both SI and H_2O_2 treated samples. Green and grey represent for the modified amino acids identified only in SI and H_2O_2 samples respectively. Methionine (m) was modified to met sulfone, proline was modified to Glu-γ-semialdehyde, Lysine (k) modified to aminiadipic semialdehyde and Histidine (h) was modified to 2-oxohistidin. All the modifications are irreversible.

The 14-3-3 family proteins are extremely conserved throughout the eukaryotic kingdom and perform as signalling regulators. They have been shown to be involved in many cellular processes such as signal transduction, apoptosis and cell-cycle control (DeLille *et al*., 2001, van Hemert *et al.*, 2001, Ferl *et al*., 2002), hence of relevance to SI and PCD. Plant 14-3-3 isoforms, comparable to their highly conserved homologues in mammals, bind to phosphorylated target proteins (another process involved in SI) to modulate their function. The 14-3-3 proteins are affected by the environment of the plant, both intracellular and extracellular, consequently playing a vital role in the response to environmental stress, pathogens and light conditions (Denison *et al*., 2011). The control of interaction with 14-3-3 proteins via phosphorylation of the target protein is well-known and it is also becoming clear that the phosphorylation of 14-3-3 isoforms on specific residues has a significant guiding role- in many cases by reducing interaction (Aitken, 2006, Aitken, 2011).

Identification of modified 14-3-3 proteins in both SI and H_2O_2 treated samples and their irreversible modifications in methionine (m) and proline (p) suggest that this protein might be involved in SI signalling and this modification might affect the function of the protein. 14-3-3 protein was identified as an actin interactor by an actin pull down assay. It has been demonstrated that numerous proteins bind to 14-3-3 which are involved in regulation of the actin cytoskeleton, polarity endocytosis and focal adhesions (Jin *et al*., 2004). The implication of these proteomic data was supported by the effects of inhibiting 14-3-3 phosphopeptide binding in living cells, which markedly affects actin polymerization, perturbs cell morphology and membrane dynamics. Therefore,

the modification of several amino acid residues on a 14-3-3 protein might interfere the binding ability of this protein and thus affect actin polymerisation and many other cellular processes.

It has been reported that the dimeric structure is necessary for normal functioning of 14-3-3, and destabilization of the dimer decreases the interaction of 14-3-3 with different target proteins (Shen *et al*., 2003, Gu *et al.*, 2006). The dimeric structure of 14-3-3ζ from Human is probably stabilized by three salt bridges formed by Arg18-Glu89, Glu5-Lys74, and Asp21-Lys85 (Gardino *et al.*, 2006). The amino acid sequence in **Figure 5.7** shows Lys75 (conserved with Lsy74 in human 14-3-3), was identified as a target of oxidative modification. Modification of this amino acid might affect the bridge formation which is important for the stabilization of dimeric structure, and thus hamper the interaction of 14-3-3 with other proteins.

Elongation factor 1α (EF1α) has been documented as an actin/ microtubule-binding protein which has a vital role to connect the protein translation apparatus and the cytoskeleton (Liu *et al*., 2002). The actin pull down assay and mass spectrometry identified several elongation factor peptides as targets of oxidative modification during SI. Peptides identical to *Capsicum chinense* Elongation factor 1α was identified in both SI and H_2O_2 treated samples where the irreversible modification occurred on Methionine (m), Proline (p) and Lysine (k) (**Figure 5.8**).

DATTPKYSKARYDEIVKEVSSYLKKVGYNPDKIPFVpISGFEGDNmIERSTNLDWYKGPTLLEALDQ
INEPKRpSDKPLRLPLQDVYkIGGIGTVpVGRVETGVIKpGmVVTFGPTGLTTEVkSVE

Figure 5.8. Sequence of Elongation factor 1 alpha of *Capsicum chinense* showing the identified peptides (yellow highlight) and the modified amino acids (red, grey and green highlight). Modified amino acids identified only in the SI samples are highlighted in green, amino acids from only H_2O_2 are in grey and the red highlighted peptides are identified in both SI and H_2O_2 treated samples.

As this EF1α protein was identified in SI and H_2O_2 treated samples, not in the untreated samples, this indicates that this peptide might be a target in actin mediated SI signalling. The identified peptides are located in the domain I and domain II on the *Capsicum* EF1α protein (**Figure 5.8**). Several studies have identified different domains of EF1α as actin binding domains. In *Dictyostelium* EF1α, domain I and domain III were identified as actin binding domain (Liu *et al*., 1996b) and it has been demonstrated that the actin filament binding on the *Dictyostelium* EF1α and vertebrate EF1α is pH dependent (Edmonds *et al*., 1995, Edmonds *et al*., 1996). EF1α binds to cytoskeletal proteins on domains II and III and mediates their interaction, though this actin binding function seems not to be connected to its role during polypeptide elongation (Gross and Kinzy, 2005, Gross and Kinzy, 2007). In this study, irreversible modification of different amino acids identified in domain I and II might affect the interaction of actin with EF1α. This will be discussed later (**Section 5.3.2**)

5.2.3.3 Stress related proteins are modified by ROS

Another class of modified proteins that were detected at a higher frequency in the SI and H_2O_2 treated samples compared to untreated sample was the stress related proteins; mainly heat shock proteins (HSP) and chaperone proteins. HSP are a family of proteins which are up regulated during a stress

response and act as intracellular chaperones for other proteins. SI can be considered as a form of stress response because it results eventually in programmed cell death (PCD) of the incompatible pollen; therefore heat shock protein could play a pivotal role in SI. Several heat shock protein 70 (HSP70) peptides were identified in both SI and H_2O_2 treated samples.

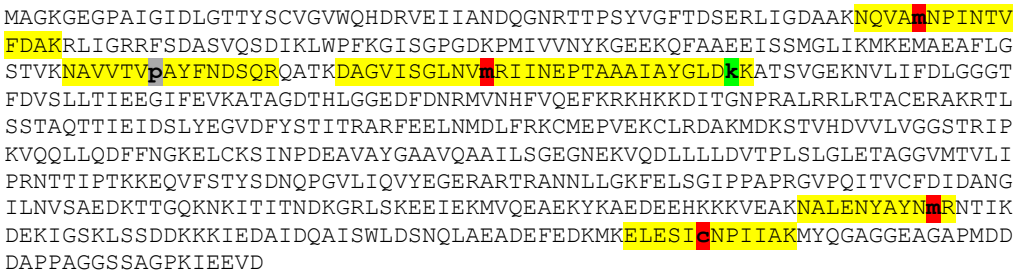

Figure 5.9. Sequence of Heat shock protein 70 of *Nicotiana tabacum*.
Identified peptides are highlighted in yellow. Modified amino acids highlighted in red are identified in both SI and H_2O_2 treated samples. Green and grey highlighted amino acids are identified only in SI or H_2O_2 treated samples respectively.

Methionine (m) modified to Met sulfone, Proline (p) to Glu-γ-semialdehyde and Lysine (k) to Aminoadipic semialdehyde which are all irreversible modifications (**Figure 5.9**). Cysteine (c) was also modified where the modification was carbamidomethylation which is a reversible modification. This protein can interfere with the process of apoptotic cell death. HSP70 has been reported to be involved in blocking apoptosis by binding apoptosis protease activating factor-1 (Apaf-1)(Beere *et al*., 2000). It has been demonstrated that oxidation of HSP70 can alter its protein structure and signalling properties, causing modification on its modulatory effects on macrophage function and viability (Grunwald *et al*., 2014). Therefore, modification of several amino acids identified in this study might alter the function of HSP70 to block apoptosis and

thus might play a role in the SI-mediated PCD. This will be further discussed later (**Section 5.3.3**).

5.2.3.4 Clathrin heavy chain is target of ROS

Clathrin heavy chain was another interesting protein that was identified in SI and H_2O_2 treated samples but not in the UT sample. From SI treated sample, only one clathrin heavy chain protein was obtained, which was also found in H_2O_2 treated samples. 6 different clathrin heavy chain proteins with 10 identical peptides to different green plants were found from H_2O_2 treated samples. The peptides FQSV**p**VQAGQTPPLLQYFGTLLTR and EAAELAAES**p**QGLLR were identified in both SI and H_2O_2 treated samples where proline was modified to Glu-γ-semialdehyde, which is an irreversible modification. **Figure 5.10** shows CHC sequence from *Zea mays*. Two peptides identical to *Zea mays* have been identified in both SI and H_2O_2 treated samples and plotted in the sequence (**Figure 5.10**). Other identified peptides are also plotted onto the sequence. The position of the modified amino acids are located in the linker domain (331-483 residues), ankle domain (484-838 residues), distal leg domain (839-1073 residues) and in the proximal leg domain (1198-1575 residues) (Brodsky, 2012).

MAAANAPIAMREALTFVTFTHVTMESEKYICVRETSPQNSVVIIDMAMPMQPLRRPITADSALMN 65
PNARILALKAQIPGTTQDHLQIFNIEAKTKIKSHQMPEQVVFWKWITPKLLGLVTQTSVYHWSIE 130
GDSEPTKMFDRTANLANNQIINYRCDPAEKWLVLIGIAPGAPERPQLVKGNMQLFSVDQQRSQAL 195
EAHAASFATFKVVGNENPSTLICFASKTTNAGQITSKLHVIELGAQPGKPGFSKKQADLFFPPDF 260
QDDFPVAMQVSQKYGLIYVITKLGLLFVYDLETAAAVYRNRISPDPIFLTAESSSTGGFYAINRR 325
GQVLHATVNDATVVPFVSGQLNNLELAVNLAKRANLPGAENLVVQRFQELFAQTKYKEAAELAAE 390
SpQGLLRTPETVAKFQSVpVQAGQTPPLLQYFGTLLTRGKLNAFESLELSRLVVNQNKKNLLENW 455
LAEDKLECSEELGDLVKTVDNDLALKIYIKARATPKVVAAFAERREFDKILIYSKQVGYTPDYLF 520
LLQTILRTDPQGAVNFALMMSQMEGGCPVDYNTITDLFLQRNMIREATAFLLDVLKPNLPEHAFL 585
QTKVLEINLVTYPNVADAILANGmFSHYDRPRIAQLCEKAGLYLRALQHYSELPDIKRAIVNTHA 650
IEPQALVEFFGTLSREWALECMKDLLLVNLRGNLQIVVQAAKEYCEQLGVDACIKLFEQFKSYEG 715
LYFFLGSYLSSSEDPDIHFKYIEAAARTGQIKEVERVTRESNFYDAEKTKNFLMEAKLPDARPLI 780
NVCDRFGFVPDLTHYLYTNNmLRYIEGYVQKVNPGNAPLVVGQLLDDECPEDFIKGLILSVRSLL 845
PVEPLVDECEKRNRLRLLTQFLEHLVSEGSQDVHVHNALGKIIIDSNNNPEHFLTTNPFYDSRVV 910
GKYCEKRDPTLAVVAYRRGQCDDELINVTNKNSLFKLQARYVVERmDGDLWDKVLQPENEYRRQL 975
IDQVVSTALPESkSPEQVSAAVKAFMTADLPHELIELLEKIVLQNSAFSGNFNLQNLLILTAIKA 1040
DPSRVMDYVNRLDNFDGPAVGEVAVEAQLYEEAFAIFKKFNLNVQAVDVLLDNIRSIERAEEFAF 1105
RVEEDAVWSQVAKAQLREGLVSEAIESFIRADDAAHFLDVIRAAEEANVYNDLVKYLLMVRQKAR 1170
EPKVDGELIFAYAKIDRLSDIEEFILMPNVANLQNVGDRLFEEELYEAAKIIYAFISNWAKLAVT 1235
LVKLKQFQGAVDAARKANSAKTWKEVCFACVDAEEFRLAQICGLNIIVQVDDLEEVSEYYQNRGc 1300
FSELIALmESGLGLERAHmGIFTELGVLYARYRSEKLMEHIKLFSTRLNIPKLIRACDEQQHWKE 1365
LTYLYIQYDEFDNAATTIMNHSPDAWDHMQFKDVCVKVANVELYYKAVHFYLQEHPDLINDMLNV 1430
LALRLDHTRVVDIMRKAGQLHLVKPYMVAVQSNNVSAVNEALNELYVEEEDYERLRESVDMHDNF 1495
DQICLAQKLEKHELLEMRRIAAYIYKKAGRWKQSIALSKKDNMYKDCMETCSQSGDRELSEDLLV 1560
YFIEQGKKECFASCLFICYDLIRPDVALELAWMNNMMDFAFPYLLQFIREYTSKVDDLVKDKIES 1625
QKEERAKEKEEKDLVAQQNMYAQLLPLALPAPPMPGMGGPPPPMGGMGMPPMGMPPMPAFGMPPM 1690
GSY 1693

Figure 5.10. Sequence of clathrin heavy chain 1 from *Zea mays*. Identified peptides are highlighted in yellow. Modified amino acids highlighted in red are identified in both SI and H_2O_2 treated samples and grey highlighted amino acids are identified only in H_2O_2 treated samples. Proline (p) and lysine (k) were modified to Glu-γ-semialdihyde and Aminoadipic-semialdihyde respectively which are irreversible modifications. Cystein modification was carbamidomethylation (reversible). Four of the methionine modification was irreversible while the methionine adjacent to the modified cysteine was modified reversibly.

None of the modifications were observed in the N-terminal domain (TD) which generally binds adaptor or other proteins during clathrin mediated endosytosis (Hirst and Robinson, 1998). An additional binding site for adaptors is localized in the ankle domain (Knuehl *et al*., 2006). A linker segment joins terminal domain to the distal leg (ter Haar *et al*., 1998). Two modified (irreversible) proline were identified in the linker domain, one methionine in the ankle domain, five methionine, one lysine and one cysteine were identified in the leg region. Although the effect of these modified peptides is not known yet, we propose that they might affect protein binding in the ankle region and might

play a role in the clathrin lattice formation for clathrin coat as proximal and distal legs participate to hold the lattice together (Crowther and Pearse, 1981, Ungewickell *et al*., 1982), because the modified peptides were identified in these region.

The clathrin heavy chain (CHC) is the main component of clathrin-coated vesicles which is well characterized for its role in intracellular membrane traffic and endocytosis from the plasma membrane (PM). Clathrin mediated endocytosis is used by all known eukaryotic cells (McMahon and Boucrot, 2011). In plant, pollen tube growth is based on carriage of secretory vesicles into the apical part of the pollen tube where they fuse with the plasma membrane in a small area (Onelli and Moscatelli, 2013). The transport of secretory vesicles to the tip is generated by actin-myosin-dependent reverse fountain cytoplasmic streaming (Cárdenas *et al*., 2005, Vidali *et al.*, 2001). Involvement of the endocytosis of proteins into tobacco pollen tubes during S-RNase based SI has been reported (Goldraij *et al*., 2006). Our finding of CHC not only is actin-associated but also a target of ROS for incompatible poppy pollen SI signals suggests a role for CHC protein in poppy pollen tube inhibition and in SI-PCD.

5.2.4 Alteration of F-actin cytoskeleton by ROS and NO in pollen tube

Previous studies have shown that the actin cytoskeleton is a target for ROS and NO signals (Wilkins *et al*., 2011). However, these studies were indirect, using ROS and NO scavengers TEMPOL (4-Hydroxy-2,2,6,6-tetramethylpiperidine 1-oxyl) and/or c-PTIO (2-(4-carboxyphenyl)-4,4,5,5-

tetramethylimidazoline-1-oxyl-3-oxide). We had not previously investigated the direct effect of ROS/NO donors on the pollen actin cytoskeleton configuration. Having analysed so many ROS modifications by mass spectrometry analysis, we decided to see if ROS can affect the actin dynamics in the pollen tube. To detect alterations in F-actin in the pollen tube triggered by ROS and NO during SI induction we treated the pollen tubes with either recombinant PrsS to induce SI, H_2O_2 or NO donor GSNO. Pollen was examined using microscopy at different time points to observe the alterations in F-actin configuration over time. F-actin was stained using rhodamine-phalloidin (Rh-Ph) which is commonly used in imaging to selectively stain F-actin (see **Chapter 2, Section 2.3**).

In the control pollen tubes (untreated, **Figure 5.11a**) F-actin filament bundles were clearly visible. After 5-12 min of SI induction F-actin organization was affected by the SI treatment, F-actin bundles were distributed near to the plasma membrane (also seen in Snowman *et al*., 2002) and most of the F-actin filaments were not visible (**Figure 5.11 b & c**). This is the time point (5-12min) at which increases in SI-induced ROS signals was found to be highest after SI induction (Wilkins *et al*., 2011).

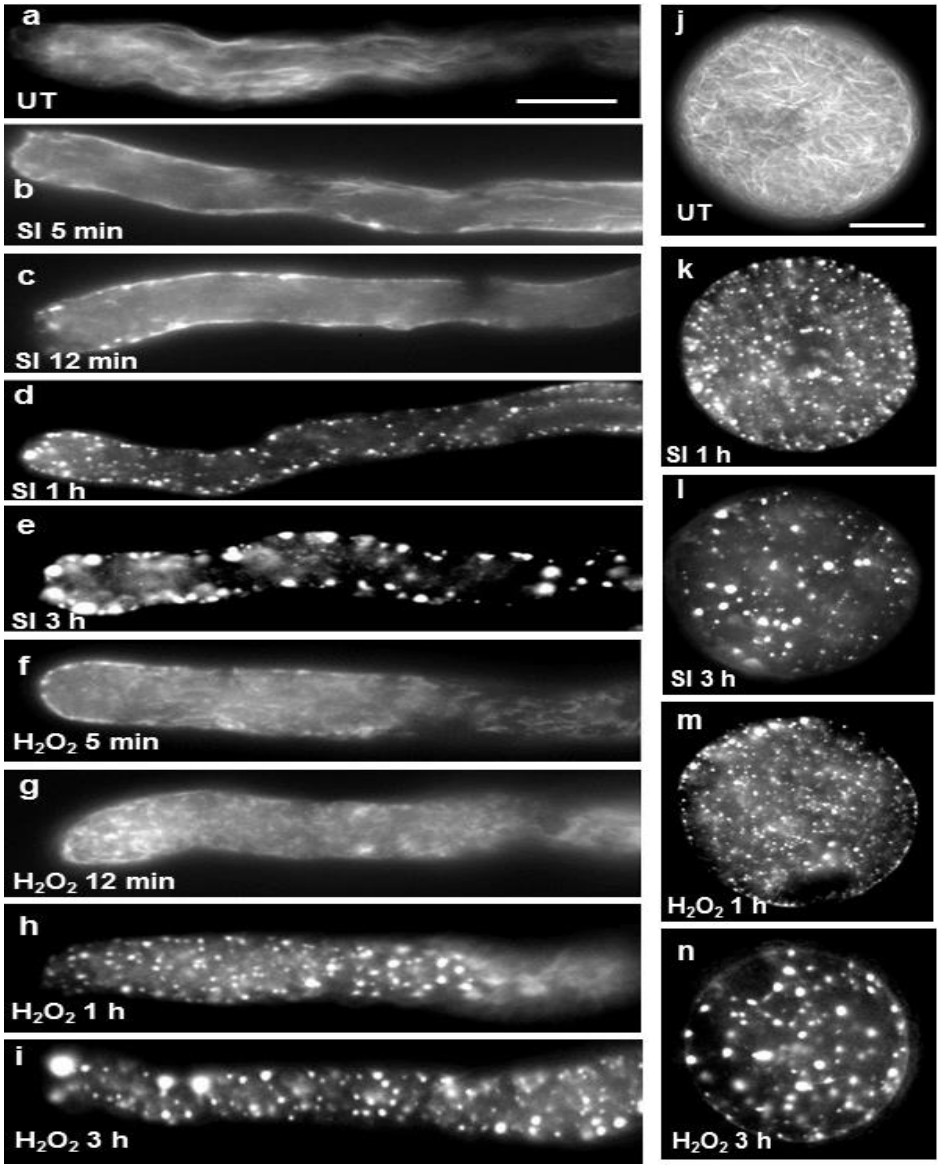

Figure 5.11. F-actin alteration by ROS during SI induction in the pollen tube.

Alterations in F-actin organization started as early as 5-12min after the treatment of both SI and H_2O_2. After 1hr of treatment (with both SI and H_2O_2) small actin foci were formed which became larger and turned into large punctate foci after 3hr of treatment. Non germinated pollen grains (j-n) also showed similar response to the treatments as we could see in the pollen tubes.

a. F-actin organization in a representative untreated pollen tube.
b – e. SI induced pollen tubes at 5min, 12min, 1hr and 3hr after treatment
f – i. H_2O_2 treated pollen tubes after 5min, 12min, 1hr and 3hr of treatment
j. Untreated pollen grain (not germinated) showing F-actin filament bundles
k, l. SI induced pollen grain after 1hr and 3hr of treatment
m, n. Pollen grains treated with H_2O_2 after 1hr and 3hr of treatment

F-actin was visualized by rhodamine-phalloidin using fluorescence microscopy.

Scale bar = 10μm

After 1h of treatment small F-actin foci were formed all through the pollen tubes (**Figure 5.11 d**) and large punctate foci were observed after 3h of treatment. Filaments were no longer visible (**Figure 5.11 e**).

When pollen tubes were treated with H_2O_2 to investigate the effect of ROS on actin morphology, alterations in the F-actin cytoskeleton organization were observed as early as 5-12 min after treatment with H_2O_2 (**Figure 5.11 f & g**). The typical F-actin filament bundle arrangement which was observed in untreated pollen tubes (**Figure 5.11 a**) was not clearly visible (**Figure 5.11 f**) and disappeared.

After 1h of treatment small actin foci was formed (**Figure 5.11 h**) and the pollen tubes that had undergone 3h of H_2O_2 treatment had large F-actin foci (**Figure 5.11i**), very similar to SI induced pollen. Interestingly, the non-germinated pollen grains also showed similar response as the pollen tubes (**Figure 5.11 j-n**), suggesting ungerminated pollen grains can also respond to SI and ROS.

These are the first data to directly show that ROS can stimulate major changes in actin configuration in pollen tube and they are very similar to those observed during SI.

Although we could not identify any modified proteins from NO donor GSNO treated samples from mass spectrometry, we wanted to investigate the effect of NO on the actin organization in the pollen tube. A previous study showed that SI induced increases in NO were much slower than ROS and took 25-30min to reach their peak after SI induction (Wilkins *et al*., 2011). We therefore

decided to observe the pollen tubes at 30min, 1hr and 3hr after the treatment with NO donor GSNO.

Figure 5.12 showed that after 30 min of treatment the F-actin filaments were not visible and small foci was formed (**Figure 5.12 a**) which also found after 1h of treatment (**Figure 5.12 b**). 3h of NO donor treatment resulted in numerous large punctate F-actin foci (**Figure 5.12 c**), which is very similar to what was observed in SI induced pollen. Non-germinated pollen grains with the same treatment also showed similar alterations (**Figure 5.12 d-f**), suggesting ungerminated pollen grains also respond to NO. These are the first data to directly show that NO can stimulate major alterations in actin configuration in pollen tube. Moreover, they are very similar to those observed during SI.

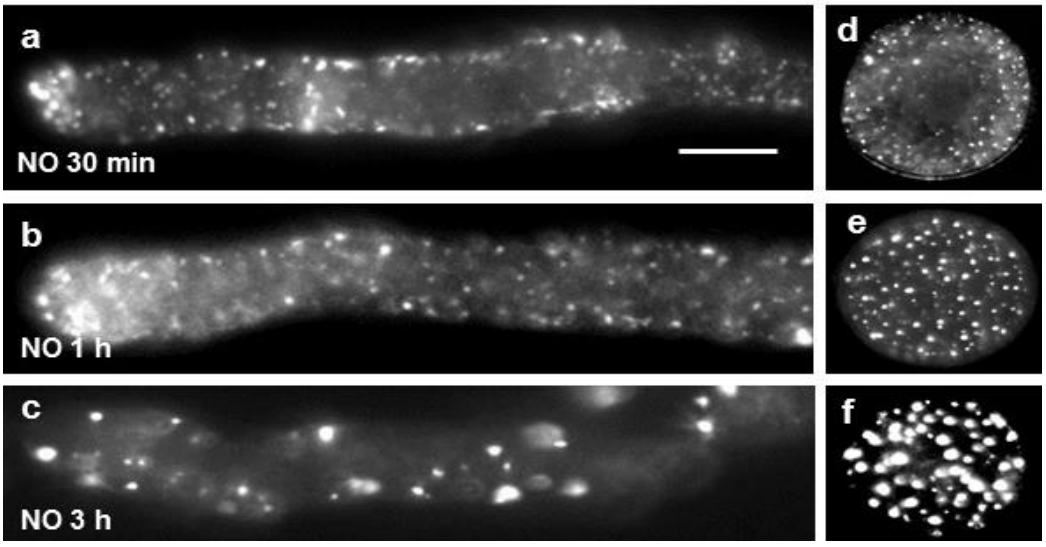

Figure 5.12. NO signal to SI-induced formation of actin punctate foci.

30min after treatment with NO donor GSNO, small actin foci was started to form **(a)** and 1hr after treatment the number of small actin foci increased **(b).** Large punctate foci were observed after 3hr of treatment **(c).** Non-germinated pollen grain also showed similar actin chaneges (d–f). Actin was visualized by rhodamine-phalloidin using fluorescence microscopy. Scale bar = 10μm

Alterations in the F-actin cytoskeleton configuration and formation of large foci in response to H_2O_2 and NO donor treatment together with identification of ROS and NO modified peptides using Mass spectrometry suggest the direct involvement of ROS and NO in the formation of SI-stimulated F-actin punctate foci.

5.2.5 Quantification of the number of pollen tube exhibiting punctate actin foci

Quantification of the number of the pollen tubes which showed actin punctate foci, revealed that, as expected, most untreated pollen tubes had normal F-actin configuration and rarely had actin foci (**Figure 5.13 a, b & c**). After 5 min and 12 min of SI treatment resulted in 7.3% and 18.3% of the tubes respectively containing foci, where 12 min was significantly different from the 5 min treatment (p=0.001***; **Figure 5.13 a**). This suggests a progressive increase in the number of foci formed over time. 81% and 86% of pollen tubes contained foci when they had undergone 1hr and 3hr of SI treatment respectively having no significant difference to each other (p=0.069, NS; **Figure 5.13 a**). 1h and 3h of SI treatment showed significantly higher percentage of actin foci than that of 12 min treatment (p=0.000***; **Figure 5.13 a**).

Pollen tubes treated with H_2O_2 also showed a similar result to that of SI treated pollen tubes. H_2O_2 treatments at 5min and 12 min resulted in 18% and 33% of pollen tubes containing foci respectively where 12 min treatment was significantly different from 5min treatment (p=0.010*, **Figure 5.13 b**). 79% and 84% pollen tubes contained actin foci at 1hr and 3hr treatment respectively

which was significantly higher than the number of foci found with 12 min H_2O_2 treatment (p=0.000***; **Figure 5.13 b**). The number of pollen tubes with foci did not show any significant difference at 1hr and 3hr treatment (NS; p=0.214; **Figure 5.13 b**).

We treated pollen tubes with NO donor GSNO for 30 min 1h and 3h. **Figure 5.13 c** shows that 47%, 83.67% and 85% pollen tubes contained actin foci when they undergone 30min, 1hr and 3hr of NO donor treatment respectively. Although nearly 50% pollen tubes was found with actin foci after 30min of treatment, the number was significantly lower that the pollen tubes found with foci at 1hr and 3hr treatment (p=0.001**; **Figure 5.13 c**).

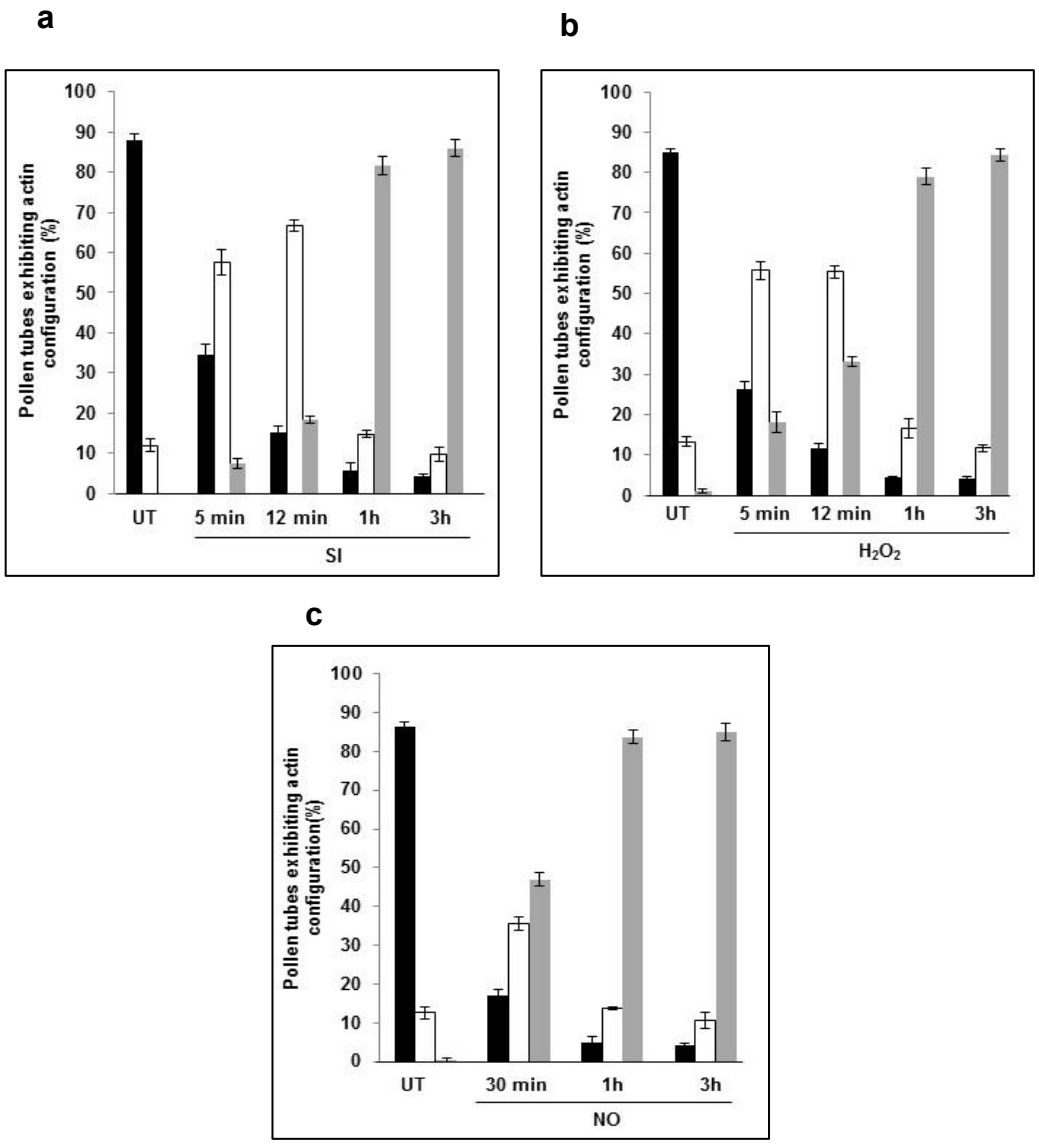

Figure 5.13. ROS and NO signal to SI-mediated actin foci formation.

Pollen tubes were pre-treated with PrsS, H_2O_2 or NO donor GSNO, Samples was collected at 5 min, 12 min, 1h and 3h after treated with PrsS or H_2O_2. NO donor treated samples were collected at 30 min, 1h and 3h after treatment. F-actin was stained with rhodamine-phalloidin and examined with fluorescence Microscopy. Actin configuration was evaluated by placing each pollen tubes into one of the three categories: Actin filaments only (Black bars), foci only (grey bars) or intermediate (i.e. filaments and foci; open bars). Three independent experiments scoring 100 pollen tubes for each treatment expressed as percentage of total. Data are mean ± SEM (n=100)

5.3 Discussion

In this chapter we identified actin and several proteins that are associated with actin which have been modified by ROS during SI signalling using a combination of actin pull down assay and mass spectrometry. SI in *Papaver* triggers rapid depolymerisation of F-actin bundles within 60 seconds after SI induction which plays a vital role in the inhibition of pollen tube tip growth (Geitmann *et al*., 2000, Snowman *et al*., 2002). This SI-induced depolymerisation of F-actin is mediated by increases in $[Ca^{2+}]_I$ and formation of stable F-actin foci later is a striking SI marker (Poulter *et al*., 2011). Recent studies have shown that increases in ROS and NO signal to the SI-stimulated formation of actin foci (Wilkins *et al*., 2011). In this chapter we have investigated the possible role of actin and proteins that bind to actin as a target of ROS and NO during SI signal in *Papaver.*

5.3.1 Actin pull-down assay and mass spectrometry

We used a previously developed method (Poulter *et al*., 2011) for the enrichment and isolation of F-actin from pollen samples. The results show that this method worked efficiently as it could enrich for F-actin and the samples could be purified through an F-actin pull down assay. To identify the actin and proteins associated with actin modified by ROS and NO signalling during SI, we used mass spectrometry analysis.

5.3.2 14-3-3 proteins and EF1α may be involved in SI

4 different peptides from two 14-3-3 signalling proteins were identified as modified peptides by FT-ICR-MS from SI treated and H_2O_2 treated actin pull-down pollen samples. The identified peptides match to sequences from *Hevea brasiliensis* and *Vitis vinifera* 14-3-3 proteins for both SI and H_2O_2 treated samples.

The 14-3-3s are small (28-33 kDa) proteins found in all eukaryotes organism investigated (Aitken, 2006). 14-3-3 proteins can regulate functions of many proteins by effecting direct protein-protein interactions. First, 14-3-3 proteins bind to phosphorylated proteins at specific sites on the target protein. This interactions result in alteration to the target proteins structure that regulates its activity (DeLille *et al*., 2001). In the signalling pathways, environmental condition can control the interactions with 14-3-3 proteins by influencing the binding sites on 14-3-3. In higher plants, during stress condition, 14-3-3 proteins play various levels of role by controlling activities of many signalling proteins (Roberts *et al*., 2002).

An increasing number of work have been begun to clarify the roles of 14-3-3s in stress response pathways in plants. 14-3-3 proteins are altered by many stress stimuli; 14-3-3s interact, although mostly *in vitro*, with targets known to be involved in stress signalling pathways (reviewed by Denison *et al*., 2011). Environmental and biotic stresses can directly influence 14-3-3 proteins by changing expression of specific isoforms. These stresses frequently have different effects on different isoforms in terms of level of expression and the time course of changed transcription. Studies of 14-3-3 genes in rice have

identified *cis* elements that can be regulated by a number of environmental and biotic stresses (Yao *et al*., 2007, Chen *et al*., 2006). The SI signal of *Papaver* is a stress response that involves rearrangements of actin cytoskeleton and results in PCD (Bosch *et al*., 2008). 14-3-3 proteins were also been identified in the poppy pollen in H_2O_2 treated samples which represented the oxidative stress response. Therefore, the 14-3-3 proteins could be good candidates that might be involved in SI signalling.

Previous studies by Poulter *et al.* (2011) identified several 14-3-3 proteins as interactors of actin foci during SI response. Some published proteomic data also provide evidence for interaction of 14-3-3 proteins with actin (Liang *et al*., 2009, Jin *et al*., 2004). Here we have provided data that 14-3-3 proteins interacting with F-actin have been modified during SI response. These data suggest the involvement of 14-3-3 proteins in the SI stress response and also somehow interacting with mediating this via actin interactions. We are not certain exactly how 14-3-3 proteins might be involved in SI response. Further studies will be needed to elucidate the role of these proteins in SI.

The FT-ICR-MS analysis of poppy pollen actin-associated peptides modified by ROS identified another group of signalling proteins: different isoforms of Elongation factors in SI and H_2O_2 treated samples. The apparatus of eukaryotic protein synthesis is found in association with the actin cytoskeleton. A key component of this translational mechanism is the actin binding protein Elongation factor 1α (EF1α), which is involved in the shuttling of aa-tRNA (Liu *et al*., 1996b). The first evidence of EF1α being an actin binding protein was found in *Dictyostelium* (Demma *et al*., 1990, Yang *et al*., 1990). Consequently,

EF1α has been shown to colocalize with actin filaments. Moreover, this colocalization alters with chemo-attractant stimulus in *Dictyostelium* and adenocarcinoma cells (Dharmawardhane *et al*., 1991, Okazaki and Yumura, 1995). Here, we also have identified EF-1α from SI samples through an actin pull-down assay, suggesting its interaction with F-actin in poppy pollen. EF1α was also modified by ROS and NO during SI as target of oxidation and *S*-nitrosylation which has been discussed in **Chapter 4.**

Study from several laboratories has confidently established a relationship between cytoskeletal organization and translation where actin plays a crucial role in regulating the efficiency of translation (Stapulionis *et al.*, 1997). After the discovery of EF1α as an actin binding protein (Yang *et al.*, 1990) a wide number of studies *in vitro* have been performed to characterize the interactions. It has been demonstrated that the binding of EF1α to actin in *Dictyostelium* and vertebrate is pH dependent (Edmonds *et al*., 1995, Edmonds *et al*., 1996). Competitive binding experiment shows that as pH increases, the attraction of EF1α for actin reduced while that for aa-tRNA increased (Liu *et al.*, 1996b). As a result cytosolic acidification would result in EF1α-actin binding which sequesters it from interaction with aa-tRNA which inhibits protein synthesis. Using a genetic screen, a series of EF1A mutants with reduced actin bundling activity has been identified in yeast (Gross and Kinzy, 2005). These mutations modify the organization of the actin cytoskeleton, but not translation, demonstrating that actin bundling activity of EF1A is not essential for its function in protein synthesis but required for its role in the actin cytoskeleton organization. An earlier study has shown that a

shift from slightly acidic to slightly alkaline pH caused a loss of EF1α-mediated F-actin crosslinking and a associated increase in binding single filaments (Liu *et al.*, 1996b). During SI-signalling in *Papaver* a rapid dramatic cytosolic acidification occurs (Wilkins *et al.*, 2015). Therefore, the SI-induced acidification is likely to have the reverse effect, increasing EF1α-mediated bundling of actin filaments. Definitely, this needs further investigation of the involvement of EF1α in the SI-induced pH-dependent F actin organization mediating PCD.

Several studies on oxidative modification of plant proteins have identified different isoforms of elongation factors to be modified. Lindermayr *et al*. (2005) identified Elongation factors from *Arabidopsis* cell culture which represented candidates for *S*-nitrosylation. Carbonylation of elongation factors and other proteins have been observed during seed germination in *Arabidopsis* (Job *et al*., 2005). Other studies in *Arabidopsis* also identified EF-1α and confirmed to undergo oxidation in H_2O_2 treated samples (Wang *et al*., 2011). Inhibition of protein synthesis in response to oxidative stress, mediated by phosphorylation of the elongation initiation factors eIF2α, has been reported in mammalian cells and yeast (Harding *et al*., 2003, Dunand-Sauthier *et al.*, 2005). Here we identified EF1α proteins as a target of ROS signalling during SI in *Papaver*. The irreversible modification occurred on Methionine (m) and Proline (p) in both SI and H_2O_2 treated samples. Our data suggest another level of regulation of protein synthesis by regulation of translational elongation by oxidative modification of EF1-α protein. However, the consequence of the

modification of EF-1α under SI signalling, as well as, oxidative stress requires further studies.

5.3.3 Stress related proteins may interact with F-actin during SI

In the poppy pollen SI-induced sample associated with F-actin pull down, four heat shock proteins (HSP) and chaperone proteins and 10 different peptides were identified, while 5 heat shock and chaperone proteins were identified as target of oxidative modification form H_2O_2 treated samples. We identified only one heat shock protein from the untreated sample. In SI-induced sample, 3 HSP70 were identified as a target of oxidative modification. It is quite interesting as HSPs were also identified as target of ROS in the SI response in poppy pollen (**Chapter 4**). HSPs act as molecular chaperones, able to facilitate many cellular processes through an influence on higher order protein structure. For instance, molecular chaperones assist in the transport of proteins into mitochondria and chloroplasts, along with influencing clathrin lattice dynamics, viral replication and transcriptional activation. HSP70 are a family of ubiquitously expressed proteins important for protein folding, and helps the cell to protect against stress factors. Many heat shock proteins are up-regulated during stress response; some of them function as molecular chaperone to prevent denaturation of some proteins and other separate protein aggregates, refolding monomers from this aggregates or targeting them for proteolytic degradation (Liang and MacRae, 1997). Heat shock proteins (HSP) are divided into five major families according to their average molecular weight, structure and function; HSP100, 90, 70, 60 and the small HSP(sHSP)/α-crystallins (Craig *et al.*, 1994, Morimoto *et al.*, 1991, Morimoto

et al., 1994). A HSP70 isoform was identified in the pollen tube of tobacco which binds to microtubules in an ATP-dependent manner (Parrotta *et al.*, 2013). HSP70 protects the centrosome and possibly intermediate filaments during heat shock. Small heat shock proteins interact with microfilaments and intermediate filaments, affect their polymerization and protect them from heat shock by a phosphorylation-dependent mechanism (Liang and MacRae, 1997).

Previous studies by Poulter *et al*. (2011) identified several HSPs including HSP70, HSP90, and chaperonin CPN60 as associated with SI-induced F-actin foci. Though this finding was not very surprising, given what we already know largely about SI acting as a stress response, these data made available the first evidence implicating a possible role for heat-shock proteins and chaperonins in the SI response. Here we have shown that HSPs associated with F-actin are a target of ROS signalling during SI response. There is evidence that oxidative stress can modify HSPs, for example, HSP90, which resulted in 99% inactivation of the protein (Carbone *et al*., 2005). Therefore, inactivation of HSPs during SI-signalling would restrict these proteins from their natural protective role in the cell and thus might be involved in the actin depolymerisation.

5.3.4 Involvement of clathrin heavy chain in SI

Although only one clathrin heavy chain protein (CHC) was identified as modified by oxidation in the SI sample we found it interesting because of its cellular function and to our knowledge it has not been found previously as a target of oxidative stress response. In eukaryotic cells, the clathrin heavy chain

(CHC) is a major component of clathrin-coated vesicles that function in the endocytosis. In plant cellular function endocytosis plays an indispensable role. Pollen tube and root growth are dependent on endocytosis (Derksen *et al.*, 1995, Voigt *et al*., 2005). Involvement of endocytosis in hormonal signalling, nutrient delivery, toxin avoidance, and pathogen defense has been documented (Chen *et al*., 2011). Pollen tube growth is based on transport of secretory vesicles in to the apex where the vesicles fuse with a small area of plasma membrane (Onelli and Moscatelli, 2013). Recent studies on endocytosis in pollen tubes using fluorescent probes, such as FM 4-64 or FM 1-43 and charged nanogold, suggest that vesicles are accumulated in the clear zone as a V-shape which include secretory vesicles and newly internalized endocytic vesicles (Bove *et al*., 2008, Moscatelli *et al*., 2007, Zonia and Munnik, 2008). Transportation of secretory vesicles to the tip region is regulated by actin-myosin-dependent reverse-fountain cytoplasmic streaming (Cárdenas *et al.*, 2005, Vidali *et al*., 2001). The polarized growth of pollen tubes is supported by an elusive equilibrium between exocytic and endocytic pathways.

Structure of clathrin have been solved by a number of research works (Kirchhausen and Harrison, 1984, ter Haar *et al*., 1998). Clathrin is a molecular scaffold protein that surrounds coated vesicles (Pearse, 1976). Clathrin is basically composed of three leged assembly unit called ‘triskelion’ which form lattice that organizes recruitment of proteins to coated pits. The structure includes the terminal domain and the linker that joins the terminal domain to the leg domain at the end of the triskelion (ter Haar *et al*., 1998).

Three legs contain three heavy chain with a light chain attached to each heavy chain (Kirchhausen and Harrison, 1984). During CME, clathrin does not bind directly to the cargo and instead binds to adaptors that mediate this function (Willox and Royle, 2012). N-terminal domain (TD) of clathrin generally bind to the adaptors and other proteins in its different sites (for recent review see Lemmon and Traub, 2012, Brodsky, 2012). An additional binding site for adaptors is localized in the ankle domain (Knuehl *et al*., 2006). We have shown here that several clathrin heavy chain peptides have been identified from FT-ICR-MS from SI and H_2O_2 treated sample as target of oxidative modification. None of the modified peptides were in the TD region; however they were situated in the linker domain, ankle domain and in the leg domain. Although we are not certain about the effect of these modified peptides, we assumed that they might affect protein binding in the ankle region and might play a role in the clathrin lattice formation for clathrin coat where proximal and distal legs participate in the interactions that hold the lattice together (Crowther and Pearse, 1981, Ungewickell *et al*., 1982). Identification of CHC in the current study associated with F-actin as a target of SI-ROS signal implicates a role for clathrin-mediated endocytosis (CME) in SI-PCD, as CHC is a major component of clathrin coated vesicles.

5.4 Future studies

We have identified several potential interesting protein targets of ROS during SI signalling in poppy that are likely to interact with the actin cytoskeleton, as we used the combination of actin pull-down assay and mass spectrometry. This identified several different subsets of proteins modified in the SI

compared to the untreated samples. Though we identified more oxidatively modified proteins in the H_2O_2 treated sample compared to SI samples, they have several common 'hits' in terms of modified proteins and peptides as well as their type of modifications. This helped to identify proteins of interest. Identification of several proteins as target of oxidative modification in a signalling pathway like SI is a starting point to get insight in the functions of these proteins in SI response. Now it is a challenge of validation and functionally characterization of these proteins in terms of their biochemical, functional and structural aspects in order to get insight into the SI signal in the molecular level. So, in future it is required to focus on a single protein at a time for their detailed characterization in relation to SI signalling pathways. Specially, 14-3-3 proteins, Elongation factors, actin itself, and clathrin heavy chain are worthy of further closer investigation. Identification of clathrin heavy chain connected with F-actin and their modification after SI-induced ROS implicates a role for clathrin-mediated endocytosis in SI-ROS-PCD as CHC is a major component of clathrin coated vesicle. Establishing a role for CME in plant PCD would be totally novel. Our identification of EF1α as an F-actin binding target and of SI-induced ROS and its pH-dependent binding to actin make EF1α a priority for its further investigation. How cytosolic pH affects EF1α function/localization will be a key question to answer. As the SI-induced acidification completely inhibits the activity of soluble inorganic pyrophosphatase, Pr-p26.1, this suggests that pH is likely to affect the activity of EF1α. Thus, further investigation of the relationship between actin-associated EF1α, cytosolic acidification in a SI-mediated ROS signalling will be able to provide novel data.

We cloned poppy actin from poppy pollen. Because of time restrictions we could not prepare recombinant actin. It would be of considerable interest to prepare recombinant poppy actin and investigate whether the modified peptides identified in this study can also be identified in the recombinant actin after ROS treatment *in vitro.* Also biochemical assays could be performed to see if ROS affects the polymerisation status of poppy actin binding to certain ABPs such as CAP, ADF.

In summary, in this current study we identified several actins and proteins associated with actin as targets of ROS during SI signalling which might play important role in the SI-mediated actin alteration and SI-PCD. To our knowledge, identification of clathrin heavy chain associated with F-actin and a target of SI- induced ROS is novel. Establishing a role of clathrin mediated endocytosis in poppy pollen and the SI-PCD response would be a promising avenue for future study.

Chapter 6

General Discussion

The work presented in this thesis has investigated various targets of the *Papaver rhoeas* SI response. The main focus was using mass spectrometry to identify targets of ROS and NO during SI signalling (**Chapter 4**) and also to examine the role of actin and proteins associated with actin as targets of ROS and NO during SI signalling (**Chapter 5**). Another part of the thesis was involved in characterizing two important sPPases Pr-p26.1a and Pr-p26.1b (**Chapter 3**). The function of Pr-p26.1 sPPases has been discussed thoroughly in **Chapter 3**; hence we will only mention their involvement in different mechanisms of SI here. Together, the studies in this thesis have revealed new aspects of SI which appear to involve mechanisms modulating pollen tube tip growth. We mainly will focus our discussion here on the modified proteins (oxidation and S-nitrosylation) and also the proteins associated with actin which were modified by oxidation. Together they throw light on potential new mechanisms involved in SI.

6.1 Modification of proteins by ROS and NO during the SI response

Mass spectrometry analysis identified hundreds of proteins which were modified by oxidation from SI induced pollen samples as well as from the H_2O_2 treated sample. Modified proteins from untreated pollen were also examined as a control to make comparisons with the protein modification under normal conditions and those that were modified artificially by H_2O_2 and *in vivo* SI conditions. We searched for several common oxidative modifications on amino acids, such as: cysteine to cysteic acid, methionine to met sulfone, arginine or proline to glu-γ-semialdehyde, histidine to 2-oxohistidin, lysine to aminoadepic semialdehyde, tryptophane to kynurenine etc (Møller *et al*., 2007, Cárdenas *et*

al., 2005). Cysteine modification to highest level of oxidation to cyteic acid is an irreversible modification, though until this step, the modifications are reversible. Methionine also modified to met sulfoxide which is a reversible modification, but further oxidation of methionine to met sulfone is irreversible. The other modifications searched are all irreversible modifications. Among the identified peptides from the SI induced and H_2O_2 treated samples more than 85% of peptides were modified irreversibly in both the samples. In contrast, only ~15% peptides identified in the untreated sample were modified irreversibly, the rest of the modifications in the untreated samples were reversible. It has been suggested that reversible modifications may be an important regulatory mechanism (Sundby *et al*., 2005) while the irreversible modifications appear to be damaging to the protein function (Ghezzi and Bonetto, 2003). Oxidative modification of proline, lysine, tryptophan, arginine, histidine and threonine gives a free carbonyl group which is termed as carbonylation. Carbonylation is an irreversible modification of proteins and because of this oxidation the function of proteins is generally inhibited (Berlett and Stadtman, 1997). Studies show inhibition of wheat root growth due to the carbonylation of several proteins modified by the Cd^{2+} induced ROS (Pena et al., 2012). In this thesis, we showed most of the SI modifications were irreversible compared to untreated controls, which were reversible modifications. Thus these irreversible modifications identified in the SI samples are possibly damaging to the proteins.

We also identified several *S*-nitrosylated proteins in the SI-induced and NO donor-treated pollen samples. As mentioned in **Chapter 4** (**Section 4.2.1.2**),

detection of S-nitrosylated protein is much more difficult than oxidatively modified proteins. It was a challenge to identify S-nitrosylated proteins from the SI-induced pollen samples because of several reasons. Firstly, the S-nitrosothioles are labile as they can easily react with intracellular reducing agents like ascorbic acid, glutathione (GSH), or reduced metal ions especially Cu^{+}. Low abundance of S-nitrosothiol in endogenous condition is another issue which should be kept in mind. As mentioned in **Chapter 4** (**Section 4.2.1.2**), use of a suitable method for detection of S-nitrosothiol is key for the analysis of the SNO-proteome. Here we used resin-assisted capture of S-nitrosothiols (SNO-RAC) method (Thompson *et al*., 2013) to identify S-nitrosylated proteins from *Papaver* pollen during SI response.The majority of NO affected proteins appear to be regulated by *S*-nitrosylation of thiol group of a single cysteine residue (Stamler *et al*., 1992).

6.2 Characterization of unique and overlapping peptides identified in the SI-induced H_2O_2 and NO donor treated samples

In chapter 4, we identified many modified peptides in *Papaver* pollen as targets of oxidation and *S*-nitrosylation by ROS and NO respectively during SI. We identified protein targets of ROS and NO during SI-signalling using recombinant PrsS for SI-induction. We also used H_2O_2 to increase ROS level and GSNO (S-nitrosoglutathione) as a NO donor to analyse their effects on protein targets of *Papaver* pollen tubes and to compare the modified proteins identified in the SI-induced samples.

Our FT-ICR-MS analysis of pollen proteins identified 14 and 12 *S*-nitrosylated proteins from the NO donor GSNO-treated sample and SI-induced samples

respectively. Importantly, no S-nitrosylated proteins were identified in the untreated samples, while four proteins were common in both SI and NO donor treated samples. Although the number of identified *S*-nitrosylated proteins was low, these proteins were of great interest because of their function and/or previous identification as a target of S-nitrosylated proteins in other systems.

We constructed a Venn diagram to observe the unique and overlapping modified peptides identified in SI-induced, H_2O_2 and NO donor treated samples (**Figure 6.1**).

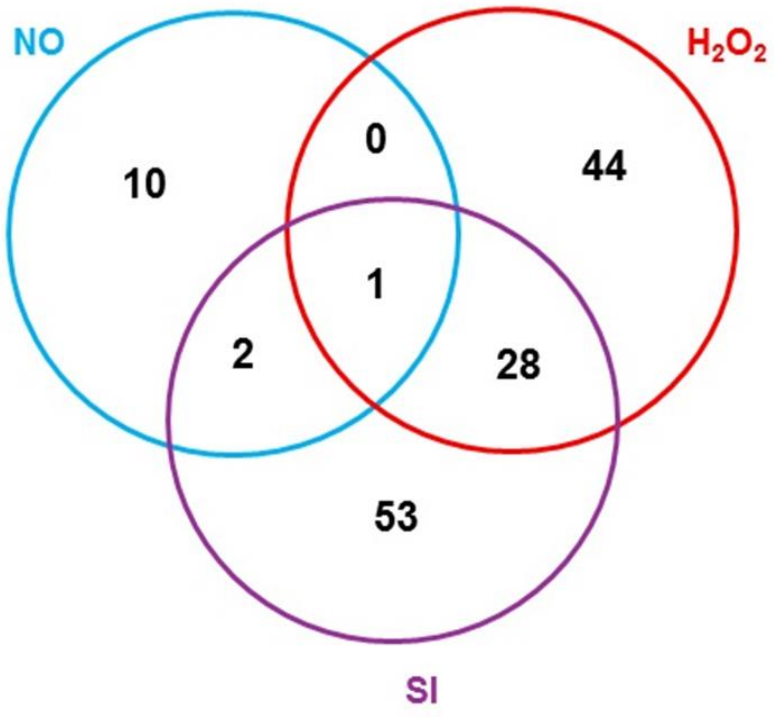

Figure 6.1. Venn diagram showing the number of modified peptides (not proteins) identified in SI-induced, H_2O_2 and NO donor GSNO treated samples and the overlap among the treatments.

The results were quite unexpected. **Figure 6.1** shows that 53 modified peptides out of 109 modified peptides were unique to SI-induced samples which were not identified in the other two samples. In the H_2O_2 treated and NO donor treated samples the number of unique modified peptides is 44 and 10 respectively (also see **Figure 6.2**). The Venn diagrams revealed that 28 oxidatively modified peptides were identified in both SI-induced and H_2O_2 treated samples which were identical in terms of peptides and types of modifications of the amino acids. Two peptides were found in both SI and NO donor treated samples and only one modified peptide with same modification was identified in the all three samples. H_2O_2 and NO-donor treated samples did not show any modified peptides common among them (see **Figure 6.3**).

We created a diagram by putting all the modified peptides which are unique in the SI-induced, H_2O_2 or NO donor treated samples to get an overall picture of events (**Figure 6.2**). The number of modified peptides in the cytoskeleton protein group in SI sample was higher than the H_2O_2 treated samples indicating that cytoskeleton proteins are a major target of SI response. We also identified the overlapping peptides where same amino acids were modified similarly among the three treatments and plotted them (see **Figure 6.3**). Thus, although there are many SI-specific modifications, there are also some key general events triggered. The proteins identified were discussed in detail in **Chapter 4.** Briefly, their identity suggest several crucial mechanisms involved in SI, like inhibition of pollen tube growth, stress response, which are also general ROS and NO responses.

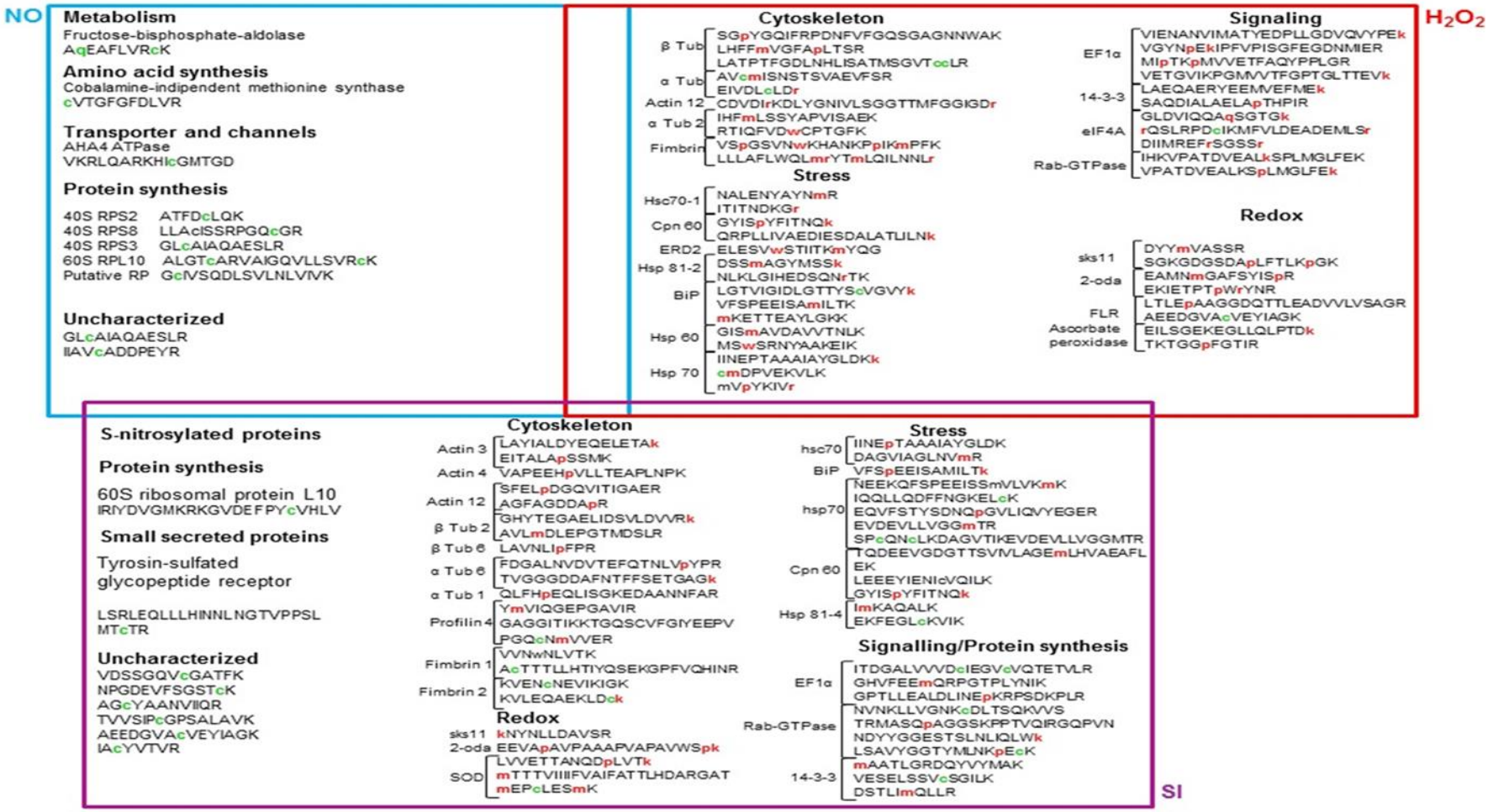

Figure 6.2. Figure showing the unique modified peptides identified only in the SI-induced, H_2O_2 or NO donor treated samples. Modified amino acids are indicated with lowercase bold letters where red letters represent irreversible modifications and green letters show the reversible modifications

As mentioned earlier, 53 modified peptides were identified in the SI-induced sample, which were not identified in the H_2O_2 or NO donor-treated samples. These includes cytoskeletal proteins; mainly actin, tubulin, and actin binding proteins (ABPs), stress and redox proteins, proteins related to signalling and protein synthesis, which were discussed in detail earlier in **Chapter 4**. Briefly, this suggests several new mechanisms implicated in SI, like alteration of actin cytoskeleton, inhibition of protein synthesis, stress response.

It is worth mentioning here that, ROS triggers as early as 5 min and peaking at 10-12 min after SI-induction in poppy. It is a rapid event. Our ROS-SI samples were also examined 10-12 min after adding the treatments. On the other hand, SI-induced NO is comparatively slower event starts at ~20 min and peaking at ~30 min after SI (Wilkins *et al.*, 2011). We examined the NO treated samples 30 min after the treatments. Therefore, the oxidative modifications of the proteins would be within few minutes of SI and linking with the inhibition of pollen tip growth as pollen tube growth stops rapidly after SI induction. NO modification is later events, related to inhibition of metabolisms.

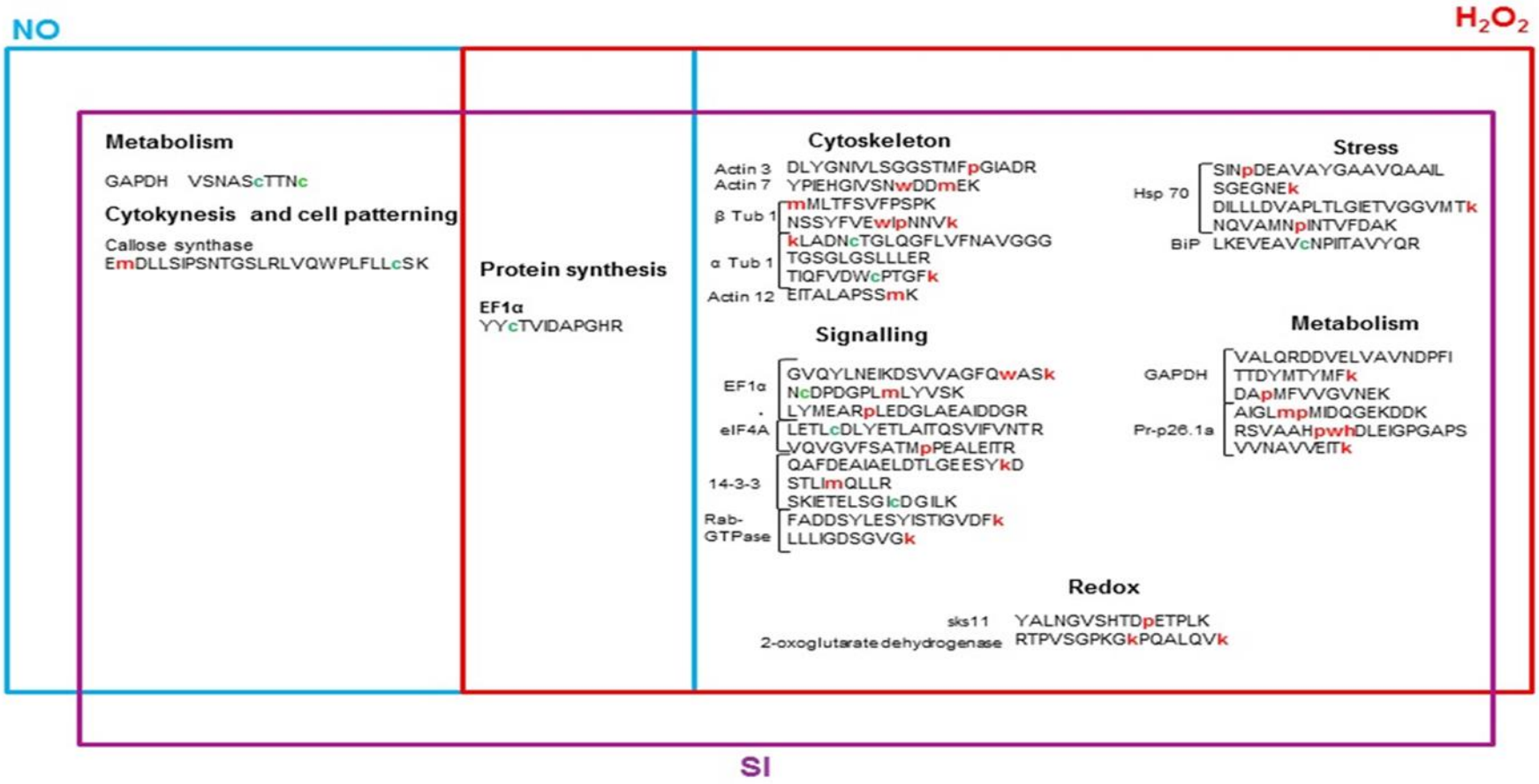

Figure 6.3. Figure showing the modified peptides overlap among the SI-induced H_2O_2 and NO donor treated samples. Lowercase bold coloured letters show the modified amino acids. Red= irreversiblely modified peptides; green= reversibly modified peptides

We will next consider how knowledge about these SI-induced protein targets helps us understand the mechanisms involved in SI better. The results presented in this thesis cover a range of mechanisms involved in the *Papaver* SI response, from the mechanisms associated with the inhibition of pollen tube growth to some potential new further mechanistic processes likely to be involved in mediating SI through actin. In this chapter, first we will briefly talk about what we knew so far about SI in *Papaver* and then will describe the findings of this thesis to include new mechanisms involved in SI.

6.3 Previously identified mechanisms in SI

In *Papaver rhoeas*, an incompatible interaction between PrsS (Pistil S-determinant) and PrpS (Pollen S-determinant) in a *S*-specific manner triggers a signalling cascade, as a result pollen tube growth is halted and finally death of 'self' pollen occur by programmed cell death (PCD) because of the activation of a caspase-3-like activity (Thomas and Franklin-Tong, 2004, Bosch and Franklin-Tong, 2007). This is summarized in **Figure 6.4**. SI stimulates increases in $[Ca^{2+}]_{cyt}$ and involves influx of Ca^{2+} and K^+ in SI-induced pollen tubes (Franklin-Tong *et al*., 1997, Wu *et al*., 2011). Increases in $[Ca^{2+}]_{cyt}$ are required for many downstream events including phosphorylation and inactivation of Pr-p26.1a/b sPPases, which occurs within 90s of SI induction and actin depolymerisation, which occurs within 2 minutes of SI (Rudd *et al*., 1996, Snowman *et al*., 2002) (**Figure 6.4**). Moreover, alterations to both actin and microtubules are associated in mediating PCD (Thomas *et al*., 2006, Poulter *et al*., 2008).

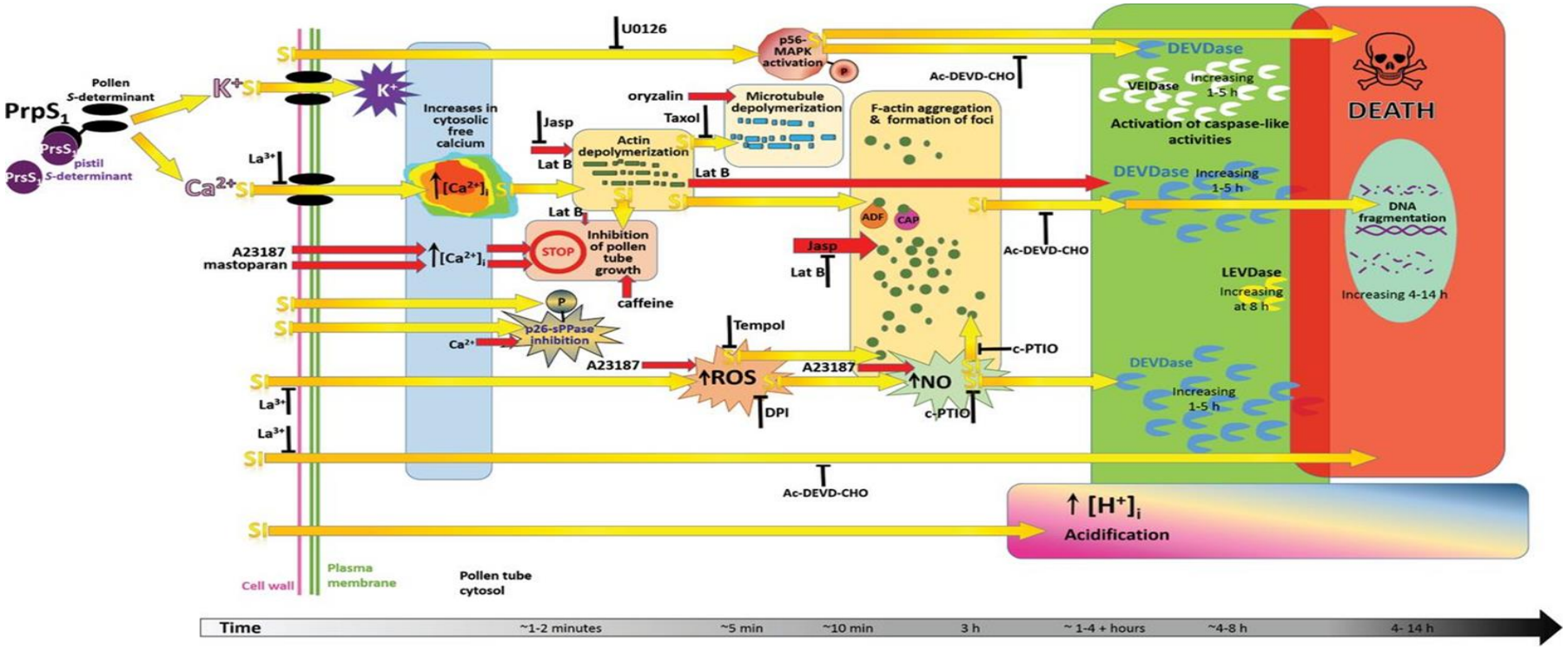

Figure 6.4. Cartoon shows a model of the integration of Self-incompatibility (SI) mediated programmed cell death (PCD) signalling network in *Papaver* pollen tube. Pistil *S*-determinant PrsS interacts with pollen *S*-determinants in an S-specific manner and rapidly triggers both K^+ and Ca^{2+} influx. Increases in cytosolic Ca^{2+} triggers a signalling network required for many SI events, including phosphorylation and inhibition the activity of Pr-p26.1a/1b sPPases and actin depolymerisation which contributed to inhibit pollen tube growth. Later in the SI response F-actin produces large punctate foci. Depolymerisation of microtubules occur which changes to the cytoskeleton signal to PCD mediated by a DEVDases activity. Increases of reactive oxygen species (ROS) and nitric oxide (NO) are also involved in PCD signalling, actin upstream of formation of actin foci and DEVDases activity. Increases in cytosolic acidification occurs which helps to activate DEVDase activity and it has been shown to be required for DNA fragmentation. Together these events ensure that fertilization cannot take place in incompatible *Papaver* pollen. Figure is adapted from Wilkins *et a*l. (2014).

Rapid increases in reactive oxygen species (ROS) are documented as early at 6 minutes after SI and increases in nitric oxide (NO) occurs after ~15 minutes of SI induction (Wilkins *et al*., 2011). Increases in ROS are stimulated by increases in $[Ca^{2+}]_{cyt}$, and are also linked to several downstream events like formation of actin foci and activation of a DEVDase/caspase-3-like activity (Wilkins *et al*., 2011) (**Figure 6.4**).

Another early event of SI in *Papaver,* which occurs within 10 minutes of SI-induction, is the activation of MAPK p56 (Li *et al.*, 2007, Rudd and Franklin-Tong, 2003). MAPK inhibitor U0126 prevented the SI-induced activation of MAPK, which resulted in the alleviation of several downstream SI-induced events such as DNA fragmentation, caspase-3-like/DEVDase activity and loss of viability (Li *et al.*, 2007).

Cytosolic acidification is another event of SI occurs within 10 minutes of SI-induction and reaches pH 5.5, which is the most acidic point, within 1 h (**Figure 6.4**). Artificial acidification of the cytosol of pollen tubes shows that cytosolic acidification is essential for SI-induced PCD, found to be necessary to trigger many important distinct features of the SI-PCD signalling pathway. Cytosolic acidification resulted in SI-induced formation of actin punctate foci and activation of a DEVDase/caspase-3-like activity both of which are linked with PCD (Wilkins *et al*., 2015)(**Figure 6.4**).

Increases in caspase-3-like activities occur 1 h after SI-induction, peaking at 5 hrs post-SI-induction (Bosch and Franklin-Tong, 2007). After 4 hrs of SI-induction DNA fragmentation has been documented and increase up to 10 hrs

after SI (Bosch and Franklin-Tong, 2008, Bosch *et al*., 2008). Many of the SI-induced events identified to date are involved in integrating signals to PCD.

6.4 Identified new mechanisms involved in SI

As we described in **Chapter 4** and earlier in this chapter (see **Figure 6.2 and 6.3**) , it is clear that many of the proteins modified by ROS and NO during SI are involved in metabolism, protein synthesis, pollen tip growth, redox and stress responses. Below we will discuss the identified proteins and their overall potential biological functions in SI.

6.4.1 Proteins involved in tip growth are identified as targets of both ROS and NO

Mass spectrometry analysis identified several proteins, which play role in pollen tip growth, in the SI-induced and H_2O_2-treated pollen samples as a target of ROS. These proteins, which are Pr-p26.1a/b, actin, Rab GTPase, callose synthase, glyceraldehyde-3-phosphate dehydrogenase (GAPDH), Fructose bisphosphate adolase (FBA), Elongation factor1α, will be discussed below.

6.4.1.1 Pr-p26.1 sPPases activities are modulated by several SI-induced events

Chapter 3 described the characterization of Pr-p26.1a and Pr-p26.1b and their multiple phospho-mutants for the first time. It had previously been established that Pr-p26.1a and Pr-p26.1b sPPases are phosphorylated in a *S*-specific manner within 90s of SI induction and their activity was reduced by both Ca^{2+} and phosphorylation (Rudd *et al.*, 1996, de Graaf *et al*., 2006). In

this thesis we have shown that pH has a dramatic effect on sPPase activity of Pr-p26.1a and Pr-p26.1b. Pr-p26.1 sPPase activity declines with the decreasing pH. The effect of pH on the phophomimic mutant was even more extreme where at pH 5.5 the activity was nearly zero. Previous studies have shown a rapid and dramatic cytosolic acidification after SI induction in *Papaver* pollen. Pr-p26.1a and Pr-p26.1b shows high sensitivity to pH, as after only 0.2 to 0.4 units of pH drops, 50% of their activity was reduced. Therefore, the cytosolic pH drop during SI, which occurs ~10 min after SI, has a dramatic effect on Pr-p26.1 sPPase activity which provides us with an additional mechanism for Pr-p26.1 sPPase activity to be reduced during early SI.

We also identified an effect of H_2O_2 (as a mimic of ROS) on the Pr-p26.1 sPPases activity. The sPPases activity was reduced in the presence of H_2O_2, and in combination with Ca^{2+}, their activities were even lower. The phosphomimic mutants showed greater loss of activity compared to the wild type Pr-p26.1 suggesting an additional effect of phosphorylation under these conditions. Moreover, mass spectrometry analysis also identified Pr-p26.1a and Pr-p26.1b as target of ROS during SI signalling, where the modifications were irreversible. These studies provide us with good evidence confirming that not only Ca^{2+} and phosphorylation, which occur within ~1min after SI, inhibit sPPase activity but also that other key SI events, pH and ROS (together with Ca^{2+}) have dramatic effect on Pr-p26.1 sPPase activity. This would effectively and rapidly inhibit the pollen tube growth. All of these events would be quite rapid and very early in SI (within few minutes). We know pollen tube growth is

inhibited in this short time frame. So, all of this happens before PCD started. This is an important crucial early step in SI.

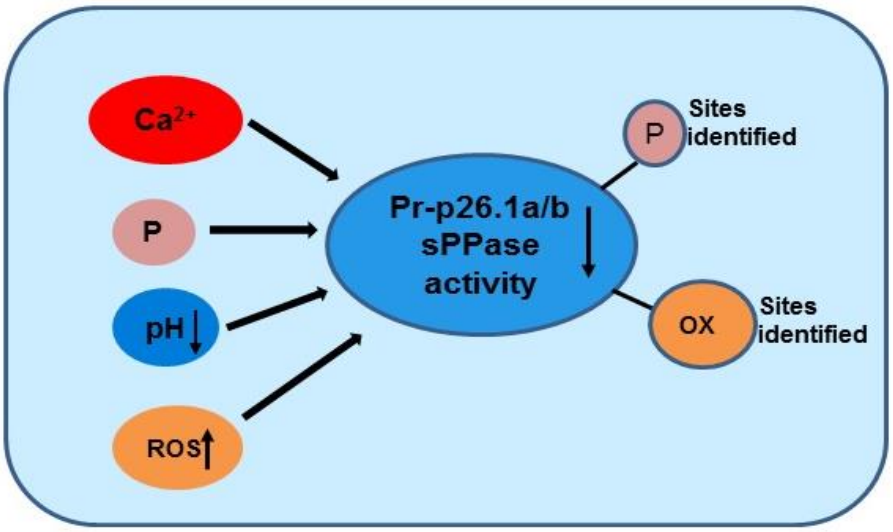

Figure 6.5. SI induced events affecting Pr-p26.1 sPPase activity. Pr-p26.1a and Pr-p26.1b are phosphorylated as early as 90s after SI induction in a Ca^{2+} dependent manner. Increases in ROS and drop of cytosolic pH occur within 5-10 min of SI which plays a vital role to inhibit the sPPase activity of phosphorylated Pr-p26.1

6.4.1.2 Cytoskeletal proteins as targets of oxidation

Several cytoskeletal proteins (mainly actin and tubulin, and some actin binding proteins (ABPs) like fimbrin and profilin) were identified by mass spectrometry in both SI and H_2O_2 treated samples as target of ROS (**Figure 6.2 and 6.3**) The actin cytoskeleton plays an essential role in pollen tube growth (Gibbon *et al*., 1999, Vidali *et al*., 2001). As previously mentioned in **Chapter 1** (**Section 1.6.2.1.4**) it has been demonstrated in early studies that actin cytoskeleton is an early target of SI signalling cascade in *Papaver* (Geitmann *et al*., 2000, Snowman *et al*., 2002). The alterations of actin cytoskeleton during SI in the pollen tube follows a distinctive and reproducible pattern that begins with

depolymerisation of the F-actin (Snowman *et al*., 2002), afterward the formation of small actin foci and later, larger, stable punctate F-actin foci (Geitmann *et al*., 2000, Snowman *et al*., 2002, Poulter *et al*., 2010). The early depolymerisation of F-actin during SI contributes to the inhibition of pollen tube growth, to ensure that fertilisation is unable to happen. More recently, studies have revealed that the actin cytoskeleton is a target of ROS and NO signals during SI in *Papaver* incompatible pollen (Wilkins *et al*., 2011). Increases in both ROS and NO contribute to the signalling events facilitating the formation of the actin punctate foci which are characteristic of the SI response in incompatible pollen of *Papaver.* In this current study, we identified actin and tubulin, as well as ABPs fimbrin and profilin, as targets of oxidative modifications by ROS signalling. Considering the importance of the involvement of actin cytoskeleton in SI-ROS-PCD signal we investigate actin modifications by ROS further detail which has been discussed in detail in **Chapter 5**. Clearly the cytoskeleton and its associated proteins are an important target during SI and we have shown for the first time that several are oxidatively modified (**Figure 6.6**).This may affect cytoskeletal dynamics. As mentioned in **Chapter 5** (**Section 5.2.3.1** and **5.2.3.1.1**), several irreversible modifications occur in the binding domain of actin which would restrict actin or ABPs to bind with actin and thus might alter actin dynamics. Pollen tube growth is dependent on the intact actin cytoskeleton, so alteration in the actin cytoskeleton would affect pollen tube growth. Thus, these modifications to actin could represent a newly identified key role in modulating pollen tube growth via actin.

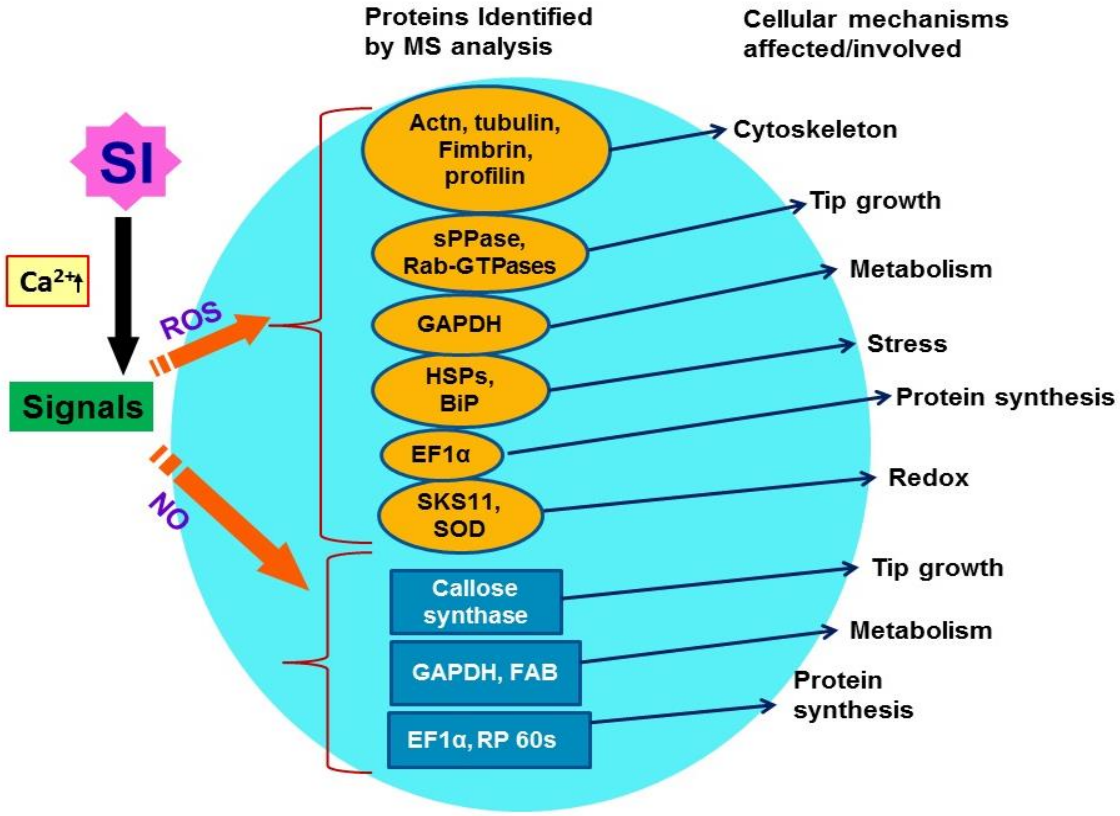

Figure 6.6. A cartoon shows the major targets of ROS and NO during SI signalling in the cell.

6.4.1.3 Rab-GTPase may be involved in SI

Rab-GTPase was also identified as oxidatively modified in the SI-induced and H_2O_2-treated pollen samples. Rab-GTPases are vital regulators for endomembrane trafficking, endocytosis, exocytosis, and recycling of membrane, processes that are important for continuing normal cellular functions (Grunwald *et al*., 2014). Several researches have shown the importance of Rab-GTPases for pollen tube growth. Tobacco pollen-expressed Rab2 has been revealed to be significant for pollen tube growth. Rab2 functions as regulator of vesicle trafficking between endoplasmic

reticulum (ER) and Golgi bodies (Cheung *et al*., 2002). Another Rab-GTPase from tobacco pollen (Rab11b) has also been identified to be vital for pollen tube growth. This protein localizes to the very apex of growing pollen tubes. The function of this Rab11b is to regulate the direction of secretory proteins and recycled membranes to the pollen tube clear zone. The activity of Rab11b is also vital for male fertility, growth rate of pollen tube and pollen tube directionality (de Graaf *et al.*, 2005). In *Arabidopsis*, mutation of the pollen expressed RABA4D disrupted the polar growth of pollen tubes and altered cell wall patterning (Szumlanski and Nielsen, 2009). We did not examine the effect of the modifications on the activity of Rab-GTPases. However, as Rab-GTPase is involved in the pollen tube growth and vesicle trafficking, it seems likely that the modifications that we identified during SI signalling might inhibit Rab-GTPase activity and thus inhibit pollen tube growth (**Figure 6.6**). Further investigation should be carried out to confirm this possibility.

6.4.1.4 Callose synthase as target of *S*-nitrosylation

Callose synthase is another protein identified being *S*-nitrosylated in both SI-induced and NO donor-treated samples (**Figure 6.6**). In developing anthers of angiosperms, microsporocytes synthesize a specialized provisional cell wall consisting of callose (a β-1,3-linked glucan) between the cell wall and the plasma membrane. Several roles of this temporary wall have been suggested over the last 40 years. It is believed that the function of callose layer is to prevent cell cohesion and fusion (Waterkeyn, 1962). The callose wall may also act to protect the developing microspores from surrounding diploid tissues (Heslop-Harrison and Mackenzie, 1967). It also provides a physical blockade

that may support prevent premature swelling and bursting of the microspores. (Stanley and Linskens, 1974). Callose is a structural component of pollen, involved at many stages of pollen development (Stone and Clarke, 1992, McCormick, 1993). Callose is synthesized by callose synthases (Verma and Hong, 2001, Brownfield *et al*., 2007, Brownfield *et al*., 2008). There is evidence that, because of mutation of callose synthase, callose production can be hampered which would ultimately affect development of pollen cell wall (Dong *et al*., 2005). Although the effect of S-nitrosylation of callose synthase has not been demonstrated yet, it could affect its activity and function and so prevent the formation of callose in the poppy pollen tubes. In this way modification of this important protein might interfere pollen tube growth.

6.4.1.5 Metabolic proteins are *S*-nitrosylated during SI

It was interesting to identify several proteins in SI-induced and H_2O_2 treated samples as well as NO donor treated sample. For example, glyceraldehyde-3-phosphate dehydrogenase (GAPDH) was identified in SI-induced oxidation and *S*-nitrosylated samples, H_2O_2 and NO donor treated samples (**Figure 6.3 and 6.6**). Thus this protein is certainly an important identification and this protein has been reported as a major target of oxidative stress response and post translational modification can inhibit its function (Lindermayr *et al*., 2005, Holtgrefe *et al*., 2008). In the glycolytic pathway, GAPDH catalyzes the conversion of glyceraldehyde-3-phosphate to 1,3 bisphosphoglycerate. Through this reaction GAPDH play an important role to produce energy and byproducts for cellular metabolism (Plaxton, 1996). However, recent studies provide evidence that GAPDH is a multifunctional protein with significant

function in a number of fundamental cell pathways (reviewed by Sirover, 1999, Sirover, 2005). Recent studies suggest that GAPDH oxidized at its active site cysteine residue changes its interacting proteins and controls its functions (Hwang *et al*., 2009). Another study showed that the deficiency in the plastidial GAPDH leads to male sterility in *Arabidopsis.* Pollen from homozygous double mutant plants (*gapcp1gapcp2*) exhibited shrunken and collapsed forms and were incapable of germinating when cultured *in vitro* (Muñoz-Bertomeu *et al*., 2010). The identified modified cys-155 and cys-159 in this current study on GAPDH is very likely to inhibit the enzymes activity. The inhibition of GAPDH enzyme would block the conversion of glucose into ethanol via glycolysis. Thus regulating glycolysis through oxidation would be involved in controlling cellular metabolism. We postulate that this metabolic enzyme might be involved in developmental process as well as pollen growth and inhibition of activity would affect growth of the pollen tubes.

Another metabolic protein, Fructose bisphosphate adolase (FBA) was identified as *S*-nitrosylated in the NO donor GSNO treated poppy pollen sample. As stated in Chapter 4, FBA has also been reported in several studies as a target of *S*-nitrosylation in different plant species, eg. *A. thaliana, Kalanchoe pinnata, Brassica juncea and in Citrus aurantium* (Lindermayr *et al*., 2005, Abat *et al*., 2008, Abat and Deswal, 2009, Tanou *et al*., 2009) as well as in yeast (Shenton and Grant, 2003), but the effect of this is not known. Thus we have identified two key metabolic proteins as new targets of SI modification. Assuming their activity is inhibited, this could contribute to pollen tube inhibited growth.

6.4.1.6 Protein synthesis might be interrupted during SI

Elongation factor (EF1α) was identified as a common target of ROS and NO during poppy SI. It was identified as an oxidatively modified protein in the SI-induced and H_2O_2 treated samples and also as a target of S-nitrosylation in both SI-induced and NO donor treated samples. Thus, it was the single protein identified to overlap all samples (see **Figure 6.1**). Interestingly, EF1α was also identified from the actin pull down assay as an actin binding protein (**Chapter 5**). This suggests it may be a key target protein for SI. Actin associated EF1α will be discussed further in **Section 6.5.2**. EF1α is involved in protein synthesis as well as in the signalling/regulatory function. Several studies have shown EF1α as target of oxidation and S-nitrosylation (Lindermayr *et al*., 2005, Tanou *et al*., 2014). It has been reported in mammalian cells and yeast that oxidative stress of EF1α caused inhibition of protein synthesis (Harding *et al*., 2003, Dunand-Sauthier *et al*., 2005). The oxidative modification of EF1α identified in this thesis is thus likely to inhibit protein synthesis in the poppy pollen tube during SI response. This modification would affect pollen tube growth.

In summary, all these proteins, identified here are modified by oxidation or nitrosylation are mostly newly identified proteins previously not known to be involved in SI. If their function were affected by the modifications occurred, would affect pollen tube growth, thus contribute to early SI events involving inhibition of pollen tube growth.

6.4.2 Stress and redox proteins might play role in SI

As discussed in **Chapter 4**, oxidative modification of stress related proteins, mainly heat shock proteins (HSPs) and chaperonins, were identified in both SI-induced and H_2O_2-treated samples (**Figure 6.6**). As mentioned in **Chapter 4** (**Section 4.2.1.1.3**), in different stress conditions, many HSPs are up-regulated in the cell and play role in protecting the cell. Several studies have shown that oxidative stress can alter the function of HSP70 (Grunwald *et al*., 2014) and also may inactivate HSP90 (Carbone *et al*., 2005) by modify these proteins. Thus, the irreversible modification of stress related proteins identified here might inhibit their activity restricting them to perform their protective role in the cell.

Another stress-related protein, luminal binding protein (BiP) was identified in SI induced samples. As stated in **Chapter 4** (**Section 4.2.2.3.4**), BiP is related to molecular chaperone activity and participate in protein folding and in specific stress responses, BiP shows protective functions (Costa et al., 2008). It has been demonstrated in tobacco that overexpressed BiP function as a positive regulator in the Cd stress (Guan et al., 2015). We discussed in **Chapter 4**, oxidation might decreases in BiP ATPase activity, protein folding and BiP mediated functions in aged mice (Hepler *et al*., 2001). Oxidative modification of BiP identified in this thesis would affect its activity. As a result this protein might not be able to protect the cell during the stress condition of SI and might affect correct folding of proteins.

Three redox proteins in the SI induced sample were identified as targets of oxidative modification and 4 in the H_2O_2-treated sample; none of them were

identified in the untreated sample. Amongst the redox proteins, SKS11 (SKU5 similar 11) proteins were identified in both SI and H_2O_2-treated samples, they were of interest. We will discuss 2 of them as there is not any information about the third one related to our story. SKS11 protein is involved in regulating pollen germination and tube growth where its function is to achieve the metabolic process (Zhang *et al*., 2013). When pollen grains land on a compatible stigma, stored BcSKS11 is possibly used to achieve the metabolic requirements of pollen germination and initial pollen-tube growth (Zhang *et al*., 2013). Other examples of SKS protein family exist; NTP303, a pollen-specific gene of tobacco, also plays a role in the pollen tube growth *in vivo*. Silencing of NTP303 caused a slowed pollen tube growth rate and growth of pollen tube was arrested prematurely in transgenic ntp303 plants (de Groot *et al*., 2004). In the current study we identified SKS11 protein as a target of oxidative modification in poppy pollen in both SI induced and H_2O_2 treated sample. From the information in the literature it seems that this protein is likely to have a role in the growth of pollen tubes, so modification of this protein is likely to affect its activity. This could result in inhibited pollen tube growth. So this modification of SKS11 may play a key role in inhibition of pollen tube growth during SI.

Superoxide dismutase (SOD) was another redox protein identified only in the SI-induced sample. The role of SOD is assumed in the detoxification of reactive oxygen species (ROS), and has a role in adaptation to heat stress (Cárdenas *et al*., 2005). So, the irreversible modification of this protein might cause damage to the proteins and thus its function might be affected. Thus

these redox proteins may be important newly identified targets of SI signals (**Figure 6.6**). Further studies are needed to verify their functional effects.

Thus the modification of these stress and redox related proteins would affect the cellular function negatively as most of these proteins have protective function in the cell.

In summary, we identified several proteins as targets of ROS and NO during SI signalling which are shown as a cartoon earlier (**Figure 6.6)**. During SI signalling in *Papaver* incompatible pollen, increases in cytosolic Ca^{2+} stimulates the increases in ROS and NO signal. ROS and NO modify several key proteins including cytoskeletal proteins, metabolic proteins or proteins involved in protein synthesis. Therefore, their modification is likely to cause inhibition of pollen tube growth. After blocking metabolism/energy for pollen tube growth via inactivation of sPPase, Rab-GTPase, GAPDH etc. protein synthesis is affected. Therefore, no new proteins can be made to replace the ones already inhibited or irreversibly modified, which provide another layer in our understanding, contributing to how inhibition of pollen tube growth is achieved. The other proteins identified are stress and redox proteins, which could be involved in later PCD events.

In **chapter 5**, we further investigated the role of actin in SI, as it clearly plays a major role. We identified many proteins that were associated with actin using an actin pull down assay as targets of ROS that were oxidatively modified during SI signalling. The modification of these proteins provides us with further new mechanisms potentially involved in SI.

6.5 Modification of actin associated proteins by ROS implicates new mechanisms involved in SI-PCD

Two key actin-associated proteins identified by mass spectrometry were clathrin heavy chain-1(CHC1) and elongation factor-1α (EF1α) as modified by oxidation in both SI induced and H_2O_2 treated samples. EF1α was also identified as the sole protein overlapping H_2O_2-, NO-donor and SI-induced modifications. As these proteins were identified in association with actin, these data provide us insights into new mechanism likely to be involved in SI through actin. As actin is involved in SI-PCD, these may give new insights into PCD-related events.

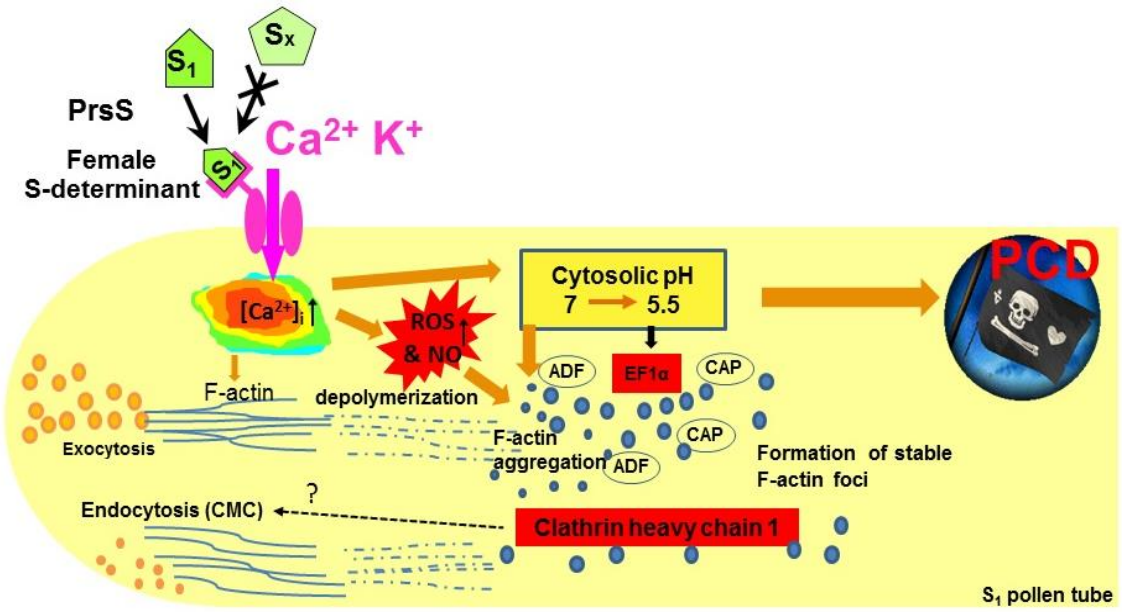

Figure 6.7 Cartoon shows the key components associated with SI-PCD in *Papaver* pollen.

Elongation factor α1 (EF1α) and clathrin heavy chain (CHC1) proteins are associated with F-actin during SI (in punctate actin foci, they are associated with actin binding protein CAP and ADF). pH sensitivity of EF1α has been reported in other studies. CHC1 plays role in endocytosis where endo and exocytosis are required for pollen tube growth. Yellow and orange indicate the previously known PCD signals. Components newly identified as ROS-NO & SI-induced modifications associated with F-actin are in red.

6.5.1 Endocytosis might be involved in the SI-PCD response

Identification of CHC1 associated with actin links the functional involvement of endocytosis mechanisms involved in SI of poppy. For polarized growth of the pollen, the secretory vesicles and other organelles move towards the apical zone of the pollen (Hepler *et al*., 2001). Secretory vesicles provide new cell wall materials for pollen tube elongation and largely accumulated in the clear zone (Heslop-Harrison and Heslop-Harrison, 1990). The dynamics of the actin cytoskeleton provide tracks for the movement of organelles and vesicles (**Figure 6.7**). In response to outside signals, the actin cytoskeleton reorganizes to transport the vesicles towards the apical zone and maintain membrane trafficking (reviewed by Cai *et al*., 2015). Involvement of endocytosis of proteins carried in the secretory vesicles by actin filaments in cytoplasmic streaming into the growth of pollen tube is well recognized (Lind *et al*., 1996, Kim *et al*., 2006). However, it is unknown exactly how endocytosis is involved in the growth of pollen tube and downstream signalling. In the *Nicotiana* S-RNase system, endocytosis of proteins into the pollen tubes through SI has been described (Goldraij *et al*., 2006). In Brassica, an endocytosis and endosomal-based regulatory mechanism for female *S*-determinant, the S-receptor kinase during the SI response has been established (Ivanov and Gaude, 2009). Our finding of CHC1 not only associated with F-actin , but also a target of SI-ROS signal (**Chapter 5**, **Section 5.2.3.4**) implicates a role for clathrin-mediated endocytosis (CME) in SI, as CHC1 is a chief component of clathrin coated vesicles. In mammalian systems, CME is the main endocytotic pathways. Recently several components involved in the CME pathways have been identified in plant cells

(Gadeyne *et al.*, 2014) and it is known to operate in the plant cell (Dhonukshe *et al*., 2007, Hao *et al*., 2014). However, the molecular mechanism responsible in this process and the role of actin is poorly understood in plant cells. Therefore, this is a novel, exciting and potentially high impact area worth investigating in the future.

6.5.2 Actin dynamics, ROS, pH and PCD might be linked by EF1α

EF1α was identified as an F-actin associated target of SI-induced ROS by mass spectrometry. Its pH-sensitive binding to actin (Liu *et al*., 1996b) provides a new potential link to acidification-mediated PCD (**Figure 6.7**). We discussed EF1α and its pH dependent association with actin in detail in **Chapter 5** (**Section 5.3.2**) that in lower pH, EF1α binds to actin more effectively (Liu *et al*., 1996b). This provided us the hypothesis that the SI-induced acidification in poppy might increase the EF1α-mediated bundling of actin filament. However, a key question is how exactly cytosolic pH affects function of EF1α. We demonstrated that the huge SI-induced acidification completely inhibits the activity of Pr-p26.1 sPPases (**Chapter 3**). Therefore, it is expected that pH would affects the activity of EF1α and probably many other proteins. It has been reported that EF1α is involved in the disorganization of F-actin in the S-RNase based SI system (Soulard *et al*., 2014). EF1α is also associated in oxidative stress-induced apoptosis in animal cells (Duttaroy *et al*., 1998, Chen *et al*., 2000). So, actin-associated EF1α might be involved PCD in poppy. This provides a convincing case to investigate the involvement of EF1α in the SI response in further detail, especially in relation to its potential role in SI-induced pH-dependent F-actin

rearrangements mediated PCD. Thus our identification of CHC1 and EF1α as SI-ROS and pH modified, F-actin associated proteins offers us with a strong platform to expose the functional involvement of previously unidentified significant cellular mechanisms in the SI response leading to PCD. These would be novel and important area for future studies.

6.6 Summary

Oxidative modification and S-nitrosylation of plant proteins is now the subject of increasing research effort. Although ROS signalling in mammalian cell is relatively well understood, in the plant cell only a handful of reports on protein modification by ROS/NO are available to date (Lindermayr *et al*., 2005, Tanou *et al*., 2009). Very few studies have been undertaken to understand the functional effect of modifications on the proteins. Therefore, it is a major challenge to identify the effect of the modification on the activity of these proteins.

In this thesis we have presented data identifying several new targets of *Papaver* SI signalling. We showed distinct targets of ROS and NO during the SI response in poppy pollen providing us with several potential new important mechanisms involved in SI via ROS and NO signalling modification. Many appear to point to mechanisms involved in regulating tip growth. These studies have also insights into novel mechanistic processes likely to be involved in mediating SI through actin. As actin plays a central role in SI-PCD, and earlier studies implicated ROS and NO in SI-PCD (Wilkins *et al*., 2011). These data further implicate ROS/NO involvement in SI-PCD. Moreover, we have shown that ROS and NO can directly trigger SI-like actin-configuration responses in

pollen tubes. We also showed that the soluble inorganic pyrophosphatases Pr-p261.a/b, were involved in new pathways, playing previously unidentified roles in the poppy SI response. These newly identified events of SI, together with the events identified previously are presented in **Figure 6.8.** An incompatible Interaction between pollen and pistil *S*-determinants triggers an influx of Ca^{2+}, resulted in increases in $[Ca^{2+}]_i$. This induces a signalling network, resulting in the inhibition of pollen tube growth and finally, death of the pollen tube occurs because of programmed cell death (PCD). During SI many downstream events take place, among them, Ca^{2+} dependent phosphorylation and inhibition of Pr-p26.1 sPPase, alteration of F-actin, increases in ROS and NO happen between 90s to 40 min of SI. Within this time point, a mitogen activated protein kinase, p56 is activated which is known to be involved in PCD. Reduction of cytosolic pH is another event of SI which provides the optimal pH level in the cytosol to activate SI-induced DEVDase activities to be functional and leading the pollen tube to its final mechanism of PCD (**Figure 6.8**). The work in this thesis has also identified several new mechanisms to further our understanding. Besides Ca^{2+} induced phosphorylation of Pr-p26.1a and 1b, increases in cytosolic pH and ROS also involved in the inhibition of their sPPase activity. SI-induced increases in ROS and NO modify several proteins which are involved in pollen tip growth, metabolic function, protein synthesis and so on. Oxidative modification and nitrosylation of these proteins are likely to affect pollen tip growth, a very important mechanism involved in the poppy SI (**Figure 6.8**). Together, all these events confirm the inhibition of pollen tube growth through the pistil and death of incompatible pollen so that it cannot fertilize the ovule.

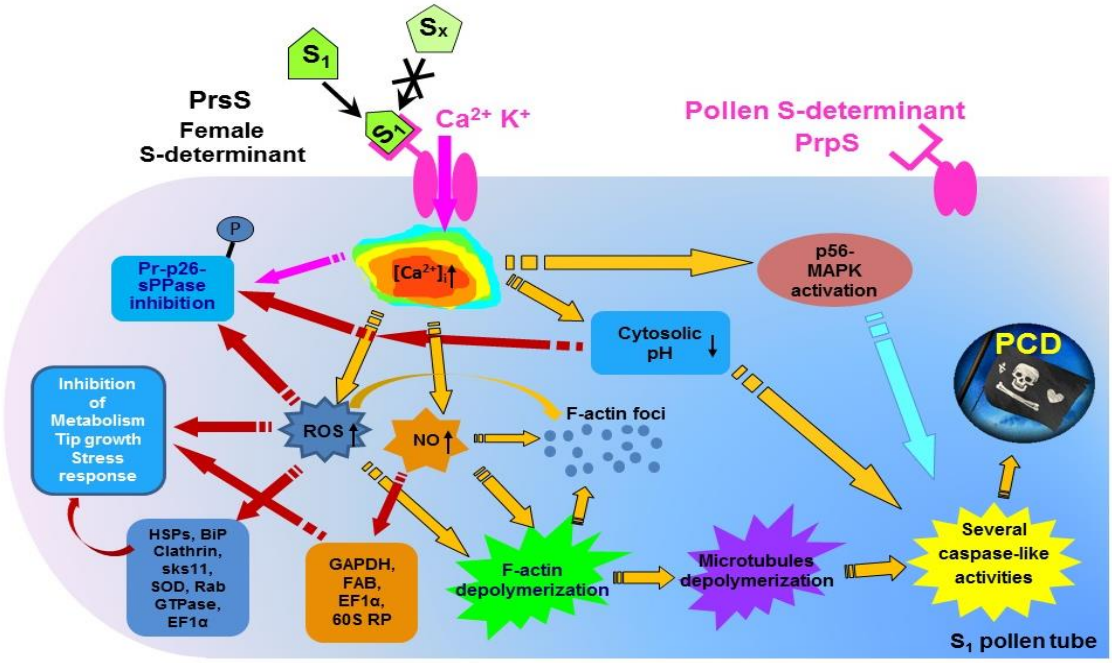

Figure 6.8. A proposed model of SI in *Papaver rhoeas* pollen.

During an incompatible interaction, *Papaver rhoeas* stigmatic S (PrsS), interacts with pollen S (PrpS) and triggers a rapid influx of both K^+ and Ca^{2+}. The increases in cytosolic Ca^{2+} trigger a signalling cascade, resulting in the inhibition of pollen tip growth and finishes to PCD. Increases in Ca^{2+} induces many SI events, including phosphorylation and inhibition of sPPase activity of Pr-p26.1a/b, alterations in the actin cytoskeleton, including the depolymerization of F-actin, later which forms large punctate foci. Rapid increases in both reactive oxygen species (ROS) and nitric oxide (NO) are observed during SI. ROS and NO are linked to actin foci formation and caspase-3-like activities. Furthermore, reduction of cytosolic pH and the release of cytochrome *c* occur which is involved in programmed cell death (PCD). Activation of mitogen activated protein kinases (MAPK) p56 is involved to PCD. SI-induced rapid acidification and ROS also inhibit Pr-p26.1a/b sPPases activity to ensure its complete inactivation. ROS and NO are involved in modification of several proteins, including metabolic enzyme, proteins involved in protein synthesis, pollen tube growth, stress and redox related proteins, which are likely to inhibit their functions towards pollen tube growth. Together, these events confirm the death of incompatible pollen so that fertilization cannot take place. Yellow arrows indicate the old events already published, red arrows show the newly identified events. ROS events are shown by blue box (black writing), NO events are shown by orange box.

Chapter 7

List of References

ABAT, J. K. & DESWAL, R. 2009. Differential modulation of S-nitrosoproteome of Brassica juncea by low temperature: Change in S-nitrosylation of Rubisco is responsible for the inactivation of its carboxylase activity. *Proteomics,* 9**,** 4368-4380.

ABAT, J. K., MATTOO, A. K. & DESWAL, R. 2008. S-nitrosylated proteins of a medicinal CAM plant Kalanchoe pinnata–ribulose-1, 5-bisphosphate carboxylase/oxygenase activity targeted for inhibition. *FEBS journal,* 275**,** 2862-2872.

AITKEN, A. 14-3-3 proteins: a historic overview. Seminars in cancer biology, 2006. Elsevier, 162-172.

AITKEN, A. Post-translational modification of 14-3-3 isoforms and regulation of cellular function. Seminars in cell & developmental biology, 2011. Elsevier, 673-680.

AL-WHAIBI, M. H. 2011. Plant heat-shock proteins: a mini review. *Journal of King Saud University-Science,* 23**,** 139-150.

ALLWOOD, E. G., ANTHONY, R. G., SMERTENKO, A. P., REICHELT, S., DROBAK, B. K., DOONAN, J. H., WEEDS, A. G. & HUSSEY, P. J. 2002. Regulation of the pollen-specific actin-depolymerizing factor LlADF1. *The Plant Cell Online,* 14**,** 2915-2927.

ALVAREZ, M. A. E., PENNELL, R. I., MEIJER, P.-J., ISHIKAWA, A., DIXON, R. A. & LAMB, C. 1998. Reactive oxygen intermediates mediate a systemic signal network in the establishment of plant immunity. *Cell,* 92**,** 773-784.

ALVIM, F. C., CAROLINO, S. M., CASCARDO, J. C., NUNES, C. C., MARTINEZ, C. A., OTONI, W. C. & FONTES, E. P. 2001. Enhanced accumulation of BiP in transgenic plants confers tolerance to water stress. *Plant Physiology,* 126**,** 1042-1054.

AMANO, Y., TSUBOUCHI, H., SHINOHARA, H., OGAWA, M. & MATSUBAYASHI, Y. 2007. Tyrosine-sulfated glycopeptide involved in cellular proliferation and expansion in Arabidopsis. *Proceedings of the National Academy of Sciences,* 104**,** 18333-18338.

AMPE, C., MARKEY, F., LINDBERG, U. & VANDEKERCKHOVE, J. 1988. The primary structure of human platelet profilin: reinvestigation of the calf spleen profilin sequence. *FEBS letters,* 228**,** 17-21.

APEL, K. & HIRT, H. 2004. Reactive oxygen species: metabolism, oxidative stress, and signal transduction. *Annu. Rev. Plant Biol.,* 55**,** 373-399.

ASPINALL, G. & KESSLER, G. 1957. The structure of callose from the grape vine. *J. Soc. Chem. & Ind,* 1296.

AVAEVA, S. 2000. Active site interactions in oligomeric structures of inorganic pyrophosphatases. *Biochemistry C/C of Biokhimiia,* 65**,** 361-372.

BAIS, H. P., VEPACHEDU, R., GILROY, S., CALLAWAY, R. M. & VIVANCO, J. M. 2003. Allelopathy and exotic plant invasion: from molecules and genes to species interactions. *Science,* 301**,** 1377-1380.

BAYKOV, A., COOPERMAN, B., GOLDMAN, A. & LAHTI, R. 1999. Cytoplasmic inorganic pyrophosphatase. *Inorganic Polyphosphates.* Springer.

BAYKOV, A. A., ALEXANDROV, A. P. & SMIRNOVA, I. N. 1992. A two-step mechanism of fluoride inhibition of rat liver inorganic pyrophosphatase. *Archives of biochemistry and biophysics,* 294**,** 238-243.

BAYKOV, A. A., FABRICHNIY, I. P., POHJANJOKI, P., ZYRYANOV, A. B. & LAHTI, R. 2000. Fluoride Effects along the Reaction Pathway of Pyrophosphatase: Evidence for a Second Enzyme. Pyrophosphate Intermediate. *Biochemistry,* 39**,** 11939-11947.

BAYKOV, A. A., SHESTAKOV, A. S., KASHO, V. N., VENER, A. V. & IVANOV, A. H. 1990. Kinetics and thermodynamics of catalysis by the inorganic pyrophosphatase of *Escherichia coli* in both directions. *European journal of biochemistry,* 194**,** 879-887.

BAYLIAK, M., SEMCHYSHYN, H. & LUSHCHAK, V. 2006. Effect of hydrogen peroxide on antioxidant enzyme activities in *Saccharomyces cerevisiae* is strain-specific. *Biochemistry (Moscow),* 71**,** 1013-1020.

BEERE, H. M., WOLF, B. B., CAIN, K., MOSSER, D. D., MAHBOUBI, A., KUWANA, T., TAILOR, P., MORIMOTO, R. I., COHEN, G. M. & GREEN, D. R. 2000. Heat-shock protein 70 inhibits apoptosis by preventing recruitment of procaspase-9 to the Apaf-1 apoptosome. *Nature cell biology,* 2**,** 469-475.

BELENGHI, B., ROMERO-PUERTAS, M. C., VERCAMMEN, D., BRACKENIER, A., INZÉ, D., DELLEDONNE, M. & VAN BREUSEGEM, F. 2007. Metacaspase activity of *Arabidopsis thaliana* is regulated by *S*-nitrosylation of a critical cysteine residue. *Journal of Biological Chemistry,* 282**,** 1352-1358.

BELL, C. D., SOLTIS, D. E. & SOLTIS, P. S. 2010. The age and diversification of the angiosperms re-revisited. *American Journal of Botany,* 97**,** 1296-1303.

BERLETT, B. S. & STADTMAN, E. R. 1997. Protein oxidation in aging, disease, and oxidative stress. *Journal of Biological Chemistry,* 272**,** 20313-20316.

BETHKE, P. C. & JONES, R. L. 2001. Cell death of barley aleurone protoplasts is mediated by reactive oxygen species. *The Plant Journal,* 25**,** 19-29.

BITEAU, B., LABARRE, J. & TOLEDANO, M. B. 2003. ATP-dependent reduction of cysteine–sulphinic acid by *S. cerevisiae* sulphiredoxin. *Nature,* 425**,** 980-984.

BOLLER, T. & FELIX, G. 2009. A renaissance of elicitors: perception of microbe-associated molecular patterns and danger signals by pattern-recognition receptors. *Annual review of plant biology,* 60**,** 379-406.

BOND, M., CHIU, N. & COOPERMAN, B. 1980. Identification of an arginine important for enzymic activity within the covalent structure of yeast inorganic pyrophosphatase. *Biochemistry,* 19**,** 94-102.

BONNEAU, L., GE, Y., DRURY, G. E. & GALLOIS, P. 2008. What happened to plant caspases? *Journal of experimental botany,* 59**,** 491-499.

BOSCH, M. & FRANKLIN-TONG, V. E. 2007. Temporal and spatial activation of caspase-like enzymes induced by self-incompatibility in *Papaver* pollen. *Proceedings of the National Academy of Sciences,* 104**,** 18327-18332.

BOSCH, M. & FRANKLIN-TONG, V. E. 2008. Self-incompatibility in *Papaver*: signalling to trigger PCD in incompatible pollen. *Journal of experimental botany,* 59**,** 481-490.

BOSCH, M., POULTER, N. S., PERRY, R. M., WILKINS, K. A. & FRANKLIN-TONG, V. E. 2010. Characterization of a legumain/vacuolar processing enzyme and YVADase activity in *Papaver* pollen. *Plant molecular biology,* 74**,** 381-393.

BOSCH, M., POULTER, N. S., VATOVEC, S. & FRANKLIN-TONG, V. E. 2008. Initiation of programmed cell death in self-incompatibility: role for cytoskeleton modifications and several caspase-like activities. *Molecular plant,* 1**,** 879-887.

BOSSIO, R. E. & MARSHALL, A. G. 2002. Baseline resolution of isobaric phosphorylated and sulfated peptides and nucleotides by electrospray ionization FTICR ms: another step toward mass spectrometry-based proteomics. *Analytical chemistry,* 74**,** 1674-1679.

BOU DAHER, F. & GEITMANN, A. 2011. Actin is involved in pollen tube tropism through redefining the spatial targeting of secretory vesicles. *Traffic,* 12**,** 1537-1551.

BOVE, J., VAILLANCOURT, B., KROEGER, J., HEPLER, P. K., WISEMAN, P. W. & GEITMANN, A. 2008. Magnitude and direction of vesicle dynamics in growing pollen tubes using spatiotemporal image

correlation spectroscopy and fluorescence recovery after photobleaching. *Plant Physiology,* 147**,** 1646-1658.

BRADFORD, M. M. 1976. A rapid and sensitive method for the quantitation of microgram quantities of protein utilizing the principle of protein-dye binding. *Analytical biochemistry,* 72**,** 248-254.

BRETSCHER, A. 1981. Fimbrin is a cytoskeletal protein that crosslinks F-actin in vitro. *Proceedings of the National Academy of Sciences,* 78**,** 6849-6853.

BRODSKY, F. M. 2012. Diversity of clathrin function: new tricks for an old protein. *Annual review of cell and developmental biology,* 28**,** 309.

BROWNFIELD, L., FORD, K., DOBLIN, M. S., NEWBIGIN, E., READ, S. & BACIC, A. 2007. Proteomic and biochemical evidence links the callose synthase in *Nicotiana alata* pollen tubes to the product of the NaGSL1 gene. *The Plant Journal,* 52**,** 147-156.

BROWNFIELD, L., WILSON, S., NEWBIGIN, E., BACIC, A. & READ, S. 2008. Molecular control of the glucan synthase-like protein NaGSL1 and callose synthesis during growth of *Nicotiana alata* pollen tubes. *Biochem. J,* 414**,** 43-52.

BUCKE, C. 1970. The distribution and properties of alkaline inorganic pyrophosphatase from higher plants. *Phytochemistry,* 9**,** 1303-1309.

BUNIK, V. I. 2003. 2-Oxo acid dehydrogenase complexes in redox regulation. *European Journal of Biochemistry,* 270**,** 1036-1042.

CABRILLAC, D., COCK, J. M., DUMAS, C. & GAUDE, T. 2001. The S-locus receptor kinase is inhibited by thioredoxins and activated by pollen coat proteins. *Nature,* 410**,** 220-223.

CAI, G. & CRESTI, M. 2009. Organelle motility in the pollen tube: a tale of 20 years. *Journal of experimental botany,* 60**,** 495-508.

CAI, G., PARROTTA, L. & CRESTI, M. 2015. Organelle trafficking, the cytoskeleton, and pollen tube growth. *Journal of integrative plant biology,* 57**,** 63-78.

CAMACHO, L. & MALHÓ, R. 2003. Endo/exocytosis in the pollen tube apex is differentially regulated by Ca^{2+} and GTPases. *Journal of experimental botany,* 54**,** 83-92.

CANO, M. L., LAUFFENBURGER, D. A. & ZIGMOND, S. H. 1991. Kinetic analysis of F-actin depolymerization in polymorphonuclear leukocyte lysates indicates that chemoattractant stimulation increases actin filament number without altering the filament length distribution. *The Journal of cell biology,* 115**,** 677-687.

CARBONE, D. L., DOORN, J. A., KIEBLER, Z., ICKES, B. R. & PETERSEN, D. R. 2005. Modification of heat shock protein 90 by 4-hydroxynonenal in a rat model of chronic alcoholic liver disease. *Journal of Pharmacology and Experimental Therapeutics,* 315**,** 8-15.

CÁRDENAS, L., LOVY-WHEELER, A., WILSEN, K. L. & HEPLER, P. K. 2005. Actin polymerization promotes the reversal of streaming in the apex of pollen tubes. *Cell motility and the cytoskeleton,* 61**,** 112-127.

CASATI, P. & WALBOT, V. 2004. Crosslinking of ribosomal proteins to RNA in maize ribosomes by UV-B and its effects on translation. *Plant physiology,* 136**,** 3319-3332.

CHARLESWORTH, D. & CHARLESWORTH, B. 1987. Inbreeding depression and its evolutionary consequences. *Annual review of ecology and systematics***,** 237-268.

CHÁVEZ-RIOS, R., ARIAS-ROMERO, L. E., DE JESÚS ALMARAZ-BARRERA, M., HERNÁNDEZ-RIVAS, R., GUILLÉN, N. & VARGAS, M. 2003. L10 ribosomal protein from Entamoeba histolytica share structural and functional homologies with QM/Jif-1: proteins with extraribosomal functions. *Molecular and biochemical parasitology,* 127**,** 151-160.

CHEN, C. Y., WONG, E. I., VIDALI, L., ESTAVILLO, A., HEPLER, P. K., WU, H.-M. & CHEUNG, A. Y. 2002. The regulation of actin organization by actin-depolymerizing factor in elongating pollen tubes. *The Plant Cell Online,* 14**,** 2175-2190.

CHEN, E., PROESTOU, G., BOURBEAU, D. & WANG, E. 2000. Rapid up-regulation of peptide elongation factor EF-1α protein levels is an immediate early event during oxidative stress-induced apoptosis. *Experimental cell research,* 259**,** 140-148.

CHEN, F., LI, Q., SUN, L. & HE, Z. 2006. The rice 14-3-3 gene family and its involvement in responses to biotic and abiotic stress. *DNA research,* 13**,** 53-63.

CHEN, J., BREVET, A., FROMANT, M., LEVEQUE, F., SCHMITTER, J., BLANQUET, S. & PLATEAU, P. 1990. Pyrophosphatase is essential for growth of *Escherichia coli*. *Journal of bacteriology,* 172**,** 5686-5689.

CHEN, X., IRANI, N. G. & FRIML, J. 2011. Clathrin-mediated endocytosis: the gateway into plant cells. *Current opinion in plant biology,* 14**,** 674-682.

CHEUNG, A. Y., CHEN, C. Y.-H., GLAVEN, R. H., DE GRAAF, B. H., VIDALI, L., HEPLER, P. K. & WU, H.-M. 2002. Rab2 GTPase regulates vesicle trafficking between the endoplasmic reticulum and the Golgi bodies and is important to pollen tube growth. *The Plant Cell Online,* 14**,** 945-962.

CHEUNG, A. Y., NIROOMAND, S., ZOU, Y. & WU, H.-M. 2010. A transmembrane formin nucleates subapical actin assembly and controls tip-focused growth in pollen tubes. *Proceedings of the National Academy of Sciences,* 107**,** 16390-16395.

CHEUNG, A. Y. & WU, H.-M. 2004. Overexpression of an Arabidopsis formin stimulates supernumerary actin cable formation from pollen tube cell membrane. *The Plant Cell Online,* 16**,** 257-269.

CHEUNG, A. Y. & WU, H.-M. 2008. Structural and signaling networks for the polar cell growth machinery in pollen tubes. *Annu. Rev. Plant Biol.,* 59**,** 547-572.

CHI, Y. H., PAENG, S. K., KIM, M. J., HWANG, G. Y., MELENCION, S. M. B., OH, H. T. & LEE, S. Y. 2013. Redox-dependent functional switching of plant proteins accompanying with their structural changes. *Frontiers in plant science,* 4.

CHRISTOFFERSON, D. E. & YUAN, J. 2010. Necroptosis as an alternative form of programmed cell death. *Current opinion in cell biology,* 22**,** 263-268.

COLL, N., EPPLE, P. & DANGL, J. 2011. Programmed cell death in the plant immune system. *Cell Death & Differentiation,* 18**,** 1247-1256.

COLL, N., SMIDLER, A., PUIGVERT, M., POPA, C., VALLS, M. & DANGL, J. 2014. The plant metacaspase AtMC1 in pathogen-triggered programmed cell death and aging: functional linkage with autophagy. *Cell Death & Differentiation*.

COOPERMAN, B. S. 1982. The mechanism of action of yeast inorganic pyrophosphatase. *Methods in enzymology,* 87**,** 526-548.

COOPERMAN, B. S., BAYKOV, A. A. & LAHTI, R. 1992. Evolutionary conservation of the active site of soluble inorganic pyrophosphatase. *Trends in biochemical sciences,* 17**,** 262-266.

COSTA, M. D., REIS, P. A., VALENTE, M. A. S., IRSIGLER, A. S., CARVALHO, C. M., LOUREIRO, M. E., ARAGÃO, F. J., BOSTON, R. S., FIETTO, L. G. & FONTES, E. P. 2008. A new branch of endoplasmic reticulum stress signaling and the osmotic signal converge on plant-specific asparagine-rich proteins to promote cell death. *Journal of Biological Chemistry,* 283**,** 20209-20219.

CRAIG, E. A., WEISSMAN, J. S. & HORWICH, A. L. 1994. Heat shock proteins and molecular chaperones: mediators of protein conformation and turnover in the cell. *Cell,* 78**,** 365-372.

CROWTHER, R. & PEARSE, B. 1981. Assembly and packing of clathrin into coats. *The Journal of cell biology,* 91**,** 790-797.

CRUZ-GARCIA, F., NATHAN HANCOCK, C., KIM, D. & MCCLURE, B. 2005. Stylar glycoproteins bind to S-RNase in vitro. *The Plant Journal,* 42**,** 295-304.

DA SILVA, D., LACHAUD, C., COTELLE, V., BRIÈRE, C., GRAT, S., MAZARS, C. & THULEAU, P. 2011. Nitric oxide production is not required for dihydrosphingosine-induced cell death in tobacco BY-2 cells. *Plant signaling & behavior,* 6**,** 736-739.

DALLE-DONNE, I., ROSSI, R., GIUSTARINI, D., GAGLIANO, N., DI SIMPLICIO, P., COLOMBO, R. & MILZANI, A. 2002. Methionine oxidation as a major cause of the functional impairment of oxidized actin. *Free Radical Biology and Medicine,* 32**,** 927-937.

DALLE-DONNE, I., ROSSI, R., GIUSTARINI, D., GAGLIANO, N., LUSINI, L., MILZANI, A., DI SIMPLICIO, P. & COLOMBO, R. 2001a. Actin carbonylation: from a simple marker of protein oxidation to relevant signs of severe functional impairment. *Free Radical Biology and Medicine,* 31**,** 1075-1083.

DALLE-DONNE, I., ROSSI, R., MILZANI, A., DI SIMPLICIO, P. & COLOMBO, R. 2001b. The actin cytoskeleton response to oxidants: from small heat shock protein phosphorylation to changes in the redox state of actin itself. *Free Radical Biology and Medicine,* 31**,** 1624-1632.

DANGL, J. L. 1995. Piece de resistance: novel classes of plant disease resistance genes. *Cell,* 80**,** 363-366.

DANGL, J. L. & JONES, J. D. 2001. Plant pathogens and integrated defence responses to infection. *nature,* 411**,** 826-833.

DANON, A., DELORME, V., MAILHAC, N. & GALLOIS, P. 2000. Plant programmed cell death: a common way to die. *Plant Physiology and Biochemistry,* 38**,** 647-655.

DAVIDSON, A. M. & HALESTRAP, A. P. 1989. Inhibition of mitochondrial-matrix inorganic pyrophosphatase by physiological [Ca^{2+}], and its role in the hormonal regulation of mitochondrial matrix volume. *Biochem. J,* 258**,** 817-821.

DE GRAAF, B. H., CHEUNG, A. Y., ANDREYEVA, T., LEVASSEUR, K., KIELISZEWSKI, M. & WU, H.-M. 2005. Rab11 GTPase-regulated membrane trafficking is crucial for tip-focused pollen tube growth in tobacco. *The Plant Cell Online,* 17**,** 2564-2579.

DE GRAAF, B. H., RUDD, J. J., WHEELER, M. J., PERRY, R. M., BELL, E. M., OSMAN, K., FRANKLIN, F. C. H. & FRANKLIN-TONG, V. E. 2006. Self-incompatibility in *Papaver* targets soluble inorganic pyrophosphatases in pollen. *Nature,* 444**,** 490-493.

DE GRAAF, B. H., VATOVEC, S., JUÁREZ-DÍAZ, J. A., CHAI, L., KOOBLALL, K., WILKINS, K. A., ZOU, H., FORBES, T., FRANKLIN, F. C. H. & FRANKLIN-TONG, V. E. 2012. The *Papaver* self-incompatibility pollen S-determinant, PrpS, functions in *Arabidopsis thaliana*. *Current Biology,* 22**,** 154-159.

DE GROOT, P., WETERINGS, K., DE BEEN, M., WITTINK, F., HULZINK, R., CUSTERS, J., VAN HERPEN, M. & WULLEMS, G. 2004. Silencing of the pollen-specific gene NTP303 and its family members in tobacco affects in vivo pollen tube growth and results in male sterile plants. *Plant molecular biology,* 55**,** 715-726.

DELILLE, J. M., SEHNKE, P. C. & FERL, R. J. 2001. The Arabidopsis 14-3-3 family of signaling regulators. *Plant Physiology,* 126**,** 35-38.

DELLEDONNE, M. 2005. NO news is good news for plants. *Current opinion in plant biology,* 8**,** 390-396.

DEMMA, M., WARREN, V., HOCK, R., DHARMAWARDHANE, S. & CONDEELIS, J. 1990. Isolation of an abundant 50,000-dalton actin filament bundling protein from *Dictyostelium amoebae*. *Journal of Biological Chemistry,* 265**,** 2286-2291.

DENISON, F. C., PAUL, A.-L., ZUPANSKA, A. K. & FERL, R. J. 14-3-3 proteins in plant physiology. Seminars in cell & developmental biology, 2011. Elsevier, 720-727.

DERKSEN, J., RUTTEN, T., AMSTEL, T., WIN, A., DORIS, F. & STEER, M. 1995. Regulation of pollen tube growth. *Acta botanica neerlandica,* 44**,** 93-119.

DHARMAWARDHANE, S., DEMMA, M., YANG, F. & CONDEELIS, J. 1991. Compartmentalization and actin binding properties of ABP-50: The elongation factor-1 alpha of Dictyostelium. *Cell motility and the cytoskeleton,* 20**,** 279-288.

DHONUKSHE, P., ANIENTO, F., HWANG, I., ROBINSON, D. G., MRAVEC, J., STIERHOF, Y.-D. & FRIML, J. 2007. Clathrin-mediated constitutive endocytosis of PIN auxin efflux carriers in Arabidopsis. *Current Biology,* 17**,** 520-527.

DIAZ-VIVANCOS, P., FAIZE, M., BARBA-ESPIN, G., FAIZE, L., PETRI, C., HERNÁNDEZ, J. A. & BURGOS, L. 2013. Ectopic expression of cytosolic superoxide dismutase and ascorbate peroxidase leads to salt stress tolerance in transgenic plums. *Plant biotechnology journal,* 11**,** 976-985.

DICKMAN, M., PARK, Y., OLTERSDORF, T., LI, W., CLEMENTE, T. & FRENCH, R. 2001. Abrogation of disease development in plants

expressing animal antiapoptotic genes. *Proceedings of the National Academy of Sciences,* 98**,** 6957-6962.

DONG, X., HONG, Z., SIVARAMAKRISHNAN, M., MAHFOUZ, M. & VERMA, D. P. S. 2005. Callose synthase (CalS5) is required for exine formation during microgametogenesis and for pollen viability in Arabidopsis. *The Plant Journal,* 42**,** 315-328.

DOS REMEDIOS, C., CHHABRA, D., KEKIC, M., DEDOVA, I., TSUBAKIHARA, M., BERRY, D. & NOSWORTHY, N. 2003. Actin binding proteins: regulation of cytoskeletal microfilaments. *Physiological reviews,* 83**,** 433-473.

DRESSELHAUS, T. & FRANKLIN-TONG, N. 2013. Male–female crosstalk during pollen germination, tube growth and guidance, and double fertilization. *Molecular Plant,* 6**,** 1018-1036.

DU JARDIN, P., ROJAS-BELTRAN, J., GEBHARDT, C. & BRASSEUR, R. 1995. Molecular cloning and characterization of a soluble inorganic pyrophosphatase in potato. *Plant Physiology,* 109**,** 853-860.

DUAN, Q., KITA, D., JOHNSON, E. A., AGGARWAL, M., GATES, L., WU, H.-M. & CHEUNG, A. Y. 2014. Reactive oxygen species mediate pollen tube rupture to release sperm for fertilization in Arabidopsis. *Nature communications,* 5.

DUNAND-SAUTHIER, I., WALKER, C. A., NARASIMHAN, J., PEARCE, A. K., WEK, R. C. & HUMPHREY, T. C. 2005. Stress-activated protein kinase pathway functions to support protein synthesis and translational adaptation in response to environmental stress in fission yeast. *Eukaryotic cell,* 4**,** 1785-1793.

DUTTAROY, A., BOURBEAU, D., WANG, X.-L. & WANG, E. 1998. Apoptosis rate can be accelerated or decelerated by overexpression or reduction of the level of elongation factor-1α. *Experimental cell research,* 238**,** 168-176.

EAVES, D. J., FLORES-ORTIZ, C., HAQUE, T., LIN, Z., TENG, N. & FRANKLIN-TONG, V. E. 2014. Self-incompatibility in *Papaver*: advances in integrating the signalling network. *Biochemical Society transactions,* 42**,** 370-376.

EDMONDS, B. T., MURRAY, J. & CONDEELIS, J. 1995. pH regulation of the F-actin binding properties of Dictyostelium elongation factor 1α. *Journal of Biological Chemistry,* 270**,** 15222-15230.

EDMONDS, B. T., WYCKOFF, J., YEUNG, Y.-G., WANG, Y., STANLEY, E. R., JONES, J., SEGALL, J. & CONDEELIS, J. 1996. Elongation factor-1 alpha is an overexpressed actin binding protein in metastatic rat mammary adenocarcinoma. *Journal of cell science,* 109**,** 2705-2714.

EISINGER, D. P., DICK, F. A. & TRUMPOWER, B. L. 1997. Qsr1p, a 60S ribosomal subunit protein, is required for joining of 40S and 60S subunits. *Molecular and Cellular Biology,* 17**,** 5136-5145.

ELMORE, S. 2007. Apoptosis: a review of programmed cell death. *Toxicologic pathology,* 35**,** 495-516.

ENGLAND, K. & COTTER, T. 2005. Direct oxidative modifications of signalling proteins in mammalian cells and their effects on apoptosis. *Redox Report,* 10**,** 237-245.

FABBRIZIO, E., BONET-KERRACHE, A., LEGER, J. J. & MORNET, D. 1993. Actin-dystrophin interface. *Biochemistry,* 32**,** 10457-10463.

FAIZE, M., BURGOS, L., FAIZE, L., PIQUERAS, A., NICOLAS, E., BARBA-ESPIN, G., CLEMENTE-MORENO, M., ALCOBENDAS, R., ARTLIP, T. & HERNANDEZ, J. 2011. Involvement of cytosolic ascorbate peroxidase and Cu/Zn-superoxide dismutase for improved tolerance against drought stress. *Journal of experimental botany***,** erq32.

FARAH, M. E. & AMBERG, D. C. 2007. Conserved actin cysteine residues are oxidative stress sensors that can regulate cell death in yeast. *Molecular biology of the cell,* 18**,** 1359-1365.

FARES, A., ROSSIGNOL, M. & PELTIER, J.-B. 2011. Proteomics investigation of endogenous *S*-nitrosylation in *Arabidopsis*. *Biochemical and Biophysical Research Communications,* 416**,** 331-336.

FARRÉ, E. M., GEIGENBERGER, P., WILLMITZER, L. & TRETHEWEY, R. N. 2000. A possible role for pyrophosphate in the coordination of cytosolic and plastidial carbon metabolism within the potato tuber. *Plant Physiology,* 123**,** 681-688.

FARRÉ, E. M., TECH, S., TRETHEWEY, R. N., FERNIE, A. R. & WILLMITZER, L. 2006. Subcellular pyrophosphate metabolism in developing tubers of potato (*Solanum tuberosum*). *Plant molecular biology,* 62**,** 165-179.

FEECHAN, A., KWON, E., YUN, B.-W., WANG, Y., PALLAS, J. A. & LOAKE, G. J. 2005. A central role for S-nitrosothiols in plant disease resistance. *Proceedings of the National Academy of Sciences,* 102**,** 8054-8059.

FEIJÓ, J., SAINHAS, J., HACKETT, G., KUNKEL, J. & HEPLER, P. 1999. Growing pollen tubes possess a constitutive alkaline band in the clear zone and a growth-dependent acidic tip. *The Journal of cell biology,* 144**,** 483-496.

FEIJO, J. A., SAINHAS, J., HOLDAWAY-CLARKE, T., CORDEIRO, M. S., KUNKEL, J. G. & HEPLER, P. K. 2001. Cellular oscillations and the regulation of growth: the pollen tube paradigm. *Bioessays,* 23**,** 86-94.

FERL, R. J., MANAK, M. S. & REYES, M. F. 2002. The 14-3-3s. *Genome biology,* 3**,** reviews3010.

FERREYRA, M. L. F., PEZZA, A., BIARC, J., BURLINGAME, A. L. & CASATI, P. 2010. Plant L10 ribosomal proteins have different roles during development and translation under ultraviolet-B stress. *Plant physiology,* 153**,** 1878-1894.

FEUER, G. & MOLNAR, F. 1948. Studies on the composition and polymerization of actin. *Hungarica acta physiologica,* 1**,** 150.

FISKE, C. H. & SUBBAROW, Y. 1925. The colorimetric determination of phosphorus. *J. biol. Chem,* 66**,** 375-400.

FOOTE, H., RIDE, J. P., FRANKLIN-TONG, V. E., WALKER, E. A., LAWRENCE, M. J. & FRANKLIN, F. 1994. Cloning and expression of a distinctive class of self-incompatibility (S) gene from *Papaver rhoeas* L. *Proceedings of the National Academy of Sciences,* 91**,** 2265-2269.

FOREMAN, J., DEMIDCHIK, V., BOTHWELL, J. H., MYLONA, P., MIEDEMA, H., TORRES, M. A., LINSTEAD, P., COSTA, S., BROWNLEE, C. & JONES, J. D. 2003. Reactive oxygen species produced by NADPH oxidase regulate plant cell growth. *Nature,* 422**,** 442-446.

FORRESTER, M. T., THOMPSON, J. W., FOSTER, M. W., NOGUEIRA, L., MOSELEY, M. A. & STAMLER, J. S. 2009. Proteomic analysis of S-nitrosylation and denitrosylation by resin-assisted capture. *Nature biotechnology,* 27**,** 557-559.

FOWLER, J. E. & QUATRANO, R. S. 1997. Plant cell morphogenesis: plasma membrane interactions with the cytoskeleton and cell wall. *Annual review of cell and developmental biology,* 13**,** 697-743.

FOYER, C. H. & NOCTOR, G. 2009. Redox regulation in photosynthetic organisms: signaling, acclimation, and practical implications. *Antioxidants & redox signaling,* 11**,** 861-905.

FRAICHARD, A., TROSSAT, C., PEROTTI, E. & PUGIN, A. 1996. Allosteric regulation by Mg^{2+} of the vacuolar H^{+}-PPase from Acer pseudoplatanus cells. Ca^{2+} -Mg^{2+} interactions. *Biochimie,* 78**,** 259-266.

FRANKLIN-TONG, N. V. & FRANKLIN, C. F. 1993. Gametophytic self-incompatibility: contrasting mechanisms for *Nicotiana* and *Papaver*. *Trends in cell biology,* 3**,** 340-345.

FRANKLIN-TONG, N. V. & FRANKLIN, F. C. H. 2003. Gametophytic self-incompatibility inhibits pollen tube growth using different mechanisms. *Trends in plant science,* 8**,** 598-605.

FRANKLIN-TONG, V. & GOURLAY, C. 2008. A role for actin in regulating apoptosis/programmed cell death: evidence spanning yeast, plants and animals. *Biochem. J,* 413**,** 389-404.

FRANKLIN-TONG, V. E. 1999. Signaling and the modulation of pollen tube growth. *The Plant Cell Online,* 11**,** 727-738.

FRANKLIN-TONG, V. E., DROBAK, B. K., ALLAN, A. C., WATKINS, P. A. & TREWAVAS, A. J. 1996. Growth of pollen tubes of *Papaver rhoeas* is regulated by a slow-moving calcium wave propagated by inositol 1, 4, 5-trisphosphate. *The Plant Cell,* 8**,** 1305-1321.

FRANKLIN-TONG, V., LAWRENCE, M. & FRANKLIN, F. 1988a. An in vitro bioassay for the stigmatic product of the self-incompatibility gene in *Papaver rhoeas L.* 110.

FRANKLIN-TONG, V., LAWRENCE, M. & FRANKLIN, F. 1988b. An in vitro bioassay for the stigmatic product of the self-incompatibility gene in *Papaver rhoeas* L. *New phytologist,* 110**,** 109-118.

FRANKLIN-TONG, V. E., HACKETT, G. & HEPLER, P. K. 1997. Ratio-imaging of Ca^{2+} i in the self-incompatibility response in pollen tubes of *Papaver rhoeas*. *The Plant Journal,* 12**,** 1375-1386.

FRANKLIN-TONG, V. E., RIDE, J. P., READ, N. D., TREWAVAS, A. J. & FRANKLIN, F. C. H. 1993. The self-incompatibility response in *Papaver rhoeas* is mediated by cytosolic free calcium. *The Plant Journal,* 4**,** 163-177.

FRANKLIN-TONG, V. E., RIDE, J. P., READ, N. D., TREWAVAS, A. J. & FRANKLIN, F. C. H. 2002. The self-incompatibility response in *Papaver rhoeas* is mediated by cytosolic free calcium. *The Plant Journal,* 4**,** 163-177.

FRANKLIN, F., LAWRENCE, M. & FRANKLIN-TONG, V. 1995. Cell and molecular biology of self-incompatibility in flowering plants. *International Review of Cytology,* 158**,** 1-64.

FRATELLI, M., DEMOL, H., PUYPE, M., CASAGRANDE, S., EBERINI, I., SALMONA, M., BONETTO, V., MENGOZZI, M., DUFFIEUX, F. & MICLET, E. 2002. Identification by redox proteomics of glutathionylated proteins in oxidatively stressed human T lymphocytes. *Proceedings of the National Academy of Sciences,* 99**,** 3505-3510.

FRICKER, M., WHITE, N. & OBERMEYER, G. 1997. pH gradients are not associated with tip growth in pollen tubes of *Lilium longiflorum*. *Journal of cell science,* 110**,** 1729-1740.

FRIDOVICH, I. 1995. Superoxide radical and superoxide dismutases. *Annual review of biochemistry,* 64**,** 97-112.

FU, Y. 2010. The actin cytoskeleton and signaling network during pollen tube tip growth. *Journal of integrative plant biology,* 52**,** 131-137.

FU, Y., WU, G. & YANG, Z. 2001. Rop GTPase–dependent dynamics of tip-localized F-actin controls tip growth in pollen tubes. *The Journal of cell biology,* 152**,** 1019-1032.

GADEYNE, A., SÁNCHEZ-RODRÍGUEZ, C., VANNESTE, S., DI RUBBO, S., ZAUBER, H., VANNESTE, K., VAN LEENE, J., DE WINNE, N., EECKHOUT, D. & PERSIAU, G. 2014. The TPLATE adaptor complex drives clathrin-mediated endocytosis in plants. *Cell,* 156**,** 691-704.

GALLI, F., ROVIDATI, S., GHIBELLI, L. & CANESTRARI, F. 1998. S-nitrosylation of glyceraldehyde-3-phosphate dehydrogenase decreases the enzyme affinity to the erythrocyte membrane. *Nitric Oxide,* 2**,** 17-27.

GARDINO, A. K., SMERDON, S. J. & YAFFE, M. B. Structural determinants of 14-3-3 binding specificities and regulation of subcellular localization of 14-3-3-ligand complexes: a comparison of the X-ray crystal structures of all human 14-3-3 isoforms. Seminars in cancer biology, 2006. Elsevier, 173-182.

GECHEV, T., PETROV, V. & MINKOV, I. 2010. Reactive oxygen species and programmed cell death. *Reactive oxygen species and antioxidants in higher plants***,** 65.

GECHEV, T. S., VAN BREUSEGEM, F., STONE, J. M., DENEV, I. & LALOI, C. 2006. Reactive oxygen species as signals that modulate plant stress responses and programmed cell death. *Bioessays,* 28**,** 1091-1101.

GEITMANN, A. 2010. How to shape a cylinder: pollen tube as a model system for the generation of complex cellular geometry. *Sexual plant reproduction,* 23**,** 63-71.

GEITMANN, A., SNOWMAN, B. N., EMONS, A. M. C. & FRANKLIN-TONG, V. E. 2000. Alterations in the actin cytoskeleton of pollen tubes are induced by the self-incompatibility reaction in *Papaver rhoeas*. *The Plant Cell Online,* 12**,** 1239-1251.

GHEZZI, P. & BONETTO, V. 2003. Redox proteomics: identification of oxidatively modified proteins. *Proteomics,* 3**,** 1145-1153.

GIBBON, B. C., KOVAR, D. R. & STAIGER, C. J. 1999. Latrunculin B has different effects on pollen germination and tube growth. *The Plant Cell Online,* 11**,** 2349-2363.

GLENNEY, J., KAULFUS, P., MATSUDAIRA, P. & WEBER, K. 1981. F-actin binding and bundling properties of fimbrin, a major cytoskeletal protein of microvillus core filaments. *Journal of Biological Chemistry,* 256**,** 9283-9288.

GOLDRAIJ, A., KONDO, K., LEE, C. B., HANCOCK, C. N., SIVAGURU, M., VAZQUEZ-SANTANA, S., KIM, S., PHILLIPS, T. E., CRUZ-GARCIA, F. & MCCLURE, B. 2006. Compartmentalization of S-RNase and HT-B degradation in self-incompatible *Nicotiana*. *Nature,* 439**,** 805-810.

GOLDSCHMIDT-CLERMONT, P. J., MACHESKY, L. M., DOBERSTEIN, S. K. & POLLARD, T. D. 1991. Mechanism of the interaction of human platelet profilin with actin. *The Journal of cell biology,* 113**,** 1081-1089.

GÓMEZ-GARCíA, M. A. R., RUIZ-PÉREZ, L. M., GONZÁLEZ-PACANOWSKA, D. & SERRANO, A. 2004. A novel calcium-dependent soluble inorganic pyrophosphatase from the trypanosomatid *Leishmania major*. *FEBS letters,* 560**,** 158-166.

GÓMEZ-GARCÍA, M. R., LOSADA, M. & SERRANO, A. 2006. A novel subfamily of monomeric inorganic pyrophosphatases in photosynthetic eukaryotes. *Biochemical Journal,* 395**,** 211.

GÓMEZ-GARCÍA, M. R., LOSADA, M. & SERRANO, A. 2007. Comparative biochemical and functional studies of family I soluble inorganic pyrophosphatases from photosynthetic bacteria. *FEBS Journal,* 274**,** 3948-3959.

GORING, D. R., INDRIOLO, E. & SAMUEL, M. A. 2014. The ARC1 E3 ligase promotes a strong and stable self-incompatibility response in *Arabidopsis species*: response to the Nasrallah and Nasrallah commentary. *The Plant Cell,* 26**,** 3842-3846.

GREENBERG, J. T. & YAO, N. 2004. The role and regulation of programmed cell death in plant–pathogen interactions. *Cellular microbiology,* 6**,** 201-211.

GROSS, P. & AP REES, T. 1986. Alkaline inorganic pyrophosphatase and starch synthesis in amyloplasts. *Planta,* 167**,** 140-145.

GROSS, S. R. & KINZY, T. G. 2005. Translation elongation factor 1A is essential for regulation of the actin cytoskeleton and cell morphology. *Nature structural & molecular biology,* 12**,** 772-778.

GROSS, S. R. & KINZY, T. G. 2007. Improper organization of the actin cytoskeleton affects protein synthesis at initiation. *Molecular and cellular biology,* 27**,** 1974-1989.

GRUNWALD, M. S., PIRES, A. S., ZANOTTO-FILHO, A., GASPAROTTO, J., GELAIN, D. P., DEMARTINI, D. R., SCHÖLER, C. M., DE BITTENCOURT JR, P. I. H. & MOREIRA, J. C. F. 2014. The oxidation of HSP70 is associated with functional impairment and lack of stimulatory capacity. *Cell Stress and Chaperones,* 19**,** 913-925.

GRZECHOWIAK, M., SIKORSKI, M. & JASKOLSKI, M. 2013. Inorganic pyrophosphatase (PPase) from a higher plant. *BioTechnologia. Journal of Biotechnology Computational Biology and Bionanotechnology,* 94.

GU, T., MAZZURCO, M., SULAMAN, W., MATIAS, D. D. & GORING, D. R. 1998. Binding of an arm repeat protein to the kinase domain of the S-locus receptor kinase. *Proceedings of the National Academy of Sciences,* 95**,** 382-387.

GU, Y.-M., JIN, Y.-H., CHOI, J.-K., BAEK, K.-H., YEO, C.-Y. & LEE, K.-Y. 2006. Protein kinase A phosphorylates and regulates dimerization of 14-3-3ζ. *FEBS letters,* 580**,** 305-310.

GU, Y., FU, Y., DOWD, P., LI, S., VERNOUD, V., GILROY, S. & YANG, Z. 2005. A Rho family GTPase controls actin dynamics and tip growth via two counteracting downstream pathways in pollen tubes. *The Journal of cell biology,* 169**,** 127-138.

GUAN, C., JIN, C., JI, J., WANG, G. & LI, X. 2015. LcBiP, a endoplasmic reticulum chaperone binding protein gene from *Lycium chinense*, confers cadmium tolerance in transgenic tobacco. *Biotechnology progress,* 31**,** 358-368.

GUPTA, K. J., FERNIE, A. R., KAISER, W. M. & VAN DONGEN, J. T. 2011. On the origins of nitric oxide. *Trends in plant science,* 16**,** 160-168.

HAFFANI, Y., GAUDE, T., COCK, J. & GORING, D. 2004. Antisense suppression of thioredoxinhmRNA in *Brassica napus* cv. *Plant molecular biology,* 55**,** 619-630.

HALLIWELL, B. 2006. Reactive species and antioxidants. Redox biology is a fundamental theme of aerobic life. *Plant Physiology,* 141**,** 312-322.

HALLIWELL, B. & GUTTERIDGE, J. M. 1999. Free radicals in biology and medicine, Oxford university press Oxford.

HAN, J., DANELL, R. M., PATEL, J. R., GUMEROV, D. R., SCARLETT, C. O., SPEIR, J. P., PARKER, C. E., RUSYN, I., ZEISEL, S. & BORCHERS, C. H. 2008. Towards high-throughput metabolomics using ultrahigh-field Fourier transform ion cyclotron resonance mass spectrometry. *Metabolomics,* 4**,** 128-140.

HAO, H., FAN, L., CHEN, T., LI, R., LI, X., HE, Q., BOTELLA, M. A. & LIN, J. 2014. Clathrin and membrane microdomains cooperatively regulate RbohD dynamics and activity in Arabidopsis. *The Plant Cell,* 26**,** 1729-1745.

HARA-NISHIMURA, I. & HATSUGAI, N. 2011. The role of vacuole in plant cell death. *Cell Death & Differentiation,* 18**,** 1298-1304.

HARA, M. R., AGRAWAL, N., KIM, S. F., CASCIO, M. B., FUJIMURO, M., OZEKI, Y., TAKAHASHI, M., CHEAH, J. H., TANKOU, S. K. & HESTER, L. D. 2005. S-nitrosylated GAPDH initiates apoptotic cell death by nuclear translocation following Siah1 binding. *Nature cell biology,* 7**,** 665-674.

HARDING, H. P., ZHANG, Y., ZENG, H., NOVOA, I., LU, P. D., CALFON, M., SADRI, N., YUN, C., POPKO, B. & PAULES, R. 2003. An integrated stress response regulates amino acid metabolism and resistance to oxidative stress. *Molecular cell,* 11**,** 619-633.

HARPER, J. F., BRETON, G. & HARMON, A. 2004. Decoding Ca^{2+} signals through plant protein kinases. *Annu. Rev. Plant Biol.,* 55**,** 263-288.

HE, F., HENDRICKSON, C. L. & MARSHALL, A. G. 2001. Baseline mass resolution of peptide isobars: A record for molecular mass resolution. *Analytical chemistry,* 73**,** 647-650.

HE, P., SHAN, L. & SHEEN, J. 2007. Elicitation and suppression of microbe-associated molecular pattern-triggered immunity in plant–microbe interactions. *Cellular microbiology,* 9**,** 1385-1396.

HEIKINHEIMO, P., LEHTONEN, J., BAYKOV, A., LAHTI, R., COOPERMAN, B. S. & GOLDMAN, A. 1996a. The structural basis for pyrophosphatase catalysis. *Structure,* 4**,** 1491-1508.

HEIKINHEIMO, P., POHJANJOKI, P., HELMINEN, A., TASANEN, M., COOPERMAN, B. S., GOLDMAN, A., BAYKOV, A. & LAHTI, R. 1996b. A Site-Directed Mutagenesis Study of *Saccharomyces cerevisiae* Pyrophosphatase. *European journal of biochemistry,* 239**,** 138-143.

HEIKINHEIMO, P., TUOMINEN, V., AHONEN, A.-K., TEPLYAKOV, A., COOPERMAN, B., BAYKOV, A., LAHTI, R. & GOLDMAN, A. 2001. Toward a quantum-mechanical description of metal-assisted phosphoryl transfer in pyrophosphatase. *Proceedings of the National Academy of Sciences,* 98**,** 3121-3126.

HEPLER, P. K., VIDALI, L. & CHEUNG, A. Y. 2001. Polarized cell growth in higher plants. *Annual review of cell and developmental biology,* 17**,** 159-187.

HESLOP-HARRISON, J. & HESLOP-HARRISON, Y. 1990. Dynamic aspects of apical zonation in the angiosperm pollen tube. *Sexual Plant Reproduction,* 3**,** 187-194.

HESLOP-HARRISON, J. & MACKENZIE, A. 1967. Autoradiography of soluble [2-14C] thymidine derivatives during meiosis and microsporogenesis in *Lilium* anthers. *Journal of cell science,* 2**,** 387-400.

HESLOP HARRISON, J. 1987. Pollen germination and pollen-tube growth. *Intn. Rev. Cytol,* 107**,** 1-78.

HESS, D. T., MATSUMOTO, A., KIM, S.-O., MARSHALL, H. E. & STAMLER, J. S. 2005. Protein S-nitrosylation: purview and parameters. *Nature Reviews Molecular Cell Biology,* 6**,** 150-166.

HESS, D. T. & STAMLER, J. S. 2012. Regulation by S-nitrosylation of protein post-translational modification. *Journal of Biological Chemistry,* 287**,** 4411-4418.

HIRST, J. & ROBINSON, M. S. 1998. Clathrin and adaptors. *Biochimica et Biophysica Acta (BBA)-Molecular Cell Research,* 1404**,** 173-193.

HISCOCK, S. J. & ALLEN, A. M. 2008. Diverse cell signalling pathways regulate pollen-stigma interactions: the search for consensus. *New phytologist,* 179**,** 286-317.

HISCOCK, S. J. & MCINNIS, S. M. 2003. Pollen recognition and rejection during the sporophytic self-incompatibility response: Brassica and beyond. *Trends in plant science,* 8**,** 606-613.

HOE, H.-S., KIM, H.-K. & KWON, S.-T. 2001. Expression in *Escherichia coli* of the thermostable inorganic pyrophosphatase from the Aquifex aeolicus and purification and characterization of the recombinant enzyme. *Protein expression and purification,* 23**,** 242-248.

HOEBERICHTS, F. A. & WOLTERING, E. J. 2003. Multiple mediators of plant programmed cell death: Interplay of conserved cell death mechanisms and plant-specific regulators. *Bioessays,* 25**,** 47-57.

HÖHNE, W. & HEITMANN, P. 1973. Tripolyphosphate as a substrate of the inorganic pyrophosphatase from baker's yeast; the role of divalent metal ions. *Acta biologica et medica Germanica,* 33**,** 1-14.

HOLDAWAY-CLARKE, T. L., FEIJÓ, J. A., HACKETT, G. R., KUNKEL, J. G. & HEPLER, P. K. 1997. Pollen tube growth and the intracellular cytosolic calcium gradient oscillate in phase while extracellular calcium influx is delayed. *The Plant Cell Online,* 9**,** 1999-2010.

HOLDAWAY-CLARKE, T. L., WEDDLE, N. M., KIM, S., ROBI, A., PARRIS, C., KUNKEL, J. G. & HEPLER, P. K. 2003. Effect of extracellular calcium, pH and borate on growth oscillations in *Lilium formosanum* pollen tubes. *Journal of Experimental Botany,* 54**,** 65-72.

HOLMES, K. C., POPP, D., GEBHARD, W. & KABSCH, W. 1990. Atomic model of the actin filament. *Nature,* 347**,** 44-49.

HOLTGREFE, S., GOHLKE, J., STARMANN, J., DRUCE, S., KLOCKE, S., ALTMANN, B., WOJTERA, J., LINDERMAYR, C. & SCHEIBE, R. 2008.

Regulation of plant cytosolic glyceraldehyde 3-phosphate dehydrogenase isoforms by thiol modifications. *Physiologia plantarum,* 133**,** 211-228.

HONTS, J. E., SANDROCK, T. S., BROWER, S. M., O'DELL, J. L. & ADAMS, A. 1994. Actin mutations that show suppression with fimbrin mutations identify a likely fimbrin-binding site on actin. *The Journal of cell biology,* 126**,** 413-422.

HUA, Z.-H., FIELDS, A. & KAO, T.-H. 2008. Biochemical models for S-RNase-based self-incompatibility. *Molecular plant,* 1**,** 575-585.

HUA, Z. & KAO, T.-H. 2006. Identification and characterization of components of a putative Petunia S-locus F-box–containing E3 ligase complex involved in S-RNase–based self-incompatibility. *The Plant Cell Online,* 18**,** 2531-2553.

HWANG, N., YIM, S., KIM, Y., JEONG, J., SONG, E., LEE, Y., LEE, J., CHOI, S. & LEE, K. 2009. Oxidative modifications of glyceraldehyde-3-phosphate dehydrogenase play a key role in its multiple cellular functions. *Biochem. J,* 423**,** 253-264.

IGIC, B. & KOHN, J. R. 2006. The distribution of plant mating systems: study bias against obligately outcrossing species. *Evolution,* 60**,** 1098-1103.

IVANOV, R., FOBIS-LOISY, I. & GAUDE, T. 2010. When no means no: guide to Brassicaceae self-incompatibility. *Trends in plant science,* 15**,** 387-394.

IVANOV, R. & GAUDE, T. 2009. Endocytosis and endosomal regulation of the S-receptor kinase during the self-incompatibility response in *Brassica oleracea*. *The Plant Cell Online,* 21**,** 2107-2117.

IWANO, M. & TAKAYAMA, S. 2012. Self/non-self discrimination in angiosperm self-incompatibility. *Current opinion in plant biology,* 15**,** 78-83.

JACOB, J.-L., PREVOT, J.-C., CLEMENT-VIDAL, A. & D'AUZAC, J. 1989. Inorganic pyrophosphate metabolism in *Hevea brasiliensis* latex. Characteristics of cytosolic alkaline inorganic pyrophosphatase. *Plant physiology and biochemistry,* 27**,** 355-364.

JAFFREY, S. R. & SNYDER, S. H. 2001. The biotin switch method for the detection of S-nitrosylated proteins. *Science Signaling,* 2001**,** pl1.

JAJIC, I., SARNA, T. & STRZALKA, K. 2015. Senescence, Stress, and Reactive Oxygen Species. *Plants,* 4**,** 393-411.

JELITTO, T., SONNEWALD, U., WILLMITZER, L., HAJIREZEAI, M. & STITT, M. 1992. Inorganic pyrophosphate content and metabolites in potato

and tobacco plants expressing *E. coli* pyrophosphatase in their cytosol. *Planta,* 188**,** 238-244.

JEON, S.-J. & ISHIKAWA, K. 2005. Characterization of the Family I inorganic pyrophosphatase from *Pyrococcus horikoshii* OT3. *Archaea,* 1**,** 385-389.

JIANG, X., GAO, Y., ZHOU, H., CHEN, J., WU, J. & ZHANG, S. 2014. Apoplastic calmodulin promotes self-incompatibility pollen tube growth by enhancing calcium influx and reactive oxygen species concentration in Pyrus pyrifolia. *Plant cell reports,* 33**,** 255-263.

JIN, J., SMITH, F. D., STARK, C., WELLS, C. D., FAWCETT, J. P., KULKARNI, S., METALNIKOV, P., O'DONNELL, P., TAYLOR, P. & TAYLOR, L. 2004. Proteomic, functional, and domain-based analysis of in vivo 14-3-3 binding proteins involved in cytoskeletal regulation and cellular organization. *Current Biology,* 14**,** 1436-1450.

JOB, C., RAJJOU, L., LOVIGNY, Y., BELGHAZI, M. & JOB, D. 2005. Patterns of protein oxidation in Arabidopsis seeds and during germination. *Plant Physiology,* 138**,** 790-802.

JONES, J. D. & DANGL, J. L. 2006. The plant immune system. *nature,* 444**,** 323-329.

JOO, J. H., BAE, Y. S. & LEE, J. S. 2001. Role of auxin-induced reactive oxygen species in root gravitropism. *Plant Physiology,* 126**,** 1055-1060.

JORDAN, N. D., FRANKLIN, F. C. H. & FRANKLIN-TONG, V. E. 2000. Evidence for DNA fragmentation triggered in the self-incompatibility response in pollen of *Papaver rhoeas*. *The Plant Journal,* 23**,** 471-479.

JOSSE, J. 1966. Constitutive Inorganic Pyrophosphatase of *Escherichia coli* II. Nature and binding of active substrate and the role of magnesium. *Journal of Biological Chemistry,* 241**,** 1948-1954.

KACHROO, A., SCHOPFER, C. R., NASRALLAH, M. E. & NASRALLAH, J. B. 2001. Allele-specific receptor-ligand interactions in Brassica self-incompatibility. *Science Signaling,* 293**,** 1824.

KANKARE, J., SALMINEN, T., LAHTI, R., COOPERMAN, B., BAYKOV, A. & GOLDMAN, A. 1996. Sructure of *Escherichia coli* Inorganic Pyrophosphatase at 2.2 Å Resolution. *Acta Crystallographica Section D: Biological Crystallography,* 52**,** 551-563.

KARUPPANAPANDIAN, T., MOON, J.-C., KIM, C., MANOHARAN, K. & KIM, W. 2011. Reactive oxygen species in plants: their generation, signal transduction, and scavenging mechanisms.

KAYA, H., NAKAJIMA, R., IWANO, M., KANAOKA, M. M., KIMURA, S., TAKEDA, S., KAWARAZAKI, T., SENZAKI, E., HAMAMURA, Y. & HIGASHIYAMA, T. 2014a. Ca^{2+}-activated reactive oxygen species production by Arabidopsis RbohH and RbohJ is essential for proper pollen tube tip growth. *The Plant Cell Online,* 26**,** 1069-1080.

KAYA, H., NAKAJIMA, R., IWANO, M., KANAOKA, M. M., KIMURA, S., TAKEDA, S., KAWARAZAKI, T., SENZAKI, E., HAMAMURA, Y. & HIGASHIYAMA, T. 2014b. Ca^{2+}-activated reactive oxygen species production by *Arabidopsis RbohH* and *RbohJ* is essential for proper pollen tube tip growth. *The Plant Cell,* 26**,** 1069-1080.

KERSCHER, O., FELBERBAUM, R. & HOCHSTRASSER, M. 2006. Modification of proteins by ubiquitin and ubiquitin-like proteins. *Annu. Rev. Cell Dev. Biol.,* 22**,** 159-180.

KIM, J. H., WOO, H. R., KIM, J., LIM, P. O., LEE, I. C., CHOI, S. H., HWANG, D. & NAM, H. G. 2009. Trifurcate feed-forward regulation of age-dependent cell death involving miR164 in Arabidopsis. *Science,* 323**,** 1053-1057.

KIM, S. T., ZHANG, K., DONG, J. & LORD, E. M. 2006. Exogenous free ubiquitin enhances lily pollen tube adhesion to an in vitro stylar matrix and may facilitate endocytosis of SCA. *Plant Physiology,* 142**,** 1397-1411.

KIRCHHAUSEN, T. & HARRISON, S. C. 1984. Structural domains of clathrin heavy chains. *The Journal of cell biology,* 99**,** 1725-1734.

KLEMME, B. & JACOBI, G. 1974. Separation and characterization of two inorganic pyrophosphatases from spinach leaves. *Planta,* 120**,** 147-153.

KLEMME, J. 1976. Regulation of intracellular pyrophosphatase-activity and conservation of the phosphoanhydride-energy of inorganic pyrophosphate in microbial metabolism. *Zeitschrift fur Naturforschung. Section C: Biosciences,* 31**,** 544.

KNOWLES, J. R. 1980. Enzyme-catalyzed phosphoryl transfer reactions. *Annual review of biochemistry,* 49**,** 877-919.

KNUEHL, C., CHEN, C. Y., MANALO, V., HWANG, P. K., OTA, N. & BRODSKY, F. M. 2006. Novel binding sites on clathrin and adaptors regulate distinct aspects of coat assembly. *Traffic,* 7**,** 1688-1700.

KOBAYASHI, I., KOBAYASHI, Y. & HARDHAM, A. R. 1994. Dynamic reorganization of microtubules and microfilaments in flax cells during the resistance response to flax rust infection. *Planta,* 195**,** 237-247.

KOBAYASHI, Y., KOBAYASHI, I., FUNAKI, Y., FUJIMOTO, S., TAKEMOTO, T. & KUNOH, H. 1997a. Dynamic reorganization of microfilaments and

microtubules is necessary for the expression of non-host resistance in barley coleoptile cells. *The Plant Journal,* 11**,** 525-537.

KOBAYASHI, Y., YAMADA, M., KOBAYASHI, I. & KUNOH, H. 1997b. Actin microfilaments are required for the expression of nonhost resistance in higher plants. *Plant and cell physiology,* 38**,** 725-733.

KOMORI, R., AMANO, Y., OGAWA-OHNISHI, M. & MATSUBAYASHI, Y. 2009. Identification of tyrosylprotein sulfotransferase in Arabidopsis. *Proceedings of the National Academy of Sciences,* 106**,** 15067-15072.

KOPYRA, M. & GWÓŹDŹ, E. A. 2003. Nitric oxide stimulates seed germination and counteracts the inhibitory effect of heavy metals and salinity on root growth of Lupinus luteus. *Plant Physiology and Biochemistry,* 41**,** 1011-1017.

KORN, E. D., CARLIER, M.-F. & PANTALONI, D. 1987. Actin polymerization and ATP hydrolysis. *Science,* 238**,** 638-644.

KORNBERG, A. 1962. On the metabolic significance of phosphorolytic and pyrophosphorolytic reactions. *Horizons in biochemistry***,** 251-264.

KOVAR, D. R., STAIGER, C. J., WEAVER, E. A. & MCCURDY, D. W. 2000. AtFim1 is an actin filament crosslinking protein from *Arabidopsis thaliana*. *The Plant Journal,* 24**,** 625-636.

KRICHEVSKY, A., KOZLOVSKY, S. V., TIAN, G.-W., CHEN, M.-H., ZALTSMAN, A. & CITOVSKY, V. 2007. How pollen tubes grow. *Developmental biology,* 303**,** 405-420.

KROEMER, G., GALLUZZI, L., VANDENABEELE, P., ABRAMS, J., ALNEMRI, E., BAEHRECKE, E., BLAGOSKLONNY, M., EL-DEIRY, W., GOLSTEIN, P. & GREEN, D. 2009. Classification of cell death: recommendations of the Nomenclature Committee on Cell Death 2009. *Cell Death & Differentiation,* 16**,** 3-11.

KROPF, D. L., BISGROVE, S. R. & HABLE, W. E. 1998. Cytoskeletal control of polar growth in plant cells. *Current opinion in cell biology,* 10**,** 117-122.

KUBO, K.-I., ENTANI, T., TAKARA, A., WANG, N., FIELDS, A. M., HUA, Z., TOYODA, M., KAWASHIMA, S.-I., ANDO, T. & ISOGAI, A. 2010. Collaborative non-self recognition system in S-RNase–based self-incompatibility. *Science,* 330**,** 796-799.

KUMAR, S. 2007. Caspase function in programmed cell death. *Cell Death & Differentiation,* 14**,** 32-43.

KURILOVA, S., BOGDANOVA, A., NAZAROVA, T. & AVAEVA, S. 1984. Changes in the *E. coli* inorganic pyrophosphatase activity on interaction

with magnesium, zinc, calcium and fluoride ions. *Bioorganicheskaya Khimiya,* 10**,** 1153-1160.

KURILOVA, S., NAZAROVA, T. & AVAEVA, S. 1983. Substrate hydrolysis by inorganic pyrophosphatase from *E. coli*. *Bioorganic Chemistry,* 9**,** 1032-1039.

LAEMMLI, U. K. 1970. Cleavage of structural proteins during the assembly of the head of bacteriophage T4. *Nature,* 227**,** 680-685.

LAI, Z., MA, W., HAN, B., LIANG, L., ZHANG, Y., HONG, G. & XUE, Y. 2002. An F-box gene linked to the self-incompatibility (S) locus of *Antirrhinum* is expressed specifically in pollen and tapetum. *Plant molecular biology,* 50**,** 29-41.

LAM, E. 2004. Controlled cell death, plant survival and development. *Nature Reviews Molecular Cell Biology,* 5**,** 305-315.

LASSING, I., SCHMITZBERGER, F., BJÖRNSTEDT, M., HOLMGREN, A., NORDLUND, P., SCHUTT, C. E. & LINDBERG, U. 2007. Molecular and structural basis for redox regulation of β-actin. *Journal of molecular biology,* 370**,** 331-348.

LEASE, K. A. & WALKER, J. C. 2006. The Arabidopsis unannotated secreted peptide database, a resource for plant peptidomics. *Plant Physiology,* 142**,** 831-838.

LEBART, M., MEJEAN, C., BOYER, M., ROUSTAN, C. & BENYAMIN, Y. 1990. Localization of a new α-actinin binding site in the COOH—terminal part of actin sequence. *Biochemical and biophysical research communications,* 173**,** 120-126.

LECOURIEUX, D., MAZARS, C., PAULY, N., RANJEVA, R. & PUGIN, A. 2002. Analysis and effects of cytosolic free calcium increases in response to elicitors in *Nicotiana plumbaginifolia* cells. *The Plant Cell Online,* 14**,** 2627-2641.

LEE, H.-S., HUANG, S. & KAO, T.-H. 1994. S proteins control rejection of incompatible pollen in Petunia inflata.

LEE, S. Y., JUNG, H., CHUNG, S. J., PARK, B. C. & PARK, S. G. 2012. Glyceraldehyde-3-Phosphate, a Glycolytic Intermediate, Prevents Cells from poptosis by Lowering S-Nitrosylation of Glyceraldehyde-3-Phosphate Dehydrogenase. *Journal of microbiology and biotechnology,* 22**,** 571-573.

LEITNER, M., VANDELLE, E., GAUPELS, F., BELLIN, D. & DELLEDONNE, M. 2009. NO signals in the haze: nitric oxide signalling in plant defence. *Current opinion in plant biology,* 12**,** 451-458.

LEMMON, S. K. & TRAUB, L. M. 2012. Getting in touch with the clathrin terminal domain. *Traffic,* 13**,** 511-519.

LEVINE, A., PENNELL, R. I., ALVAREZ, M. E., PALMER, R. & LAMB, C. 1996. Calcium-mediated apoptosis in a plant hypersensitive disease resistance response. *Current Biology,* 6**,** 427-437.

LEVINE, A., TENHAKEN, R., DIXON, R. & LAMB, C. 1994. H_2O_2 from the oxidative burst orchestrates the plant hypersensitive disease resistance response. *Cell,* 79**,** 583-593.

LI, S., ŠAMAJ, J. & FRANKLIN-TONG, V. E. 2007. A mitogen-activated protein kinase signals to programmed cell death induced by self-incompatibility in *Papaver* pollen. *Plant Physiology,* 145**,** 236-245.

LIANG, P. & MACRAE, T. H. 1997. Molecular chaperones and the cytoskeleton. *Journal of cell science,* 110**,** 1431-1440.

LIANG, S., YU, Y., YANG, P., GU, S., XUE, Y. & CHEN, X. 2009. Analysis of the protein complex associated with 14-3-3 epsilon by a deuterated-leucine labeling quantitative proteomics strategy. *Journal of Chromatography B,* 877**,** 627-634.

LIM, P. O., KIM, H. J. & GIL NAM, H. 2007. Leaf senescence. *Annu. Rev. Plant Biol.,* 58**,** 115-136.

LIN, A., WANG, Y., TANG, J., XUE, P., LI, C., LIU, L., HU, B., YANG, F., LOAKE, G. J. & CHU, C. 2012. Nitric oxide and protein S-nitrosylation are integral to hydrogen peroxide-induced leaf cell death in rice. *Plant Physiology,* 158**,** 451-464.

LIN, Z. 2015. *Functional transfer of the Papaver SI system into self-compatible A. thaliana and investigating the role of the proteasome in the Papaver SI response* Doctor of Philosophy, University of Birmingham.

LINCOLN, J. E., RICHAEL, C., OVERDUIN, B., SMITH, K., BOSTOCK, R. & GILCHRIST, D. G. 2002. Expression of the antiapoptotic baculovirus p35 gene in tomato blocks programmed cell death and provides broad-spectrum resistance to disease. *Proceedings of the National Academy of Sciences,* 99**,** 15217-15221.

LIND, J. L., BÖNIG, I., CLARKE, A. E. & ANDERSON, M. A. 1996. A style-specific 120-kDa glycoprotein enters pollen tubes of *Nicotiana alata* in vivo. *Sexual Plant Reproduction,* 9**,** 75-86.

LINDERMAYR, C., SAALBACH, G. & DURNER, J. 2005. Proteomic identification of S-nitrosylated proteins in *Arabidopsis*. *Plant Physiology,* 137**,** 921-930.

LINHART, Y. 2014. Plant Pollination and Dispersal. *Ecology and the Environment.* Springer.

LIU, G., EDMONDS, B. T. & CONDEELIS, J. 1996a. pH, EF-1α and the cytoskeleton. *Trends in cell biology,* 6**,** 168-171.

LIU, G., GRANT, W. M., PERSKY, D., LATHAM, V. M., SINGER, R. H. & CONDEELIS, J. 2002. Interactions of elongation factor 1α with F-actin and β-actin mRNA: implications for anchoring mRNA in cell protrusions. *Molecular biology of the cell,* 13**,** 579-592.

LIU, G., TANG, J., EDMONDS, B. T., MURRAY, J., LEVIN, S. & CONDEELIS, J. 1996b. F-actin sequesters elongation factor 1alpha from interaction with aminoacyl-tRNA in a pH-dependent reaction. *The Journal of cell biology,* 135**,** 953-963.

LOFTUS, T. M., NGUYEN, Y. H. & STANBRIDGE, E. J. 1997. The QM protein associates with ribosomes in the rough endoplasmic reticulum. *Biochemistry,* 36**,** 8224-8230.

LOMBARDO, M. C., GRAZIANO, M., POLACCO, J. C. & LAMATTINA, L. 2006. Nitric oxide functions as a positive regulator of root hair development. *Plant signaling & behavior,* 1**,** 28-33.

LOVY-WHEELER, A., KUNKEL, J. G., ALLWOOD, E. G., HUSSEY, P. J. & HEPLER, P. K. 2006. Oscillatory increases in alkalinity anticipate growth and may regulate actin dynamics in pollen tubes of lily. *The Plant Cell Online,* 18**,** 2182-2193.

LUNDIN, M., BALTSCHEFFSKY, H. & RONNE, H. 1991. Yeast *PPA2* gene encodes a mitochondrial inorganic pyrophosphatase that is essential for mitochondrial function. *Journal of Biological Chemistry,* 266**,** 12168-12172.

LUU, D.-T., QIN, X., MORSE, D. & CAPPADOCIA, M. 2000. S-RNase uptake by compatible pollen tubes in gametophytic self-incompatibility. *Nature,* 407**,** 649-651.

LYNCH, M. 1991. The genetic interpretation of inbreeding depression and outbreeding depression. *Evolution***,** 622-629.

MA, Y. & HENDERSHOT, L. M. 2004. ER chaperone functions during normal and stress conditions. *Journal of chemical neuroanatomy,* 28**,** 51-65.

MALHÓ, R. 2006. *The pollen tube: a cellular and molecular perspective*, Springer Berlin.

MALHO, R., READ, N. D., PAIS, M. S. & TREWAVAS, A. J. 1994. Role of cytosolic free calcium in the reorientation of pollen tube growth. *The Plant Journal,* 5**,** 331-341.

MALIK, S. I., HUSSAIN, A., YUN, B.-W., SPOEL, S. H. & LOAKE, G. J. 2011. GSNOR-mediated de-nitrosylation in the plant defence response. *Plant Science,* 181**,** 540-544.

MANNICK, J. B. & SCHONHOFF, C. M. 2004. Review NO Means No and Yes: Regulation of Cell Signaling by Protein Nitrosylation. *Free radical research,* 38**,** 1-7.

MASLOWSKI, P., MASLOWSKA, H. & KOWALCZYK, S. 1977. Subcellular distribution and properties of alkaline inorganic pyrophosphatase of maize leaves. *Acta Biochim. Pol,* 24**,** 117-126.

MATSUBAYASHI, Y. 2011. Post-translational modifications in secreted peptide hormones in plants. *Plant and cell physiology,* 52**,** 5-13.

MATSUYAMA, S. & REED, J. 2000. Mitochondria-dependent apoptosis and cellular pH regulation. *Cell death and differentiation,* 7**,** 1155-1165.

MAZZURCO, M., SULAMAN, W., ELINA, H., COCK, J. M. & GORING, D. R. 2001. Further analysis of the interactions between the Brassica S receptor kinase and three interacting proteins (ARC1, THL1 and THL2) in the yeast two-hybrid system. *Plant molecular biology,* 45**,** 365-376.

MCCLURE, B. 2006. New views of S-RNase-based self-incompatibility. *Current opinion in plant biology,* 9**,** 639-646.

MCCLURE, B. 2009. Darwin's foundation for investigating self-incompatibility and the progress toward a physiological model for S-RNase-based SI. *Journal of experimental botany,* 60**,** 1069-1081.

MCCLURE, B., CRUZ-GARCÍA, F. & ROMERO, C. 2011. Compatibility and incompatibility in S-RNase-based systems. *Annals of botany,* 108**,** 647-658.

MCCLURE, B., MOU, B., CANEVASCINI, S. & BERNATZKY, R. 1999. A small asparagine-rich protein required for S-allele-specific pollen rejection in *Nicotiana*. *Proceedings of the National Academy of Sciences,* 96**,** 13548-13553.

MCCLURE, B. A., HARING, V., EBERT, P. R., ANDERSON, M. A., SIMPSON, R. J., SAKIYAMA, F. & CLARKE, A. E. 1989. Style self-incompatibility gene products of *Nicotlana alata* are ribonucleases. *Nature,* 342**,** 955-957.

MCCORMICK, S. 1993. Male gametophyte development. *The Plant Cell,* 5**,** 1265.

MCCURDY, D. W., KOVAR, D. R. & STAIGER, C. J. 2001. Actin and actin-binding proteins in higher plants. *Protoplasma,* 215**,** 89-104.

MCGOUGH, A., WAY, M. & DEROSIER, D. 1994. Determination of the alpha-actinin-binding site on actin filaments by cryoelectron microscopy and image analysis. *The Journal of cell biology,* 126**,** 433-443.

MCKENNA, S. T., VIDALI, L. & HEPLER, P. K. 2004. Profilin inhibits pollen tube growth through actin-binding, but not poly-L-proline-binding. *Planta,* 218**,** 906-915.

MCLAUGHLIN, P., GOOCH, J., MANNHERZ, H.-G. & WEEDS, A. 1993. Structure of gelsolin segment 1-actin complex and the mechanism of filament severing.

MCMAHON, H. T. & BOUCROT, E. 2011. Molecular mechanism and physiological functions of clathrin-mediated endocytosis. *Nature reviews Molecular cell biology,* 12**,** 517-533.

MEAGHER, R. B. & WILLIAMSON, R. E. 1994. 38 The Plant Cytoskeleton. *Cold Spring Harbor Monograph Archive,* 27**,** 1049-1084.

MI-ICHI, F., YOUSUF, M. A., NAKADA-TSUKUI, K. & NOZAKI, T. 2009. Mitosomes in *Entamoeba histolytica* contain a sulfate activation pathway. *Proceedings of the National Academy of Sciences,* 106**,** 21731-21736.

MIACZYNSKA, M., PELKMANS, L. & ZERIAL, M. 2004. Not just a sink: endosomes in control of signal transduction. *Current opinion in cell biology,* 16**,** 400-406.

MILZANI, A., ROSSI, R., DI SIMPLICIO, P., GIUSTARINI, D., COLOMBO, R. & DALLEDONNE, I. 2000. The oxidation produced by hydrogen peroxide on Ca-ATP-G-actin. *Protein Science,* 9**,** 1774-1782.

MIMURA, N. & ASANO, A. 1987. Further characterization of a conserved actin-binding 27-kDa fragment of actinogelin and alpha-actinins and mapping of their binding sites on the actin molecule by chemical cross-linking. *Journal of Biological Chemistry,* 262**,** 4717-4723.

MITTLER, R. 2002. Oxidative stress, antioxidants and stress tolerance. *Trends in plant science,* 7**,** 405-410.

MITTLER, R. & LAM, E. 1996. Sacrifice in the face of foes: pathogen-induced programmed cell death in plants. *Trends in microbiology,* 4**,** 10-15.

MITTLER, R., VANDERAUWERA, S., GOLLERY, M. & VAN BREUSEGEM, F. 2004. Reactive oxygen gene network of plants. *Trends in plant science,* 9**,** 490-498.

MOLDOVAN, L., MYTHREYE, K., GOLDSCHMIDT-CLERMONT, P. J. & SATTERWHITE, L. L. 2006. Reactive oxygen species in vascular

endothelial cell motility. Roles of NAD (P) H oxidase and Rac1. *Cardiovascular research,* 71**,** 236-246.

MØLLER, I. M., JENSEN, P. E. & HANSSON, A. 2007. Oxidative modifications to cellular components in plants. *Annu. Rev. Plant Biol.,* 58**,** 459-481.

MOREAU, M., LINDERMAYR, C., DURNER, J. & KLESSIG, D. F. 2010. NO synthesis and signaling in plants–where do we stand? *Physiologia Plantarum,* 138**,** 372-383.

MORIMOTO, R., TISSIERES, A. & GEORGOPOULOS, C. 1991. Stress Proteins in Biology and Medicine Cold Spring Harbor Lab. *Press, Plainview*.

MORIMOTO, R. I., TISSIÈRES, A. & GEORGOPOULOS, C. 1994. *The biology of heat shock proteins and molecular chaperones*, Cold Spring Harbor Laboratory Press New York:.

MOSCATELLI, A., CIAMPOLINI, F., RODIGHIERO, S., ONELLI, E., CRESTI, M., SANTO, N. & IDILLI, A. 2007. Distinct endocytic pathways identified in tobacco pollen tubes using charged nanogold. *Journal of cell science,* 120**,** 3804-3819.

MUÑOZ-BERTOMEU, J., CASCALES-MIÑANA, B., IRLES-SEGURA, A., MATEU, I., NUNES-NESI, A., FERNIE, A. R., SEGURA, J. & ROS, R. 2010. The plastidial glyceraldehyde-3-phosphate dehydrogenase is critical for viable pollen development in Arabidopsis. *Plant physiology,* 152**,** 1830-1841.

MUR, L. A., KENTON, P., LLOYD, A. J., OUGHAM, H. & PRATS, E. 2008. The hypersensitive response; the centenary is upon us but how much do we know? *Journal of experimental Botany,* 59**,** 501-520.

MURASE, K., SHIBA, H., IWANO, M., CHE, F.-S., WATANABE, M., ISOGAI, A. & TAKAYAMA, S. 2004. A membrane-anchored protein kinase involved in Brassica self-incompatibility signaling. *Science Signaling,* 303**,** 1516.

MURFETT, J., ATHERTON, T. L., MOU, B., GASSERT, C. S. & MCCLURE, B. A. 1994. S-RNase expressed in transgenic *Nicotiana causes* S-allele-specific pollen rejection.

NASRALLAH, M. E., LIU, P. & NASRALLAH, J. B. 2002. Generation of self-incompatible *Arabidopsis thaliana* by transfer of two S locus genes from A. lyrata. *Science,* 297**,** 247-249.

NAVARRO-DE LA SANCHA, E., COELLO-COUTINO, M. P., VALENCIA-TURCOTTE, L. G., HERNÁNDEZ-DOMÍNGUEZ, E. E., TREJO-YEPES, G. & RODRÍGUEZ-SOTRES, R. 2007. Characterization of two

soluble inorganic pyrophosphatases from *Arabidopsis thaliana*. *Plant science,* 172**,** 796-807.

NEILL, S. J., DESIKAN, R. & HANCOCK, J. T. 2003. Nitric oxide signalling in plants. *New Phytologist,* 159**,** 11-35.

NICK, P. 1999. Signals, Motors, Morphogenesis-the Cytoskeleton in Plant Development1. *Plant Biology,* 1**,** 169-179.

NIKA, J., ERICKSON, F. L. & HANNIG, E. M. 1997. Ribosomal protein L9 is the product of GRC5, a homolog of the putative tumor suppressor QM in *S. cerevisiae. Yeast,* 13**,** 1155-1166.

NIMCHUK, Z., EULGEM, T., HOLT III, B. F. & DANGL, J. L. 2003. Recognition and response in the plant immune system. *Annual review of genetics,* 37**,** 579-609.

NUSS, J. E., CHOKSI, K. B., DEFORD, J. H. & PAPACONSTANTINOU, J. 2008. Decreased enzyme activities of chaperones PDI and BiP in aged mouse livers. *Biochemical and biophysical research communications,* 365**,** 355-361.

OBARA, K., KURIYAMA, H. & FUKUDA, H. 2001. Direct evidence of active and rapid nuclear degradation triggered by vacuole rupture during programmed cell death in *Zinnia*. *Plant Physiology,* 125**,** 615-626.

OBERMEYER, G. & WEISENSEEL, M. 1991. Calcium channel blocker and calmodulin antagonists affect the gradient of free calcium ions in lily pollen tubes. *European journal of cell biology,* 56**,** 319-327.

OGASAWARA, N. 2000. Systematic function analysis of *Bacillus subtilis* genes. *Research in microbiology,* 151**,** 129-134.

OHYAMA, K., OGAWA, M. & MATSUBAYASHI, Y. 2008. Identification of a biologically active, small, secreted peptide in *Arabidopsis* by in silico gene screening, followed by LC-MS-based structure analysis. *The Plant Journal,* 55**,** 152-160.

OKAZAKI, K. & YUMURA, S. 1995. Differential association of three actin-bundling proteins with microfilaments in *Dictyostelium amoebae*. *European journal of cell biology,* 66**,** 75-81.

OKUDA, S., TSUTSUI, H., SHIINA, K., SPRUNCK, S., TAKEUCHI, H., YUI, R., KASAHARA, R. D., HAMAMURA, Y., MIZUKAMI, A. & SUSAKI, D. 2009. Defensin-like polypeptide LUREs are pollen tube attractants secreted from synergid cells. *Nature,* 458**,** 357-361.

ONELLI, E. & MOSCATELLI, A. 2013. Endocytic pathways and recycling in growing pollen tubes. *Plants,* 2**,** 211-229.

ORTEGA-GALISTEO, A. P., RODRÍGUEZ-SERRANO, M., PAZMIÑO, D. M., GUPTA, D. K., SANDALIO, L. M. & ROMERO-PUERTAS, M. C. 2012. S-Nitrosylated proteins in pea (*Pisum sativum* L.) leaf peroxisomes: changes under abiotic stress. *Journal of experimental botany,* 63**,** 2089-2103.

PANTALONI, D. & CARLIER, M.-F. 1993. How profilin promotes actin filament assembly in the presence of thymosin β4. *Cell,* 75**,** 1007-1014.

PARRADO, J., BOUGRIA, M., AYALA, A., CASTAÑO, A. & MACHADO, A. 1999. Effects of aging on the various steps of protein synthesis: fragmentation of elongation factor 2. *Free Radical Biology and Medicine,* 26**,** 362-370.

PARROTTA, L., CRESTI, M. & CAI, G. 2013. Heat-shock protein 70 binds microtubules and interacts with kinesin in tobacco pollen tubes. *Cytoskeleton,* 70**,** 522-537.

PASTORE, A., TOZZI, G., GAETA, L. M., BERTINI, E., SERAFINI, V., DI CESARE, S., BONETTO, V., CASONI, F., CARROZZO, R. & FEDERICI, G. 2003. Actin Glutathionylation Increases in Fibroblasts of Patients with Friedreich's Ataxia a potential role in the pathogenesis of the disease. *Journal of Biological Chemistry,* 278**,** 42588-42595.

PEARSE, B. 1976. Clathrin: a unique protein associated with intracellular transfer of membrane by coated vesicles. *Proceedings of the National Academy of Sciences,* 73**,** 1255-1259.

PENA, L. B., BARCIA, R. A., AZPILICUETA, C. E., MÉNDEZ, A. A. & GALLEGO, S. M. 2012. Oxidative post translational modifications of proteins related to cell cycle are involved in cadmium toxicity in wheat seedlings. *Plant science,* 196**,** 1-7.

PENNELL, R. I. & LAMB, C. 1997. Programmed cell death in plants. *The Plant Cell,* 9**,** 1157.

PERELROIZEN, I., DIDRY, D., CHRISTENSEN, H., CHUA, N.-H. & CARLIER, M.-F. 1996. Role of nucleotide exchange and hydrolysis in the function of profilin in actin assembly. *Journal of Biological Chemistry,* 271**,** 12302-12309.

PÉREZ-CASTIÑEIRA, J. R., GÓMEZ-GARCÍA, R., LÓPEZ-MARQUÉS, R. L., LOSADA, M. & SERRANO, A. 2001. Enzymatic systems of inorganic pyrophosphate bioenergetics in photosynthetic and heterotrophic protists: remnants or metabolic cornerstones? *International Microbiology,* 4**,** 135-142.

PERL, A., PERL-TREVES, R., GALILI, S., AVIV, D., SHALGI, E., MALKIN, S. & GALUN, E. 1993. Enhanced oxidative-stress defense in transgenic

potato expressing tomato Cu, Zn superoxide dismutases. *Theoretical and Applied Genetics,* 85**,** 568-576.

PICTON, J. M. & STEER, M. W. 1983. Membrane recycling and the control of secretory activity in pollen tubes. *Journal of Cell Science,* 63**,** 303-310.

PIERSON, E., MILLER, D., CALLAHAM, D., VAN AKEN, J., HACKETT, G. & HEPLER, P. 1996. Tip-localized calcium entry fluctuates during pollen tube growth. *Developmental biology,* 174**,** 160-173.

PLAXTON, W. C. 1996. The organization and regulation of plant glycolysis. *Annual review of plant biology,* 47**,** 185-214.

POLLARD, T. D. & BORISY, G. G. 2003. Cellular motility driven by assembly and disassembly of actin filaments. *Cell,* 112**,** 453-465.

POLLARD, T. D. & COOPER, J. A. 2009. Actin, a central player in cell shape and movement. *Science,* 326**,** 1208-1212.

POSTEL, S. & KEMMERLING, B. Plant systems for recognition of pathogen-associated molecular patterns. Seminars in cell & developmental biology, 2009. Elsevier, 1025-1031.

POTOCKÝ, M., JONES, M. A., BEZVODA, R., SMIRNOFF, N. & ŽÁRSKÝ, V. 2007. Reactive oxygen species produced by NADPH oxidase are involved in pollen tube growth. *New Phytologist,* 174**,** 742-751.

POULTER, N., WHEELER, M., BOSCH, M. & FRANKLIN-TONG, V. 2010. Self-incompatibility in *Papaver*: identification of the pollen *S*-determinant PrpS. *Biochemical Society Transactions,* 38**,** 588.

POULTER, N. S. 2009 *Investigating the role of the cytoskeleton and signalling in the self-incompatibility response of Papaver rhoeas.* DOCTOR OF PHILOSOPHY, University of Birmingham.

POULTER, N. S., BOSCH, M. & FRANKLIN-TONG, V. E. 2011. Proteins implicated in mediating self-incompatibility-induced alterations to the actin cytoskeleton of *Papaver* pollen. *Annals of botany,* 108**,** 659-675.

POULTER, N. S., VATOVEC, S. & FRANKLIN-TONG, V. E. 2008. Microtubules are a target for self-incompatibility signaling in *Papaver* pollen. *Plant physiology,* 146**,** 1358-1367.

PRADO, A. M., COLAÇO, R., MORENO, N., SILVA, A. C. & FEIJÓ, J. A. 2008. Targeting of pollen tubes to ovules is dependent on nitric oxide (NO) signaling. *Molecular Plant,* 1**,** 703-714.

PRADO, A. M., PORTERFIELD, D. M. & FEIJÓ, J. A. 2004. Nitric oxide is involved in growth regulation and re-orientation of pollen tubes. *Development,* 131**,** 2707-2714.

PWEE, K.-H. H., KWOK-KI 1995. Identification and characterisation of two isoforms of soluble alkaline inorganic pyrophosphatase from sugar cane leaves. *Plant physiology and biochemistry,* 33**,** 39-46.

QIAO, H., WANG, F., ZHAO, L., ZHOU, J., LAI, Z., ZHANG, Y., ROBBINS, T. P. & XUE, Y. 2004. The F-box protein AhSLF-S2 controls the pollen function of S-RNase–based self-incompatibility. *The Plant Cell Online,* 16**,** 2307-2322.

QU, G.-Q., LIU, X., ZHANG, Y.-L., YAO, D., MA, Q.-M., YANG, M.-Y., ZHU, W.-H., YU, S. & LUO, Y.-B. 2009. Evidence for programmed cell death and activation of specific caspase-like enzymes in the tomato fruit heat stress response. *Planta,* 229**,** 1269-1279.

QU, X., ZHANG, H., XIE, Y., WANG, J., CHEN, N. & HUANG, S. 2013. Arabidopsis villins promote actin turnover at pollen tube tips and facilitate the construction of actin collars. *The Plant Cell Online,* 25**,** 1803-1817.

RAFF, M. 1998. Cell suicide for beginners. *Nature,* 396**,** 119-119.

RATHORE, K. S., CORK, R. J. & ROBINSON, K. R. 1991. A cytoplasmic gradient of Ca^{2+} is correlated with the growth of lily pollen tubes. *Developmental biology,* 148**,** 612-619.

REICHLER, S. A., TORRES, J., RIVERA, A. L., CINTOLESI, V. A., CLARK, G. & ROUX, S. J. 2009. Intersection of two signalling pathways: extracellular nucleotides regulate pollen germination and pollen tube growth via nitric oxide. *Journal of experimental botany,* 60**,** 2129-2138.

REINHECKEL, T., NOACK, H., LORENZ, S., WISWEDEL, I. & AUGUSTIN, W. 1998. Comparison of protein oxidation and aldehyde formation during oxidative stress in isolated mitochondria. *Free radical research,* 29**,** 297-305.

RENTEL, M. C., LECOURIEUX, D., OUAKED, F., USHER, S. L., PETERSEN, L., OKAMOTO, H., KNIGHT, H., PECK, S. C., GRIERSON, C. S. & HIRT, H. 2004. OXI1 kinase is necessary for oxidative burst-mediated signalling in *Arabidopsis*. *Nature,* 427**,** 858-861.

RICHMOND, T. A. & SOMERVILLE, C. R. 2000. The cellulose synthase superfamily. *Plant physiology,* 124**,** 495-498.

ROBERTS, M. R., SALINAS, J. & COLLINGE, D. B. 2002. 14-3-3 proteins and the response to abiotic and biotic stress. *Plant molecular biology,* 50**,** 1031-1039.

RODINA, E., SAMYGINA, V., VOROBYEVA, N., SITNIK, T., KURILOVA, S. & NAZAROVA, T. 2009. Structural and kinetic features of family I

inorganic pyrophosphatase from *Vibrio cholerae*. *Biochemistry (Moscow),* 74**,** 734-742.

RODRÍGUEZ-SERRANO, M., PAZMIÑO, D., SPARKES, I., ROCHETTI, A., HAWES, C., ROMERO-PUERTAS, M. & SANDALIO, L. 2014. 2, 4-Dichlorophenoxyacetic acid promotes *S*-nitrosylation and oxidation of actin affecting cytoskeleton and peroxisomal dynamics. *Journal of experimental botany***,** eru237.

ROMERO-PUERTAS, M. & DELLEDONNE, M. 2003. Nitric Oxide Signaling in Plant-Pathogen Interactions. *IUBMB life,* 55**,** 579-583.

ROMERO-PUERTAS, M. C., CAMPOSTRINI, N., MATTÈ, A., RIGHETTI, P. G., PERAZZOLLI, M., ZOLLA, L., ROEPSTORFF, P. & DELLEDONNE, M. 2008. Proteomic analysis of S-nitrosylated proteins in *Arabidopsis thaliana* undergoing hypersensitive response. *Proteomics,* 8**,** 1459-1469.

ROTHMAN, J. E. 1989. Polypeptide chain binding proteins: catalysts of protein folding and related processes in cells. *Cell,* 59**,** 591-601.

RUDD, J. J. & FRANKLIN-TONG, V. E. 2003. Signals and targets of the self-incompatibility response in pollen of *Papaver rhoeas*. *Journal of experimental botany,* 54**,** 141-148.

RUDD, J. J., FRANKLIN, F. C. H., LORD, J. M. & FRANKLIN-TONG, V. E. 1996. Increased Phosphorylation of a 26-kD Pollen Protein Is Induced by the Self-Incompatibility Response in *Papaver rhoeas*. *The Plant Cell Online,* 8**,** 713-724.

RUSTÉRUCCI, C., ESPUNYA, M. C., DÍAZ, M., CHABANNES, M. & MARTÍNEZ, M. C. 2007. S-nitrosoglutathione reductase affords protection against pathogens in *Arabidopsis*, both locally and systemically. *Plant Physiology,* 143**,** 1282-1292.

SAFAVIAN, D. & GORING, D. R. 2013. Secretory activity is rapidly induced in stigmatic papillae by compatible pollen, but inhibited for self-incompatible pollen in the Brassicaceae.

SAMUEL, M. A., CHONG, Y. T., HAASEN, K. E., ALDEA-BRYDGES, M. G., STONE, S. L. & GORING, D. R. 2009. Cellular pathways regulating responses to compatible and self-incompatible pollen in *Brassica* and *Arabidopsis* stigmas intersect at Exo70A1, a putative component of the exocyst complex. *The Plant Cell,* 21**,** 2655-2671.

SAWADA, H., MORITA, M. & IWANO, M. 2014. Self/non-self recognition mechanisms in sexual reproduction: new insight into the self-incompatibility system shared by flowering plants and hermaphroditic animals. *Biochemical and biophysical research communications,* 450**,** 1142-1148.

SCHOPFER, C. R., NASRALLAH, M. E. & NASRALLAH, J. B. 1999. The male determinant of self-incompatibility in *Brassica*. *Science,* 286**,** 1697-1700.

SCHWESSINGER, B. & ZIPFEL, C. 2008. News from the frontline: recent insights into PAMP-triggered immunity in plants. *Current opinion in plant biology,* 11**,** 389-395.

SEDBROOK, J. C., CARROLL, K. L., HUNG, K. F., MASSON, P. H. & SOMERVILLE, C. R. 2002. The *Arabidopsis SKU5* gene encodes an extracellular glycosyl phosphatidylinositol–anchored glycoprotein involved in directional root growth. *The Plant Cell Online,* 14**,** 1635-1648.

SEN, N., HARA, M. R., KORNBERG, M. D., CASCIO, M. B., BAE, B.-I., SHAHANI, N., THOMAS, B., DAWSON, T. M., DAWSON, V. L. & SNYDER, S. H. 2008. Nitric oxide-induced nuclear GAPDH activates p300/CBP and mediates apoptosis. *Nature cell biology,* 10**,** 866-873.

SERRANO, I., ROMERO-PUERTAS, M. C., RODRÍGUEZ-SERRANO, M., SANDALIO, L. M. & OLMEDILLA, A. 2011. Peroxynitrite mediates programmed cell death both in papillar cells and in self-incompatible pollen in the olive (*Olea europaea L.*). *Journal of experimental botany***,** err392.

SERRANO, I., ROMERO-PUERTAS, M. C., RODRÍGUEZ SERRANO, M., SANDALIO, L. M. & OLMEDILLA, A. 2012. Role of peroxynitrite in programmed cell death induced in self-incompatible pollen. *Plant signaling & behavior,* 7**,** 779-781.

SHACTER, E. 2000. Quantification and significance of protein oxidation in biological samples 1*. *Drug metabolism reviews,* 32**,** 307-326.

SHAFRANSKII, I., BAIKOV, A., ANDRUKOVICH, P. & AVAEVA, S. 1977. Comparative kinetic studies of Mg^{2+}-activated hydrolysis of tripolyphosphate and pyrophosphate by inorganic pyrophosphatase. *Biokhimiia (Moscow, Russia),* 42**,** 1244-1251.

SHEN, Y. H., GODLEWSKI, J., BRONISZ, A., ZHU, J., COMB, M. J., AVRUCH, J. & TZIVION, G. 2003. Significance of 14-3-3 self-dimerization for phosphorylation-dependent target binding. *Molecular biology of the cell,* 14**,** 4721-4733.

SHENTON, D. & GRANT, C. 2003. Protein S-thiolation targets glycolysis and protein synthesis in response to oxidative stress in the yeast *Saccharomyces cerevisiae*. *Biochem. J,* 374**,** 513-519.

SHINTANI, T., UCHIUMI, T., YONEZAWA, T., SALMINEN, A., BAYKOV, A. A., LAHTI, R. & HACHIMORI, A. 1998. Cloning and expression of a

unique inorganic pyrophosphatase from *Bacillus subtilis*: evidence for a new family of enzymes. *FEBS letters,* 439**,** 263-266.

SHIRAYA, T., MORI, T., MARUYAMA, T., SASAKI, M., TAKAMATSU, T., OIKAWA, K., ITOH, K., KANEKO, K., ICHIKAWA, H. & MITSUI, T. 2014. Golgi/plastid-type manganese superoxide dismutase involved in heat-stress tolerance during grain filling of rice. *Plant biotechnology journal*.

SIJACIC, P., WANG, X., SKIRPAN, A. L., WANG, Y., DOWD, P. E., MCCUBBIN, A. G., HUANG, S. & KAO, T.-H. 2004. Identification of the pollen determinant of S-RNase-mediated self-incompatibility. *Nature,* 429**,** 302-305.

SILVERSTEIN, K. A., MOSKAL, W. A., WU, H. C., UNDERWOOD, B. A., GRAHAM, M. A., TOWN, C. D. & VANDENBOSCH, K. A. 2007. Small cysteine-rich peptides resembling antimicrobial peptides have been under-predicted in plants. *The Plant Journal,* 51**,** 262-280.

SIMMONS, S. & BUTLER, L. G. 1969. Alkaline inorganic pyrophosphatase of maize leaves. *Biochimica et Biophysica Acta (BBA)-Bioenergetics,* 172**,** 150-157.

SIROVER, M. A. 1999. New insights into an old protein: the functional diversity of mammalian glyceraldehyde-3-phosphate dehydrogenase. *Biochimica et Biophysica Acta (BBA)-Protein Structure and Molecular Enzymology,* 1432**,** 159-184.

SIROVER, M. A. 2005. New nuclear functions of the glycolytic protein, glyceraldehyde-3-phosphate dehydrogenase, in mammalian cells. *Journal of cellular biochemistry,* 95**,** 45-52.

SIVULA, T., SALMINEN, A., PARFENYEV, A. N., POHJANJOKI, P., GOLDMAN, A., COOPERMAN, B. S., BAYKOV, A. A. & LAHTI, R. 1999. Evolutionary aspects of inorganic pyrophosphatase. *FEBS letters,* 454**,** 75-80.

SLENO, L., VOLMER, D. A. & MARSHALL, A. G. 2005. Assigning product ions from complex MS/MS spectra: the importance of mass uncertainty and resolving power. *Journal of the American Society for Mass Spectrometry,* 16**,** 183-198.

SMALL, J. V., STRADAL, T., VIGNAL, E. & ROTTNER, K. 2002. The lamellipodium: where motility begins. *Trends in cell biology,* 12**,** 112-120.

SNOWMAN, B. N., KOVAR, D. R., SHEVCHENKO, G., FRANKLIN-TONG, V. E. & STAIGER, C. J. 2002. Signal-mediated depolymerization of actin in pollen during the self-incompatibility response. *The Plant Cell Online,* 14**,** 2613-2626.

SONG, C. J., STEINEBRUNNER, I., WANG, X., STOUT, S. C. & ROUX, S. J. 2006. Extracellular ATP induces the accumulation of superoxide via NADPH oxidases in Arabidopsis. *Plant Physiology,* 140**,** 1222-1232.

SONNEWALD, U. 1992. Expression of *E. coli* inorganic pyrophosphatase in transgenic plants alters photoassimilate partitioning. *The Plant Journal,* 2**,** 571-581.

SOULARD, J., BOIVIN, N., MORSE, D. & CAPPADOCIA, M. 2014. eEF1A is an S-RNase binding factor in self-incompatible Solanum chacoense. *PloS one,* 9**,** e90206.

STAIGER, C. J. 2000. Signaling to the actin cytoskeleton in plants. *Annual review of plant biology,* 51**,** 257-288.

STAIGER, C. J., POULTER, N. S., HENTY, J. L., FRANKLIN-TONG, V. E. & BLANCHOIN, L. 2010. Regulation of actin dynamics by actin-binding proteins in pollen. *Journal of experimental botany,* 61**,** 1969-1986.

STAMLER, J. S., JARAKI, O., OSBORNE, J., SIMON, D. I., KEANEY, J., VITA, J., SINGEL, D., VALERI, C. R. & LOSCALZO, J. 1992. Nitric oxide circulates in mammalian plasma primarily as an S-nitroso adduct of serum albumin. *Proceedings of the National Academy of Sciences,* 89**,** 7674-7677.

STAMLER, J. S., LAMAS, S. & FANG, F. C. 2001. Nitrosylation. the prototypic redox-based signaling mechanism. *Cell,* 106**,** 675.

STAMLER, J. S. & TOONE, E. J. 2002. The decomposition of thionitrites. *Current opinion in chemical biology,* 6**,** 779-785.

STANLEY, R. G. & LINSKENS, H. F. 1974. *Pollen: biology, biochemistry, management*, Berlin: Springer-Verlag 307p.. Illustrations. Palynology (KR, 197506433).

STAPULIONIS, R., KOLLI, S. & DEUTSCHER, M. P. 1997. Efficient mammalian protein synthesis requires an intact F-actin system. *Journal of Biological Chemistry,* 272**,** 24980-24986.

STASKAWICZ, B. J., AUSUBEL, F. M., BAKER, B. J., ELLIS, J. G. & JONES, J. D. 1995. Molecular genetics of plant disease resistance. *SCIENCE-NEW YORK THEN WASHINGTON-***,** 661-661.

STEER, M. W. & STEER, J. M. 1989. Tansley review no. 16. Pollen tube tip growth. *New phytologist***,** 323-358.

STEIN, J. C., HOWLETT, B., BOYES, D. C., NASRALLAH, M. E. & NASRALLAH, J. B. 1991. Molecular cloning of a putative receptor protein kinase gene encoded at the self-incompatibility locus of

Brassica oleracea. *Proceedings of the National Academy of Sciences,* 88**,** 8816-8820.

STONE, B. A. & CLARKE, A. E. 1992. Chemistry and Biology of 1, 3-[beta]-Glucans, La Trobe University Press Melbourne.

SU, H., ZHU, J., CAI, C., PEI, W., WANG, J., DONG, H. & REN, H. 2012. FIMBRIN1 is involved in lily pollen tube growth by stabilizing the actin fringe. *The Plant Cell Online,* 24**,** 4539-4554.

SUNDBY, C., HÄRNDAHL, U., GUSTAVSSON, N., ÅHRMAN, E. & MURPHY, D. J. 2005. Conserved methionines in chloroplasts. *Biochimica et Biophysica Acta (BBA)-Proteins and Proteomics,* 1703**,** 191-202.

SUZUKI, G., KAI, N., HIROSE, T., FUKUI, K., NISHIO, T., TAKAYAMA, S., ISOGAI, A., WATANABE, M. & HINATA, K. 1999. Genomic organization of the *S* locus: identification and characterization of genes in SLG/SRK region of S9 haplotype of *Brassica campestris* (syn. rapa). *Genetics,* 153**,** 391-400.

SZUMLANSKI, A. L. & NIELSEN, E. 2009. The Rab GTPase RabA4d regulates pollen tube tip growth in *Arabidopsis thaliana*. *The Plant Cell Online,* 21**,** 526-544.

TAKAYAMA, S. & ISOGAI, A. 2005. Self-incompatibility in plants. *Annu. Rev. Plant Biol.,* 56**,** 467-489.

TAKAYAMA, S., SHIBA, H., IWANO, M., SHIMOSATO, H., CHE, F.-S., KAI, N., WATANABE, M., SUZUKI, G., HINATA, K. & ISOGAI, A. 2000. The pollen determinant of self-incompatibility in *Brassica campestris*. *Proceedings of the National Academy of Sciences,* 97**,** 1920-1925.

TAKAYAMA, S., SHIMOSATO, H., SHIBA, H., FUNATO, M., CHE, F.-S., WATANABE, M., IWANO, M. & ISOGAI, A. 2001. Direct ligand–receptor complex interaction controls *Brassica* self-incompatibility. *Nature,* 413**,** 534-538.

TANOU, G., JOB, C., RAJJOU, L., ARC, E., BELGHAZI, M., DIAMANTIDIS, G., MOLASSIOTIS, A. & JOB, D. 2009. Proteomics reveals the overlapping roles of hydrogen peroxide and nitric oxide in the acclimation of citrus plants to salinity. *The Plant Journal,* 60**,** 795-804.

TANOU, G., ZIOGAS, V., BELGHAZI, M., CHRISTOU, A., FILIPPOU, P., JOB, D., FOTOPOULOS, V. & MOLASSIOTIS, A. 2014. Polyamines reprogram oxidative and nitrosative status and the proteome of citrus plants exposed to salinity stress. *Plant, cell & environment,* 37**,** 864-885.

TANTIKANJANA, T., NASRALLAH, M. E. & NASRALLAH, J. B. 2010. Complex networks of self-incompatibility signaling in the Brassicaceae. *Current opinion in plant biology,* 13**,** 520-526.

TAYLOR, L. P. & HEPLER, P. K. 1997. Pollen germination and tube growth. *Annual review of plant biology,* 48**,** 461-491.

TER HAAR, E., MUSACCHIO, A., HARRISON, S. C. & KIRCHHAUSEN, T. 1998. Atomic structure of clathrin: A β propeller terminal domain joins an α zigzag linker. *Cell,* 95**,** 563-573.

TERMAN, J. R. & KASHINA, A. 2013. Post-translational modification and regulation of actin. *Current opinion in cell biology,* 25**,** 30-38.

TERTIVANIDIS, K., GOUDOULA, C., VASILIKIOTIS, C., HASSIOTOU, E., PERL-TREVES, R. & TSAFTARIS, A. 2004. Superoxide dismutase transgenes in sugarbeets confer resistance to oxidative agents and the fungus *C. beticola. Transgenic research,* 13**,** 225-233.

THOMAS, S. G. & FRANKLIN-TONG, V. E. 2004. Self-incompatibility triggers programmed cell death in *Papaver pollen*. *Nature,* 429**,** 305-309.

THOMAS, S. G., HUANG, S., LI, S., STAIGER, C. J. & FRANKLIN-TONG, V. E. 2006. Actin depolymerization is sufficient to induce programmed cell death in self-incompatible pollen. *The Journal of cell biology,* 174**,** 221-229.

THOMPSON, J. W., FORRESTER, M. T., MOSELEY, M. A. & FOSTER, M. W. 2013. Solid-phase capture for the detection and relative quantification of S-nitrosoproteins by mass spectrometry. *Methods,* 62**,** 130-137.

TORRES, M. A. 2010. ROS in biotic interactions. *Physiologia Plantarum,* 138**,** 414-429.

TORRES, M. A. & DANGL, J. L. 2005. Functions of the respiratory burst oxidase in biotic interactions, abiotic stress and development. *Current opinion in plant biology,* 8**,** 397-403.

TOWBIN, H., STAEHELIN, T. & GORDON, J. 1979. Electrophoretic transfer of proteins from polyacrylamide gels to nitrocellulose sheets: procedure and some applications. *Proceedings of the National Academy of Sciences,* 76**,** 4350-4354.

TRISTAN, C., SHAHANI, N., SEDLAK, T. W. & SAWA, A. 2011. The diverse functions of GAPDH: views from different subcellular compartments. *Cellular signalling,* 23**,** 317-323.

TSIKAS, D., SANDMANN, J., HOLZBERG, D., PANTAZIS, P., RAIDA, M. & FRÖLICH, J. C. 1999. Determination of S-nitrosoglutathione in human

and rat plasma by high-performance liquid chromatography with fluorescence and ultraviolet absorbance detection after precolumn derivatization with o-phthalaldehyde. *Analytical biochemistry,* 273**,** 32-40.

UNGEWICKELL, E., UNANUE, E. & BRANTON, D. Functional and structural studies on clathrin triskelions and baskets. Cold Spring Harbor symposia on quantitative biology, 1982. Cold Spring Harbor Laboratory Press, 723-731.

URIBE, S., RANGEL, P., PARDO, J. P. & PEREIRA-DA-SILVA, L. 1993. Interactions of calcium and magnesium with the mitochondrial inorganic pyrophosphatase from *Saccharomyces cerevisiae*. *European journal of biochemistry,* 217**,** 657-660.

VAN BREUSEGEM, F. & DAT, J. F. 2006. Reactive oxygen species in plant cell death. *Plant physiology,* 141**,** 384-390.

VAN DOORN, W., BEERS, E., DANGL, J., FRANKLIN-TONG, V., GALLOIS, P., HARA-NISHIMURA, I., JONES, A., KAWAI-YAMADA, M., LAM, E. & MUNDY, J. 2011. Morphological classification of plant cell deaths. *Cell Death & Differentiation,* 18**,** 1241-1246.

VAN GISBERGEN, P. A. & BEZANILLA, M. 2013. Plant formins: membrane anchors for actin polymerization. *Trends in cell biology,* 23**,** 227-233.

VAN HEMERT, M. J., STEENSMA, H. Y. & VAN HEUSDEN, G. P. H. 2001. 14-3-3 proteins: key regulators of cell division, signalling and apoptosis. *Bioessays,* 23**,** 936-946.

VERMA, D. P. S. & HONG, Z. 2001. Plant callose synthase complexes. *Plant molecular biology,* 47**,** 693-701.

VIDALI, L., MCKENNA, S. T. & HEPLER, P. K. 2001. Actin polymerization is essential for pollen tube growth. *Molecular biology of the cell,* 12**,** 2534-2545.

VISSER, K., HEIMOVAARA-DIJKSTRA, S., KIJNE, J. W. & WANG, M. 1998. Molecular cloning and characterization of an inorganic pyrophosphatase from barley. *Plant molecular biology,* 37**,** 131-140.

VOIGT, B., TIMMERS, A. C., ŠAMAJ, J., HLAVACKA, A., UEDA, T., PREUSS, M., NIELSEN, E., MATHUR, J., EMANS, N. & STENMARK, H. 2005. Actin-based motility of endosomes is linked to the polar tip growth of root hairs. *European journal of cell biology,* 84**,** 609-621.

VRANOVÁ, E., INZÉ, D. & VAN BREUSEGEM, F. 2002. Signal transduction during oxidative stress. *Journal of experimental botany,* 53**,** 1227-1236.

WALL, S. B., OH, J.-Y., DIERS, A. R. & LANDAR, A. 2012. Oxidative modification of proteins: an emerging mechanism of cell signaling. *Frontiers in physiology,* 3.

WANG, C.-L., WU, J., XU, G.-H., GAO, Y.-B., CHEN, G., WU, J.-Y., WU, H.-Q. & ZHANG, S.-L. 2010. S-RNase disrupts tip-localized reactive oxygen species and induces nuclear DNA degradation in incompatible pollen tubes of *Pyrus pyrifolia*. *Journal of Cell Science,* 123**,** 4301-4309.

WANG, H., WANG, S., LU, Y., ALVAREZ, S., HICKS, L. M., GE, X. & XIA, Y. 2011. Proteomic analysis of early-responsive redox-sensitive proteins in *Arabidopsis*. *Journal of proteome research,* 11**,** 412-424.

WANG, Y.-F., FAN, L.-M., ZHANG, W.-Z., ZHANG, W. & WU, W.-H. 2004. Ca^{2+}-permeable channels in the plasma membrane of *Arabidopsis* pollen are regulated by actin microfilaments. *Plant Physiology,* 136**,** 3892-3904.

WANG, Y., LOAKE, G. J. & CHU, C. 2013. Cross-talk of nitric oxide and reactive oxygen species in plant programed cell death. *Frontiers in plant science,* 4.

WANG, Y., YUN, B.-W., KWON, E., HONG, J. K., YOON, J. & LOAKE, G. J. 2006. S-nitrosylation: an emerging redox-based post-translational modification in plants. *Journal of experimental botany,* 57**,** 1777-1784.

WATERKEYN, L. 1962. Les parois microsporocytaries de nature callosique chez Helleborus et Tradescantia. *Cellule,* 62**,** 225-55.

WEINER, H., STITT, M. & HELDT, H. W. 1987. Subcellular compartmentation of pyrophosphate and alkaline pyrophosphatase in leaves. *Biochimica et Biophysica Acta (BBA)-Bioenergetics,* 893**,** 13-21.

WHEELER, M. J., DE GRAAF, B. H., HADJIOSIF, N., PERRY, R. M., POULTER, N. S., OSMAN, K., VATOVEC, S., HARPER, A., FRANKLIN, F. C. H. & FRANKLIN-TONG, V. E. 2009. Identification of the pollen self-incompatibility determinant in *Papaver rhoeas*. *Nature,* 459**,** 992-995.

WILKINS, K. A. 2013 *Investigating pollen signalling networks triggered by the self-incompatibility response in Papaver rhoeas.* DOCTOR OF PHILOSOPHY, University of Birmingham.

WILKINS, K. A., BANCROFT, J., BOSCH, M., INGS, J., SMIRNOFF, N. & FRANKLIN-TONG, V. E. 2011. Reactive oxygen species and nitric oxide mediate actin reorganization and programmed cell death in the self-incompatibility response of *Papaver*. *Plant Physiology,* 156**,** 404-416.

WILKINS, K. A., BOSCH, M., HAQUE, T., TENG, N., POULTER, N. S. & FRANKLIN-TONG, V. E. 2015. Self-Incompatibility-Induced Programmed Cell Death in Field Poppy Pollen Involves Dramatic Acidification of the Incompatible Pollen Tube Cytosol. *Plant Physiology,* 167**,** 766-779.

WILKINS, K. A., POULTER, N. S. & FRANKLIN-TONG, V. E. 2014. Taking one for the team: self-recognition and cell suicide in pollen. *Journal of experimental botany***,** ert468.

WILLIAMS, R. 1998. Calcium: outside/inside homeostasis and signalling. *Biochimica et Biophysica Acta (BBA)-Molecular Cell Research,* 1448**,** 153-165.

WILLOX, A. K. & ROYLE, S. J. 2012. Functional Analysis of Interaction Sites on the N-Terminal Domain of Clathrin Heavy Chain. *Traffic,* 13**,** 70-81.

WINDER, S. J. & AYSCOUGH, K. R. 2005. Actin-binding proteins. *Journal of cell science,* 118**,** 651-654.

WITUSZYŃSKA, W. & KARPIŃSKI, S. 2013. *Programmed Cell Death as a Response to High Light, UV and Drought Stress in Plants*, INTECH Open Access Publisher.

WOLF, B. B., SCHULER, M., LI, W., EGGERS-SEDLET, B., LEE, W., TAILOR, P., FITZGERALD, P., MILLS, G. B. & GREEN, D. R. 2001. Defective cytochrome c-dependent caspase activation in ovarian cancer cell lines due to diminished or absent apoptotic protease activating factor-1 activity. *Journal of Biological Chemistry,* 276**,** 34244-34251.

WOLTERING, E. J., VAN DER BENT, A. & HOEBERICHTS, F. A. 2002. Do plant caspases exist? *Plant Physiology,* 130**,** 1764-1769.

WOO, H. R., KIM, H. J., NAM, H. G. & LIM, P. O. 2013. Plant leaf senescence and death–regulation by multiple layers of control and implications for aging in general. *Journal of cell science,* 126**,** 4823-4833.

WOOL, I. G. 1996. Extraribosomal functions of ribosomal proteins. *Trends in biochemical sciences,* 21**,** 164-165.

WU, J., WANG, S., GU, Y., ZHANG, S., PUBLICOVER, S. J. & FRANKLIN-TONG, V. E. 2011. Self-incompatibility in *Papaver rhoeas* activates nonspecific cation conductance permeable to Ca^{2+} and K^{+}. *Plant Physiology,* 155**,** 963-973.

WU, Z., RODGERS, R. P. & MARSHALL, A. G. 2004. Characterization of vegetable oils: detailed compositional fingerprints derived from electrospray ionization fourier transform ion cyclotron resonance mass

spectrometry. *Journal of agricultural and food chemistry,* 52**,** 5322-5328.

YAKUNIN, A. F. & HALLENBECK, P. C. 1998. A luminol/iodophenol chemiluminescent detection system for western immunoblots. *Analytical biochemistry,* 258**,** 146-149.

YANG, F., DEMMA, M., WARREN, V., DHARMAWARDHANE, S. & CONDEELIS, J. 1990. Identification of an actin-binding protein from Dictyostelium as elongation factor 1a.

YAO, Y., DU, Y., JIANG, L. & LIU, J.-Y. 2007. Molecular Analysis and Expression Patterns of the 14-3-3 Gene Family from *Oryza sativa. Journal of biochemistry and molecular biology,* 40**,** 349-357.

YE, J., ZHENG, Y., YAN, A., CHEN, N., WANG, Z., HUANG, S. & YANG, Z. 2009. Arabidopsis formin3 directs the formation of actin cables and polarized growth in pollen tubes. *The Plant Cell Online,* 21**,** 3868-3884.

YE, Y., LI, Z. & XING, D. 2013. Nitric oxide promotes MPK6-mediated caspase-3-like activation in cadmium-induced *Arabidopsis thaliana* programmed cell death. *Plant, cell & environment,* 36**,** 1-15.

YOUNG, T. W., KUHN, N. J., WADESON, A., WARD, S., BURGES, D. & COOKE, G. D. 1998. *Bacillus subtilis* ORF *yybQ* encodes a manganese-dependent inorganic pyrophosphatase with distinctive properties: the first of a new class of soluble pyrophosphatase? *Microbiology,* 144**,** 2563-2571.

ZAGO, E., MORSA, S., DAT, J. F., ALARD, P., FERRARINI, A., INZÉ, D., DELLEDONNE, M. & VAN BREUSEGEM, F. 2006. Nitric oxide-and hydrogen peroxide-responsive gene regulation during cell death induction in tobacco. *Plant Physiology,* 141**,** 404-411.

ZANINOTTO, F., LA CAMERA, S., POLVERARI, A. & DELLEDONNE, M. 2006. Cross talk between reactive nitrogen and oxygen species during the hypersensitive disease resistance response. *Plant Physiology,* 141**,** 379-383.

ZHANG, H., QU, X., BAO, C., KHURANA, P., WANG, Q., XIE, Y., ZHENG, Y., CHEN, N., BLANCHOIN, L. & STAIGER, C. J. 2010. *Arabidopsis* VILLIN5, an actin filament bundling and severing protein, is necessary for normal pollen tube growth. *The Plant Cell Online,* 22**,** 2749-2767.

ZHANG, S., CHEN, D., KANG, L. & WANG, L. 2004. Effects of medium components and pH on pollen germination and tube growth in pear (*Pyrus pyrifolia*). *Acta Botanica Boreali-occidentalia Sinica,* 25**,** 225-230.

ZHANG, S. & KLESSIG, D. F. 2001. MAPK cascades in plant defense signaling. *Trends in plant science,* 6**,** 520-527.

ZHANG, Z., CAO, J., QIU, L., JIANG, J. & WU, B. 2013. *BcSKS11*, a *SKS* gene from pollinated pistils of Chinese cabbage pak choi, is expressed continuously during the male gametophyte development, pollen germination and pollen-tube growth processes. *Australian Journal of Botany,* 61**,** 446-454.

ZIPFEL, C. 2009. Early molecular events in PAMP-triggered immunity. *Current opinion in plant biology,* 12**,** 414-420.

ZONIA, L. & MUNNIK, T. 2008. Vesicle trafficking dynamics and visualization of zones of exocytosis and endocytosis in tobacco pollen tubes. *Journal of experimental botany,* 59**,** 861-873.

APPENDIX I

WILKINS, K. A., BOSCH, M., **HAQUE, T**., TENG, N., POULTER, N. S. & FRANKLIN-TONG, V. E. 2015. Self-Incompatibility-induced Programmed Cell Death in poppy pollen involves dramatic acidification of the incompatible pollen tube cytosol. Plant Physiology, 167, 766-779.

My contribution: I investigated the effect of pH on Pr-p26.1a and Pr-p26.1b sPPases activity

APPENDIX II

FT-ICR-MS DATA

The full list of proteins identified as target of ROS and NO (**Chapter 4**) and proteins identified using actin pull-down assay (**Chapter 5**) are listed in the Supplimentary tables (S1-.

Table S1. Oxidative modification of protein treated with germination medium (GM)(Untreated= UT)). (Chapter 4)

Functional group	Accession number	Name of the protein	Identified peptide	Modifications
Cytoskeleton	15238387	ACT4 (ACTIN 4); structural constituent of cytoskeleton [*Arabidopsis thaliana*]	EITALAPSS**m**K AVF**p**SIVGRPR	Met sulfoxide(rev.) Glu y-semialdehyde (irrev.)
	15242516	ACT7 (ACTIN 7); structural constituent of cytoskeleton [*Arabidopsis thaliana*]	DLYGNIVLSGGST**m**FPGIADR EITALAPSS**m**K	Met sulfoxide(rev.) Met sulfoxide(rev.)
	166582	actin-1 [*Arabidopsis thaliana*]	DLYGNIVLSGGTT**m**FPGIADR EITALAPSS**m**K	Met sulfoxide(rev.) Met sulfoxide(rev.)
	15231447	ACT12 (ACTIN-12); structural constituent of cytoskeleton [*Arabidopsis thaliana*]	EITALAPSS**m**K LDLAGRDLTDHL**m**K	Met sulfoxide(rev.) Met sulfoxide(rev.)
	227069387	actin 2 [*Picea abies*]	DLYGNIVLSGGST**m**FPGIADR EITALAPSS**m**K	Met sulfoxide(rev.) Met sulfoxide(rev.)
	18424620	TUB2; GTP binding / GTPase/ structural molecule [*Arabidopsis thaliana*]	**m**ASTFIGNSTSIQE**m**FR LHFF**m**VGFAPLTSR	Met sulfoxide(rev.); Met sulfoxide(rev.) Met sulfoxide(rev.)
Metabolism	15239843	malate dehydrogenase, cytosolic, putative [*Arabidopsis thaliana*]	VLVTGAAGQIGYALVP**m**IAR **m**ELVDAAFPLLK K**m**DLTAEELKEEK	Met sulfoxide(rev.) Met sulfoxide(rev.) Met sulfoxide(rev.)
	15231432	UXS5; UDP-glucuronate decarboxylase/ catalytic [*Arabidopsis thaliana*]	L**m**ENEKNEVIVADNYFTGSK TNVIGTLN**m**LGLAK	Met sulfoxide(rev.) Met sulfoxide(rev.)
	15238151	6-phosphogluconate dehydrogenase family protein [*Arabidopsis thaliana*]	IGLAGLAV**m**GQNLALNIADK ICSYAQG**m**NLLRAKSLEK	Met sulfoxide(rev.) Met sulfoxide(rev.)
	15222735	UGD1 (UDP-GLUCOSE DEHYDROGENASE 1) [*Arabidopsis thaliana*]	VVSS**m**FNTVSGK IFDN**m**QKPAFVFDGR	Met sulfoxide(rev.) Met sulfoxide(rev.)
	1022805	phosphoglycerate kinase [*Arabidopsis thaliana*]	GVTTIIGGGDSVAAVE**k** GVT**p**KFSLAPLVP	AASA (irrev.) Glu y-semialdehyde (irrev.)

	30678219	aconitate hydratase, cytoplasmic [*Arabidopsis thaliana*]	ATIAN**m**SPEYGAT**m**GFFPVDHVTLQYLK **q**VEIPFKPAR	Met sulfoxide(rev.); Met sulfoxide(rev.) Deamidation (rev.)
	15218869	isocitrate dehydrogenase (NADP+)/ oxidoreductase [*Arabidopsis thaliana*]	**n**ILNGTVFR IKVINPVVE**m**DGDE**m**TR	Deamidation (rev.) Met sulfoxide(rev.); Met sulfoxide(rev.)
	30686293	UTP--glucose-1-phosphate uridylyltransferase, putative [*Arabidopsis thaliana*]	DGWYPPGHGDVFPSL**m**NSGK SRFL**p**VK	Met sulfoxide(rev.) Glu y-semialdehyde (irrev.)
	15221788	isocitrate dehydrogenase[*Arabidopsis thaliana*]	LIDD**m**VAYALK **n**ILNGTVFR	Met sulfoxide(rev.) Deamidation (rev.)
	15221107	enolase, putative [*Arabidopsis thaliana*]	SGETEDNFIADLSVGLASG**q**IK AAGWGV**m**VSHR	Deamidation (rev.) Met sulfoxide(rev.)
	26185954	cytosolic phosphoglucomutase [*Arabidopsis thaliana*]	S**m**PTSAALDVVAK LSGTGSEGATI**r**	Met sulfoxide(rev.) Glu y-semialdehyde (irrev.)
	84619270	soluble inorganic pyrophosphatase [*Papaver rhoeas*] Pr-p26.1a	AIGL**m**PMIDQGEKDDK EVAVNDFLPSATAHEAIQYS**m**DLYAEYI**m**MSLR	Met sulfoxide(rev.) Met sulfoxide(rev.); Met sulfoxide(rev.)
	9758328	xylose isomerase [*Arabidopsis thaliana*]	Y**m**HGGATSSEVGVYAYAAAQVK ILEEGSLSELV**r**K**r**	Met sulfoxide(rev.) Glu y-semialdehyde (irrev.); Glu y-semialdehyde (irrev.)
	15234986	pfkB-type carbohydrate kinase family protein [*Arabidopsis thaliana*]	NPSAD**m**LLK EF**m**FYR	Met sulfoxide(rev.) Met sulfoxide(rev.)
	15221119	aminomethyltransferase, putative [*Arabidopsis thaliana*]	**m**VPFAGWSMPIQYK KNIA**m**GYVK	Met sulfoxide(rev.) Met sulfoxide(rev.)
	15236129	ASP5 (aspartate aminotransferase 5	VATI**q**GLSGTGSLR IGAI**n**VVCSSADAATRVK	Deamidation (rev.) Deamidation (rev.)
Energy production pathways	22326673	ATP synthase beta chain, mitochondrial, putative [*Arabidopsis thaliana*]	TVLI**m**ELINNVAK TIA**m**DGTEGLVR	Met sulfoxide(rev.) Met sulfoxide(rev.)
	15227987	LOS2; copper ion binding / phosphopyruvate hydratase [*Arabidopsis thaliana*]	**m**GVEVYHHLK LA**m**QEFMILPVGAASFK	Met sulfoxide(rev.) Met sulfoxide(rev.)
	15219412	PGK (PHOSPHOGLYCERATE KINASE); phosphoglycerate kinase	YL**m**GNGSRVVLCSHLGRPKG	Met sulfoxide(rev.)

		[*Arabidopsis thaliana*]	A**q**GLSVGSSLVEEDKLDLAK	Deamidation (rev.)
	17939849	mitochondrial F1 ATP synthase beta subunit [*Arabidopsis thaliana*]	TVLI**m**ELINNVAK TIA**m**DGTEGLVR	Met sulfoxide(rev.) Met sulfoxide(rev.)
	435001	H(+)-transporting ATPase [*Solanum tuberosum*]	LLEGDPLKID**q**SALTGESLPVTK EA**q**WALAQR	Deamidation (rev.) Deamidation (rev.)
	15219234	VHA-A (VACUOLAR ATP SYNTHASE SUBUNIT A); [*Arabidopsis thaliana*]	VSGPVVVADG**m**AGAAMYELVR TTLVANTSN**m**PVAAR	Met sulfoxide(rev.) Met sulfoxide(rev.)
	15224157	AHA5 (Arabidopsis H(+)-ATPase 5); ATPase [*Arabidopsis thaliana]*	**m**ITGDQLAIGK IVFGFMFIALIWQFDFSPFMVLIIAILNDGTI**m**TISKDR	Met sulfoxide(rev.) Met sulfoxide(rev.)
	15241190	pyruvate kinase, putative [*Arabidopsis thaliana*]	SVP**m**VEKLLR MA**m**IEQRPKTK	Met sulfoxide(rev.) Met sulfoxide(rev.)
Stress related	15223533	ERD2 (EARLY-RESPONSIVE TO DEHYDRATION 2); ATP binding [*Arabidopsis thaliana*]	**m**VNHFVQEFK QFAAEEISS**m**VLIK	Met sulfoxide(rev.) Met sulfoxide(rev.)
	15232682	heat shock cognate 70 kDa protein 3 (HSC70-3) (HSP70-3) [*Arabidopsis thaliana*]	NQVA**m**NPINTVFDAK **m**VNHFVQEFK	Met sulfoxide(rev.) Met sulfoxide(rev.)
	38325815	heat shock protein 70-3 [*Nicotiana tabacum*]	LIGDAAKNQVA**m**NPINT QFAAEEISS**m**VLIK	Met sulfoxide(rev.) Met sulfoxide(rev.)
	15242459	MTHSC70-2 (MITOCHONDRIAL HSP70 2); ATP binding [*Arabidopsis thaliana*]	GVNPDEAVA**m**GAALQGGILR IINEPTAAALSYG**m**TNK	Met sulfoxide(rev.) Met sulfoxide(rev.)
	15229595	chaperonin, putative [*Arabidopsis thaliana*]	EERNYILG**m**IKK ILKITGIKD**m**GR	Met sulfoxide(rev.) Met sulfoxide(rev.)
	217855	81kDa heat-shock protein [*Arabidopsis thaliana*]	GYEVLY**m**VDAIDEYAVGQLK AVENS**p**FLER	Met sulfoxide(rev.) Glu y-semialdehyde (irrev.)
	27476086	Putative heat shock 70 KD protein, mitochondrial precursor [*Oryza sativa*]	GVNPDEAVA**m**GAAIQGGILR ATNGDTFLGGEDFD**n**TLLEFLVSEFKR	Met sulfoxide(rev.) Deamidation (rev.)

Signalling/regulatory	470115786	PREDICTED: elongation factor 2-like [*Fragaria vesca subsp. vesca*]	EVAGDVR**m**TDTRADEAERGIT QRVIENANVI**m**ATYED	Met sulfoxide(rev.) Met sulfoxide(rev.)
	38564733	initiation factor eIF4A-15 [*Helianthus annuus*]	VQVGVFSAT**m**PPEALEITR **m**FVLDEADEMLSR	Met sulfoxide(rev.) Met sulfoxide(rev.)
	351725929	14-3-3 protein SGF14h [*Glycine max*]	LAEQAERYEE**m**VEFMEK IISSIE**q**KEESR	Met sulfoxide(rev.) Deamidation (rev.)
	15224916	RAB6A; GTP binding / protein binding [*Arabidopsis thaliana*]	LVFLGD**q**SVGK ELNV**m**FIETSAK	Deamidation (rev.) Met sulfoxide(rev.)
Protein degradation	79321461	UBC35 (ubiquitin-conjugating enzyme 35 [*Arabidopsis thaliana*]	YFNV**m**ILGPTQSPYEGGVFK LELFLPEEYP**m**AAPK	Met sulfoxide(rev.) Met sulfoxide(rev.)
Amino acid/Protein biosynthesis	47600741	cobalamin-independent methionine synthase [Arabidopsis thaliana]	G**m**LTGPVTILNWSFVR YGAGIGPGVYDIHS**p**R	Met sulfoxide(rev.) Glu y-semialdehyde (irrev.)
	30688090	ATMS3 (methionine synthase 3) [*Arabidopsis thaliana*]	G**m**LTGPVTILNWSFVR YGAGIGPGVYDIHS**p**R	Met sulfoxide(rev.) Glu y-semialdehyde (irrev.)
	110740085	s-adenosylmethionine synthetase like protein [*Arabidopsis thaliana*]	TN**m**V**m**VFGEITTK **q**AAKSIVASGLAR	Met sulfoxide(rev.); Met sulfoxide(rev.) Deamidation (rev.)
Protein transport	15240640	AAC2 (ADP/ATP carrier 2); ATP:ADP antiporter/ binding [*Arabidopsis thaliana*]	YFPTQAL**n**FAFK LLIQNQDE**m**LK	Deamidation (rev.) Met sulfoxide(rev.)
	2218152	type IIIa membrane protein cp-wap13 [Vigna unguiculata]	ELIGPAMYFGL**m**GDGQPIGR YIYTIDDD**c**FVAK	Met sulfoxide(rev.) Carbamidomethyl (rev.)
Uncharacterised	224055669	predicted protein [*Populus trichocarpa*]	VALQRDDVELVAVNDPFITTDY**m**TYMFK DDVELVAVNDPFITTDY**m**TYMFK LGTVIGIDLGTTYS**c**VGVYK	Met sulfoxide(rev.) Met sulfoxide(rev.) Carbamidomethyl (rev.)
	118484713	unknown [*Populus trichocarpa*]	GIELIASE**n**FTSFAVIEALGSALTNK GLVEKDFEqIGEFLHR	Deamidation (rev.) Deamidation (rev.)
	297738640	unnamed protein product [*Vitis vinifera*]	LETL**c**DLYETLAITQSVIFVNTR VQVGVFSAT**m**PPEALEITR	Carbamidomethyl (rev.) Met sulfoxide(rev.)

	224073500	predicted protein [*Populus trichocarpa*]	LETL**c**DLYETLAITQSVIFVNTR VQVGVFSAT**m**PPEALEITR	Carbamidomethyl (rev.) Met sulfoxide(rev.)
	217072994	unknown [*Medicago truncatula*]	DLYGNIVLSGGST**m**FPGIADR YPIEHGIVSNWDD**m**EK	Met sulfoxide(rev.) Met sulfoxide(rev.)
	168062156	predicted protein [*Physcomitrella patens*]	SINPDEAVAYGAAVQAAILSGEGNE**k** EQVFSTYSDNQPGVLI**q**VYEGER	AASA (irrev.) Deamidation (rev.)
	326513870	predicted protein [*Hordeum vulgare*]	G**m**LTGPVTILNWSFVR I**q**EELDIDVLVHGEPER	Met sulfoxide(rev.) Deamidation (rev.)
	219885633	unknown [*Zea mays*]	E**q**VFSTYSDNQPGVLIQVYEGER QFAAEEISS**m**VLIK	Deamidation (rev.) Met sulfoxide(rev.)
	326506132	predicted protein [*Hordeum vulgare*]	SINPDEAVAYGAAVQAAILSGEGNE**k** E**q**VFSTYSDNQPGVLIQVYEGER	AASA (irrev.) Deamidation (rev.)
	351721290	uncharacterized protein LOC100305663 [*Glycine max*]	LDYVLALTVE**n**FLER YGLLDET**q**NKLDYVLALTVENFLER	Deamidation (rev.) Deamidation (rev.)
	297733971	unnamed protein product [*Vitis vinifera*]	VAILGAAGGIGQ**p**LALLIK **m**SPLVSALHLYDIANVK	Glu y-semialdehyde (irrev.) Met sulfoxide(rev.)
	62149091	hypothetical protein [*Cucumis melo*]	LVTGGTENHLVLWDLRPLGLTGNKVE**k** INFSVFPALQGGPHNHQIGALAVAL**k**	AASA (irrev.) AASA (irrev.)
	15234797	unknown protein [*Arabidopsis thaliana*]	AGILGN**m**QNLYETVK KAQ**m**VVQVEAVRVQK	Met sulfoxide(rev.) Met sulfoxide(rev.)
	4455159	putative protein [*Arabidopsis thaliana*]	GIPAILGIIST**q**R DE**c**WYRNVPYDWINKQK	Deamidation (rev.) S-nitrosocysteine (rev.)

Table S2. Oxidative modification of protein using PrsS (Chapter 4)

Functional group	Accession number	Name of the protein	Identified peptide	Modifications
Cytoskeleton	224088196	Actin 3 [*Populus trichocarpa*]	DLYGNIVLSGGSTMF**p**GIADR LAYIALDYEQELETA**k** EITALA**p**SSMK	Glu y-semialdehyde (irrev.) AASA (irrev.) Glu y-semialdehyde (irrev.)
	15242516	Actin 7 [*Arabidopsis thaliana*]	DLYGNIVLSGGST**m**F**p**GIADR YPIEHGIVSNWDD**m**EK EITALAPSS**m**K	Met sulfone (irrev.); Glu y-semialdehyde (irrev.) Met sulfone (irrev.) Met sulfone (irrev.)
	15229955	Actin-11 [*Arabidopsis thaliana*]	DLYGNIVLSGGTT**m**FPGIADR EITALAPSS**m**K	Met sulfone (irrev.) Met sulfone (irrev.)
	227069387	actin 2 [*Picea abies*]	DLYGNIVLSGGSTMF**p**GIADR YPIEHGIVTN**w**DDMEK	Glu y-semialdehyde (irrev.) Kynurenine (irrev.)
	15238387	Actin 4 [*Arabidopsis thaliana*]	VAPEEH**p**VLLTEAPLNPK EITALAPSS**m**K	Glu y-semialdehyde (irrev.) Met sulfone (irrev.)
	18424620	TUB2 GTP binding / GTPase/ [*Arabidopsis thaliana*]	NSSYFVE**w**l**p**NNV**k** GHYTEGAELIDSVLDVVR**k** AVL**m**DLEPGTMDSLR	Kynurenine (irrev.); Glu y-semialdehyde (irrev.); AASA (irrev.) AASA (irrev.) Met sulfone (irrev.)
	15239914	TUB6 [*Arabidopsis thaliana*]	**m**MLTFSVFPSPK LAVNLI**p**FPR	Met sulfone (irrev.) Glu y-semialdehyde (irrev.)
	15231447	Actin-12 [*Arabidopsis thaliana*]	SFEL**p**DGQVITIGAER AGFAGDDA**p**R EITALAPSS**m**K	Glu y-semialdehyde (irrev.) Glu y-semialdehyde (irrev.) Met sulfone (irrev.)
	30683070	TUA6 [*Arabidopsis thaliana*]	FDGALNVDVTEFQTNLV**p**YPR TVGGGDDAFNTFFSETGAG**k**	Glu y-semialdehyde (irrev.) AASA (irrev.)

	15217737	Alpha-1 tubulin [*Arabidopsis thaliana*]	QLFH**p**EQLISGKEDAANNFAR RTIQFVDW**c**PTGFKCGINYQPPSVVPGGDLAK	Glu y-semialdehyde (irrev.) Cysteic acid (irrev.)
	15233536	Profilin 4 [*Arabidopsis thaliana*]	Y**m**VIQGEPGAVIR GAGGITIKKTGQSCVFGIYEEPVTPGQ**c**N**m**VVER	Met sulfone (irrev.) S-nitrosocysteine (rev.); Met sulfone (irrev.)
	15236837	ATFIM1; actin binding [*Arabidopsis thaliana*]	VVN**w**NLVTK A**c**TTTLLHTIYQSEKGPFVQHINR	Kynurenine (irrev.) Cysteic acid (irrev.)
	15238586	Fimbrin-like protein 2 actin binding [*Arabidopsis thaliana*]	KVEN**c**NEVIKIGK KVLEQAEKLD**ck**	Cysteic acid (irrev.) S-nitrosocysteine (rev.); AASA (irrev.)
	321437427	alpha-tubulin [*Musa acuminata*]	**k**LADN**c**TGLQGFLVFNAVGGGTGSGLGSLLLER TVGGGDDAFNTFFSETGAG**k** QLFHPEQLISG**k**EDAANNFAR TIQFVDW**c**PTGFK	AASA (irrev.); Carbamidomethyl (rev.) AASA (irrev.) AASA (irrev.) Carbamidomethyl (rev.)
Metabolism	307136112	glyceraldehyde-3-phosphate dehydrogenase [*Cucumis melo*]	VALQRDDVELVAVNDPFITTDYMTYMF**k** DDVELVAVNDPFITTDYMTYMF**k** DA**p**MFVVGVNEK	AASA (irrev.) AASA (irrev.) Glu y-semialdehyde (irrev.)
	15236375	SHM4 (serine hydroxymethyltransferase 4 [*Arabidopsis thaliana*]	ANAVALGNYL**m**SK I**m**GLDLPSGGHLTHGYYTSGGK	Met sulfone (irrev.) Met sulfone (irrev.)
	15239897	ATP citrate lyase subunit B 2; ATP citrate synthase [*Arabidopsis thaliana*]	VVIGPATVGGIQAGAF**k** IGDTAGTIDNIIQ**c**KLYRPGSVGFVSK	AASA (irrev.) Cysteic acid (irrev.)
	84619270 **Pr-p26.1a**	soluble inorganic pyrophosphatase [*Papaver rhoeas*]	AIGL**mp**MIDQGEKDDK RSVAAH**pwh**DLEIGPGAPSVVNAVVEIT**k** TL**c**EDNDPLDVLILMQEPVLPG**c**FLR	Met sulfone (irrev.); Glu y-semialdehyde (irrev.) Glu y-semialdehyde (irrev.); Kynurenine (irrev.); 2-oxohistidine (irrev.); AASA (irrev.) Carbamidomethyl (rev.); Carbamidomethyl (rev.)
	84619272 **Pr-p26.1b**	soluble inorganic pyrophosphatase [*Papaver rhoeas*]	AIGL**mp**MIDQGEKDDK KNEN**k**EVAVNDFLPAEDAS**k** TLNAIKAASYSS**h**ARPSL**n**ER	Met sulfone (irrev.); Glu-γ-semialdehyde (irrev.); AASA (irrev.); AASA (irrev.) 2-Oxohistidine (irrev.); Deamidation (rev.)

	15239843	malate dehydrogenase, cytosolic, putative [*Arabidopsis thaliana*]	VLVTGAAGQIGYALVP**m**IAR **m**ELVDAAFPLLK	Met sulfone (irrev.) Met sulfone (irrev.)
	15228048	Methionine adenosyltransferase 3 [*Arabidopsis thaliana*]	KIIIDTYGGWGAHGGGAFSG**k**DPTK KPEDIGAGDQGH**m**FGYATDETPELMPLTHVLATK	AASA (irrev.) Met sulfone (irrev.)
	15219721	malate dehydrogenase, cytosolic, putative [*Arabidopsis thaliana*]	K**m**DLTAEELKEEK GVVATTDAVEG**c**TGVNVAV**m**VGGFPRKEGMER	Met sulfone (irrev.) S-nitrosocysteine (rev.); Met sulfone (irrev.)
	15234986	pfkB-type carbohydrate kinase family protein [*Arabidopsis thaliana*]	FGDDEFGH**m**LVNILK APGGAPANVA**c**AITK	Met sulfone (irrev.) S-nitrosocysteine (rev.)
	22329337	ATSPS3F (sucrose phosphate synthase 3F)[*Arabidopsis thaliana*]	GVFINPALVEPFGLTLIEAAAHGLP**m**VATK ELANLTLI**m**GNRDDIDELSSGNASVLTTVLK	Met sulfone (irrev.) Met sulfone (irrev.)
	357498709	Enolase [*Medicago truncatula*]	KYGQDATNVGDEGGFAPNIQEN**k**EGLELLK LGANAILAVSLAV**c**K SFVSDYPIVSIEDPFDQDD**w**E**h**YS**k**	AASA (irrev.) Carbamidomethyl (rev.) Kynurenine (irrev.); 2-oxohistidine (irrev.); AASA (irrev.)
	15221107	enolase, putative [*Arabidopsis thaliana*]	SGETEDNFIADLSVGLASGQI**k** LGANAILGVSLSV**c**RAGAGAK	AASA (irrev.) Cysteic acid (irrev.)
	357113118	PREDICTED: enolase 2-like [*Brachypodium distachyon*]	KYGQDATNVGDEGGFAPNIQEN**k**EGLELLK LGANAILAVSLAV**c**K	AASA (irrev.) Carbamidomethyl (rev.)
	15228687	UDP-glucose 6-dehydrogenase, putative [*Arabidopsis thaliana*]	IFDN**m**QKPAFVFDGR **m**VKI**c**CIGAGYVGGPT**m**AVIALK	Met sulfone (irrev.) Met sulfone (irrev.); Cysteic acid (irrev.); Met sulfone (irrev.)
	240254631	ATPPC2 (phosphoenolpyruvate carboxylase 2); catalytic/ phosphoenolpyruvate carboxylase [*Arabidopsis thaliana*]	VPYNAPLIQFSSW**m**GGDR VL**m**DE**m**AIIATEEYRSVVFKEPR	Met sulfone (irrev.) Met sulfone (irrev.); Met sulfone (irrev.)
	225456550	Predicted: UDP-arabinopyranose mutase 1 [*Vitis vinifera*]	EGVPTAVSHGLWLNIPDYDAPTQLV**k**PR YIYTIDDD**c**FVAK	AASA (irrev.) Carbamidomethyl (rev.)

			ELIGPAMYFGLMGDGQ**p**lGR	Glu y-semialdehyde (irrev.)
	15218074	pyrophosphate--fructose-6-phosphate 1-phosphotransferase-related [*Arabidopsis thaliana*]	**c**GATPITA**m**MTVK KHSHVALE**c**TLQSHPN**m**VILGEEVAASK	Cysteic acid (irrev.); Met sulfone (irrev.) Cysteic acid (irrev.); Met sulfone (irrev.)
	15222735	UGD1 (UDP-glucose dehydrogenase 1 [*Arabidopsis thaliana*]	AADLTY**w**ESAAR IFDN**m**QKPAFVFDGR	Kynurenine (irrev.) Met sulfone (irrev.)
	21592905	mitochondrial NAD-dependent malate dehydrogenase [*Arabidopsis thaliana*]	S**m**LVRSSASAKQAAIR NLCTAIAKYCPHALIN**m**ISNPVNSTVPIAAEIFKK	Met sulfone (irrev.) Met sulfone (irrev.)
	15227981	fructose-bisphosphate aldolase, putative [Arabidopsis thaliana]	KP**w**SLSFSFGR GILAADESTGTIG**k**R	Kynurenine (irrev.) AASA (irrev.)
Energy production pathways	18415911	ATP synthase beta chain 2, mitochondrial [*Arabidopsis thaliana*]	NLQDIIAILG**m**DELSEDDKLTVAR TVLI**m**ELINNVAK	Met sulfone (irrev.) Met sulfone (irrev.)
	225424142	PREDICTED: ATP synthase subunit beta, mitochondrial-like [*Vitis vinifera*]	ITDEFTGAGAIGSV**c**QVIGAVVDVR **k**GSITSVQAIYVPADDLTDPAPATTFAHLDATTVLSR	Carbamidomethyl (rev.) AASA (irrev.)
	435001	H(+)-transporting ATPase [*Solanum tuberosum*]	LLEGDPL**k**IDQSALTGESLPVTK NPGDEVFSGST**c**K	AASA (irrev.) Carbamidomethyl (rev.)
	15234666	AHA2; ATPase/ hydrogen-exporting ATPase, phosphorylative mechanism [*Arabidopsis thaliana*]	NLVEVF**c**KGVEKDQVLLFAAMASR VLTAIGNF**c**I**c**SIAIG**m**VIEIIVMYPIQR	S-nitrosocysteine (rev.) Cysteic acid (irrev.); Cysteic acid (irrev.); Met sulfone (irrev.)
	15224157	AHA5 (Arabidopsis H(+)-ATPase 5); ATPase [*Arabidopsis thaliana*]	**m**ITGDQLAIGK IVFGFMFIALIWQFDFSPFMVLIIAILNDGTI**m**TISKDR	Met sulfone (irrev.) Met sulfone (irrev.)
	15225747	AHA6 (Arabidopsis H(+)-ATPase 6); ATPase [*Arabidopsis thaliana*]	GAPEQIIEL**c**DLKGETKR YTLSGKAWNN**m**IENRTAFTTK	S-nitrosocysteine (rev.) Met sulfone (irrev.)
	15220197	AHA9; hydrogen-exporting ATPase, phosphorylative mechanism [*Arabidopsis thaliana*]	HI**c**GMTGDGVNDAPALKRADIGIAVADATDAAR VLTAIGNF**c**I**c**SIAIG**m**LIEIVV**m**YPIQKR	Cysteic acid (irrev.) Cysteic acid (irrev.); S-nitrosocysteine (rev.); Met sulfone (irrev.); Met sulfone (irrev.)

	145332819	pyruvate kinase, putative [*Arabidopsis thaliana*]	YRPT**m**PVISVVIPR KL**c**AV**m**LDTVGPELQVINK	Met sulfone (irrev.) Cysteic acid (irrev.); Met sulfone (irrev.)
	15240952	PDC3 (pyruvate decarboxylase-3); carboxy-lyase transferase [*Arabidopsis thaliana*]	ILHHTIGL**p**DFSQELR KDSL**c**FIEVIVHK	Glu y-semialdehyde (irrev.) Cysteic acid (irrev.)
	2204087	enoyl-ACP reductase [*Arabidopsis thaliana*]	AGTYIVGAYPGNASWDKLS**c**TRQLSNLG**c**LR LS**c**TRQLSNLG**c**LRNNTAVPTCK VLKAGTYIVGAYPGNASWDKLS**c**TR	Cysteic acid (irrev.); Cysteic acid (irrev.) Cysteic acid (irrev.); Cysteic acid (irrev.) Cysteic acid (irrev.)
Stress related	225434984	Predicted: heat shock cognate 70 kDa protein isoform 1 [*Vitis vinifera*]	SIN**p**DEAVAYGAAVQAAILSGEGNE**k** NQVAMN**p**INTVFDAK	Glu y-semialdehyde (irrev.); AASA (irrev.) Glu y-semialdehyde (irrev.)
	15241849	HSC70-1 ATP binding [*Arabidopsis thaliana*]	IINE**p**TAAAIAYGLDK DAGVIAGLNV**m**R NQVA**m**NPVNTVFDAKRLIGR	Glu y-semialdehyde (irrev.) Met sulfone (irrev.) Met sulfone (irrev.)
	38325815	heat shock protein 70-3 [*Nicotiana tabacum*]	SIN**p**DEAVAYGAAVQAAILSGEGNE**k** NQVAMN**p**INTVFDAK	Glu y-semialdehyde (irrev.); AASA (irrev.) Glu y-semialdehyde (irrev.)
	225426230	Predicted: luminal-binding protein 5 [*Vitis vinifera*]	VFS**p**EEISAMILTK LKEVEAV**c**NPIITAVYQR DILLLDVAPLTLGIETVGGVMT**k**	Glu y-semialdehyde (irrev.) Carbamidomethyl (rev.) AASA (irrev.)
	1695719	luminal binding protein [*Arabidopsis thaliana*]	VFSPEEISAMILT**k** DILLLDVAPLTLGIETVGGV**m**TK	AASA (irrev.) Met sulfone (irrev.)
	15219109	Hsp70b [*Arabidopsis thaliana*]	NEEKQFSPEEISS**m**VLVK**m**K IQQLLQDFFNGKEL**c**K	Met sulfone (irrev.); Met sulfone (irrev.) Cysteic acid (irrev.)
	108864707	Heat shock cognate 70 kDa protein [*Oryza sativa*]	EQVFSTYSDNQ**p**GVLIQVYEGER NQVAMN**p**INTVFDAK	Glu y-semialdehyde (irrev.) Glu y-semialdehyde (irrev.)
	15223533	ERD2 (early-responsive to dehydration 2); ATP binding [*Arabidopsis thaliana*]	NQVA**m**NPVNTVFDAKRLIGR SIN**p**DEAVAYGAAVQAAILSGEGNE**k**	Met sulfone (irrev.) Glu y-semialdehyde (irrev.); AASA (irrev.)
	4467097	heat shock protein 70 like protein [*Arabidopsis thaliana*]	EVDEVLLVGG**m**TR SP**c**QN**c**LKDAGVTIKEVDEVLLVGGMTR	Met sulfone (irrev.) S-nitrosocysteine (rev.); Cysteic acid (irrev.)

	356568992	Predicted: heat shock cognate 70 kDa protein 2-like isoform 1 [*Glycine max*]	SIN**p**DEAVAYGAAVQAAILSGEGNE**k** NQVAMN**p**VNTVFDAK	Glu y-semialdehyde (irrev.); AASA (irrev.) Glu y-semialdehyde (irrev.)
	15240317	chaperonin, putative [*Arabidopsis thaliana*]	TQDEEVGDGTTSVIVLAGE**m**LHVAEAFLEK LEEEYIEN**c**VQILK	Met sulfone (irrev.) S-nitrosocysteine (rev.)
	357442729	Chaperonin CPN60-2 [*Medicago truncatula*]	TQDEEVGDGTTSVIVLAGEMLHVAEAFLE**k** GYIS**p**YFITNQ**k**	AASA (irrev.) Glu y-semialdehyde (irrev.); AASA (irrev.)
	15241102	heat shock protein 81-4 (HSP81-4) [*Arabidopsis thaliana*]	I**m**KAQALK EKFEGL**c**KVIK	Met sulfone (irrev.) S-nitrosocysteine (rev.)
Signalling/regulatory	470115786	Predicted: elongation factor 2-like [*Fragaria vesca*]	GVQYLNEIKDSVVAGFQ**w**AS**k** ITDGALVVVD**c**IEGV**c**VQTETVLR NcDPDGPL**m**LYVSK LYMEAR**p**LEDGLAEAIDDGR GFVQF**c**YEPI**k**	Kynurenine (irrev.); AASA (irrev.) Carbamidomethyl (rev.); Carbamidomethyl (rev.) Carbamidomethyl (rev.); Met sulfone (irrev.) Glu y-semialdehyde (irrev.) Carbamidomethyl (rev.); AASA (irrev.)
	38564733	initiation factor eIF4A-15 [*Helianthus annuus*]	LETL**c**DLYETLAITQSVIFVNTR VQVGVFSATM**p**PEALEITR	Carbamidomethyl (rev.) Glu y-semialdehyde (irrev.)
	29824421	putative elongation factor [*Arabidopsis thaliana*]	GVQYLNEIKDSVVAGFQ**w**AS**k** GHVFEE**m**QRPGTPLYNIK	Kynurenine (irrev.); AASA (irrev.) Met sulfone (irrev.)
	18396217	GRF7 (general regulatory factor 7) [*Arabidopsis thaliana*]	LAEQAERYEE**m**VEFMEK DSTLI**m**QLLR QAFDEAISELDTLGEESY**k**DSTLI**m**QLLR	Met sulfone (irrev.) Met sulfone (irrev.) AASA (irrev.); Met sulfone (irrev.)
	209922600	elongation factor 1-alpha [*Prunus persica*]	YY**c**TVIDAPGHR GPTLLEALDLINE**p**KRPSDKPLR	Carbamidomethyl (rev.) Glu y-semialdehyde (irrev.)
	332658507	RAB GTPase homolog 1C [*Arabidopsis thaliana*]	NVNKLLVGNK**c**DLTSQKVVS TRMASQ**p**AGGSKPPTVQIRGQPVN	Carbamidomethyl (rev.) Glu y-semialdehyde (irrev.)
	357519317	Rab GDP dissociation inhibitor [*Medicago truncatula*]	NDYYGGESTSLNLIQLW**k** LSAVYGGTYMLNK**p**E**c**K	AASA (irrev.) Glu y-semialdehyde (irrev.); Carbamidomethyl (rev.)
	18411901	14-3-3-like protein GF14 omega	QAFDEAIAELDTLGEESY**k**	AASA (irrev.)

		[*Arabidopsis thaliana*]	SKIETELSGI**c**DGILK	Carbamidomethyl (rev.)
	21553476	14-3-3-like protein GF14 iota (General regulatory factor 12) [*Arabidopsis thaliana*]	QAFDEAIAELDTLSEESY**k**DSTLI**m**QLLR DSTLI**m**QLLR	AASA (irrev.); Met sulfone (irrev.) Met sulfone (irrev.)
	7671458	14-3-3-like protein AFT1 [*Arabidopsis thaliana*]	QAFEEAIAELDTLGEESY**k**DSTLI**m**QLLR DSTLI**m**QLLR **m**AATLGRDQYVYMAK VESELSSV**c**SGILK	AASA (irrev.); Met sulfone (irrev.) Met sulfone (irrev.) Met sulfone (irrev.) Cysteic acid (irrev.)
	168030217	Rab1/RabD-family small GTPase [*Physcomitrella patens*]	FADDSYLESYISTIGVDF**k** LLLIGDSGVG**k**	AASA (irrev.) AASA (irrev.)
Protein degradation	15237159	RPT3 (regulatory particle triple-a atpase 3); ATPase [*Arabidopsis thaliana*]	ISAAEIAAI**c**QEAG**m**HAVR EAVEL**p**LT**h**HELYKQIGIDPPR	Cysteic acid (irrev.); Met sulfone (irrev.) Glu y-semialdehyde (irrev.); 2-oxohistidine (irrev.)
	18399399	RPN1A (26S proteasome regulatory subunit S2 1A) [*Arabidopsis thaliana*]	AVPLALGLL**c**ISNPKVTVMDTLSR YCDMTLLSCAYAGTGNVLKVQDLLAQ**c**GEHLEK	S-nitrosocysteine (rev.) Cysteic acid (irrev.)
	15235577	DDB1A (damaged DNA binding protein 1A) [*Arabidopsis thaliana*]	IGRPTDNGQIGIIDPD**c**R NKMEDISKSMNVQVEEL**c**K	Cysteic acid (irrev.) Cysteic acid (irrev.)
Amino acid/Protein biosynthesis	347361140	methionine synthase [*Camellia sinensis*]	DKLVVSTS**c**SLLHTAVDLVNET**k** **k**LNLPILPTTTIGSFPQTIELR LVVSTS**c**SLLHTAVDLVNET**k** FET**c**YQIALAIKDEVEDLE**k** GMLTG**p**VTILNWSFVR	Carbamidomethyl (rev.); AASA (irrev.) AASA (irrev.) Carbamidomethyl (rev.); AASA (irrev.) Carbamidomethyl (rev.); AASA (irrev.) Glu y-semialdehyde (irrev.)
	110740085	s-adenosylmethionine synthetase like protein [*Arabidopsis thaliana*]	TN**m**V**m**VFGEITTK KPEEVGAGDQGHMFGYATDETPEL**m**PLTHVLATK	Met sulfone (irrev.); Met sulfone (irrev.) Met sulfone (irrev.)
	297831158	S-adenosyl-L-homocysteine (sah) hydrolase 2 [*Arabidopsis lyrata subsp. lyrata*]	LYQMQETGTLLFPAINVNDSVT**k** LMNLG**c**ATGH**p**SFVMS**c**SFTNQVIAQLELWNE**k**	AASA (irrev.) Carbamidomethyl (rev.); Glu y-semialdehyde (irrev.); Carbamidomethyl (rev.); AASA (irrev.)
	30688090	ATMS3 (methionine synthase 3 [*Arabidopsis thaliana*]	**c**VKPPIIYGDITRPKA**m**TVFWSSMAQK EKVVVSTS**c**SLLHTAVDLVNEMKLDK	Cysteic acid (irrev.); Met sulfone (irrev.) Cysteic acid (irrev.)

	357119807	Predicted: 5-methyltetrahydropteroyltriglutamate--homocysteine methyltransferase-like [*Brachypodium distachyon*]	GMLTG**p**VTILNWSFVR D**k**LVVSTS**c**SLMhTAVDLVNET**k**	Glu y-semialdehyde (irrev.) AASA (irrev.); Carbamidomethyl (rev.) 2-oxohistidine (irrev.); AASA (irrev.)
Protein transport	30681617	clathrin heavy chain, putative [*Arabidopsis thaliana*]	GNLQIIVQA**c**KEY**c**EQLGVDA**c**IKLFEQFK LAQI**c**GLNIIIQVDDLEEVSEYYQNR	Cysteic acid (irrev.); S-nitrosocysteine (rev.); Cysteic acid (irrev.) Cysteic acid (irrev.)
	3641837	Nonclathrin coat protein gamma-like protein [*Arabidopsis thaliana*]	VA**m**THP**m**AVTN**c**NID**m**ESLISDQNRSIATLAITTLLK ITVLLKR**c**IYDSDDEVR	Met sulfone (irrev.); Met sulfone (irrev.); Cysteic acid (irrev.); Met sulfone (irrev.) Cysteic acid (irrev.)
	15220684	coatomer protein complex, subunit alpha, putative [*Arabidopsis thaliana*]	TLDVPIYITKVSGNTIF**c**LDRDGK TPSLL**m**PPTPI**mc**GGDWPLLR	Cysteic acid (irrev.) Met sulfone (irrev.); Met sulfone (irrev.); Cysteic acid (irrev.)
	2218152	type IIIa membrane protein cp-wap13 [*Vigna unguiculata*]	YIYTIDDD**c**FVAK ELIGPAMYFGLMGDGQ**p**IGR	Carbamidomethyl (rev.) Glu y-semialdehyde (irrev.)
Redox	15231228	sks11 (SKU5 Similar 11); copper ion binding / oxidoreductase [*Arabidopsis thaliana*]	YALNGVSHTD**p**ETPLK **k**NYNLLDAVSR	Glu y-semialdehyde (irrev.) AASA (irrev.)
	508725282	2-oxoacid dehydrogenases acyltransferase family protein isoform 1 [*Theobroma cacao*]	RTPVSGPKG**k**PQALQV**k** EEVA**p**AVPAAAPVAPAVWS**pk**	AASA (irrev.); AASA (irrev.) Glu y-semialdehyde (irrev.); Glu y-semialdehyde (irrev.); AASA (irrev.)
	15228896	superoxide dismutase (Mn), putative / manganese superoxide dismutase, putative [*Arabidopsis thaliana*]	LVVETTANQD**p**LVT**k** **m**TTTVIIIIFVAIFATTLHDARGAT**m**EP**c**LES**m**K	Glu y-semialdehyde (irrev.); AASA (irrev.) Met sulfone (irrev.); Met sulfone (irrev.); S-nitrosocysteine (rev.); Met sulfone (irrev.)
Uncharacterised	21593701	unknown [*Arabidopsis thaliana*]	VVDIPNS**m**TILDELLPISIEMAK **m**VADANGSSSSFNFLIYGK	Met sulfone (irrev.) Met sulfone (irrev.)
	118484713	unknown [*Populus trichocarpa*]	GIELIASENFTSFAVIEALGSALTN**k** IMGLDL**p**SGGHLTHGYYTSGG**k**	AASA (irrev.) Glu y-semialdehyde (irrev.); AASA (irrev.)

	217072994	unknown [*Medicago truncatula*]	DLYGNIVLSGGSTMF**p**GIADR YPIEHGIVSNWDD**m**EK	Glu y-semialdehyde (irrev.) Met sulfone (irrev.)
	297738640	unnamed protein product [*Vitis vinifera*]	LETL**c**DLYETLAITQSVIFVNTR VQVGVFSATM**p**PEALEITR	Carbamidomethyl (rev.) Glu y-semialdehyde (irrev.)
	224098390	predicted protein [*Populus trichocarpa*]	NQVAMN**p**VNTVFDAK DAGVIAGLNV**m**R	Glu y-semialdehyde (irrev.) Met sulfone (irrev.)
	219885633	unknown [*Zea mays*]	EQVFSTYSDNQ**p**GVLIQVYEGER NQVAMN**p**INTVFDAK	Glu y-semialdehyde (irrev.) Glu y-semialdehyde (irrev.)
	326510251	predicted protein [*Hordeum vulgare*]	GVQYLNEIKDSVVAGFQWAS**k** ITDGALVVVD**c**IEGV**c**VQTETVLR SINPDEAVAYGAAVQAAILSGEGNE**k** NQVAMN**p**INTVFDAK	AASA (irrev.) Carbamidomethyl (rev.); Carbamidomethyl (rev.) AASA (irrev.) Glu y-semialdehyde (irrev.)
	125535351	hypothetical protein OsI_37065 [*Oryza sativa Indica Group*]	QFAAEEISS**m**VLIK NQVAMN**p**INTVFDAK	Met sulfone (irrev.) Glu y-semialdehyde (irrev.)
	147857569	hypothetical protein VITISV_001328 [*Vitis vinifera*]	LIDD**m**VAYALK SDGGYVWA**c**K	Met sulfone (irrev.) Carbamidomethyl (rev.)
	363814428	uncharacterized protein LOC100781043 [*Glycine max*]	LTTPSFGDLNHLISATMSGVT**cc**LR GHYTEGAELIDSVLDVVR**k**	Carbamidomethyl (rev.); Carbamidomethyl (rev.) AASA (irrev.)
	388495536	unknown [*Lotus japonicus*]	ILLTSTSEVYGDPLIH**p**QPESY**w**GNVNPIGVR AKELLGWEP**k**	Glu y-semialdehyde (irrev.); Kynurenine (irrev.) AASA (irrev.)
	242052109	hypothetical protein SORBIDRAFT_03g006130 [*Sorghum bicolor*]	VIA**c**VGETLEQR GGAFTGEVSAEMLVNLGV**p**WVILGHSER	Carbamidomethyl (rev.) Glu y-semialdehyde (irrev.)
	462407437	hypothetical protein PRUPE_ppa008423mg [*Prunus persica*]	VLVTGAAGQIGYAIV**p**MIAR KLSSALSAASSA**c**DHIR	Glu y-semialdehyde (irrev.) Carbamidomethyl (rev.)

Table S3. Oxidative modification of protein using H_2O_2 (Chapter 4)

Functional group	Accession number	Name of the protein	Identified peptide	Modifications
Cytoskeleton	224088196	actin 3 [*Populus trichocarpa*]	DLYGNIVLSGGSTMF**p**GIADR YPIEHGIVSNWDD**m**EK	Glu y-semialdehyde (irrev.) Met sulfone (irrev.)
	15222873	TUB1; GTPas [*Arabidopsis thaliana*]	SG**p**YGQIFRPDNFVFGQSGAGNNWAK LHFF**m**VGFAPLTSR **m**MLTFSVFPSPK	Glu y-semialdehyde (irrev.) Met sulfone (irrev.) Met sulfone (irrev.)
	15451226	beta tubulin [*Arabidopsis thaliana*]	SG**p**YGQIFRPDNFVFGQSGAGNNWAK LHFF**m**VGFAPLTSR	Glu y-semialdehyde (irrev.) Met sulfone (irrev.)
	353259709	alpha-tubulin [*Rosa multiflora*]	**k**LADN**c**TGLQGFLVFNAVGGGTGSGLGSLLLER AV**cm**ISNSTSVAEVFSR TIQFVDW**c**PTGF**k** EIVDL**c**LD**r**	AASA (irrev.); Carbamidomethyl (rev.) Carbamidomethyl (rev.); Met sulfone (irrev.) Carbamidomethyl (rev.); AASA (irrev.); Carbamidomethyl (rev.); Glu y-semialdehyde (irrev.)
	225452767	PREDICTED: tubulin alpha chain [*Vitis vinifera*]	LADN**c**TGLQGFLVF**h**AVGGGTGSGLGSLLLER AV**c**MISNSTSVAEVFSR TIQFVDW**c**PTGF**k** EIVDL**c**LD**r**	Carbamidomethyl (rev.); 2-Oxohistidin (irrev.) Carbamidomethyl (rev.) Carbamidomethyl (rev.); AASA (irrev.); Carbamidomethyl (rev.); Glu y-semialdehyde (irrev.)
	15239914	TUB6 (BETA-6 TUBULIN) [*Arabidopsis thaliana*]	LHFF**m**VGFAPLTSR **m**MLTFSVFPSPK	Met sulfone (irrev.) Met sulfone (irrev.)
	227069387	actin 2 [*Picea abies*]	DLYGNIVLSGGSTMF**p**GIADR YPIEHGIVTN**w**DD**m**EK	Glu y-semialdehyde (irrev.) Kynurenine (irrev.); Met sulfone (irrev.)
	59709767	beta-tubulin [*Lolium perenne*]	LHFF**m**VGFA**p**LTSR LTTPSFGDLNHLISATMSGVT**cc**LR	Met sulfone (irrev.); Glu y-semialdehyde (irrev.) Carbamidomethyl (rev.); Carbamidomethyl (rev.)
	15231447	ACT12 (ACTIN-12) [*Arabidopsis thaliana*]	EITALAPSS**m**K CDVDI**r**KDLYGNIVLSGGTTMFGGIGD**r**	Met sulfone (irrev.) Glu y-semialdehyde (irrev.); Glu y-semialdehyde (irrev.)

	110742192	tubulin alpha-2/alpha-4 chain [*Arabidopsis thaliana*]	IHF**m**LSSYAPVISAEK RTIQFVD**w**CPTGFK	Met sulfone (irrev.) Kynurenine (irrev.)
	15224051	fimbrin-like protein, putative [*Arabidopsis thaliana*]	VS**p**GSVN**w**KHANKP**p**IK**m**PFK LLLAFLWQL**mr**YT**m**LQILNNL**r**	Glu y-semialdehyde (irrev.); Kynurenine (irrev.); Glu y-semialdehyde (irrev.); Met sulfone (irrev.) Met sulfone (irrev.); Glu y-semialdehyde (irrev.); Met sulfone (irrev.); Glu y-semialdehyde (irrev.)
	153799899	beta-tubulin [*Eucalyptus grandis*]	NSSYFVE**w**I**p**NNV**k** LATPTFGDLNHLISATMSGVT**cc**LR	Kynurenine (irrev.); Glu y-semialdehyde (irrev.); AASA (irrev.) Carbamidomethyl (rev.); Carbamidomethyl (rev.)
	166582	actin-1 [*Arabidopsis thaliana*]	DLYGNIVLSGGTT**m**FPGIADR EITALAPSS**m**K	Met sulfone (irrev.) Met sulfone (irrev.)
Metabolism	357498709	Enolase [*Medicago truncatula*]	KYGQDATNVGDEGGFAPNIQEN**k**EGLELLK LGANAILAVSLAV**c**K SFVSDYPIVSIEDPFDQDD**w**E**h**YS**k**	AASA (irrev.); Cysteic acid (irrev.) Kynurenine (irrev.); 2-oxohistidine (irrev.); AASA (irrev.);
	15239843	malate dehydrogenase, cytosolic, putative [*Arabidopsis thaliana*]	VLVTGAAGQIGYALVP**m**IAR **m**ELVDAAFPLLK	Met sulfone (irrev.) Met sulfone (irrev.)
	307136112	glyceraldehyde-3-phosphate dehydrogenase [*Cucumis melo*]	VALQRDDVELVAVNDPFITTDYMTYMF**k** DA**p**MFVVGVNEK	AASA (irrev.); Glu y-semialdehyde (irrev.)
	9758328	xylose isomerase [*Arabidopsis thaliana*]	Y**m**HGGATSSEVGVYAYAAAQV**k** ILEEGSLSELV**r**K**r**	Met sulfone (irrev.); AASA (irrev.); Glu y-semialdehyde (irrev.); Glu y-semialdehyde (irrev.)
	15239897	ACLB-2 (ATP citrate lyase subunit B 2); ATP citrate synthase [*Arabidopsis thaliana*]	EVIP**p**QIPEDLNSAIK H**p**WEDVLYTK	Glu y-semialdehyde (irrev.) Glu y-semialdehyde (irrev.)
	18404382	malate dehydrogenase (NAD), mitochondrial [*Arabidopsis thaliana*]	VAILGAAGGIGQPLALL**m**K DDLF**n**INAGIV**k**	Met sulfone (irrev.) Deamidation (rev.); AASA (irrev.);

	15230764	ACLB-1; ATP citrate synthase [*Arabidopsis thaliana*]	SIGLIGHTFDQ**k** ANNKVIIG**p**ATVGGVQAGAFK	AASA (irrev.) Glu y-semialdehyde (irrev.)
	4586021	cytoplasmic aconitate hydratase [*Arabidopsis thaliana*]	NGVTATDLVLTVTQ**m**L**r** ATIAN**m**SPEYGAT**m**GFFPVDHVTLQYLK	Met sulfone (irrev.); Glu y-semialdehyde (irrev.) Met sulfone (irrev.); Met sulfone (irrev.)
	15226950	NAD-dependent epimerase/dehydratase family protein [*Arabidopsis thaliana*]	VVS**n**FIAQALR TNVIGTLN**m**LGLAK	Deamidation (rev.) Met sulfone (irrev.)
	15231715	fructose-bisphosphate aldolase, putative [*Arabidopsis thaliana*]	K**p**WSLSFSFGR ANSEATLGTY**k**	Glu y-semialdehyde (irrev.) AASA (irrev.);
	22329337	ATSPS3F (sucrose phosphate synthase 3F); sucrose-phosphate synthase [*Arabidopsis thaliana*]	FFTNPHKPMILALS**r**PD**p**K AFGEC**r**PL**r**ELANLTLI**m**GN**r**	Glu y-semialdehyde (irrev.); Glu y-semialdehyde (irrev.) Glu y-semialdehyde (irrev.); Glu y-semialdehyde (irrev.); Met sulfone (irrev.); Glu y-semialdehyde (irrev.)
	15228048	MAT3 (methionine adenosyltransferase 3); copper ion binding / methionine adenosyltransferase [*Arabidopsis thaliana*]	IIIDTYGGWGAHGGGAFSG**k** NKT**c**PWLR**p**DGKTQVTVEYK	AASA (irrev.); Cysteic acid (irrev.); Glu y-semialdehyde (irrev.)
	508716212	Enolase [*Theobroma cacao*]	KYGQDATNVGDEGGFAPNIQEN**k**EGLELLK LGANAILAVSLAV**c**K	AASA (irrev.) Cysteic acid (irrev.)
	508713247	Serine hydroxymethyltransferase 4 isoform 1 [*Theobroma cacao*]	GIELIASENFTSFAVIEALGSALTN**k** YYGGNEFIDEIENL**c**R IMGLDL**p**SGGHLTHGYYTSGG**k**	AASA (irrev.) Carbamidomethyl (rev.) Glu y-semialdehyde (irrev.); AASA (irrev.)
	84619270	soluble inorganic pyrophosphatase [*Papaver rhoeas*] **Pr-p26.1a**	AIGL**mp**MIDQGEKDDK RSVAAH**pwh**DLEIGPGAPSVVNAVVEIT**k** TL**c**EDNDPLDVLILMQE**p**VLPG**c**FLR	Met sulfone (irrev.); Glu y-semialdehyde (irrev.) Glu y-semialdehyde (irrev.); Kynurenine (irrev.); 2-oxohistidine (irrev.); AASA (irrev.) Carbamidomethyl (rev.)Glu y-semialdehyde (irrev.); Carbamidomethyl (rev.)
	10798652	malate dehydrogenase [*Nicotiana tabacum*]	KLSSALSAASSA**c**D**h**IR	Carbamidomethyl (rev.); 2-oxohistidine (irrev.)

			VLVTGAAGQIGYALV**p**MIAR	Glu y-semialdehyde (irrev.)
	297795089	cytosolic malate dehydrogenase [*Arabidopsis lyrata subsp. lyrata*]	KLSSALSAASSA**c**DHIR VLVTGAAGQIGYALV**p**MIAR	Carbamidomethyl (rev.) Glu y-semialdehyde (irrev.)
	77416931	UDP-glucose:protein transglucosylase-like [*Solanum tuberosum*]	YDDMWAGW**c**IK GTLF**p**M**c**GMNLAFDR	Carbamidomethyl (rev.) Glu y-semialdehyde (irrev.);Carbamidomethyl (rev.)
	470141120	PREDICTED: citrate synthase, glyoxysomal-like [*Fragaria vesca*]	HLASSGVDVYTALAGAVGALYGPLHGGANEAV L**k** AMGF**p**TEFFPVLFAIPR	AASA (irrev.) Glu y-semialdehyde (irrev.)
	22330456	pfkB-type carbohydrate kinase family protein [*Arabidopsis thaliana*]	EF**m**FYR LSNSRSNLKG**r**	Met sulfone (irrev.) Glu y-semialdehyde (irrev.)
Energy production pathways	297806945	ATP synthase beta chain 1, mitochondrial [*Arabidopsis lyrata subsp. lyrata*]	TIA**m**DGTEGLVR VLNTGA**p**ITVPVGR	Met sulfone (irrev.) Glu y-semialdehyde (irrev.)
	15219412	PGK (phosphoglycerate kinase); phosphoglycerate kinase [*Arabidopsis thaliana*]	ELDYLVGAVAN**p**K K**p**FAAIVGGSKVSTK	Glu y-semialdehyde (irrev.) Glu y-semialdehyde (irrev.)
	15219234	VHA-A (vacuolar atp synthase subunit A) [*Arabidopsis thaliana*]	TTLVANTSN**m**PVAAR WAEALREISG**r**	Met sulfone (irrev.) Glu y-semialdehyde (irrev.)
	15229126	AHA8 (Arabidopsis H(+)-ATPase 8); ATPase [*Arabidopsis thaliana*]	LG**m**GTN**m**YPSTSLLGNSK ADGFAGVFPEH**k**	Met sulfone (irrev.); Met sulfone (irrev.) AASA (irrev.)
	15233891	V-type proton ATPase subunit B2 [*Arabidopsis thaliana*]	IALTTAEYLAYE**c**G**k** IPLFSAAGLPHNEIAAQI**c**R	Carbamidomethyl (rev.); AASA (irrev.) Carbamidomethyl (rev.)
	18396215	MOD1 (MOSAIC DEATH 1); [*Arabidopsis thaliana*]	HFL**p**IMNPGGASISLTYIASER RPSMSS**p**SKILK	Glu y-semialdehyde (irrev.) Glu y-semialdehyde (irrev.)
	15227987	LOS2; copper ion binding / phosphopyruvate hydratase [*Arabidopsis thaliana*]	LA**m**QEFMIL**p**VGAASFK **m**GVEVYHHLK	Met sulfone (irrev.); Glu y-semialdehyde (irrev.) Met sulfone (irrev.)

	297806945	ATP synthase beta chain 1, mitochondrial [*Arabidopsis lyrata subsp. lyrata*]	TIA**m**DGTEGLVR LGN**r**NP**r**LPS**p**SPAR	Met sulfone (irrev.) Glu y-semialdehyde (irrev.); Glu y-semialdehyde (irrev.); Glu y-semialdehyde (irrev.)
	15233891	vacuolar ATP synthase subunit B, [*Arabidopsis thaliana*]	EVSAA**r**EEV**p**GR AVVQVFEGTSGIDN**k**	Glu y-semialdehyde (irrev.); Glu y-semialdehyde (irrev.) AASA (irrev.)
Stress related	38325815	heat shock protein 70-3 [*Nicotiana tabacum*]	SIN**p**DEAVAYGAAVQAAILSGEGNE**k** NQVAMN**p**INTVFDAK	Glu y-semialdehyde (irrev.); AASA (irrev.) Glu y-semialdehyde (irrev.)
	357503161	Heat shock protein [*Medicago truncatula*]	SIN**p**DEAVAYGAAVQAAILSGEGNE**k** NQVAMN**p**VNTVFDAK	Glu y-semialdehyde (irrev.); AASA (irrev.) Glu y-semialdehyde (irrev.)
	15241849	HSC70-1 (heat shock cognate protein 70-1); ATP binding [*Arabidopsis thaliana*]	NALENYAYN**m**R ITITNDKG**r**	Met sulfone (irrev.) Glu y-semialdehyde (irrev.)
	15232682	heat shock cognate 70 kDa protein 3 (HSC70-3) [*Arabidopsis thaliana*]	NQVA**m**NPINTVFDAK NALENYAYN**m**R	Met sulfone (irrev.) Met sulfone (irrev.)
	15223533	ERD2 (early-responsive to dehydration 2); ATP binding [*Arabidopsis thaliana*]	QFAAEEISS**m**VLIK **m**VNHFVQEFK ELESV**w**STIITK**m**YQG	Met sulfone (irrev.) Met sulfone (irrev.) Kynurenine (irrev.); Met sulfone (irrev.)
	1695719	luminal binding protein [*Arabidopsis thaliana*]	VFSPEEISA**m**LTK **m**KETTEAYLGKK DAVVTV**p**AYFNDAQ**r**QATK	Met sulfone (irrev.) Met sulfone (irrev.) Glu y-semialdehyde (irrev.); Glu y-semialdehyde (irrev.)
	15219109	Hsp70b ATP binding [*Arabidopsis thaliana*]	IINEPTAAAIAYGLDK**k** **cm**DPVEKVLK	AASA (irrev.) S-nitrosocysteine (rev.); Met sulfone (irrev.)
	15242459	MTHSC70-2 (MITOCHONDRIAL HSP70 2); ATP binding [*Arabidopsis thaliana*]	GVNPDEAVA**m**GAALQGGILR **m**V**p**YKIV**r**	Met sulfone (irrev.) Met sulfone (irrev.); Glu y-semialdehyde (irrev.); Glu y-semialdehyde (irrev.)
	15229559	HSP60 (heat shock protein 60); ATP binding [*Arabidopsis thaliana*]	MS**w**SRNYAAKEIK GIS**m**AVDAVVTNLK	Kynurenine (irrev.) Met sulfone (irrev.)

	357442729	Chaperonin CPN60-2 [*Medicago truncatula*]	QRPLLIVAEDIESDALATLILN**k** GYIS**p**YFITNQ**k**	AASA (irrev.) Glu γ-semialdehyde (irrev.); AASA (irrev.)
	15241115	HSP81-2 (heat shock protein 81-2); ATP binding [*Arabidopsis thaliana*]	DSS**m**AGYMSS**k** NLKLGIHEDSQN**r**TK	Met sulfone (irrev.); AASA (irrev.) Glu γ-semialdehyde (irrev.)
	225426230	Predicted: luminal-binding protein 5 [*Vitis vinifera*]	LGTVIGIDLGTTYS**c**VGVY**k** LKEVEAV**c**NPIITAVYQR	Carbamidomethyl (rev.); AASA (irrev.) Carbamidomethyl (rev.)
	56554972	heat shock protein 70 [*Medicago sativa*]	SIN**p**DEAVAYGAAVQAAILSGEGNE**k** IINEPTAAAIAYGLDK**k**	Glu γ-semialdehyde (irrev.); AASA (irrev.) AASA (irrev.)
	476003	HSP70 [*Hordeum vulgare subsp. vulgare*]	LGTVIGIDLGTTYS**c**VGVY**k** DILLLDVAPLTLGIETVGGVMT**k**	Carbamidomethyl (rev.); AASA (irrev.) AASA (irrev.)
Signalling/regulatory	470115786	Predicted: elongation factor 2-like [*Fragaria vesca subsp. vesca*]	GVQYLNEIKDSVVAGFQ**w**AS**k** VIENANVIMATYEDPLLGDVQVYPE**k** N**c**DPDGPL**m**LYVSK LYMEAR**p**LEDGLAEAIDDGR	Kynurenine (irrev.); AASA (irrev.) AASA (irrev.) Carbamidomethyl (rev.); Met sulfone (irrev.) Glu γ-semialdehyde (irrev.)
	38564733	initiation factor eIF4A-15 [*Helianthus annuus*]	LETL**c**DLYETLAITQSVIFVNTR VQVGVFSATM**p**PEALEITR	Carbamidomethyl (rev.) Glu γ-semialdehyde (irrev.)
	48527431	elongation factor 1-alpha 1 [*Elaeis guineensis*]	VGYN**p**E**k**IPFVPISGFEGDNMIER YY**c**TVIDAPGHR	Glu γ-semialdehyde (irrev.); AASA (irrev.) Carbamidomethyl (rev.)
	326694867	14-3-3 protein 3 [*Hevea brasiliensis*]	LAEQAERYEEMVEFME**k** QAFDEAIAELDTLGEESY**k**DSTLI**m**QLLR	AASA (irrev.) AASA (irrev.); Met sulfone (irrev.)
	374256019	putative 14-3-3 regulatory [*Elaeis guineensis*]	SAQDIALAELA**p**THPIR QAFDEAISELDSLGEESY**k**DSTLI**m**QLLR LAEQAERYEEMVEFME**k**	Glu γ-semialdehyde (irrev.) AASA (irrev.); Met sulfone (irrev.) AASA (irrev.)
	1170508	Eukaryotic initiation factor 4A-8 (eIF4A-8)	GLDVIQQA**q**SGTG**k** LETL**c**DLYETLAITQSVIFVNTR	Deamidation (rev.); AASA (irrev.) Carbamidomethyl (rev.)
	18411901	14-3-3-like protein GF14 omega [*Arabidopsis thaliana*]	SKIETELSGI**c**DGILK LAEQAERYEEMVEFME**k**	Carbamidomethyl (rev.) AASA (irrev.)

	351725929	14-3-3 protein SGF14h [*Glycine max*]	LAEQAERYEEMVEFME**k** QAFDEAIAELDTLGEESY**k**DSTL**l**m**m**QLLR	AASA (irrev.) AASA (irrev.); Met sulfone (irrev.)
	359496384	PREDICTED: rab GDP dissociation inhibitor alpha [*Vitis vinifera*]	IHKVPATDVEAL**k**SPLMGLFEK VPATDVEALKS**p**LMGLFE**k**	AASA (irrev.) Glu y-semialdehyde (irrev.); AASA (irrev.)
	6015054	RecName: Full=Elongation factor 1-alpha; Short=EF-1-alpha	VETGVIKPGMVVTFGPTGLTTEV**k** MI**p**TK**p**MVVETFAQYPPLGR	AASA (irrev.) Glu y-semialdehyde (irrev.); Glu y-semialdehyde (irrev.)
	225462164	PREDICTED: elongation factor 2-like isoform 1 [*Vitis vinifera*]	GVQYLNEIKDSVVAGFQ**w**AS**k** VIENANVIMATYEDPLLGDVQVYPE**k**	Kynurenine (irrev.); AASA (irrev.) AASA (irrev.)
	359496384	PREDICTED: rab GDP dissociation inhibitor alpha [*Vitis vinifera*]	IHKVPATDVEAL**k**SPLMGLFEK VPATDVEALKS**p**LMGLFE**k**	AASA (irrev.) Glu y-semialdehyde (irrev.); AASA (irrev.)
	168030217	Rab1/RabD-family small GTPase [*Physcomitrella patens*]	FADDSYLESYISTIGVDF**k** LLLIGDSGVG**k**	AASA (irrev.) AASA (irrev.)
	15221761	EIF4A-2; ATP-dependent helicase/ translation initiation factor [*Arabidopsis thaliana*]	**r**QSLRPD**c**IKMFVLDEADEMLS**r** DIIMREF**r**SGSS**r**	Glu y-semialdehyde (irrev.); S-nitrosocysteine (rev.); Glu y-semialdehyde (irrev.) Glu y-semialdehyde (irrev.); Glu y-semialdehyde (irrev.)
Amino acid/Protein biosynthesis	14532772	putative methionine synthase [*Arabidopsis thaliana*]	G**m**LTGPVTILN**w**SFVR KLNLPILPTTTIGSF**p**QTVELR	Met sulfone (irrev.);Kynurenine (irrev.) Glu y-semialdehyde (irrev.)
	30688090	ATMS3 (methionine synthase 3); 5-methyltetrahydropteroyltriglutamate-homocysteine S-methyltransferase/ methionine synthase [*Arabidopsis thaliana*]	G**m**LTGPVTILN**w**SFVR LQ**p**LASLP**rr**PPSLPP**p**SSATPSLPCATASR	Met sulfone (irrev.); Kynurenine (irrev.) Glu y-semialdehyde (irrev.); Glu y-semialdehyde (irrev.); Glu y-semialdehyde (irrev.); Glu y-semialdehyde (irrev.)
	347361140	methionine synthase [*Camellia sinensis*]	**k**LNLPILPTTTIGSFPQTIELR GMLTG**p**VTILNWSFVR	AASA (irrev.) Glu y-semialdehyde (irrev.)
	21592545	glycyl tRNA synthetase, putative [*Arabidopsis thaliana*]	DVLAV**m**EDFS**p**EQLGAK SGTPLVAEEKFAE**p**K	Met sulfone (irrev.); Glu y-semialdehyde (irrev.) Glu y-semialdehyde (irrev.)

	17017263	methionine synthase [*Zea mays*]	GMLTG**p**VTILNWSFVR AAGASWIQFDE**p**TLVLDLDSDK	Glu y-semialdehyde (irrev.) Glu y-semialdehyde (irrev.)
	15228048	S-adenosylmethionine synthase 3 [*Arabidopsis thaliana*]	**c**NVLVNIEQQSPDIAQGVHGHLT**k** KIIIDTYGGWGAHGGGAFSGKDPT**k**	Carbamidomethyl (rev.); AASA (irrev.) AASA (irrev.)
	15237069	PSAT; O-phospho-L-serine:2-oxoglutarate aminotransferase [*Arabidopsis thaliana*]	ASIYNA**m**PLAGVEK SV**r**SL**m**NVPFTLEK	Met sulfone (irrev.) Glu y-semialdehyde (irrev.); Met sulfone (irrev.)
Protein transport	12321552	clathrin heavy chain, putative [*Arabidopsis thaliana*]	FGFVPDLTHYLYTNN**m**LR FQSV**p**VQAGQTPPLLQYFGTLLTR LFSTRLNIPKLI**r**	Met sulfone (irrev.) Glu y-semialdehyde (irrev.) Glu y-semialdehyde (irrev.)
	3641837	Nonclathrin coat protein gamma-like protein [*Arabidopsis thaliana*]	AEMVILEAARAITELDGVTS**r** SQ**p**LAEKK ID**m**YRANAI**r**VL**c**R	Glu y-semialdehyde (irrev.) Glu y-semialdehyde (irrev.) Met sulfone (irrev.); Glu y-semialdehyde (irrev.); Cysteic acid (irrev.)
Redox	15231228	sks11 (SKU5 Similar 11); copper ion binding / oxidoreductase [*Arabidopsis thaliana*]	DYY**m**VASSR SGKGDGSDA**p**LFTLK**p**GK YALNGVSHTD**p**ETPLK	Met sulfone (irrev.) Glu y-semialdehyde (irrev.); Glu y-semialdehyde (irrev.) Glu y-semialdehyde (irrev.)
	7076784	2-oxoglutarate dehydrogenase, E1 subunit-like protein [*Arabidopsis thaliana*]	EAMN**m**GAFSYIS**p**R EKIETPT**p**W**r**YNR RTPVSGPKG**k**PQALQV**k**	Met sulfone (irrev.); Glu y-semialdehyde (irrev.) Glu y-semialdehyde (irrev.); Glu y-semialdehyde (irrev.) AASA (irrev.); AASA (irrev.)
	351722675	ferric leghemoglobin reductase-2 precursor [*Glycine max*]	LTLE**p**AAGGDQTTLEADVVLVSAGR AEEDGVA**c**VEYIAGK	Glu y-semialdehyde (irrev.) Carbamidomethyl (rev.)
	6682242	putative ascorbate peroxidase [*Arabidopsis thaliana*]	EILSGEKEGLLQLPTD**k** TKTGG**p**FGTIR	AASA (irrev.) Glu y-semialdehyde (irrev.)
Uncharacterised	298204460	unnamed protein product [*Vitis vinifera*]	EGVPTAVS**h**GLWLNIPDYDAPTQLV**k**PLER YIFTIDDD**c**FVAKDPSG**k** GTLFPM**c**GMNLAFDR	2-oxohistidine (irrev.); AASA (irrev.); Carbamidomethyl (rev.); AASA (irrev.) Carbamidomethyl (rev.)
	168038068	predicted protein [*Physcomitrella patens*]	YRVE**n**LYEGPLDDQYANAIR LLEPVYLVEIQAPEGALGGIYGVLNQ**k**	Deamidation (rev.) AASA (irrev.);

	462397785	hypothetical protein PRUPE_ppa007696mg [*Prunus persica*]	VD**k**GTVELAGTNGETTTQGLDGLAQR K**pw**SLSFSFGR	AASA (irrev.); Glu y-semialdehyde (irrev.); Kynurenine (irrev.)
	224120656	predicted protein [*Populus trichocarpa*]	EGVPTAVS**h**GLWLNIPDYDAPTQLV**k**PLER YIFTIDDD**c**FVAKDPSG**k**	2-oxohistidine (irrev.); AASA (irrev.); Carbamidomethyl (rev.); AASA (irrev.);
	326510251	predicted protein [*Hordeum vulgare*]	GVQYLNEIKDSVVAGFQWAS**k** N**c**DPDG**p**LMLYVSK	AASA (irrev.); Carbamidomethyl (rev.); Glu y-semialdehyde (irrev.)
	217071826	unknown [*Medicago truncatula*]	LHFF**m**VGFAPLTSR LSTPSFGDLNHLISATMSGVT**cc**LR	Met sulfone (irrev.) Carbamidomethyl (rev.); Carbamidomethyl (rev.)
	224087339	predicted protein [*Populus trichocarpa*]	**k**AMGDAAVSAAASIGYIGVGTVEFLLDER DAPMFVMGVNE**k**SYTPDLNIISNAS**c**TTN**c**LAPL A**k**	AASA (irrev.) AASA (irrev.); Carbamidomethyl (rev.); Carbamidomethyl (rev.); AASA (irrev.);
	255642137	unknown [*Glycine max*]	NDYYGGESTSLNLIQLW**k** E**c**ILSGLLSVDGLK	AASA (irrev.) Carbamidomethyl (rev.)
	363814428	uncharacterized protein LOC100781043 [*Glycine max*]	LTTPSFGDLNHLISATMSGVT**cc**LR GHYTEGAELIDSVLDVVR**k**	Carbamidomethyl (rev.); Carbamidomethyl (rev.) AASA (irrev.)
	110741581	hypothetical protein [*Arabidopsis thaliana*]	**m**EQKSVLLSALGVGVGLGIGLASGQSLG**r** TTNL**c**FDEKLFLQSLYK	Met sulfoxide (rev.); Glu y-semialdehyde (irrev.) S-nitrosocysteine (rev.)
	147857569	hypothetical protein VITISV_001328 [*Vitis vinifera*]	GGETSTNSIASIFA**w**SR SDGGYVWA**c**K	Kynurenine (irrev.) Carbamidomethyl (rev.)
	118484164	unknown [*Populus trichocarpa*]	VNSQLISNV**c**TDALSAEK QLLLHPESDDSAQLSQIETE**k**	Carbamidomethyl (rev.) AASA (irrev.)

Table S4. Modified proteins identified by MS in F-actin pull down using germination medium (Untreated)(Chapter 5)

Functional Class	Accession number	Name of the protein	Identified peptide	Modifications
Metabolism	148508784	glyceraldehyde-3-phosphate dehydrogenase [*Triticum aestivum*]	LTG**m**AFRVPTVDVSVVDLTVR FGIVEGLMTTVHA**m**TATQK	Met sulfoxide (rev.) Met sulfoxide (rev.)
	226496759	pyruvate kinase, cytosolic isozyme [*Zea mays*]	VEN**q**EGVVNFDEILR TKLV**c**TLGPASR	Deamidation (rev.) Carbamidomethylation (rev.)
	346983237	D-3-phosphoglycerate dehydrogenase [*Pinus pinaster*]	IGEV**p**AIEEFVYLK TLAV**m**GFGK	Glu-y-semialdehyde (irrev.) Met sulfoxide(rev.)
Cytoskeleton	224088196	actin 3 [*Populus trichocarpa*]	NGTG**m**VKAGFAGDDAPRAV EITALAPSS**m**K	Met sulfoxide(rev.) Met sulfoxide(rev.)
Energy production	460367518	PREDICTED: ADP,ATP carrier protein, mitochondrial-like [*Solanum lycopersicum*]	LLIQNQDE**m**IK VKLLIQNQDE**m**IK	Met sulfoxide(rev.) Met sulfoxide(rev.)
Stress related protein	30025966	heat shock protein 70 [*Nicotiana tabacum*]	ELESI**c**NPIIAK NALENYAYN**m**R	Carbamidomethylation (rev.) Met sulfoxide (rev.)
Biosynthetic pathway	14532772	putative methionine synthase [*Arabidopsis thaliana*]	YGAGIGPGVYDIHS**p**R G**m**LTGPVTILNWSFVR	Glu-y-semialdehyde (irrev.) Met sulfoxide(rev.)
	195623672	RHM1 [*Zea mays*]	**m**PISSDLSNPR GNNVYGPN**q**FPEK	Met sulfoxide(rev.) Deamidation (rev.)
Ion transport	60592630	vacuolar H+-ATPase catalytic subunit [*Pyrus communis*]	LAE**m**PADSGYPAYLAAR TTLVANTSN**m**PVAAR	Met sulfoxide(rev.) Met sulfoxide(rev.)
	356521645	PREDICTED: V-type proton ATPase catalytic	LAE**m**PADSGYPAYLAAR	Met sulfoxide(rev.)

		subunit A-like [*Glycine max*]	TTLVANTSN**m**PVAAR	Met sulfoxide(rev.)
	508782369	H(+)-ATPase 8 [*Theobroma cacao*]	VENQDAIDASIVG**m**LGDPK LG**m**GTN**m**YPSSSLLGQSK	Met sulfoxide(rev.) Met sulfoxide(rev.); Met sulfoxide(rev.)
Uncharacterized protein	224119602	predicted protein [*Populus trichocarpa*]	SYTPDL**n**IVSNAS**c**TTN**c**LAPLA**k** LTG**m**AFRVPTVDVSVVDLTVR	Deamidation (rev.); Carbamidomethylation (rev.) Carbamidomethylation (rev.) Met sulfoxide(rev.)
	217072994	unknown [*Medicago truncatula*]	SYEL**p**DGQVITIGSER DLYGNIVLSGGST**m**FPGIADR	Glu-y-semialdehyde (irrev.) Met sulfoxide(rev.)
	194707656	unknown [*Zea mays*]	DAP**m**FVVGVNEK LTGMSFRVPTVDVSVVDLTV**r**	Met sulfoxide(rev.) Deamidation (rev.)
	388508708	unknown [*Lotus japonicus*]	TN**m**V**m**VFGEITTK IIIDTYGGWGAHGGGAFSGKDPT**k**VDR	Met sulfoxide(rev.); Met sulfoxide(rev.) AASA (irrev.)
	297740315	unnamed protein product [*Vitis vinifera*]	MKLIQIQ**p**ELGLR D**p**VLNMIAEKLG**k**	Glu-y-semialdehyde (irrev.) Glu-y-semialdehyde (irrev.); AASA (irrev.)
	6143867	hypothetical protein [*Arabidopsis thaliana*]	T**c**LEGAEVIPA**q**EIAE**c**EQSQSV**q**VVEPEVR AVRSPGYWVV**nn**RPK	Carbamidomethylation (rev.); Deamidation (rev.); Carbamidomethylation (rev.); Deamidation (rev.) Deamidation (rev.); Deamidation (rev.)

Table S5. Modified proteins identified by MS in F-actin pull down using recombinant *PrsS* (Chapter 5)

Functional Class	Accession number	Name of the protein	Identified peptide	Modifications
Signalling/regulatory/Ras related protein	115345320	Elongation factor 1 alpha [*Capsicum chinense*]	VETGIVK**p**G**m**VVTFGPTGLTTEVK IGGIGTV**p**VGR LPLQDVY**k**	Glu-y-semialdehyde (irrev.); Met sulfone (irrev.) Glu-y-semialdehyde (irrev.) AASA (irrev.)
	357496973	Elongation factor 1-alpha [*Medicago truncatula*]	IGGIGTV**p**VGR VETGIVK**p**G**m**VVTFGPTGLTTEVK	Glu-y-semialdehyde (irrev.) Glu-y-semialdehyde (irrev.); Met sulfone (irrev.)
	326694867	14-3-3 protein 3 [*Hevea brasiliensis*]	QAFDEAIAELDTLGEESY**k** YEE**m**VEF**m**EK DSTLI**m**QLLR	AASA (irrev.) Met sulfone (irrev.); Met sulfone (irrev.) Met sulfone (irrev.)
	225451995	PREDICTED: 14-3-3 protein 4 [*Vitis vinifera*]	SAQDIALAELA**p**T**hp**IR YEE**m**VEF**m**EK DSTLI**m**QLLR	Glu-y-semialdehyde (irrev.); 2-Oxohistidine (irrev.); Glu-y-semialdehyde (irrev.) Met sulfone (irrev.); Met sulfone (irrev.) Met sulfoxide (rev.)
	15232210	RAB GDP dissociation inhibitor 2 [*Arabidopsis thaliana*]	IV**c**DPSYLP**n**K VIGVTSEGETA**k**	Carbamidomethyl (rev.); Deamidation (rev.) AASA (irrev.)
Metabolism	32478662	cytosolic glyceraldehyde-3-phosphate dehydrogenase [*Triticum aestivum*]	FGIVEGL**m**TTVHA**m**TATQK AASFNII**p**SSTGAAK	Met sulfone (irrev.); Met sulfone (irrev.) Glu-y-semialdehyde (irrev.)
	307136111	glyceraldehyde-3-phosphate dehydrogenase [*Cucumis melo*]	DAP**m**FVVGVNEK FGIVEGL**m**TTVHSMTATQK DA**p**MFVVGVNEK	Met sulfone (irrev.) Met sulfone (irrev.) Glu-y-semialdehyde (irrev.)

			IGI**n**GFGR	Deamidation (rev.)
	508708076	ATP synthase alpha/beta family protein isoform 1 [*Theobroma cacao*]	l**p**SAVGYQPTLATDLGGLQER TVLI**m**ELINNVAK TIA**m**DGTEGLVR	Glu-y-semialdehyde (irrev.) Met sulfone (irrev.) Met sulfoxide (rev.)
	514815392	PREDICTED: UDP-glucose 6-dehydrogenase 2-like [*Setaria italica*]	ETPAIDV**c**NGLLGDK STV**p**VKTAEAIEK	Carbamidomethyl (rev.) Glu-y-semialdehyde (irrev.)
Cytoskeleton	93359562	alpha-tubulin [*Phaseolus vulgaris*]	AIFVDLE**p**TVIDEVR TVGGGDDAFNTFFSETGAG**k**	Glu-y-semialdehyde (irrev.) AASA (irrev.)
	224088196	actin 3 [*Populus trichocarpa*]	VAPEEH**p**VLLTEAPLNPK EITALAPSS**m**K	Glu-y-semialdehyde (irrev.) Met sulfone (irrev.)
	324331817	actin [*Camellia sinensis*]	SYEL**p**DGQVITIGAER EITALAPSS**m**K	Glu-y-semialdehyde (irrev.) Met sulfone (irrev.)
	15242516	actin 7 [*Arabidopsis thaliana*]	VAPEEH**p**VLLTEAPLNPK DLYGNIVLSGGST**m**FPGIADR NYELPDG**q**VITIGAER	Glu-y-semialdehyde (irrev.) Met sulfone (irrev.) Deamidation (rev.)
	2944389	actin 4 [*Glycine max*]	LAYIALDYEQELETS**k** SYEL**p**DGQVITIGAER	AASA (irrev.) Glu-y-semialdehyde (irrev.)
	1498344	actin, partial [*Glycine max*]	LAYIALDYEQELETS**k** SYEL**p**DGQVITIGSER	AASA (irrev.) Glu-y-semialdehyde (irrev.)

Electron transport	460413924	Cytochrome c1-1, heme protein, mitochondrial-like isoform 2 [*Solanum lycopersicum*]	DLVGVAYTEEET**k** FANGGAY**p**PDLSLITK	AASA (irrev.) Glu-y-semialdehyde (irrev.)
Energy production pathways	508704803	ADP/ATP carrier 2 [*Theobroma cacao*]	VKLLIQNQDE**m**IK LLIQNQDE**m**LK **m**M**m**TSGEAVKYK	Met sulfone (irrev.) Met sulfone (irrev.) Met sulfone (irrev.); Met sulfone (irrev.)
Stress/Chaperonin	470143740	PREDICTED: heat shock cognate 70 kDa protein-like [*Fragaria vesca*]	DAGVIAGLNV**m**R ELESL**c**NPIIAK	Met sulfone (irrev.) Carbamidomethyl (rev.)
	56202189	putative heat shock protein 82 [*Oryza sativa*]	GIVDSEDL**p**LNISR SDLV**n**NLGTIAR	Glu-y-semialdehyde (irrev.) Deamidation (rev.)
	356534858	PREDICTED: chaperonin CPN60-2, mitochondrial-like isoform 2 [*Glycine max*]	AGIID**p**LKVIR NVVIEQSFGAP**k**	Glu-y-semialdehyde (irrev.) AASA (irrev.)
	30025966	heat shock protein 70 [*Nicotiana tabacum*]	IINEPTAAAIAYGLD**k**K ELESI**c**NPIIAK NALENYAYN**m**R NQVA**m**NPINTVFDAK	AASA (irrev.) Carbamidomethyl (rev.) Met sulfone (irrev.) Met sulfoxide (rev.)
	470111876	PREDICTED: heat shock cognate 70 kDa protein-like [*Fragaria vesca*]	IINE**p**TAAAIAYGLDK **n**AVITVPAYFNDAQR	Glu-y-semialdehyde (irrev.) Deamidation (rev.)
Biosynthetic pathway	195623672	RHM1 [*Zea mays*]	VV**n**IP**n**SMTILDELLPISVEMA**k** AGAE**m**LV**m**AYGR	Deamidation (rev.); Deamidation (rev.); AASA (irrev.) Met sulfone (irrev.); Met sulfone (irrev.)
	460373499	PREDICTED: phosphoserine aminotransferase,	VFNFAAG**p**ATLPENVLQK	Glu-y-semialdehyde (irrev.);

		chloroplastic-like [*Solanum lycopersicum*]	ASIYNA**m**PLAGVEK	Met sulfone (irrev.)
Ion transport	356521645	PREDICTED: V-type proton ATPase catalytic subunit A-like [*Glycine max*]	LAE**m**PADSGYPAYLAAR TTLVANTSN**m**PVAAR	Met sulfone (irrev.) Met sulfone (irrev.)
	15220197	H(+)-ATPase 9 [*Arabidopsis thaliana*]	**w**SEQEAAILVPGDIISIK LS**q**QGAIT**k**	Kynurenine (irrev) Deamidation (rev.); AASA (irrev.)
	15219234	V-type proton ATPase catalytic subunit A [*Arabidopsis thaliana*]	LAE**m**PADSGYPAYLAAR TTLVANTSN**m**PVAAR	Met sulfone (irrev.) Met sulfone (irrev.)
	225442287	PREDICTED: plasma membrane ATPase-like isoform 1 [*Vitis vinifera*]	LG**m**GTN**m**Y**p**SSSLLGQSK **m**ITGDQLAIGK	Met sulfone (irrev.); Met sulfone (irrev.); Glu-y-semialdehyde (irrev.) Met sulfone (irrev.)
	225462986	PREDICTED: ATPase 8, plasma membrane-type [*Vitis vinifera*]	VENQDAIDASIVG**m**LGDPK LG**m**GTN**m**YPSSSLLGQSK	Met sulfone (irrev.) Met sulfone (irrev.); Met sulfone (irrev.)
Vesicle trafficking pathways	443299013	clathrin heavy chain 1 [*Zea mays*]	EAAELAAES**p**QGLLR FQSV**p**VQAGQTPPLLQYFGTLLTR	Glu-y-semialdehyde (irrev.) Glu-y-semialdehyde (irrev.)
Uncharacterized proteins	326496176	predicted protein [*Hordeum vulgare*]	**n**YELPDGQVITIGSER VA**p**EEHPVLLTEAPLNPK FGIVEGLMTTV**h**AMTATQK LTG**m**AFR	Deamidation (rev.) Glu-y-semialdehyde (irrev.) 2-oxohistidine (irrev.) Met sulfone (irrev.)
	217071944	unknown [*Medicago truncatula*]	GL**c**GGINSTSVK	Carbamidomethyl (rev.)

			qASITTELIEIISGASALTG	Deamidation (rev.)
	219887485	unknown [*Zea mays*]	ALGIDTVPVLVGPVSYLLLSKPA**k** YGAGIG**p**GVYDIHSPR	AASA (irrev.) Glu-y-semialdehyde (irrev.)
	296085909	unnamed protein product [*Vitis vinifera*]	YGAGIG**p**GVYDIHSPR I**p**STEEIADR	Glu-y-semialdehyde (irrev.) Glu-y-semialdehyde (irrev.)
	255642128	unknown [*Glycine max*]	LII**c**GGSAYPR ANAVALGNYL**m**G**k**	Carbamidomethyl (rev.) Met sulfone (irrev.); AASA (irrev.)

Table S6. Modified proteins identified by MS in F-actin pull down using H_2O_2 (Chapter 5)

Functional class	Accession number	Name of the protein	Identified peptied	Type of modification
Signalling/regulatory/ Ras related protein	326694867	14-3-3 protein 3 [*Hevea brasiliensis*]	YEE**m**VEF**m**EK DSTLI**m**QLLR	Met sulfone (irrev.); Met sulfone (irrev.) Met sulfone (irrev.)
	359488689	PREDICTED: ADP-ribosylation factor [*Vitis vinifera*]	MLNEDELRDSVLLVFANKQDL**p**NAMNAAEITDK QDLPNA**m**NAAEITDK IL**m**VGLDAAGK	Glu-y-semialdehyde (irrev.) Met sulfone (irrev.) Met sulfone (irrev.)
	3122071	Elongation factor 1-alpha [*Zea mays*]	VETGVIK**p**GMVVTFGPTGLTTEVK EALDLINEPKR**p**SDKPLR	Glu-y-semialdehyde (irrev.) Glu-y-semialdehyde (irrev.)
	470107062	Rac-like GTP-binding protein ARAC3-like [*Fragaria vesca*]	DDKQFFTD**h**PGAV**p**ITTAQGEELKK GADVFLLAFSLIS**k**	2-Oxohistidine (irrev.); Glu-y-semialdehyde (irrev.) AASA (irrev.)
	359484301	Eeukaryotic initiation factor 4A-15-like [*Vitis vinifera*]	**m**FVLDEADE**m**LSR SLLGL**p**VAE**p**NCFLQGHDGPA**y**DVK	Met sulfone (irrev.); Met sulfone (irrev.) Glu-y-semialdehyde (irrev.); 3-Nitrotyrosine (rev.)
	390195442	Elongation factor E1 [*Brassica oleracea var. capitata*]	ELLSFYKF**p**GDDIPIIR EDIQRG**m**VIAKPGS**c**KTYK	Glu-y-semialdehyde (irrev.) Met sulfone (irrev.); Cysteic acid (irrev.)
	225451995	PREDICTED: 14-3-3 protein 4 [*Vitis vinifera*]	SAQDIALAELAPT**h**PIR SAQDIALAELA**p**TH**p**IR IISSIEQ**k**EESR	2-Oxohistidine (irrev.) Glu-y-semialdehyde (irrev.); Glu-y-semialdehyde (irrev.) AASA (irrev.)
	115345320	Elongation factor 1 alpha [*Capsicum chinense*]	VETGVIK**p**GMVVTFGPTGLTTEV**k** V**p**ISGFEGDN**m**	Glu-y-semialdehyde (irrev.); AASA (irrev.) Glu-y-semialdehyde (irrev.); Met sulfoxide (rev.)

Cytoskeleton	33339126	actin [*Musa acuminata*]	DLYGNIVLSGGSTMF**p**GIADR **m**SKEITALAPSS**m**K YPIEHGIVSNWDD**m**EK **c**DVDIRRDLYGNIVLSGGST**m**FPGIADR HTGV**m**VG**m**GQKDAYVGDEAQSKR	Glu-y-semialdehyde (irrev.) Met sulfone (irrev.); Met sulfoxide (rev.); Met sulfoxide (rev.) S-nitrosocysteine (rev.); Met sulfoxide (rev.) Met sulfone (irrev.); Met sulfone (irrev.)
	227069387	actin 2 [*Picea abies*]	DLYGNIVLSGGSTMF**p**GIADR LDLAGRDLTDAL**m**KILTER DLTDAL**m**KILTER KDLYGNIVLSGGST**m**FPGIADR **m**SKEITALAPSS**m**K	Glu-y-semialdehyde (irrev.) Met sulfone (irrev.) Met sulfone (irrev.) Met sulfone (irrev.) Met sulfoxide (rev.); Met sulfoxide (rev.)
	356558127	PREDICTED: actin-like [*Glycine max*]	DLYGNIVLSGGSTMF**p**GIADR LDLAGRDLTDAL**mk**ILTER DLTDAL**m**KILTER KDLYGNIVLSGGST**m**FPGIADR FR**c**PEVLFQPSMIG**m**EAVGIHETTYNSI**m**K	Glu-y-semialdehyde (irrev.) Met sulfone (irrev.); AASA (irrev.) Met sulfoxide (rev.) Met sulfoxide (rev.) S-nitrosocysteine (rev.); Met sulfone (irrev.); Met sulfone (irrev.)
	159482014	actin [*Camellia sinensis*]	SYEL**p**DGQVITIGAER EITALAPSS**m**K	Glu-y-semialdehyde (irrev.) Met sulfone (irrev.)
	15242516	actin 7 [*Arabidopsis thaliana*]	VAPEEH**p**VLLTEAPLNPK DLYGNIVLSGGST**m**FPGIADR NYELPDG**q**VITIGAER	Glu-y-semialdehyde (irrev.) Met sulfone (irrev.) Deamidation (rev.)
	93359562	alpha-tubulin [*Phaseolus vulgaris*]	TVGGGDDAFNTFFSETGAG**k** AIFVDLE**p**TVIDEVR	AASA (irrev.) Glu-y-semialdehyde (irrev.)
	224088196	actin 3 [*Populus trichocarpa*]	NGTGMV**k**AGFAGDDAPRAV VAPEEH**p**VLLTEAPLNPK	AASA (irrev.) Glu-y-semialdehyde (irrev.)
	1498344	actin, partial [*Glycine max*]	LAYIALDYEQELETS**k** LDLAGRDLTDAL**m**KILTER DLTDAL**m**KILTER SYEL**p**DGQVITIGSER	AASA (irrev.) Met sulfone (irrev.) Met sulfone (irrev.) Glu-y-semialdehyde (irrev.)

Metabolism	4539543	glyceraldehyde-3-phosphate dehydrogenase [*Nicotiana tabacum*]	LTG**m**AFRVPTVDVSVVDLTVR KVIISAPSKDAP**m**FVVGVNEK DA**p**MFVVGVNEKE**y**K**p**ELNIVSNASCTTNCLA**p**LAK	Met sulfone (irrev.) Met sulfone (irrev.) Glu-y-semialdehyde (irrev.); 3-Nitrotyrosine (rev.); Glu-y-semialdehyde (irrev.); Glu-y-semialdehyde (irrev.)
	15219412	phosphoglycerate kinase [*Arabidopsis thaliana*]	GVTTIIGGGDSVAAVE**k** ELDYLVGAVAN**p**K	AASA (irrev.) Glu-y-semialdehyde (irrev.)
	162464059	pyruvate dehydrogenase2 [*Zea mays*]	SNY**m**SAGQISVPIVFR LGSGCVLAQLAQALR**p**AAA**p**AR	Met sulfone (irrev.) Glu-y-semialdehyde (irrev.); Glu-y-semialdehyde (irrev.)
	357477179	Glyceraldehyde-3-phosphate dehydrogenase [*Medicago truncatula*]	VALKRDDVELVAVNDPFITTDY**m**TY**m**FK LTG**m**AFRVPTVDVSVVDLTVR DDVELVAVNDPFITTDY**m**TYMFK TVDG**p**SAKDWR	Met sulfone (irrev.); Met sulfone (irrev.) Met sulfone (irrev.) Met sulfone (irrev.) Glu-y-semialdehyde (irrev.)
	514802145	PREDICTED: isocitrate dehydrogenase [NAD] regulatory subunit 1, mitochondrial-like isoform X2 [*Setaria italica*]	ANPVALLLSSA**mm**LR LVSASSPPAPQPLPGH**c**GGLARRTVTY**m**PRPGDGTPR	Met sulfone (irrev.); Met sulfone (irrev.) S-nitrosocysteine (rev.); Met sulfone (irrev.)
	32478662	cytosolic glyceraldehyde-3-phosphate dehydrogenase [*Triticum aestivum*]	FGIVEGL**m**TTVHA**m**TATQK AASFNII**p**SSTGAAK	Met sulfone (irrev.); Met sulfoxide (rev.); Glu-y-semialdehyde (irrev.)
Electron transport	460413924	PREDICTED: cytochrome c1-1, heme protein, mitochondrial-like isoform 2 [*Solanum lycopersicum*]	HNGQNYVFALLTGYRD**p**PAGVSIR DVVSFLSWAAEPE**m**EER EGLHYNPYFPGGAIA**m**PK FANGGAY**p**PDLSLITK	Glu-y-semialdehyde (irrev.) Met sulfone (irrev.) Met sulfone (irrev.) Glu-y-semialdehyde (irrev.)

Energy production pathways	508704803	ADP/ATP carrier 2 [*Theobroma cacao*]	VKLLIQNQDE**m**IK LLIQNQDE**m**IK **m**MMTSGEAVKYK	Met sulfone (irrev.) Met sulfone (irrev.) Met sulfone (irrev.)
	357137335	PREDICTED: ADP,ATP carrier protein, mitochondrial-like isoform 1 [*Brachypodium distachyon*]	VKLLIQNQDE**m**IK MM**m**TSGEAVKYK LLIQNQDE**m**IKAGR NMC**p**SAPA**y**ER	Met sulfone (irrev.) Met sulfone (irrev.) Met sulfone (irrev.) Glu-y-semialdehyde (irrev.); 3-Nitrotyrosine (rev.)
	195644888	ATP synthase gamma chain [*Zea mays*]	NAGD**m**LDRLTLTYNR N**p**INYTQVAVLADDILKNVEYDALR MA**m**AALRR	Met sulfone (irrev.) Glu-y-semialdehyde (irrev.) Met sulfone (irrev.)
Protein transport	508778346	Coatomer epsilon subunit isoform 2 [*Theobroma cacao*]	IQEAYLIFQDFSEKY**p**MTGLILNGK HTNAGGT**m**ELHALNVQIFIK	Glu-y-semialdehyde (irrev.) Met sulfone (irrev.)
Vesicle trafficking pathways	357161325	PREDICTED: clathrin heavy chain 1-like [*Brachypodium distachyon*]	YKEAAELAAES**p**QGLLR G**c**FHELISL**m**ESGLGLER	Glu-y-semialdehyde (irrev.) Cysteic acid (irrev.); Met sulfone (irrev.)
	470143989	PREDICTED: clathrin heavy chain 1-like [*Fragaria vesca*]	YKEAAELAAES**p**QGILR FGFVPDLTHYLYTNN**m**LR	Glu-y-semialdehyde (irrev.) Met sulfone (irrev.)
	30681617	Clathrin, heavy chain [*Arabidopsis thaliana*]	FQSV**p**VQAGQTPPLLQYFGTLLTR QLIDQVVSTALPES**k** FGFVPDLTHYLYTNN**m**LR AH**m**GIFTELGVLYAR	Glu-y-semialdehyde (irrev.) AASA (irrev.) Met sulfone (irrev.); Met sulfone (irrev.)
	356495434	PREDICTED: clathrin heavy chain 1-like [*Glycine max*]	AH**m**GIFTELGVLYAR VLEINLVTFPNVADAILANG**m**FSHYDRPR YVVER**m**DSDLWEK	Met sulfone (irrev.) Met sulfone (irrev.) Met sulfone (irrev.)
	225434540	PREDICTED: clathrin heavy chain 2 [*Vitis vinifera*]	YKEAAELAAES**p**QGLLR AQLPGTTQDHLQIFNIE**m**K FGFV**p**DLTHYLYTNN**m**LR AH**m**GIFTELGVLYAR	Glu-y-semialdehyde (irrev.) Met sulfone (irrev.) Glu-y-semialdehyde (irrev.); Met sulfone (irrev.) Met sulfoxide (rev.)

	443299013	clathrin heavy chain 1 [*Zea mays*]	FQSV**p**VQAGQTPPLLQYFGTLLTR EAAELAAES**p**QGLLR	Glu-y-semialdehyde (irrev.) Glu-y-semialdehyde (irrev.)
Redox related protein	508725282	2-oxoacid dehydrogenases acyltransferase family protein isoform 1 [*Theobroma cacao*]	EIF**m**PALSST**m**TEGK N**m**VESLSVPTFR GVT**m**TALLAK	Met sulfone (irrev.); Met sulfone (irrev.) Met sulfone (irrev.) Met sulfone (irrev.)
Biosynthetic pathways	195623672	RHM1 [*Zea mays*]	VR**m**PISSDLSNPR AGAE**m**LV**m**AYGR	Met sulfone (irrev.) Met sulfone (irrev.); Met sulfone (irrev.)
	473993302	5-methyltetrahydropteroyltriglutamate--homocysteine methyltransferase [*Triticum urartu*]	G**m**LTGPVTILNWSFVR WFDTNYHFIV**p**ELA**p**STK	Met sulfone (irrev.) Glu-y-semialdehyde (irrev.); Glu-y-semialdehyde (irrev.)
Ion Transport	7378769	H+-ATPase [*Medicago truncatula*]	**m**ITGDQLAIGKETGR **h**PGEGl**y**SGSTCKQGEIEAIVIATGVHTFFGK LLEGDPLKIDQSALTGESLPVTK**h**PGEGl**y**SGSTCK	Met sulfone (irrev.); 2-Oxohistidine (irrev.); 3-Nitrotyrosine (rev.) 2-Oxohistidine (irrev.); 3-Nitrotyrosine (rev.)
	15220197	H(+)-ATPase 9 [*Arabidopsis thaliana*]	**m**ITGDQLAIGKETGR GAPEQIIEL**c**NLR	Met sulfone (irrev.) Cysteic acid (irrev.)
Stress	514812924	PREDICTED: heat shock cognate 70 kDa protein 2-like [*Setaria italica*]	NQVA**m**NPINTVFDAK DAGVIAGLNV**m**R	Met sulfone (irrev.) Met sulfone (irrev.)
	356534858	PREDICTED: chaperonin CPN60-2, mitochondrial-like isoform 2 [*Glycine max*]	AGIID**p**LKVIR NVVIEQSFGAP**k**	Glu-y-semialdehyde (irrev.) AASA (irrev.)
	470143740	PREDICTED: heat shock cognate 70 kDa protein-like [*Fragaria vesca*]	DAGVIAGLNV**m**R ELESL**c**NPIIAK	Met sulfone (irrev.) Carbamidomethylation (rev.)

	30025966	heat shock protein 70 [*Nicotiana tabacum*]	NAVVTV**p**AYFNDSQR ELESI**c**NPIIAK NALENYAYN**m**R	Glu-y-semialdehyde (irrev.) Carbamidomethylation (rev.) Met sulfone (irrev.)
	145342421	Luminal binding protein precursor, probable [*Ostreococcus lucimarinus*]	GVNPDEAVAYGAAV**q**GGILSGEGGDET**k** IINEPTAAAIAYGLDK**k**	Deamidation (rev.); AASA (irrev.) AASA (irrev.)
Uncharacterized protein	217072626	unknown [*Medicago truncatula*]	GLWQ**p**FTALLGDATSVDVKK NAGD**m**LDRLTLTYNR	Glu-y-semialdehyde (irrev.) Met sulfone (irrev.)
	224097392	predicted protein [*Populus trichocarpa*]	VENQEGVVNFDEILRETDSF**m**VAR GDLGMEI**p**VEKIFLAQK	Met sulfone (irrev.) Glu-y-semialdehyde (irrev.)
	388508708	unknown [*Lotus japonicus*]	TN**m**V**m**VFGEITTK FVIGG**p**HGDAGLTGR	Met sulfoxide (rev.); Met sulfoxide (rev.); Glu-y-semialdehyde (irrev.)